Oxidative Medicine and Cellular Longevity

Applications of Antioxidants in Ameliorating Drugs and Xenobiotics Toxicity: Mechanistic Approach

Lead Guest Editor: Mohamed M. Abdel-Daim
Guest Editors: Yasser M. Moustafa, Masakazu Umezawa, Kota V. Ramana, and Elena Azzini

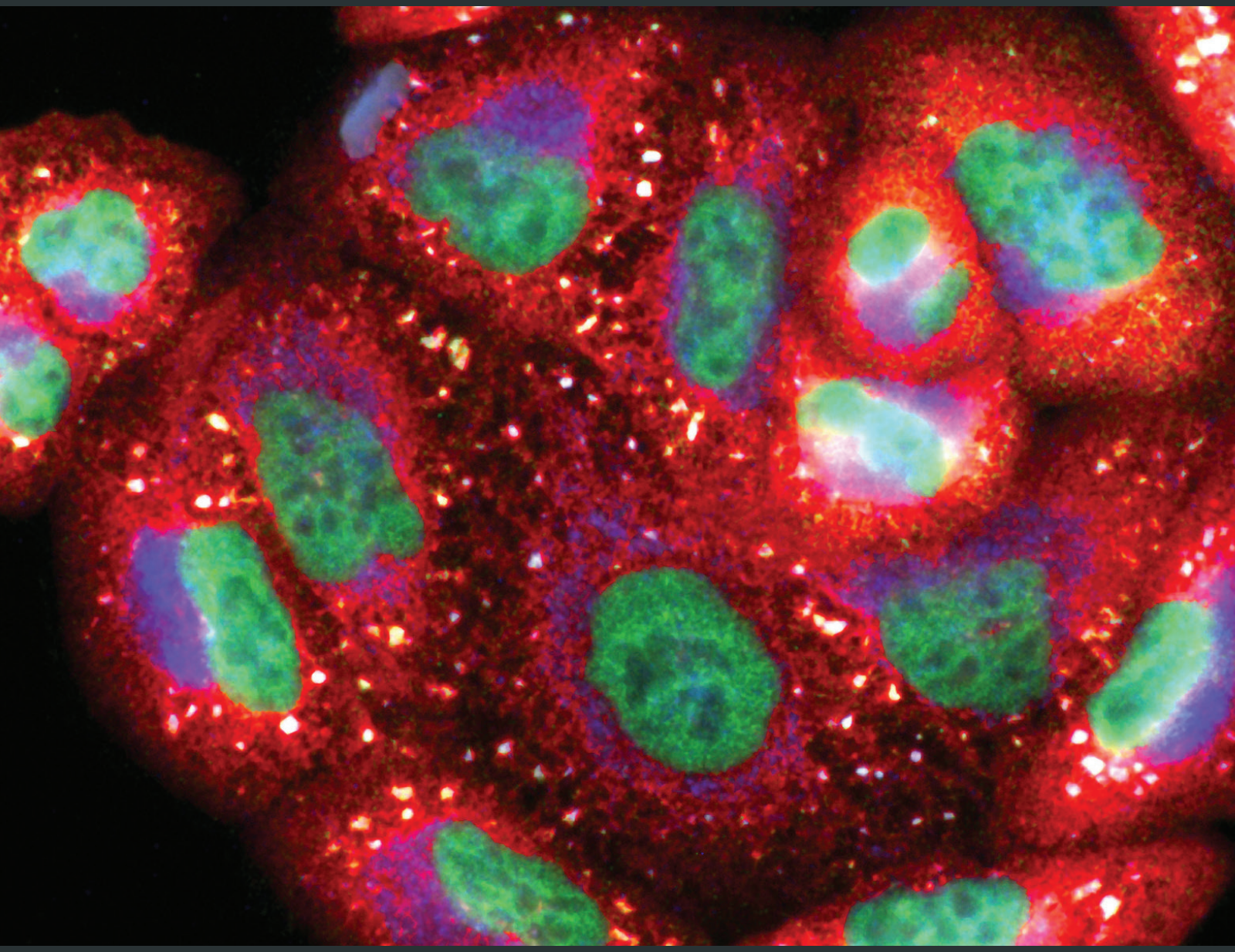

Applications of Antioxidants in Ameliorating Drugs and Xenobiotics Toxicity: Mechanistic Approach

Oxidative Medicine and Cellular Longevity

Applications of Antioxidants in Ameliorating Drugs and Xenobiotics Toxicity: Mechanistic Approach

Lead Guest Editor: Mohamed M. Abdel-Daim
Guest Editors: Yasser M. Moustafa, Masakazu Umezawa, Kota V. Ramana, and Elena Azzini

Copyright © 2017 Hindawi. All rights reserved.

This is a special issue published in "Oxidative Medicine and Cellular Longevity." All articles are open access articles distributed under the Creative Commons Attribution License, which permits unrestricted use, distribution, and reproduction in any medium, provided the original work is properly cited.

Editorial Board

Antonio Ayala, Spain
Peter Backx, Canada
Damian Bailey, UK
Consuelo Borrás, Spain
Vittorio Calabrese, Italy
Angel Catalá, Argentina
Shao-Yu Chen, USA
Zhao Zhong Chong, USA
Giuseppe Cirillo, Italy
Massimo Collino, Italy
Mark Crabtree, UK
Manuela Curcio, Italy
Andreas Daiber, Germany
Felipe Dal Pizzol, Brazil
Francesca Danesi, Italy
Domenico D'Arca, Italy
Yolanda de Pablo, Sweden
Grégory Durand, France
Javier Egea, Spain
Ersin Fadillioglu, Turkey
Qingping Feng, Canada
Giuseppe Filomeni, Italy
Swaran J. S. Flora, India
Rodrigo Franco, USA
José Luís García-Giménez, Spain
Janusz Gebicki, Australia
Husam Ghanim, USA
Daniela Giustarini, Italy
Saeid Golbidi, Canada
Tilman Grune, Germany
Tim Hofer, Norway
Silvana Hrelia, Italy
Maria G. Isaguliants, Sweden
Vladimir Jakovljevic, Serbia
Peeter Karihtala, Finland
Eric E. Kelley, USA
Kum Kum Khanna, Australia
Neelam Khaper, Canada
Thomas Kietzmann, Finland
Jean-Claude Lavoie, Canada
Christopher Horst Lillig, Germany
Paloma B. Liton, USA
Nageswara Madamanchi, USA
Kenneth Maiese, USA
Tullia Maraldi, Italy
Reiko Matsui, USA
Steven McAnulty, USA
Bruno Meloni, Australia
Trevor A. Mori, Australia
Ryuichi Morishita, Japan
Ange Mouithys-Mickalad, Belgium
Hassan Obied, Australia
Pál Pacher, USA
Valentina Pallottini, Italy
Serafina Perrone, Italy
Tiziana Persichini, Italy
Vincent Pialoux, France
Ada Popolo, Italy
José L. Quiles, Spain
Walid Rachidi, France
Kota V. Ramana, USA
Sidhartha D. Ray, USA
Alessandra Ricelli, Italy
Francisco J. Romero, Spain
H.P. Vasantha Rupasinghe, Canada
Gabriele Saretzki, UK
Honglian Shi, USA
Cinzia Signorini, Italy
Shane Thomas, Australia
Rosa Tundis, Italy
Giuseppe Valacchi, Italy
Jeannette Vasquez-Vivar, USA
Victor M. Victor, Spain
Michal Wozniak, Poland
Sho-ichi Yamagishi, Japan
Liang-Jun Yan, USA
Guillermo Zalba, Spain
Jacek Zielonka, USA

Contents

Applications of Antioxidants in Ameliorating Drugs and Xenobiotics Toxicity: Mechanistic Approach
Mohamed M. Abdel-Daim, Yasser M. Moustafa, Masakazu Umezawa, Kota V. Ramana, and Elena Azzini
Volume 2017, Article ID 4565127, 2 pages

Genetic Transformation and Hairy Root Induction Enhance the Antioxidant Potential of *Lactuca serriola* L.
Mohamed A. El-Esawi, Amr Elkelish, Hosam O. Elansary, Hayssam M. Ali, Mohamed Elshikh, Jacques Witczak, and Margaret Ahmad
Volume 2017, Article ID 5604746, 8 pages

Diosmin Attenuates Methotrexate-Induced Hepatic, Renal, and Cardiac Injury: A Biochemical and Histopathological Study in Mice
Mohamed M. Abdel-Daim, Hesham A. Khalifa, Abdelrahman Ibrahim Abushouk, Mohamed A. Dkhil, and Saleh A. Al-Quraishy
Volume 2017, Article ID 3281670, 10 pages

Effects of Antioxidant Supplements on the Survival and Differentiation of Stem Cells
Sara Shaban, Mostafa Wanees Ahmed El-Husseny, Abdelrahman Ibrahim Abushouk, Amr Muhammad Abdo Salem, Mediana Mamdouh, and Mohamed M. Abdel-Daim
Volume 2017, Article ID 5032102, 16 pages

Modulatory Effect of Monochromatic Blue Light on Heat Stress Response in Commercial Broilers
Safaa E. Abdo, Seham El-Kassas, Abeer F. El-Nahas, and Shawky Mahmoud
Volume 2017, Article ID 1351945, 13 pages

***Camellia sinensis* Prevents Perinatal Nicotine-Induced Neurobehavioral Alterations, Tissue Injury, and Oxidative Stress in Male and Female Mice Newborns**
Jamaan S. Ajarem, Gadh Al-Basher, Ahmed A. Allam, and Ayman M. Mahmoud
Volume 2017, Article ID 5985219, 16 pages

MitoTEMPO Prevents Oxalate Induced Injury in NRK-52E Cells via Inhibiting Mitochondrial Dysfunction and Modulating Oxidative Stress
Jiaqiao Zhang, Qing Wang, Chuou Xu, Yuchao Lu, Henglong Hu, Baolong Qin, Yufeng Wang, Deng He, Cong Li, Xiao Yu, Shaogang Wang, and Jihong Liu
Volume 2017, Article ID 7528090, 9 pages

Nephroprotective Effects of N-Acetylcysteine Amide against Contrast-Induced Nephropathy through Upregulating Thioredoxin-1, Inhibiting ASK1/p38MAPK Pathway, and Suppressing Oxidative Stress and Apoptosis in Rats
Xuezhong Gong, Yiru Duan, Junli Zheng, Yiquan Wang, Guohua Wang, Svante Norgren, and Tom K. Hei
Volume 2016, Article ID 8715185, 11 pages

Dietary Supplementation of *Phoenix dactylifera* Seeds Enhances Performance, Immune Response, and Antioxidant Status in Broilers
Ali H. El-Far, Hamada A. Ahmed, and Hazem M. Shaheen
Volume 2016, Article ID 5454963, 9 pages

Hindawi
Oxidative Medicine and Cellular Longevity
Volume 2017, Article ID 4565127, 2 pages
https://doi.org/10.1155/2017/4565127

Editorial

Applications of Antioxidants in Ameliorating Drugs and Xenobiotics Toxicity: Mechanistic Approach

Mohamed M. Abdel-Daim,[1,2] Yasser M. Moustafa,[3] Masakazu Umezawa,[4] Kota V. Ramana,[5] and Elena Azzini[6]

[1]*Pharmacology Department, Faculty of Veterinary Medicine, Suez Canal University, Ismailia 41522, Egypt*
[2]*Department of Ophthalmology and Micro-Technology, Yokohama City University, Yokohama, Japan*
[3]*Pharmacology Department, Faculty of Pharmacy, Suez Canal University, Ismailia, Egypt*
[4]*Research Institute of Science and Technology, Tokyo University of Science, Tokyo, Japan*
[5]*Department of Biochemistry and Molecular Biology, University of Texas Medical Branch, Galveston, TX 77555, USA*
[6]*Council for Agricultural Research and Economics (CREA), Research Center for Food and Nutrition, Via Ardeatina 546, 00178 Rome, Italy*

Correspondence should be addressed to Mohamed M. Abdel-Daim; abdeldaim.m@vet.suez.edu.eg

Received 10 August 2017; Accepted 10 August 2017; Published 29 August 2017

Copyright © 2017 Mohamed M. Abdel-Daim et al. This is an open access article distributed under the Creative Commons Attribution License, which permits unrestricted use, distribution, and reproduction in any medium, provided the original work is properly cited.

Biotransformation of drugs, xenobiotics, and environmental pollutants leads to the overproduction of free radicals in the body leading to lipid peroxidation, oxidative stress, and oxidative damage. The free radicals interact with various macromolecules, such as nucleic acids, proteins, and lipids and alter critical intracellular signaling pathways, responsible for the maintenance of cellular homeostasis. The free radicals, either directly or indirectly through the mediation of oxidative and inflammatory signals, disrupt the cellular equilibrium and cause mitogenesis, mutagenesis, genotoxicity, and cytotoxicity. The involvement of free radical-mediated damage in the pathophysiology of a variety of diseases including diabetes, hypertension, atherosclerosis, cancer, Parkinsonism, and Alzheimer's has been well established.

Currently, a plethora of phytochemical antioxidants have been developed in the therapeutic management to maintain normal homeostasis and for the prevention and treatment of many diseases and toxicities. The investigations on the molecular mechanisms through which antioxidants restrict free radical-mediated toxicity still remain the primary focus of many investigators for a better understanding of their biological activities as well as future drug development opportunities. The articles published in this special issue provide an in-depth understanding of antioxidants in the regulation of free radical-mediated disease pathologies.

An excellent review article by S. Shaban et al. discussed the cellular and molecular effects of antioxidant supplements on mitigation of oxidative stress, improvement of transplanted or cultured stem cell survival, potency, and differentiation. Further, they discussed how antioxidants enhance genomic stability, improve the stem cell adhesion to culture media, and enable researchers to manipulate cellular proliferation. This review nicely described the possible clinical applications of antioxidant-supplemented stem cells in improving neurogenesis in patients with neurodegenerative diseases and regeneration of infarcted myocardial tissue as well as in spermatogonial stem cell banking.

In this special issue, two research articles describe the benefit of antioxidants in protection against drugs and xenobiotics, using mouse models. The first study by M. Abdel-Daim et al. examined the beneficial role of citrus fruit-derived flavonoid (diosmin) on the oxidative damage induced by the antineoplastic and antirheumatic drug (methotrexate) in mice hepatic, renal, and cardiac tissues.

Specifically, they have shown that diosmin prevents methotrexate-induced oxidative as well as inflammatory markers. Based on these results, they concluded that diosmin could be a promising agent to protect against methotrexate-induced toxicities in patients with cancer and autoimmune diseases. The second study by J. S. Ajarem et al. examined the protective effects of green tea (*Camellia sinensis*) on nicotine exposure-induced oxidative damage in mice leading to behavioral alterations in early childhood and young adulthood animals. This study demonstrates that green tea significantly improved the nicotine-induced abnormalities such as physical development, neuromotor maturation, and behavioral performance in newborn male and female mice.

Another interesting research article by X. Gong et al. highlighted a nephroprotective role of N-acetylcysteine amide (NACA) against contrast-induced nephropathy using rat model. They have shown that NACA ameliorates contrast-induced nephropathy by modulating the thioredoxin-1 and ASK1/p38 MAPK pathway, leading to inhibition of renal cell oxidative stress and apoptosis.

Further, two research articles describe the significance of antioxidants in broiler chicken. A. El-Far et al. demonstrated the improvement of growth performance, immunity, and antioxidant status in chickens, fed with a diet containing antioxidant-rich *Phoenix dactylifera* seeds, as compared to mannon-oligosaccharide-fed chicken. On the other hand, S. E. Abdo et al. reported the improvement of antioxidant gene expression as well as enhancement of chicken's resistance to heat stress in two commercial broiler strains (Ross 308 and Cobb 500), as a result of exposure to monochromatic blue light.

Another research article by J. Zhang et al. used NRK-52E cells to investigate whether the mitochondria-targeted antioxidant (MitoTEMPO) could protect against oxalate-mediated cell injury. Specifically, they found that MitoTEMPO regulates oxalate-induced cytotoxicity by modulating the oxidative stress and inhibiting the mitochondrial dysfunction. Thus, the authors suggested that MitoTEMPO could be a new candidate for the protection against oxalate-induced renal injury as well as urolithiasis.

Finally, M. El-Esawi et al. investigated the increased production of antioxidants, such as phenolics and flavonoids by hairy root cultures of *L. serriola*, transformed with *Agrobacterium rhizogenes* bearing the rolB gene. This study showed significant increases in the total phenolic and flavonoid contents as well as in the total reducing power of transgenic hairy lines, indicating the potential efficiency of hairy root induction platform in enhancing the antioxidant potential in *L. serriola*.

Acknowledgments

We would like to thank all the authors and reviewers who took part in the success of this special issue.

Mohamed M. Abdel-Daim
Yasser M. Moustafa
Masakazu Umezawa
Kota V. Ramana
Elena Azzini

Hindawi
Oxidative Medicine and Cellular Longevity
Volume 2017, Article ID 5604746, 8 pages
https://doi.org/10.1155/2017/5604746

Research Article

Genetic Transformation and Hairy Root Induction Enhance the Antioxidant Potential of *Lactuca serriola* L.

Mohamed A. El-Esawi,[1,2] Amr Elkelish,[3] Hosam O. Elansary,[4] Hayssam M. Ali,[5,6] Mohamed Elshikh,[5] Jacques Witczak,[2] and Margaret Ahmad[2,7]

[1]*Botany Department, Faculty of Science, Tanta University, Tanta, Egypt*
[2]*UMR CNRS 8256 (B2A), IBPS, Université Paris VI, Paris, France*
[3]*Botany Department, Faculty of Science, Suez Canal University, Ismailia, Egypt*
[4]*Floriculture, Ornamental Horticulture and Garden Design Department, Faculty of Agriculture (El-Shatby), Alexandria University, Alexandria, Egypt*
[5]*Botany and Microbiology Department, College of Science, King Saud University, Riyadh 11451, Saudi Arabia*
[6]*Timber Trees Research Department, Sabahia Horticulture Research Station, Horticulture Research Institute, Agriculture Research Center, Alexandria, Egypt*
[7]*Department of Biology, Xavier University, Cincinnati, OH, USA*

Correspondence should be addressed to Mohamed A. El-Esawi; mohamed.elesawi@science.tanta.edu.eg

Received 24 March 2017; Revised 18 May 2017; Accepted 31 May 2017; Published 1 August 2017

Academic Editor: Kota V. Ramana

Copyright © 2017 Mohamed A. El-Esawi et al. This is an open access article distributed under the Creative Commons Attribution License, which permits unrestricted use, distribution, and reproduction in any medium, provided the original work is properly cited.

Lactuca serriola L. is a herbaceous species, used for human nutrition and medicinal purposes. The high antioxidant capacity of *L. serriola* indicates the possibility of enhancing its edible and health potential by increasing the flavonoid and phenolic contents. The present study aimed at enhancing the production of phenolics and flavonoids by hairy root cultures in *Lactuca serriola* transformed with *Agrobacterium rhizogenes* strain AR15834 harbouring the *rolB* gene. The genetic transformation of *rolB* in transformed roots was validated, and *rolB* expression level was evaluated using real-time qPCR analysis. Expression levels of flavonoid biosynthesis genes (CHI, PAL, FLS, and CHS) were assessed in the hairy and nontransformed roots. Results showed higher expression levels in the transgenic roots than in the nontransformed ones ($p < 0.01$). Transgenic hairy roots exhibited a 54.8–96.7% increase in the total phenolic content, 38.1–76.2% increase in the total flavonoid content, and 56.7–96.7% increase in the total reducing power when compared with the nontransgenic roots ($p < 0.01$). DPPH results also revealed that the transgenic hairy roots exhibited a 31.6–50% increase in antioxidant potential, when compared to normal roots. This study addressed the enhancement of secondary metabolite biosynthesis by hairy root induction in *L. serriola*.

1. Introduction

Cellular reactive oxygen species (ROS) may arise during the process of mitochondrial oxidative metabolism or due to interactions with some agents like xenobiotics [1, 2]. Oxidative stress occurs because of the imbalance between ROS production and antioxidant defence activity [1, 2]. Oxidative stress causes ROS-mediated macromolecular damage which results in severe diseases [1–4]. Phenolics and flavonoids are natural antioxidants and effective ROS scavengers [2], widely distributed in plants. Therefore, human diet plants have a key role in disease prevention and maintaining health [2].

Lactuca serriola L. of the family Asteraceae is a herbaceous species [5, 6], cultivated in Europe, Siberia, Pakistan, Iran, and India [7]. The plant is used for human nutrition and in various medicinal purposes as sedative, expectorant, purgative, cough suppressant, antiseptic, diuretic, and antispasmodic [7]. The

plant is rich in lactucarium and comprises a wide range of mineral nutrients, vitamins, natural antioxidants, flavonoids, and phenolics [7]. Pharmacological evaluation of the plant extract showed its anti-inflammatory, anticarcinogenic, and antioxidant potential due to its high phenolic content that revealed effective free radical scavenging activity [7–10]. Though the phytochemical level is relatively less in *Lactuca serriola*, its high antioxidant capacity indicates the possibility of enhancing its edible and health potential upon increasing the flavonoid and phenolic content. The enhancement of secondary metabolites through field cultivation has many defects such as slow growth and low and variable yield due to the environmental and biotic factors [11]. Therefore, hairy root culture has been developed as a more efficient alternative biotechnological technology for secondary metabolite synthesis, regardless of environmental, seasonal, and climatic variations [11, 12]. In vitro hairy roots formed by genetic transformation have been efficiently utilized for the synthesis of higher levels of secondary metabolites due to their biochemical and genetic stability as well as their fast growth in media without phytohormones [11, 13].

Several studies have demonstrated that *Agrobacterium rhizogenes*-mediated transformation with root locus (*rol*) genes induces secondary metabolite biosynthesis in transgenic roots by activating biosynthetic genes [14–18]. Few earlier studies on the hairy root induction of *Lactuca sativa* have been reported [16–18]. However, the secondary metabolite synthesis by *Lactuca serriola* hairy roots has never been reported yet. Our current study aimed to assess and enhance the production of phenolics and flavonoids by hairy root cultures, for the first time, in *Lactuca serriola* transformed with *Agrobacterium rhizogenes* strain AR15834 harbouring the *rolB* gene. The genetic transformation of the *rolB* gene in transgenic roots was validated, and *rolB* expression level was evaluated using real-time quantitative PCR analysis (RT-qPCR). We also evaluated the expression levels of four flavonoid biosynthetic genes (chalcone isomerase (CHI), chalcone synthase (CHS), phenylalanine ammonia-lyase (PAL), and flavonol synthase (FLS)) of transformed and nontransformed roots. Additionally, we estimated the total flavonoid and phenolic contents of hairy and nontransgenic roots of the plant. Finally, we assessed the antioxidant and cytotoxic activities of transformed and normal root extracts of *Lactuca serriola*.

2. Material and Methods

2.1. Plant Material and Bacterial Strain. Lactuca serriola L. seeds were received from the Centre for Genetic Resources (CGN) in the Netherlands. Seeds were first sterilized using 5% NaClO for 5 min, washed 5 times in sterile H_2O, and then grown on 1/2 MS medium [19, 20] for 16 h light/8 h dark at 24°C.

Agrobacterium rhizogenes strain AR15834 harbouring the *rolB* gene was used for transformation and was cultured on liquid Luria-Bertani (LB) media in darkness at 28°C for 48 hours with shaking.

2.2. Transformation, Hairy Root Induction, and Root Biomass. Cotyledonary leafy explants of 2-week-old seedlings were cut and infected with the bacterial suspension ($OD_{600} = 0.5$) for 10 minutes, dried with an autoclaved filter paper, and cultivated on MS media in darkness at 26°C for 4 days. The explants were then transferred onto fresh media of the same constituents and supplemented with cefotaxime. The formed roots were then transferred onto liquid Woody Plant Media (WPM) lacking growth regulators. Cultures were put on a rotary shaker at 80 rpm in darkness. Subcultures were performed every 30 days (0.5 g fresh root biomass was transferred onto new media). Hairy root biomass (fresh and dry weights) was estimated after 30 days of culture. For each hairy root line, 3 flasks from 3 successive subcultures were utilized. The hairy roots showed stability with regard to a root biomass increase. The untransformed (control) roots were also grown on the same media.

2.3. Molecular Analysis of Hairy Roots by PCR. To validate transformation, total genomic DNA was prepared from transgenic roots (5 survived lines) and nontransformed roots (negative control) using the DNeasy Plant kit from Qiagen in UK, following the manufacturer's procedures. Plasmid DNA was also purified from *A. rhizogenes* strain AR15834 and used as a control. A primer pair designed by Skała et al. [21] was used for amplification of the *rolB* gene (a fragment size of 386 bp; Table 1). Additionally, to confirm the correct transformation of hairy roots without bacterial contamination, PCR amplification included the *vir*G gene (Table 1) [21]. Amplification was conducted in reactions of a final volume of 25 μl (1.5 μl of each primer (50 ng/μl), 2 μl of DNA (25 ng/μl), 12.5 μl of master mix, and 7.5 μl of dist. H_2O. PCR amplification programme was set up: 3 min at 95°C; 33 cycles of 30 sec at 95°C, 30 seconds at 55°C, and 2 min at 72°C; and then 3 min at 72°C. PCR products amplified were then visualized on 1.2% agarose gel and photographed.

2.4. Expression Analysis of the rolB Gene and Flavonoid Biosynthetic Genes. Real-time quantitative PCR (RT-qPCR) was performed to evaluate the expression level of the *rolB* gene in transgenic roots as well as changes in expression levels of four flavonoid biosynthesis genes (CHI, PAL, FLS, and CHS) of transformed and nontransformed roots. Total RNA was prepared from the transformed (5 lines) and nontransformed roots using the RNeasy Plant Mini kit, and cDNA synthesis was done using the Reverse Transcription kit (Qiagen). RT-qPCR was done in triplicates with the QuantiTect SYBR Green PCR kit from Qiagen. PCR amplification programme used was set up: 95°C for 5 min and 35 cycles of 95°C for 30 sec, 57°C for 30 sec, and 72°C for 2 min. The primers of genes analyzed are shown in Table 1. Analysis of the melting curve was then used to test the amplification specificity. Gene expression level was normalized to ubiquitin (UBQ1) housekeeping gene level [22] and calculated using the $2^{-\Delta\Delta Ct}$ method.

2.5. Extract Preparation. To conduct antioxidant assays, extracts from the transgenic and nontransformed roots of

Table 1: Primers of *rolB* and flavonoid biosynthetic pathway genes used in RT-qPCR analysis.

Gene	Primer sequence (5′–3′)	Reference
rolB	F: GCTCTTGCAGTGCTAGATTT R: GAAGGTGCAAGCTACCTCTC	Skała et al. [21]
*vir*G	F: AGTTCAATCGTGTACTTTCCT R: CTGATATTCAGTGTCCAGTCT	Skała et al. [21]
CHI	F: TGGTGGCCTAGACAACGATGAGTT R: TCACACTCCCAACTTGGTTTCCCT	Chung et al. [11]
PAL	F: AGAACGGTGTCGCTCTTCAG R: TGTGGCGGAGTGTGGTAATG	Chung et al. [11]
FLS	F: TTAAAGGAAGGTCTCGGTGGCGAA R: TCATTGGTGACGATGAGTGCGAGT	Chung et al. [11]
CHS	F: AGGCTAACAGAGGAGGGTA R: CCAATTTACCGGCTTTCT	Dilshad et al. [27]
UBQ1	F: TTCCTTGATGATGCTTGCTC R: TTGACAGCTCTTGGGTGAAG	Chen et al. [22]

Lactuca serriola were prepared. For each type, 5 grams of dried plant material was soaked in 100 ml methanol in a sonication bath for 2 hours. The extracts were then filtered and concentrated. The concentration of extracts used in antioxidant assays is 50 mg/ml sterile water.

2.6. Total Phenolic Content (TPC). TPC of the transformed and nontransformed extracts was estimated following the Folin-Ciocalteu reagent assay [18, 23] with minor modifications. In brief, 4 μl of plant extract was added and mixed with 98 μl of diluted Folin-Ciocalteu solution and kept at 26°C for 10 min; then, 98 μl of 5% Na_2CO_3 was added to the mixture and kept for 2 hours at 26°C. Solution absorbance was then determined at 725 nm. TPC was represented as a gallic acid equivalent. Triplicate analyses were done.

2.7. Total Flavonoid Content (TFC). TFC of the transformed and normal extracts was estimated following the reported assay [24] with minor modifications. In brief, 4 μl of each extract was mixed with a solution (10 μl of 1 M potassium acetate, 10 μl of 10% $AlCl_3$, and 176 μl of H_2O) and kept at 26°C for 30 min. Mixture absorbance was then determined at 405 nm. TFC was represented as a quercetin equivalent.

2.8. Total Reducing Power (TRP). TRP of the transgenic and nontransformed extracts was estimated following the reported method [24] with minor modifications. Twenty microliter of each extract was added to 490 μl 1% potassium ferricyanide and 490 μl 0.2 M phosphate buffer and mixed and kept for 20 min at 50°C. 500 μl of 10% TCA was then added to the solution and centrifuged; then, 500 μl of the upper layer was mixed with 100 μl of 0.1% ferric cyanide in a new Eppendorf tube. The solution absorbance was then determined at 630 nm. TRP was represented as an ascorbic acid equivalent. Analyses were done in triplicate.

2.9. 2,2-Diphenyl-1-picryl-hydrazyl (DPPH) Free Radical Scavenging Assay. DPPH of the transformed and untransformed extracts was estimated following the DPPH protocol [18]. Ascorbic acid was utilized as a control. Triplicate analyses were conducted.

2.10. Cytotoxicity Screening Assay. HepG2 human liver cancer cells (obtained from VACSERA, Egypt) were utilized for the cytotoxicity test of root extracts of *Lactuca serriola*. Cell viability was recorded with the MTT method [25]. Human cells were added to each well of 96-well plates and were subjected to various concentrations of transformed and nontransformed extracts of the transgenic line of *rolB2* (12.5, 25, 50, 100, and 200 μg/ml) for 48 hrs. Cells were incubated with MTT (20 μl per well) at 37°C for 2 hours. DMSO was then used. Optical density was measured at 492 nm. Cell growth inhibition percentage was estimated as reported by Chung et al. [11]. Analyses were done in triplicate.

2.11. Data Analysis. Results were represented as means with standard deviation. ANOVA analysis and test for significant difference ($p < 0.05$) were done using SPSS software.

3. Results and Discussion

3.1. Transformation, Hairy Root Induction, and Root Biomass. Lactuca serriola L. was transformed with *A. rhizogenes* strain AR15834 containing the *rolB* gene. Approximately, 250 explants were transformed, and transformation efficiency of producing hairy roots was high (74%). However, only five transformed lines survived till the maturity stage. Similar high transformation efficiency with *A. rhizogenes* AR15834 was found in *Tribulus terrestris* L. by Sharifi et al. [26]. Efficiency of transformation and hairy root induction relies on *A. rhizogenes* strain as well as on the type of hairy root culture used [16]. In the current study, we used liquid Woody Plant Media (WPM). After 30 days of culture, fresh and dry weights of hairy roots of each of the 5 transformed lines were approximately 81 $g \cdot l^{-1}$ and 8 $g \cdot l^{-1}$, respectively (Figure 1). For each hairy root line, 3 flasks from 3 successive subcultures were utilized. The hairy roots showed stability with regard to a root biomass increase. WPM was the best

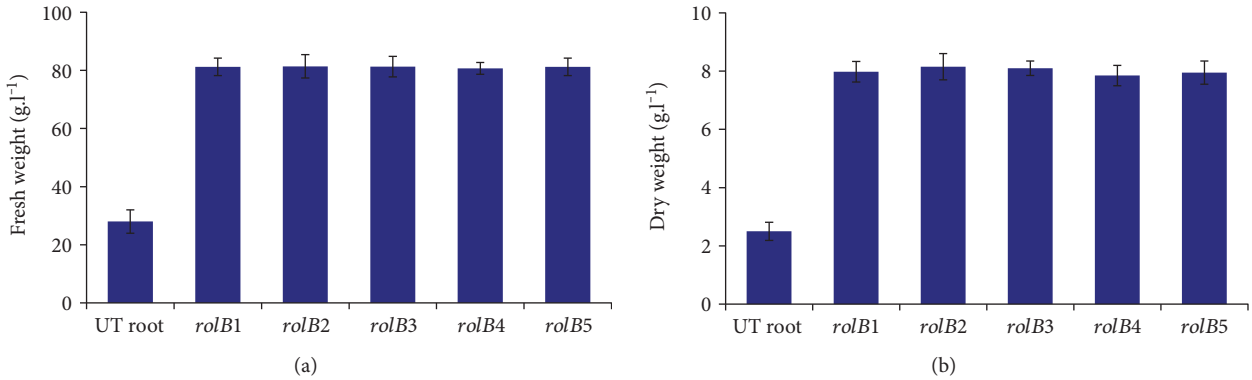

Figure 1: Fresh and dry weights of the untransformed root (UT root) and the 5 transgenic hairy root lines after 30 days in liquid media. (a) Fresh weight (g) of biomass per liter; (b) dry weight (g) of biomass per liter.

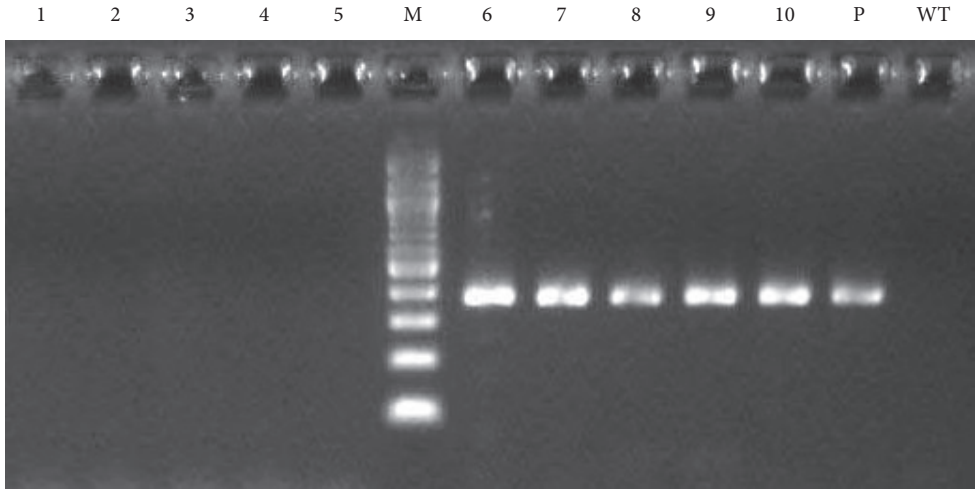

Figure 2: PCR-amplified products of the *rolB* gene in *Lactuca serriola*. Lanes 1–5 show the absence of the *virG* gene in the 5 transgenic hairy root lines. Lanes 6–10 show *rolB* gene fragment amplified in the 5 transgenic hairy root lines. Lane P stands for the plasmid DNA. WT refers to the nontransformed root. Lane M refers to the 100 bp DNA ladder.

growth medium for the transgenic roots of other plant species such as *Rhaponticum carthamoides* [21].

3.2. Integration and Expression Analysis of the rolB Gene. PCR confirmed *rolB* integration in *Lactuca serriola*, and a fragment of the same size (386 bp) was amplified from each of the 5 survived hairy root lines (Figure 2). A fragment having similar size was also amplified from the plasmid DNA of *A. rhizogenes* AR15834 (positive control). However, no such fragment was amplified from the nontransformed roots (negative control). The *vir*G gene was not amplified from any of the 5 transgenic hairy root lines, confirming the true transformation of hairy roots without *A. rhizogenes* contamination (Figure 2, lanes 1–5). RT-qPCR confirmed *rolB* gene expression in all the 5 survived transgenic lines (Figure 3). The transgenic hairy root lines *rolB1*, *rolB2*, *rolB3*, and *rolB5* exhibited higher levels of *rolB* transcript as compared to *rolB4* line ($p < 0.05$).

3.3. Expression Analysis of Flavonoid Biosynthetic Genes. Analysis of gene expression provides a comprehensive insight into how metabolic pathways regulate flavonoid synthesis in the transgenic and nontransformed roots. RT-qPCR was done to evaluate the expression of 4 flavonoid biosynthetic genes (CHI, PAL, FLS, and CHS) in the transgenic and nontransformed roots. Expression levels of flavonoid

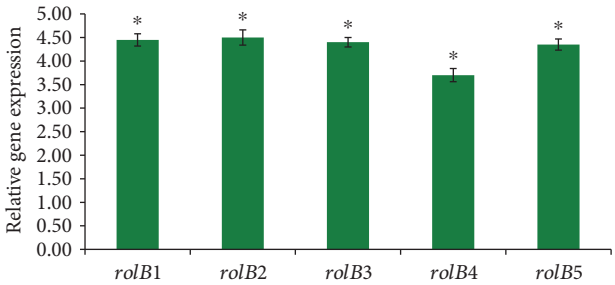

Figure 3: Expression level of the *rolB* gene in the 5 transgenic hairy root lines using real-time qPCR. Data represent three replicates. $^{*}p < 0.05$ statistically significant.

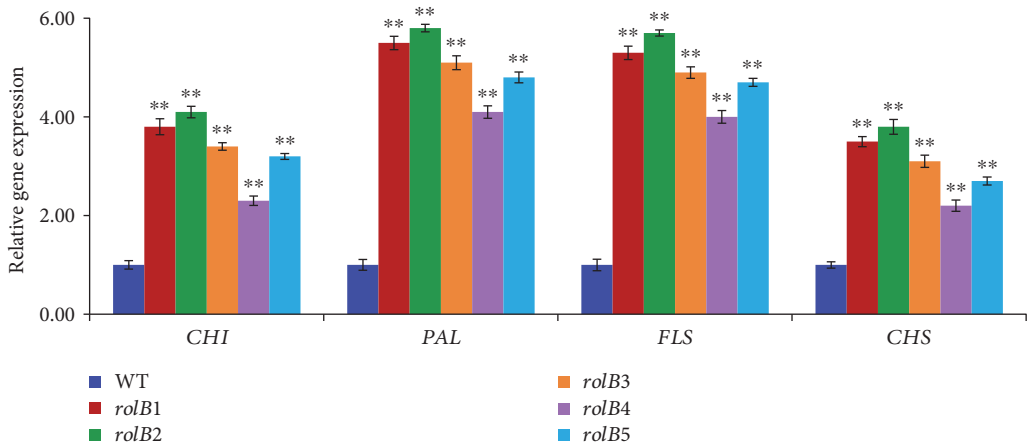

Figure 4: Flavonoid biosynthetic gene expression level in the transgenic roots and nontransformed roots (WT). Data represent three replicates; bars indicate ±standard deviation. $^{**}p < 0.01$ statistically significant.

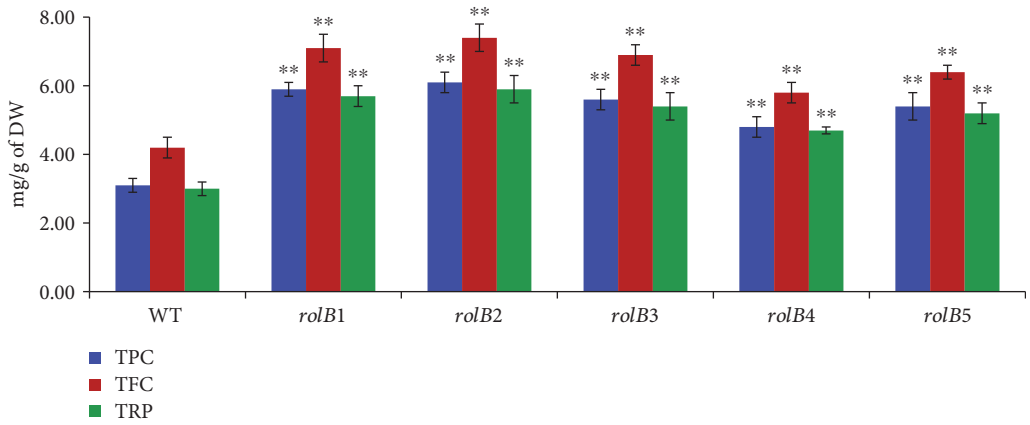

Figure 5: Results of TPC, TFC, and TRP in the 5 transgenic hairy root lines of the *rolB* gene and nontransformed roots (WT). Data are represented in mean ± standard deviation, in milligrams/gram of dry weight (DW). $^{**}p < 0.01$ statistically significant.

biosynthetic genes were higher in the transformed roots as compared to the normal roots ($p < 0.01$; Figure 4). These results could be attributed to the functional role of the *rolB* gene in inducing secondary metabolite biosynthesis in hairy roots by activating their biosynthetic genes. These results are in accordance with those revealed by Chung et al. [11] and Dilshad et al. [27] who found that the expression levels of flavonoid biosynthetic genes in the hairy roots of *Brassica rapa* and *Artemisia carvifolia*, respectively, were higher than those in the normal roots.

3.4. Evaluation of Total Phenolic and Flavonoid Content and Total Reducing Power. TPC results exhibited a 90.3%, 96.7%, 80.6%, 54.8%, and 74.2% increase in the hairy root lines of *rolB1*, *rolB2*, *rolB3*, *rolB4*, and *rolB5*, respectively, compared to the nontransformed root (Figure 5). TFC data revealed a 69%, 76.2%, 64.3%, 38.1%, and 52.4% increase in the hairy root lines of *rolB1*, *rolB2*, *rolB3*, *rolB4*, and *rolB5*, respectively, compared to the nontransformed root (Figure 5). TRP also showed a 90%, 96.7%, 80%, 56.7%, and 73.3% increase in the hairy root lines of *rolB1*, *rolB2*, *rolB3*, *rolB4*, and *rolB5*, respectively, compared to the nontransformed root (Figure 5).

In conclusion, the total flavonoid and phenolic contents and total reducing power were higher in the transformed roots as compared to the normal roots ($p < 0.01$). The results were in accordance with those recorded by Vojin et al. [16] and Ismail et al. [17] who found that the total flavonoid and phenolic contents and total reducing power were higher in the transformed roots as compared to the nontransformed ones of *Lactuca sativa*. Results also showed high significant correlations with the expression levels of *rolB* and flavonoid biosynthetic genes (Table 2). This is the first study that compares the phenolic and flavonoid contents and the corresponding gene expression (CHI, PAL, FLS, and CHS) of transgenic and nontransgenic roots in *Lactuca serriola*.

3.5. DPPH Free Radical Scavenging Assay. The DPPH assay was effective for estimating the enhanced antioxidant potential in the transgenic lines of the *rolB* gene. The extract of

Table 2: Pearson's correlation among total phenolic and flavonoid contents, total reducing power, DPPH, *rolB*, and flavonoid biosynthetic genes.

	rolB	*TPC*	*TFC*	*TRP*	*DPPH*	*CHI*	*PAL*	*FLS*
TPC	0.92*	1						
TFC	0.90*	0.99**	1					
TRP	0.90*	0.99**	0.99**	1				
DPPH	−0.80ns	−0.95*	−0.95*	−0.96*	1			
CHI	0.93*	0.99**	0.98**	0.99**	−0.95*	1		
PAL	0.90*	0.99**	0.99**	0.99**	−0.96*	0.99**	1	
FLS	0.89*	0.99**	0.98**	0.99**	−0.98*	0.99**	0.99**	1
CHS	0.86ns	0.99**	0.99**	0.99**	−0.96*	0.98**	0.99**	0.99**

*Significant at $p < 0.05$; **Significant at $p < 0.01$; NS: non significant.

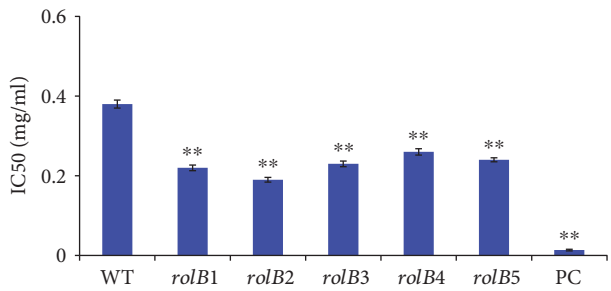

Figure 6: Results of the DPPH assay of the 5 transgenic hairy root lines of the *rolB* gene and nontransformed roots (WT). Data are represented in mean ± standard deviation. PC is a positive control (ascorbic acid). $^{**}p < 0.01$ statistically significant.

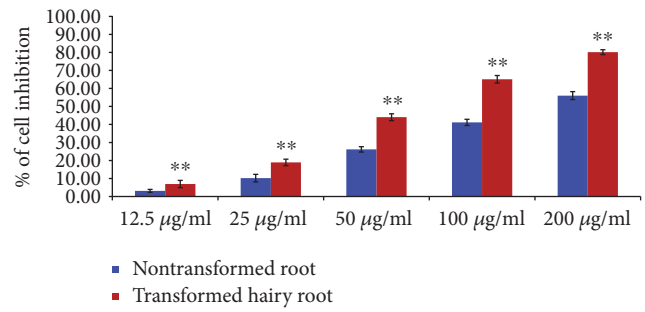

Figure 7: Percentage of cell inhibition of transgenic hairy root and nontransformed root extracts of *Lactuca serriola* against HepG2 human liver cancer cells. Data represent three replicates. $^{**}p < 0.01$ statistically significant.

rolB2-transformed line exhibited the highest radical scavenging capacity (IC50 = 0.19 mg/ml) with a 50% increase as compared to that of the normal roots (0.38 mg/ml) ($p < 0.01$; Figure 6). The extracts of *rolB1*, *rolB3*, *rolB4*, and *rolB5* exhibited a 42.1%, 39.5%, 31.6%, and 36.8% increase as compared to those of the nontransformed roots ($p < 0.01$; Figure 6). This increasing DPPH scavenging potential could be attributed to the high secondary metabolites formed in the transgenic hairy root [17]. The results were in accordance with those recorded by Vojin et al. [16] and Ismail et al. [17].

3.6. Cytotoxicity Activity. Screening cytotoxic activity of the extracts of the transgenic and nontransgenic roots against HepG2 human liver cancer cells was investigated. The human cells were subjected to several concentrations of the extracts of the transgenic hairy root *rolB2* line and nontransformed roots. The results showed that the percentage of cancer inhibition relies on the concentration of the extract used (Figure 7). The greater inhibition was recorded at the highest extract concentration (200 μg/ml) ($p < 0.01$; Figure 7), at which the hairy root extracts exhibited 80.21% cancer inhibition whereas the nontransformed root extracts showed 56.02% inhibition. This high cytotoxic activity in hairy roots may be due to the high flavonoid and phenolic content. Our results agreed with various earlier studies which demonstrated that the transgenic roots showed higher antibacterial and cytotoxic activities compared to the nontransgenic roots [28, 29]. In conclusion, the present study suggests that transgenic hairy roots of *Lactuca serriola* could be efficiently used for the antioxidant and medicinal treatments.

4. Conclusions

This is the first study that addresses the enhancement of secondary metabolite biosynthesis by hairy root induction in *L. serriola*. The genetic transformation and expression levels of *rolB* in transgenic roots of *Lactuca serriola* were validated by PCR and real-time qPCR analyses. The flavonoid biosynthetic genes (CHI, PAL, FLS, and CHS) exhibited higher levels in the hairy roots than in the nontransformed roots. Hairy roots exhibited significant increases in the total flavonoid and phenolic contents and the total reducing power as compared to the nontransformed roots. Additionally, the cytotoxicity assay revealed that the hairy root extracts exhibited a maximum percentage of 80.21% cancer inhibition whereas the nontransformed root extracts showed a maximum percentage of 56.02% inhibition. The study highlights that the transformation of *Lactuca serriola* with the *rolB* gene may be efficiently used to develop plants with enhanced secondary metabolites and improved medicinally important properties.

Conflicts of Interest

The authors state that no conflict of interests exists.

Authors' Contributions

Mohamed A. El-Esawi designed the research, carried out the experiments, analyzed the data, and wrote the whole manuscript. Hayssam M. Ali, Amr Elkelish, Hosam O. Elansary, Mohamed Elshikh, Jacques Witczak, and Margaret Ahmad helped in the data analysis and revisions. All authors revised and approved the paper.

Acknowledgments

The authors would like to thank the Deanship of Scientific Research at King Saud University for funding this work through research Grant no. RG1435-011. This work was also supported by Tanta University in Egypt and University of Paris VI in France.

References

[1] P. D. Ray, B. W. Huang, and Y. Tsuji, "Reactive oxygen species (ROS) homeostasis and redox regulation in cellular signalling," *Cellular Signalling*, vol. 24, no. 5, pp. 981–990, 2012.

[2] E. Skała, P. Sitarek, M. Różalski et al., "Antioxidant and DNA repair stimulating effect of extracts from transformed and normal roots of *Rhaponticum carthamoides* against induced oxidative stress and DNA damage in CHO cells," *Oxidative Medicine and Cellular Longevity*, vol. 2016, Article ID 5753139, 11 pages, 2016.

[3] B. N. Ames, M. K. Shigenaga, and T. M. Hagen, "Oxidants, antioxidants, and degenerative diseases of aging," *Proceedings of the National Academy of Sciences*, vol. 90, no. 17, pp. 7915–7922, 1993.

[4] M. Stankovic, M. Topuzovic, S. Solujic, and V. Mihailovic, "Antioxidant activity and concentration of phenols and flavonoids in the whole plant and plant parts of *Teucrium chamaerdys* L. var. *Glanduliferum Haussk*," *Journal of Medicinal Plants Research*, vol. 4, no. 20, pp. 2092–2098, 2010.

[5] M. A. El-Esawi and R. Sammour, "Karyological and phylogenetic studies in the genus *Lactuca* L. (Asteraceae)," *Cytologia*, vol. 79, pp. 269–275, 2014.

[6] M. A. El-Esawi, A. Mustafa, S. Badr, and R. Sammour, "Isozyme analysis of genetic variability and population structure of *Lactuca* L. germplasm," *Biochemical Systematics and Ecology*, vol. 70, pp. 73–79, 2017.

[7] K. H. Janbaz, M. F. Latif, F. Saqib, I. Imran, M. Zia-Ul-Haq, and V. D. Feo, "Pharmacological effects of *Lactuca serriola* L. in experimental model of gastrointestinal, respiratory, and vascular ailments," *Evidence-Based Complementary and Alternative Medicine*, vol. 2013, Article ID 304394, 9 pages, 2013.

[8] D. K. Kim, "Antioxidative components from the aerial parts of *Lactuca scariola* L," *Archives of Pharmacal Research*, vol. 24, no. 5, pp. 427–430, 2001.

[9] B. Tepe and A. Sokmen, "Screening of the antioxidative properties and total phenolic contents of three endemic *Tanacetum* subspecies from Turkish flora," *Bioresource Technology*, vol. 98, no. 16, pp. 3076–3079, 2007.

[10] S. M. Nabavi, S. F. Nabavi, S. H. Eslami, and A. H. Moghaddam, "In vivo protective effects of quercetin against sodium-fluoride-induced oxidative stress in the hepatic tissue," *Food Chemistry*, vol. 132, no. 2, pp. 931–935, 2012.

[11] I. M. Chung, K. Rekha, G. Rajakumar, and M. Thiruvengadam, "Production of glucosinolates, phenolic compounds and associated gene expression profiles of hairy root cultures in turnip (*Brassica rapa ssp. rapa*)," *3 Biotech*, vol. 6, p. 175, 2016.

[12] S. A. Wilson and S. C. Roberts, "Metabolic engineering approaches for production of biochemicals in food and medicinal plants," *Current Opinion in Biotechnology*, vol. 26, pp. 174–182, 2014.

[13] S. Chandra, "Natural plant genetic engineer *Agrobacterium rhizogenes*: role of T-DNA in plant secondary metabolism," *Biotechnology Letters*, vol. 34, pp. 407–415, 2012.

[14] V. P. Bulgakov, "Functions of rol genes in plant secondary metabolism," *Biotechnology Advances*, vol. 26, no. 4, pp. 318–324, 2008.

[15] E. Dilshad, S. Zafar, H. Ismail et al., "Effect of *rol* genes on polyphenols biosynthesis in *Artemisia annua* and their effect on antioxidant and cytotoxic potential of the plant," *Applied Biochemistry and Biotechnology*, vol. 179, no. 8, pp. 1456–1468, 2016.

[16] T. Vojin, M. Snežana, C. Aleksandar et al., "Production of hairy root cultures of lettuce (*Lactuca sativa* L.)," *Central European Journal of Biology*, vol. 9, no. 12, pp. 1196–1205, 2014.

[17] H. Ismail, E. Dilshad, M. T. Waheed, M. Sajid, W. K. Kayani, and B. Mirza, "Transformation of *Lactuca sativa* L. with *rol C* gene results in increased antioxidant potential and enhanced analgesic, anti-inflammatory and antidepressant activities in vivo," *3 Biotech*, vol. 6, no. 2, p. 215, 2016.

[18] H. Ismail, E. Dilshad, M. T. Waheed, and B. Mirza, "Transformation of lettuce with *rol ABC* genes: extracts show enhanced antioxidant, analgesic, anti-inflammatory, antidepressant, and anticoagulant activities in rats," *Applied Biochemistry and Biotechnology*, vol. 181, no. 3, pp. 1179–1198, 2017.

[19] T. Murashige and F. Skoog, "A revised medium for rapid growth and bio assays with tobacco tissue cultures," *Physiologia Plantarum*, vol. 15, pp. 473–497, 1962.

[20] T. A. Brown, *Gene Cloning*, Blackwell Science LTD, West Sussex, UK, 3rd edition, 1998.

[21] E. Skała, A. Kicel, M. A. Olszewska, A. K. Kiss, and H. Wysokińska, "Establishment of hairy root cultures of *Rhaponticum carthamoides* (Willd.) Iljin for the production of biomass and caffeic acid derivatives," *BioMed Research International*, vol. 2015, Article ID 181098, 11 pages, 2015.

[22] D. Chen, G. Xu, W. Tang et al., "Antagonistic basic helix-loop-helix/bZIP transcription factors form transcriptional modules that integrate light and reactive oxygen species signaling in *Arabidopsis*," *The Plant Cell*, vol. 25, pp. 1657–1673, 2013.

[23] X. Liu, S. Ardo, M. Bunning et al., "Total phenolic content and DPPH radical scavenging activity of lettuce (*Lactuca sativa* L.) grown in Colorado," *LWT-Food Science and Technology*, vol. 40, pp. 552–557, 2017.

[24] M. R. Moein, S. Moein, and S. Ahmadizadeh, "Radical scavenging and reducing power of *Salvia mirzayanii* subfractions," *Molecules*, vol. 13, pp. 2804–2813, 2008.

[25] A. M. Gabr, H. B. Mabrok, K. Z. Ghanem, M. Blaut, and I. Smetanska, "Lignan accumulation in callus and *Agrobacterium rhizogenes*-mediated hairy root cultures of flax (*Linum*

usitatissimum)," *Plant Cell, Tissue and Organ Culture*, vol. 126, pp. 255–267, 2016.

[26] S. Sharifi, T. N. Sattari, A. Zebarjadi, A. Majd, and H. Ghasempour, "The influence of *Agrobacterium rhizogenes* on induction of hairy roots and ß-carboline alkaloids production in *Tribulus terrestris* L," *Physiology and Molecular Biology of Plants*, vol. 20, no. 1, pp. 69–80, 2014.

[27] E. Dilshad, H. Ismail, R. M. Cusido, J. Palazon, K. Ramirez-Estrada, and B. Mirza, "*Rol* genes enhance the biosynthesis of antioxidants in *Artemisia carvifolia* Buch," *BMC Plant Biology*, vol. 16, p. 125, 2016.

[28] M. Thiruvengadam, N. Praveen, K. M. Maria John, Y. S. Yang, S. H. Kim, and I. M. Chung, "Establishment of *Momordica charantia* hairy root cultures for the production of phenolic compounds and determination of their biological activities," *Plant Cell, Tissue and Organ Culture*, vol. 118, pp. 545–557, 2014.

[29] K. Syklowska-Baranek, A. Pietrosiuk, A. Gawron et al., "Enhanced production of antitumour naphthoquinones in transgenic hairy root lines of *Lithospermum canescens*," *Plant Cell, Tissue and Organ Culture*, vol. 108, pp. 213–219, 2012.

Hindawi
Oxidative Medicine and Cellular Longevity
Volume 2017, Article ID 3281670, 10 pages
https://doi.org/10.1155/2017/3281670

Research Article

Diosmin Attenuates Methotrexate-Induced Hepatic, Renal, and Cardiac Injury: A Biochemical and Histopathological Study in Mice

Mohamed M. Abdel-Daim,[1] Hesham A. Khalifa,[2] Abdelrahman Ibrahim Abushouk,[3] Mohamed A. Dkhil,[4,5] and Saleh A. Al-Quraishy[4]

[1]*Pharmacology Department, Faculty of Veterinary Medicine, Suez Canal University, Ismailia, Egypt*
[2]*Department of Pharmacology, Faculty of Veterinary Medicine, Zagazig University, Zagazig, Egypt*
[3]*Faculty of Medicine, Ain Shams University, Cairo, Egypt*
[4]*Department of Zoology, College of Science, King Saud University, Riyadh, Saudi Arabia*
[5]*Department of Zoology and Entomology, College of Science, Helwan University, Cairo, Egypt*

Correspondence should be addressed to Mohamed M. Abdel-Daim; abdeldaim.m@vet.suez.edu.eg

Received 22 March 2017; Revised 8 June 2017; Accepted 12 June 2017; Published 27 July 2017

Academic Editor: Francisco J. Romero

Copyright © 2017 Mohamed M. Abdel-Daim et al. This is an open access article distributed under the Creative Commons Attribution License, which permits unrestricted use, distribution, and reproduction in any medium, provided the original work is properly cited.

The current study was designed to investigate the beneficial role of diosmin, a biologically active flavonoid, against methotrexate- (MTX-) induced hepatic, renal, and cardiac injuries in mice. Male Swiss albino mice received a single intraperitoneal injection of MTX (at 20 mg/kg, body weight) either alone or in combination with oral diosmin (at 50 or 100 mg/kg body weight, for 10 days). Serum was used to evaluate tissue injury markers, while hepatic, renal, and cardiac tissue samples were obtained for determination of antioxidant activity as well as histopathological examination. Diosmin treatment ameliorated the MTX-induced elevation of serum alkaline phosphatase, aminotransferases, urea, creatinine, lactate dehydrogenase, and creatine kinases as well as plasma proinflammatory cytokines (interleukin-1-beta, interleukin-6, and tumor necrosis factor-alpha). Additionally, both diosmin doses significantly reduced tissue levels of malondialdehyde and nitric oxide and increased those of glutathione, glutathione peroxidase, glutathione reductase, glutathione S-transferase, superoxide dismutase, and catalase, compared to the MTX-intoxicated group. Histopathological examination showed that diosmin significantly minimized the MTX-induced histological alterations and nearly restored the normal architecture of hepatic, renal, and cardiac tissues. Based on these findings, diosmin may be a promising agent for protection against MTX-induced cytotoxicity in patients with cancer and autoimmune diseases.

1. Introduction

Methotrexate (MTX) is a widely known folate antimetabolite agent, used to treat several types of cancer [1] and autoimmune diseases [2]. Using MTX at cyclic high doses to treat malignant tumors can be associated with severe hepatotoxicity and acute renal failure [3, 4], while its chronic use at lower doses may cause progressive liver fibrosis, uremia, and hematuria [4, 5]. Moreover, few articles have reported an acute toxic effect of MTX on the cardiovascular system [6]. Methotrexate-induced cytotoxicity can be a product of the interaction of several factors including the patient's risk factors, type of disease, dosing schedule, and treatment duration, as well as the presence of genetic apoptotic factors [7].

Long-term use of MTX leads to accumulation of its intracellular storage form "MTX polyglutamates," which has been suggested as a mechanism for MTX hepatotoxicity [8]. It also inhibits the cytosolic nicotinamide adenosine diphosphate- [NAD(P)-] dependent dehydrogenases, decreasing the cellular availability of NADP [9], which is normally used by glutathione reductase (GR) to maintain

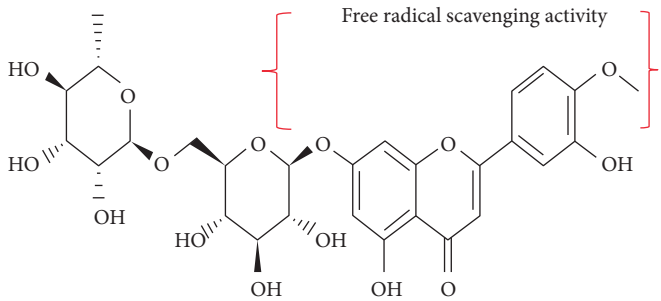

Figure 1: The chemical structure of diosmin. The area (in brackets) refers to the main antioxidant component of diosmin molecule.

the reduced state of glutathione (GSH) [10]. Moreover, its high affinity to dihydrofolate reductase inhibits the production of thymidylate, suppressing DNA synthesis [11]. Despite these side effects, MTX is a highly effective chemotherapeutic agent; therefore, research efforts should be directed at preventing and treating its cytotoxicity.

Diosmin (3′,5,7-trihydroxy-4′-methoxyflavone 7-rutinoside) is an unsaturated flavonoid glycoside, present in citrus fruits (Figure 1) [12]. It is a biologically active polyphenol that has anti-inflammatory [13], antioxidant, antihyperglycemic [14], and antimutagenic properties [15]. In rat models, Ahmed and colleagues showed a nephroprotective role for diosmin against alloxan-induced nephropathy [16], while Tahir et al. highlighted its beneficial effect against alcoholic liver injury [13]. Moreover, diosmin could successfully improve cardiac function [17] and exert antihyperlipidemic effects against isopropanol-induced myocardial injury in rats [18].

A literature survey retrieved no scientific reports on the protective effects of diosmin against MTX toxicity. Therefore, in light of the above inferences from other evidence, we designed this study to investigate the beneficial role of diosmin against MTX-induced injuries to mouse hepatic, renal, and cardiac tissues.

2. Materials and Methods

2.1. Chemicals. Methotrexate was purchased from Shanxi PUDE Pharmaceutical Company (Shanxi, China), while diosmin was purchased from Sigma (St. Louis, MO, USA). All the assay kits were purchased from Biodiagnostics Co. (Cairo, Egypt), except for the kits of creatine kinase (CK) and CK-myoglobin binding (CK-MB) (Stanbio™, TX, USA), lactate dehydrogenase (LDH) enzymes (Randox Laboratories Ltd., UK), tumor necrosis factor- (TNF-) α (BioSource International Inc., Camarillo, CA, USA), interleukin- (IL-) 1β, and IL-6 (Glory Science Co. Ltd., Del Rio, TX, USA).

2.2. Mice. Thirty-two adult male Swiss albino mice, weighing 22 to 27 g, were obtained from the Egyptian Organization for Biological Products and Vaccines. The animals were first acclimatized for seven days at the experiment site (animal house of the Department of Pharmacology, Faculty of Veterinary Medicine, Suez Canal University) under optimal environmental conditions (12-hour light-dark cycles, temperature [20 ± 2°C] with moderate humidity [60 ± 5%]). All the animal handling procedures, used in this study, were approved by the Research Ethical Committee at the Faculty of Veterinary Medicine, Suez Canal University, Egypt (Approval number 201608).

2.3. Experimental Design. The mice were divided into four groups, each of eight. Mice in group I served as a negative control, receiving saline only during the entire experimental period. Mice in group II received a single intraperitoneal injection of MTX at a dose of 20 mg/kg bw (mimicking the acute exposure to an acute large dose in humans) [19]. Mice in groups III and IV received oral diosmin for 10 days at doses of 50 and 100 mg/kg bw [20], respectively. On the sixth day of the experiment, mice in groups III and IV received i.p MTX injection, at the same dose used in group II mice.

All animals were sacrificed on the 11th day after blood sample collection via direct cardiac puncture. The liver, heart, and kidneys were dissected into two parts: the 1st part was fixed with 10% formalin for further histopathological examination and the 2nd part was used for biochemical analysis. For the latter purpose, tissue pieces (each of 0.5 g) were washed with cold normal saline and homogenized in 2.5 volumes of ice-cold 0.1 M potassium phosphate buffer (pH 7.4). The resulting homogenate underwent two cycles of centrifugation at 600g and 10000g, and the supernatant was collected and stored at −70°C to measure the tissue content of oxidative biomarkers and antioxidant enzymes.

2.4. Serum Biochemical Analysis. The obtained blood samples were allowed to clot for 30 minutes then centrifuged at 3000 rpm for 15 minutes in order to obtain clear sera. The sera were then stored at −20°C for further biochemical analysis. The methods described by Reitman and Frankel [21] to measure the serum levels of alanine transferase (ALT) and aspartate transferase (AST) and those described by Kind and King [22] to measure the serum level of alkaline phosphatase (ALP) were used. To estimate the serum levels of renal injury markers, we used the methods described by Larsen for measurement of serum creatinine [23] and those described by Coulombe and Favreau for measurement of serum urea [24]. In addition, the cardioprotective effect of diosmin was evaluated enzymatically by estimating the serum activity of CK and CK-MB, using Stanbio CK-NAC (UV-Rate)/CK-MB kits (TX, USA), according to the

Table 1: Ameliorative effects of diosmin on serum concentrations of hepatic, cardiac, and renal injury markers in mice exposed to methotrexate.

Group	AST (U/ml)	ALT (U/ml)	ALP (U/l)	LDH (U/l)	CK (U/l)	CK-MB (U/l)	Urea (mg/dl)	Creatinine (mg/dl)
Control	30.7 ± 1.8	27.2 ± 1.3	68.3 ± 1.6	290.5 ± 7.3	116 ± 3.1	36.6 ± 1.3	22.3 ± 1.5	0.41 ± 0.02
MTX	$83 \pm 4.6^{*}$	$71.5 \pm 2.7^{*}$	$132.7 \pm 3.03^{*}$	$440.7 \pm 10.3^{*}$	$394 \pm 17.6^{*}$	$190.3 \pm 15.6^{*}$	$73.5 \pm 3.5^{*}$	$2.1 \pm 0.15^{*}$
MTX-DM50	$52 \pm 4.7^{*\#}$	$42 \pm 2^{*\#}$	$84.6 \pm 2.5^{*\#}$	$347.2 \pm 15.7^{*\#}$	$221 \pm 11.6^{*\#}$	$89.4 \pm 4.3^{*\#}$	$39 \pm 2.3^{*\#}$	$1.2 \pm 0.13^{*\#}$
MTX-DM100	$36.9 \pm 2.8^{\#}$	$30 \pm 1.4^{\#}$	$71.2 \pm 2.6^{\#}$	$307.6 \pm 9^{\#}$	$146 \pm 9.7^{\#}$	$45.7 \pm 4.3^{\#}$	$26.4 \pm 2.4^{\#}$	$0.57 \pm 0.04^{\#}$

Values are means ± SEM. *Significant change at $p < 0.01$ with respect to the negative control group. #Significant change at $p < 0.01$ with respect to the MTX group as the positive control group. ALP: alkaline phosphatase; ALT: alanine transferase; AST: aspartate transferase; CK: creatine kinase; LDH: lactate dehydrogenase.

methods described by Szasz et al. [25] and Würzburg et al. [26], respectively. Later, serum levels of LDH were measured according to Babson SR and Babson AL [27].

2.5. Evaluation of Tissue Lipid Peroxidation, Nitric Oxide, and Antioxidant Enzymes. For evaluation of lipid peroxidation, the methods described by Uchiyama and Mihara were used to measure the hepatic, cardiac, and renal tissue content of malondialdehyde (MDA) [28]. The concentration of nitric oxide (NO) in these tissues was assessed according to Green et al. [29]. Later, tissue levels of reduced GSH, superoxide dismutase (SOD), and catalase (CAT) were determined according to the methods described by Beutler et al. [30], Nishikimi et al. [31], and Aebi [32], respectively. Moreover, we measured tissue levels of glutathione S-transferase (GST), GR, and glutathione peroxidase (GPx) according to Habig et al. [33], Zanetti [34], and Paglia and Valentine [35], respectively.

2.6. Estimation of Proinflammatory Cytokines. Enzyme-linked immunosorbent assay (ELISA) kits were used to measure the serum levels of TNF-α (BioSource International Inc., Camarillo, CA, USA), IL-1β, and IL-6 (Glory Science Co. Ltd., Del Rio, TX, USA). The measurements were performed according to the manufacturer's instructions, and absorbance was read using an automated ELISA reader at 420 nm.

2.7. Histopathological Examination. Using a rotatory microtome, 5 μm thick sections were sliced from the liver, heart, and kidneys for histopathological examination. These sections were later stained with hematoxylin-eosin (H&E) dye (Merck) and examined at 200x magnification using a power light microscope (Zeiss, Germany). We used a semiquantitative analysis to assess the tissue injury index in examined sections. The results were expressed as the sum of individual score grades (0: no findings, 1: mild, 2: moderate, or 3: severe) for each of the following parameters: degeneration, cellular swelling, cellular vacuolization, necrosis, congestion, and hemorrhage.

2.8. Statistical Analysis. We used SPSS (Statistical Package for Social Sciences) software (version 20) to perform the statistical analysis. All values were expressed as the mean and the standard error of mean (SEM). The means of different groups were compared using the one-way analysis of variance (ANOVA), followed by Tukey's post hoc comparison tests. A p value <0.05 was considered statistically significant.

3. Results

3.1. Biochemical Findings

3.1.1. Serum Concentrations. Intraperitoneal injection of MTX significantly increased serum concentrations of AST, ALT, and ALP enzymes, compared to normal control levels ($p < 0.01$). However, treatment of MTX-injected mice with diosmin (at 50 and 100 mg/kg bw) significantly reduced the elevation of AST levels by 37.3% and 55.6%, ALT levels by 41.3% and 58.1%, and ALP levels by 36.2% and 46.4%, respectively. Treatment of MTX-injected mice with 100 mg/kg of diosmin restored serum concentrations of these parameters to normal control levels.

Similarly, MTX-injected mice showed a significant increase in serum concentrations of cardiac (CK and CK-MB enzymes) as well as renal injury markers (urea and creatinine) in comparison to normal control mice ($p < 0.01$). Upon treatment of MTX-injected mice with diosmin (at 50 and 100 mg/kg bw), we recorded significant reductions in elevated serum levels of LDH by 21.2% and 30.2%, CK by 44% and 63%, CK-MB by 53% and 76%, urea by 47.1% and 64.1%, and creatinine by 42.2% and 73%, respectively. As shown before, only the 100 mg/kg dose of diosmin could restore serum concentrations of these parameters to normal control levels (Table 1).

Plasma concentrations of inflammatory markers (IL-1β, IL-6, and TNF-α) were significantly higher ($p < 0.01$) in the MTX group than in the normal control group. Consistent with previous findings, diosmin treatment (at 50 and 100 mg/kg bw) significantly reduced plasma concentrations of IL-1β by 33.6% and 56.1%, IL-6 by 31.5% and 65.1%, and TNF-α by 38% and 64.2%, respectively. Interestingly, restoration of IL-1β and IL-6 plasma concentrations in MTX-injected mice to normal control levels was noted only in the 100 mg/kg diosmin group; however, neither doses (50 and 100 mg/kg bw) could restore the plasma concentration of TNF-α in MTX-injected mice to normal levels (Figure 2).

3.1.2. Antioxidant Activity in Isolated Tissue Samples. Biochemical analysis of hepatic, cardiac, and renal tissues in MTX-injected mice showed a marked reduction in GSH concentration and antioxidant enzymes' levels (GST, GR, GPx, SOD, and CAT), as well as significant increases in MDA and NO tissue concentrations ($p < 0.01$). Administration

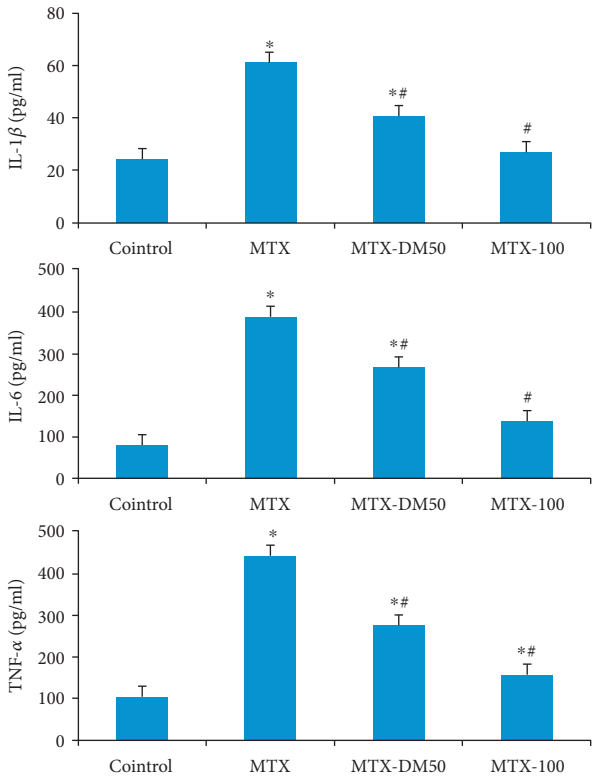

Figure 2: Effect of MTX with or without diosmin on proinflammatory cytokines IL-1β, IL-6, and TNF-α. DM: diosmin; IL: interleukin; MTX: methotrexate; TNF: tumor necrosis factor. *Significant change at $p < 0.01$ with respect to the negative control group. #Significant change at $p < 0.01$ with respect to the MTX group as the positive control group.

of diosmin significantly ameliorated the elevations of MDA and NO tissue concentrations in MTX-injected mice ($p < 0.01$). Moreover, it could increase tissue concentrations ($p < 0.05$) of GSH, as well as the activities of GST, GR, GPx, SOD, and CAT enzymes (Table 2).

3.2. Histopathological Findings

3.2.1. Liver. Liver tissue samples from the negative control group showed normal hepatic cells, arranged in cords around normal central veins. However, liver tissue samples from the MTX group showed focal areas of necrosis around the central vein, sinusoidal dilatation, vacuolar degeneration, and focal infiltration with leukocytes, mainly lymphocytes. In group III (MTX + diosmin 50 mg/kg), moderate hepatocyte vacuolization, sinusoidal dilatation, and partial disruption of hepatic cords' arrangement were observed, while group IV (MTX + diosmin 100 mg/kg) liver sections showed remarkable improvements of all MTX-induced histological changes (Figure 3).

3.2.2. Heart. Cardiac tissue microscopic slices from the negative control group showed normal histological appearance of cardiomyocytes with normal cigar-shaped nuclei. Conversely, we observed massive degenerative changes, cardiomyocyte necrosis, severe congestion, intermuscular edema, and intermuscular hemorrhage in mice that received MTX alone. In group III (MTX + diosmin 50 mg/kg), we detected mild-to-moderate intermuscular hemorrhage and edema, while group IV (MTX + diosmin 100 mg/kg) cardiac muscles showed minimal intermuscular edema with restoration of the normal cardiac tissue architecture (Figure 4).

3.2.3. Kidney. Microscopic examination of H&E-stained renal tissue slices from the negative control group showed normal histological appearance with tubular arrangement of epithelial cells. On the contrary, tissue samples from the kidneys of group II mice (MTX) showed intensive degenerative changes and swelling of epithelial cells of the proximal tubules. Minimal areas of necrosis with pyknotic and karryorrhetic nuclei, as well as focal areas of severe vacuolar degeneration of proximal convoluted tubules, were also observed. In group III (MTX + diosmin 50 mg/kg), we observed a moderate-to-severe swelling of tubular epithelial cells along with areas of mild vacuolar degeneration, while group IV (MTX + diosmin 100 mg/kg) microscopic renal slices showed an improvement in tubular structure and minimal cellular swelling, compared to those of the MTX group (Figure 5).

Quantitative analysis showed that in comparison to the control group, MTX administration caused significantly higher tissue lesion scores ($p < 0.01$) in all examined organs. Interestingly, treatment with diosmin (both doses) caused a significant decrease in all tissue lesion scores, when compared to the MTX group (Table 3).

4. Discussion

This study highlights—for the first time—the protective role of diosmin against MTX-induced injuries to mouse hepatic, renal, and cardiac tissues. In experimental mice, diosmin was able to significantly reduce the biochemical and histological alterations, induced by MTX. These findings are mostly mediated via its antioxidant, anti-inflammatory, and antiapoptotic effects as shown by the decrease in oxidative and nitrative stress markers (MDA and NO), enhanced antioxidant defense mechanisms (GSH, SOD, and CAT), reduced serum levels of inflammatory cytokines (IL-1β, IL-6, and TNF-α), and the reduction in necrosis and vacuolar degeneration on histopathological examination after diosmin treatment.

The cytotoxic effects of MTX on the liver and kidneys were investigated in previous reports. Chladek et al. showed that MTX is metabolized in the liver by an enzymatic system [36]. The increased level of its cellular metabolites could induce oxidative and inflammatory tissue damages [37], which could be demonstrated in the form of histopathological changes [38] and elevation of serum liver enzymes [39]. Moreover, MTX metabolites were found to precipitate in renal tubules, causing marked nephrotoxicity in rats [40, 41].

Methotrexate can induce oxidative stress through inhibition of NADP synthesis, which is used by GR to maintain the reduced state of GSH. It can also induce nitrative stress by increasing the levels of TNF-α and IL-1β, which increase

Table 2: Ameliorative effects of diosmin on tissue concentrations of lipid peroxidation and antioxidant markers in mice exposed to methotrexate.

Group	MDA (nmol/g)	NO (μmol/g)	GSH (mg/g)	GST (U/g)	GR (U/g)	GPx (U/g)	SOD (U/g)	CAT (U/g)
I. Hepatic tissue concentrations								
Control	28.9 ± 1.8	53.3 ± 2.9	0.41 ± 0.02	49.13 ± 1.62	43.95 ± 1.45	37.78 ± 1.64	116.4 ± 3.99	41.39 ± 3.16
MTX	$84.1 \pm 3.07^{*}$	$104.8 \pm 2.9^{*}$	$0.16 \pm 0.02^{*}$	$19.84 \pm 1.74^{*}$	$17.98 \pm 0.93^{*}$	$15.92 \pm 1.75^{*}$	$42.2 \pm 1.28^{*}$	$19.9 \pm 2.24^{*}$
MTX-DM50	$66.2 \pm 4.5^{*\#}$	$83.3 \pm 2.5^{*\#}$	$0.23 \pm 0.02^{*}$	$32.26 \pm 2.08^{*\#}$	$28.32 \pm 1.99^{*\#}$	$24.38 \pm 1.94^{*\#}$	$84.8 \pm 3.59^{*\#}$	30.07 ± 2.52
MTX-DM100	$35.2 \pm 2.5^{\#}$	$58.2 \pm 3.6^{\#}$	$0.33 \pm 0.02^{\#}$	$43.01 \pm 1.28^{\#}$	$37.45 \pm 1.31^{*\#}$	$28.70 \pm 3.92^{*\#}$	$106.04 \pm 4.25^{\#}$	$39.33 \pm 2.37^{\#}$
II. Cardiac tissue concentrations								
Control	49.47 ± 2.7	57.1 ± 2.2	26.8 ± 1.0	33.58 ± 1.78	5.76 ± 0.34	16.69 ± 0.96	57.32 ± 2.3	3.1 ± 0.14
MTX	$138.7 \pm 5.2^{*}$	$158.7 \pm 5.5^{*}$	$12.35 \pm 0.6^{*}$	$16.65 \pm 0.57^{*}$	$2.45 \pm 0.13^{*}$	$7.20 \pm 0.29^{*}$	$29.58 \pm 1.1^{*}$	$0.73 \pm 0.05^{*}$
MTX-DM50	$89.6 \pm 3.4^{*\#}$	$97.5 \pm 3.4^{*\#}$	$16.44 \pm 1.2^{*}$	$24.42 \pm 0.92^{*\#}$	$3.67 \pm 0.18^{*\#}$	$10.62 \pm 0.62^{*\#}$	$44.29 \pm 2.4^{*\#}$	$1.3 \pm 0.08^{*\#}$
MTX-DM100	$56.3 \pm 3.4^{\#}$	$62.2 \pm 3.4^{\#}$	$24.3 \pm 1.2^{\#}$	$32.19 \pm 1.13^{\#}$	$5.59 \pm 0.28^{\#}$	$15.48 \pm 0.18^{\#}$	$53 \pm 2.4^{\#}$	$2.7 \pm 0.2^{\#}$
III. Renal tissue concentrations								
Control	36.8 ± 2.42	43.8 ± 1.47	9.04 ± 0.12	9.39 ± 0.34	13.06 ± 0.48	6.16 ± 0.14	57.2 ± 1.24	4.3 ± 0.27
MTX	$77.3 \pm 5.02^{*}$	$87.6 \pm 3.6^{*}$	$4.52 \pm 0.30^{*}$	$5.23 \pm 0.27^{*}$	$6.51 \pm 0.40^{*}$	$2.96 \pm 0.19^{*}$	$27.55 \pm 1.9^{*}$	$2.05 \pm 0.31^{*}$
MTX-DM50	$49.5 \pm 3.13^{\#}$	$63.6 \pm 2.45^{*\#}$	$6.04 \pm 0.43^{*\#}$	$7.24 \pm 0.20^{*\#}$	$9.30 \pm 0.28^{*\#}$	$4.76 \pm 0.16^{*\#}$	$43.9 \pm 3.9^{*\#}$	$3.46 \pm 0.27^{\#}$
MTX-DM100	$39.2 \pm 2.2^{\#}$	$45.9 \pm 1.04^{\#}$	$8.25 \pm 0.18^{\#}$	$9.26 \pm 0.26^{\#}$	$12.08 \pm 0.33^{\#}$	$6.02 \pm 0.15^{\#}$	$53.5 \pm 2.6^{\#}$	$4.09 \pm 0.28^{\#}$

Values are means ± SEM. *Significant change at $p < 0.01$ with respect to the negative control group. $^{\#}$Significant change at $p < 0.01$ with respect to the MTX group as the positive control group. CAT: catalase; MDA: malondialdehyde; NO: nitric oxide; GPx: glutathione peroxidase; GR: glutathione reductase; GSH: glutathione; GST: glutathione S-transferase; SOD: superoxide dismutase.

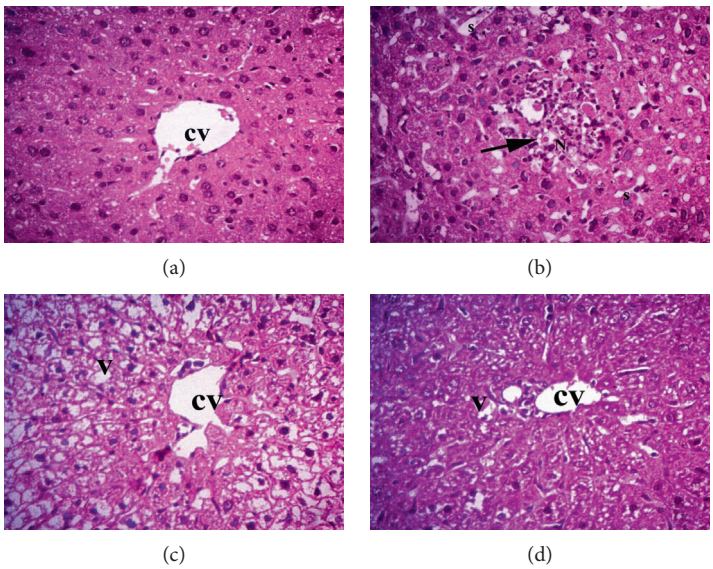

Figure 3: Histopathologic examination of liver tissue by H&E at ×400. CV: central vein; V: vacuolar degeneration; S: sinusoids. The arrow indicates necrosis and lymphocytic infiltrations. Groups are (a) normal liver tissue in the negative control group, (b) MTX group, (c) MTX + diosmin 50 mg/kg group, and (d) MTX + diosmin 100 mg/kg group.

the expression of inducible nitric oxide synthase (iNOS) and the production of NO and cyclic guanosine monophosphate (cGMP) [42]. Moreover, TNF-α can directly induce cytotoxicity to hepatocytes and glomerular and epithelial cells of the proximal convoluted tubules [43, 44]. In addition, IL-1β stimulates the synthesis of prostaglandin E2 in renal mesangial cells, changing the glomerular hemodynamics [45], while IL-6 increases the expression of fibronectin, causing thickening of the glomerular basement membrane [46].

Our study showed that diosmin mitigated MTX-induced oxidative and nitrative stresses by increasing GSH levels, lowering NO levels, and enhancing the activity of antioxidant enzymes. Tahir et al. showed that diosmin could alleviate ethanol-induced liver injury by reducing the activation of nuclear factor kappa B (NF-κB) and inhibiting the expression

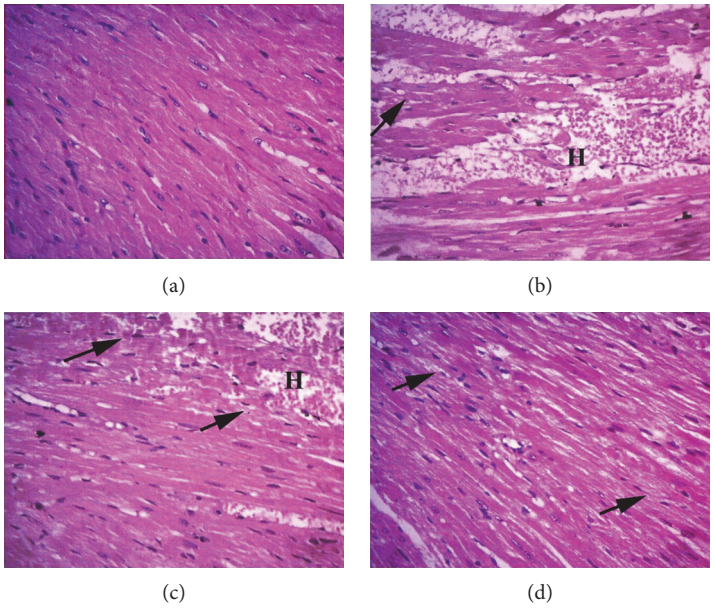

Figure 4: Histopathologic examination findings of cardiac tissue sections by H&E at ×400. Arrows point to myocardiocyte degeneration. H: hemorrhage. Groups are (a) control group showing normal myocardium, (b) MTX group, (c) MTX + diosmin 50 mg/kg group, and (d) MTX + diosmin 100 mg/kg group.

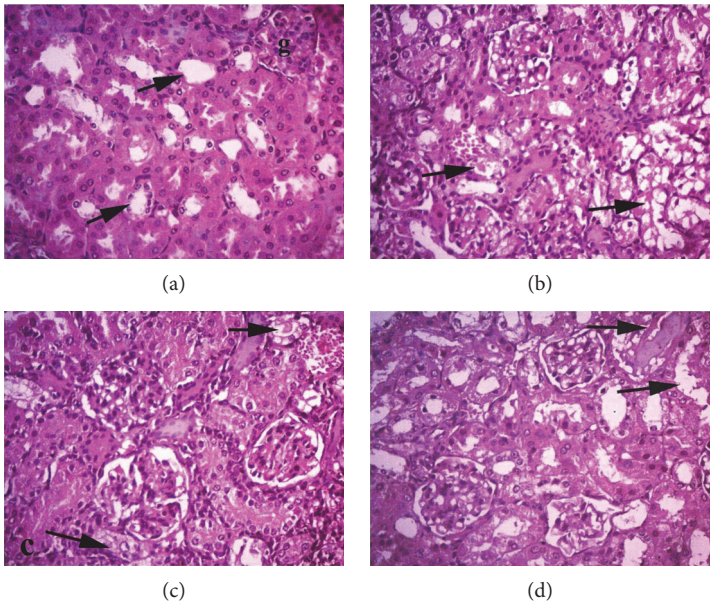

Figure 5: Histopathologic examination findings of kidney tissue by H&E at ×400. Arrows point to renal tubules. Groups are (a) control group showing normal renal tubules, (b) MTX group showing severe vacuolation, (c) MTX + diosmin 50 mg/kg group showing moderate degeneration, and (d) MTX + diosmin 100 mg/kg showing mild degeneration.

Table 3: Organ lesion scores in control and different experimental groups.

Lesion	Experimental groups			
	Control	MTX	MTX-DM50	MTX-DM100
Hepatic lesions	0.00	$3.00 \pm 0.00^{*}$	$1.80 \pm 0.13^{*\#}$	$1.20 \pm 0.13^{*\#}$
Renal lesions	0.00	$3.00 \pm 0.00^{*}$	$2.30 \pm 0.15^{*\#}$	$1.90 \pm 0.31^{*\#}$
Cardiac lesions	0.00	$3.00 \pm 0.00^{*}$	$2.00 \pm 0.21^{*\#}$	$1.40 \pm 0.16^{*\#}$

Data are expressed as means ± SEM. *Significant change at $p < 0.01$ with respect to the negative control group. #Significant change at $p < 0.01$ with respect to the MTX group as the positive control group.

of TNF-α, iNOS, and cyclooxygenase-II [13]. Rehman et al. used kidney injury molecule-1 (KIM-1), a highly sensitive biomarker for renal injury, to evaluate the protective role of diosmin against trichloroethylene (TCE) nephrotoxicity [47]. In agreement with other studies [48, 49], they reported that TCE administration increased the levels of renal KIM-1, while adding diosmin to TCE could effectively reduce these elevations.

To our knowledge, there is no study about the histological effects of MTX on the cardiac tissue. However, our data showed that MTX induces marked cardiac tissue damage in mice as indicated by the previously mentioned histopathological changes and elevation of plasma levels of cardiac enzymes (CK and CK-MB). These biochemical and histological changes were significantly reduced after diosmin treatment. In the same vein, previous reports showed the ability of diosmin to protect against isopropanol-induced myocardial infarction (at a daily dose of 5 to 10 mg/kg bw) and ischemia-/reperfusion-related cardiac dysfunction (at a daily dose of 50 to 100 mg/kg bw), as evidenced by restoration of normal echocardiographic patterns and reduction in plasma levels of cardiac troponins [17, 18]. Diosmin can offer additional cardioprotection through its antihyperlipidemic (via inhibition of hepatic HMG CoA reductase), antihyperglycemic [14], and antihypertensive effects [50].

Histopathological analysis showed that MTX administration induced an acute inflammatory reaction, marked by vascular congestion, tissue edema, and infiltration by leukocytes. This reaction was explained in earlier studies by the ability of MTX to induce oxidative and nitrative stresses, as well as activation of nuclear factor-κB (NF-κB) and p38 pathways [19, 51]. Several degenerative changes were also noted, such as pyknotic and karryorrhetic nuclei, cellular vacuolization (reflecting dilatation of the smooth endoplasmic reticulum), and disturbance of tissue architecture.

The observed reduction in cellular necrosis and vacuolar degeneration following diosmin treatment may be related to (a) reduction in DNA damage indirectly through alleviation of MTX-induced oxidative stress and inflammation and (b) the possible antiapoptotic role of diosmin, demonstrated in previous experimental studies. For example, Liu et al. reported that diosmin protected against cerebral ischemia/reperfusion injury in mice through activation of the JAK2/STAT3 signaling pathway, a key regulator of cellular proliferation [52]. Moreover, Rehman et al. showed that diosmin offered nephroprotection in TCE-intoxicated mice by reducing the expression of Bax, p53, caspase-3, caspase-7, and caspase-9 [47].

Interestingly, several animal studies showed an antimutagenic effect of diosmin against esophageal [53], hepatic [54], colon [55], and buccal pouch tumors [56]. Rajasekar et al. concluded that diosmin (at a daily dose of 100 mg/kg bw) suppressed cellular proliferation and tumor progression in 7,12-dimethylbenz(a)anthracene- (DMBA-) induced hamster buccal pouch carcinoma through inhibition of the IL-6/STAT3 signaling pathway [56]. Additionally, Tahir et al. and Tanaka et al. attributed the antimutagenic effect of diosmin to inhibition of cellular proliferation and downregulation of inflammatory markers [54, 55]. Therefore, adding diosmin to MTX does not only protect against its cytotoxicity but may also provide synergistic antimutagenic effects.

Based on our results, as well as those of previous reports, diosmin can exert its antioxidant effect directly (by free radical scavenging [57]) and indirectly (by upregulating cellular antioxidant enzymes, such as GR, GPx, CAT, and SOD). Earlier investigations have shown that several antioxidants, such as N-acetylcysteine [58, 59], carvacrol [60, 61], curcumin [38, 62], and silymarin [63], can protect against MTX-induced hepatic and renal injury in animal models. Future studies should directly compare diosmin to these antioxidants to determine the optimal chemoprotective agent in this regard and whether diosmin has additional cytoprotective effects against MTX.

An earlier report by Iqbal and colleagues showed that MTX-induced nephrotoxicity can be ameliorated by folinic acid administration [64]; therefore, the effects of adding folinic acid as a supplement to diosmin should be investigated. Future studies should also test the protective role of diosmin against other chemotherapeutic agents. The antimutagenic and the cytoprotective effects of diosmin against chemotherapeutic drugs have been studied separately; therefore, further research should investigate the effects of diosmin on animal models with malignant tumors, receiving chemotherapeutic agents.

5. Conclusion

In experimental mice, diosmin significantly reduced the biochemical as well as the histological alterations, induced by MTX due to its antioxidant and anti-inflammatory activities. Therefore, diosmin may be a promising agent for protection against MTX-induced cytotoxicity in patients with cancer and autoimmune diseases. Future studies should investigate the effects of diosmin on animal models with malignant tumors and its potential for cytoprotection against other chemotherapeutic agents.

Abbreviations

ALP: Alkaline phosphatase
ALT: Alanine transferase
AST: Aspartate transferase
CK: Creatine kinase
CK-MB: Creatine kinase-myocardial B fraction
IL: Interleukin
LDH: Lactate dehydrogenase
MTX: Methotrexate
TNF: Tumor necrosis factor.

Conflicts of Interest

None was declared.

Acknowledgments

The authors would like to thank Professor Amina A. Dessouki, the professor of pathology, Faculty of Veterinary Medicine, Suez Canal University, for her help in the

histopathological evaluations of this study. The authors would like to appreciate the Deanship of Scientific Research at King Saud University for funding this study through the research group project (no. RG-198).

References

[1] J. Jolivet, K. H. Cowan, G. A. Curt, N. J. Clendeninn, and B. A. Chabner, "The pharmacology and clinical use of methotrexate," *New England Journal of Medicine*, vol. 309, no. 18, pp. 1094–1104, 1983.

[2] J. A. M. Wessels, T. W. J. Huizinga, and H.-J. Guchelaar, "Recent insights in the pharmacological actions of methotrexate in the treatment of rheumatoid arthritis," *Rheumatology*, vol. 47, no. 3, pp. 249–255, 2008.

[3] E. M. Hersh, V. G. Wong, E. S. Henderson, and E. J. Freireich, "Hepatotoxic effects of methotrexate," *Cancer*, vol. 19, no. 4, pp. 600–606, 1966.

[4] P. E. Kintzel, "Anticancer drug—induced kidney disorders," *Drug Safety*, vol. 24, no. 1, pp. 19–38, 2001.

[5] H. Tobias and R. Auerbach, "Hepatotoxicity of long-term methotrexate therapy for psoriasis," *Archives of Internal Medicine*, vol. 132, no. 3, pp. 391–396, 1973.

[6] A. Perez-Verdia, F. Angulo, F. L. Hardwicke, and K. M. Nugent, "Acute cardiac toxicity associated with high-dose intravenous methotrexate therapy: case report and review of the literature," *Pharmacotherapy: The Journal of Human Pharmacology and Drug Therapy*, vol. 25, no. 9, pp. 1271–1276, 2005.

[7] M. G. Neuman, R. G. Cameron, J. A. Haber, G. G. Katz, I. M. Malkiewicz, and N. H. Shear, "Inducers of cytochrome P450 2E1 enhance methotrexate-induced hepatocytotoxicity," *Clinical Biochemistry*, vol. 32, no. 7, pp. 519–536, 1999.

[8] B. A. Kamen, P. A. Nylen, B. M. Camitta, and J. R. Bertino, "Methotrexate accumulation and folate depletion in cells as a possible mechanism of chronic toxicity to the drug," *British Journal of Haematology*, vol. 49, no. 3, pp. 355–360, 1981.

[9] W. H. Vogel, R. Snyder, and M. P. Schulman, "The inhibition of dehydrogenases by folic acid and several of its analogs," *Biochemical and Biophysical Research Communications*, vol. 10, pp. 97–101, 1963.

[10] K. Kurosawa, H. Shibata, N. Hayashi, N. Sato, T. Kamada, and K. Tagawa, "Kinetics of hydroperoxide degradation by NADP-glutathione system in mitochondria," *The Journal of Biochemistry*, vol. 108, no. 1, pp. 9–16, 1990.

[11] J. W. Williams, J. F. Morrison, and R. G. Duggleby, "Methotrexate, a high-affinity pseudosubstrate of dihydrofolate reductase," *Biochemistry*, vol. 18, no. 12, pp. 2567–2573, 1979.

[12] M. Szymański, D. Młynarek, A. Szymański, and I. Matławska, "Simultaneous determination of diosmin and hesperidin in pharmaceuticals by RPLC using ionic liquids as mobile phase modifiers," *Iranian Journal of Pharmaceutical Research: IJPR*, vol. 15, no. 1, p. 141, 2016.

[13] M. Tahir, M. U. Rehman, A. Lateef et al., "Diosmin protects against ethanol-induced hepatic injury via alleviation of inflammation and regulation of TNF-α and NF-κB activation," *Alcohol*, vol. 47, no. 2, pp. 131–139, 2013.

[14] S. Srinivasan and L. Pari, "Ameliorative effect of diosmin, a citrus flavonoid against streptozotocin-nicotinamide generated oxidative stress induced diabetic rats," *Chemico-Biological Interactions*, vol. 195, no. 1, pp. 43–51, 2012.

[15] T. Tanaka, H. Makita, M. Ohnishi et al., "Chemoprevention of 4-nitroquinoline 1-oxide-induced oral carcinogenesis in rats by flavonoids diosmin and hesperidin, each alone and in combination," *Cancer Research*, vol. 57, no. 2, pp. 246–252, 1997.

[16] S. Ahmed, N. Mundhe, M. Borgohain et al., "Diosmin modulates the NF-kB signal transduction pathways and downregulation of various oxidative stress markers in alloxan-induced diabetic nephropathy," *Inflammation*, vol. 39, no. 5, pp. 1783–1797, 2016.

[17] O. Senthamizhselvan, J. Manivannan, T. Silambarasan, and B. Raja, "Diosmin pretreatment improves cardiac function and suppresses oxidative stress in rat heart after ischemia/reperfusion," *European Journal of Pharmacology*, vol. 736, pp. 131–137, 2014.

[18] S. S. Queenthy and B. John, "Diosmin exhibits antihyperlipidemic effects in isoproterenol induced myocardial infarcted rats," *European Journal of Pharmacology*, vol. 718, no. 1–3, pp. 213–218, 2013.

[19] S. Mukherjee, S. Ghosh, S. Choudhury et al., "Pomegranate reverses methotrexate-induced oxidative stress and apoptosis in hepatocytes by modulating Nrf2-NF-κB pathways," *The Journal of Nutritional Biochemistry*, vol. 24, no. 12, pp. 2040–2050, 2013.

[20] F. Imam, N. O. Al-Harbi, M. M. Al-Harbi et al., "Diosmin downregulates the expression of T cell receptors, proinflammatory cytokines and NF-κB activation against LPS-induced acute lung injury in mice," *Pharmacological Research*, vol. 102, pp. 1–11, 2015.

[21] S. Reitman and S. Frankel, "A colorimetric method for the determination of serum glutamic oxalacetic and glutamic pyruvic transaminases," *American Journal of Clinical Pathology*, vol. 28, no. 1, pp. 56–63, 1957.

[22] P. R. N. Kind and E. J. King, "Estimation of plasma phosphatase by determination of hydrolysed phenol with amino-antipyrine," *Journal of Clinical Pathology*, vol. 7, no. 4, p. 322, 1954.

[23] K. Larsen, "Creatinine assay in the presence of protein with LKB 8600 reaction rate analyser," *Clinica Chimica Acta*, vol. 38, no. 2, pp. 475-476, 1972.

[24] J. J. Coulombe and L. Favreau, "A new simple semimicro method for colorimetric determination of urea," *Clinical Chemistry*, vol. 9, pp. 102–108, 1963.

[25] G. Szasz, J. Waldenström, and W. Gruber, "Creatine kinase in serum: 6. Inhibition by endogenous polyvalent cations, and effect of chelators on the activity and stability of some assay components," *Clinical Chemistry*, vol. 25, no. 3, pp. 446–452, 1979.

[26] U. Würzburg, N. Hennrich, H. Lang, W. Prellwitz, D. Neumeier, and M. Knedel, "Determination of creatine kinase-MB in serum using inhibiting antibodies (author's transl)," *Klinische Wochenschrift*, vol. 54, no. 8, pp. 357–360, 1976.

[27] S. R. Babson and A. L. Babson, "An improved amylase assay using dyed amylopectin," *Clinica Chimica Acta*, vol. 44, no. 2, pp. 193–197, 1973.

[28] M. Uchiyama and M. Mihara, "Determination of malonaldehyde precursor in tissues by thiobarbituric acid test," *Analytical Biochemistry*, vol. 86, no. 1, pp. 271–278, 1978.

[29] L. C. Green, D. A. Wagner, J. Glogowski, P. L. Skipper, J. S. Wishnok, and S. R. Tannenbaum, "Analysis of nitrate, nitrite,

and [^{15}N] nitrate in biological fluids," *Analytical Biochemistry*, vol. 126, no. 1, pp. 131–138, 1982.

[30] E. Beutler, O. Duron, and B. M. Kelly, "Improved method for the determination of blood glutathione," *The Journal of Laboratory and Clinical Medicine*, vol. 61, pp. 882–888, 1963.

[31] M. Nishikimi, N. A. Rao, and K. Yagi, "The occurrence of superoxide anion in the reaction of reduced phenazine methosulfate and molecular oxygen," *Biochemical and Biophysical Research Communications*, vol. 46, no. 2, pp. 849–854, 1972.

[32] H. Aebi, "Catalase in vitro," *Methods in Enzymology*, vol. 105, pp. 121–126, 1984.

[33] W. H. Habig, M. J. Pabst, and W. B. Jakoby, "Glutathione S-transferases the first enzymatic step in mercapturic acid formation," *Journal of Biological Chemistry*, vol. 249, no. 22, pp. 7130–7139, 1974.

[34] G. Zanetti, "Rabbit liver glutathione reductase. Purification and properties," *Archives of Biochemistry and Biophysics*, vol. 198, no. 1, pp. 241–246, 1979.

[35] D. E. Paglia and W. N. Valentine, "Studies on the quantitative and qualitative characterization of erythrocyte glutathione peroxidase," *The Journal of Laboratory and Clinical Medicine*, vol. 70, no. 1, pp. 158–169, 1967.

[36] J. Chladek, J. Martinkova, and L. Sispera, "An in vitro study on methotrexate hydroxylation in rat and human liver," *Physiological Research*, vol. 46, no. 5, pp. 371–379, 1997.

[37] T. Çakır, A. Baştürk, C. Polat et al., "Does alfa lipoic acid prevent liver from methotrexate induced oxidative injury in rats?" *Acta Cirurgica Brasileira*, vol. 30, no. 4, pp. 247–252, 2015.

[38] R. A. Hemeida and O. M. Mohafez, "Curcumin attenuates methotraxate-induced hepatic oxidative damage in rats," *Journal of the Egyptian National Cancer Institute*, vol. 20, no. 2, pp. 141–148, 2008.

[39] A. Aslaner, T. Çakır, B. Çelik et al., "The protective effect of intraperitoneal medical ozone preconditioning and treatment on hepatotoxicity induced by methotrexate," *International Journal of Clinical and Experimental Medicine*, vol. 8, no. 8, pp. 13303–13309, 2015.

[40] H. B. Ulusoy, İ. Öztürk, and M. F. Sönmez, "Protective effect of propolis on methotrexate-induced kidney injury in the rat," *Renal Failure*, vol. 38, no. 5, pp. 744–750, 2016.

[41] Y. Yuksel, R. Yuksel, M. Yagmurca et al., "Effects of quercetin on methotrexate-induced nephrotoxicity in rats," *Human & Experimental Toxicology*, vol. 36, pp. 51–61, 2017.

[42] A. K. Kiemer, T. Hartung, and A. M. Vollmar, "cGMP-mediated inhibition of TNF-α production by the atrial natriuretic peptide in murine macrophages," *The Journal of Immunology*, vol. 165, no. 1, pp. 175–181, 2000.

[43] J. J. Navarro, F. F. Milena, C. Mora et al., "Tumor necrosis factor-α gene expression in diabetic nephropathy: relationship with urinary albumin excretion and effect of angiotensin-converting enzyme inhibition," *Kidney International*, vol. 68, pp. S98–S102, 2005.

[44] M. Jo, T.-H. Kim, D.-W. Seol et al., "Apoptosis induced in normal human hepatocytes by tumor necrosis factor-related apoptosis-inducing ligand," *Nature Medicine*, vol. 6, no. 5, pp. 564–567, 2000.

[45] M. B. Duran-Salgado and A. F. Rubio-Guerra, "Diabetic nephropathy and inflammation," *World Journal of Diabetes*, vol. 5, no. 3, pp. 393–398, 2014.

[46] J. F. Navarro-González and C. Mora-Fernández, "The role of inflammatory cytokines in diabetic nephropathy," *Journal of the American Society of Nephrology*, vol. 19, no. 3, pp. 433–442, 2008.

[47] M. U. Rehman, M. Tahir, A. Q. Khan et al., "Diosmin protects against trichloroethylene-induced renal injury in Wistar rats: plausible role of p53, Bax and caspases," *British Journal of Nutrition*, vol. 110, no. 4, pp. 699–710, 2013.

[48] Y. Zhou, V. S. Vaidya, R. P. Brown et al., "Comparison of kidney injury molecule-1 and other nephrotoxicity biomarkers in urine and kidney following acute exposure to gentamicin, mercury, and chromium," *Toxicological Sciences*, vol. 101, no. 1, pp. 159–170, 2008.

[49] S. T. Ahmad, W. Arjumand, A. Seth et al., "Preclinical renal cancer chemopreventive efficacy of geraniol by modulation of multiple molecular pathways," *Toxicology*, vol. 290, no. 1, pp. 69–81, 2011.

[50] T. Silambarasan and B. Raja, "Diosmin, a bioflavonoid reverses alterations in blood pressure, nitric oxide, lipid peroxides and antioxidant status in DOCA-salt induced hypertensive rats," *European Journal of Pharmacology*, vol. 679, no. 1–3, pp. 81–89, 2012.

[51] Y.-J. Kim, M. Song, and J.-C. Ryu, "Inflammation in methotrexate-induced pulmonary toxicity occurs via the p38 MAPK pathway," *Toxicology*, vol. 256, no. 3, pp. 183–190, 2009.

[52] X. Liu, X. Zhang, J. Zhang et al., "Diosmin protects against cerebral ischemia/reperfusion injury through activating JAK2/STAT3 signal pathway in mice," *Neuroscience*, vol. 268, pp. 318–327, 2014.

[53] T. Tanaka, H. Makita, K. Kawabata et al., "Modulation of N-methyl-N-amylnitrosamine-induced rat oesophageal tumourigenesis by dietary feeding of diosmin and hesperidin, both alone and in combination," *Carcinogenesis*, vol. 18, no. 4, pp. 761–769, 1997.

[54] M. Tahir, M. U. Rehman, A. Lateef et al., "Diosmin abrogates chemically induced hepatocarcinogenesis via alleviation of oxidative stress, hyperproliferative and inflammatory markers in murine model," *Toxicology Letters*, vol. 220, no. 3, pp. 205–218, 2013.

[55] T. Tanaka, H. Makita, K. Kawabata et al., "Chemoprevention of azoxymethane-induced rat colon carcinogenesis by the naturally occurring flavonoids, diosmin and hesperidin," *Carcinogenesis*, vol. 18, no. 5, pp. 957–965, 1997.

[56] M. Rajasekar, K. Suresh, and K. Sivakumar, "Diosmin induce apoptosis through modulation of STAT-3 signaling in 7,12 dimethylbenz(a)anthracene induced harmster buccal pouch carcinogenesis," *Biomedicine & Pharmacotherapy*, vol. 83, pp. 1064–1070, 2016.

[57] H. H. Arab, S. A. Salama, H. A. Omar, E. S. Arafa, and I. A. Maghrabi, "Diosmin protects against ethanol-induced gastric injury in rats: novel anti-ulcer actions," *PloS One*, vol. 10, no. 3, article e0122417, 2015.

[58] A. Cetinkaya, E. Bulbuloglu, E. B. Kurutas, and B. Kantarceken, "N-acetylcysteine ameliorates methotrexate-induced oxidative liver damage in rats," *Medical Science Monitor*, vol. 12, no. 8, pp. BR274–BR278, 2006.

[59] Y. Cağlar, H. Özgür, I. Matur et al., "Ultrastructural evaluation of the effect of N-acetylcysteine on methotrexate nephrotoxicity in rats," *Histology and Histopathology*, vol. 28, no. 7, pp. 865–874, 2013.

[60] M. Bozkurt, M. N. Bodakci, G. Turkcu et al., "Protective effects of carvacrol against methotrexate-induced liver toxicity in rats," *Acta Chirurgica Belgica*, vol. 114, no. 6, pp. 404–409, 2014.

[61] M. Bozkurt, S. Em, P. Oktayoglu et al., "Carvacrol prevents methotrexate-induced renal oxidative injury and renal damage in rats," *Clinical & Investigative Medicine*, vol. 37, pp. 19–25, 2014.

[62] M. A. Morsy, S. A. Ibrahim, E. F. Amin, M. Y. Kamel, R. A. Rifaai, and M. K. Hassan, "Curcumin ameliorates methotrexate-induced nephrotoxicity in rats," *Advances in Pharmacological Sciences*, vol. 2013, Article ID 387071, 7 pages, 2013.

[63] D. O. Dabak and N. Kocaman, "Effects of silymarin on methotrexate-induced nephrotoxicity in rats," *Renal Failure*, vol. 37, no. 4, pp. 734–739, 2015.

[64] M. Perwaiz Iqbal, F. Sultana, N. Mehboobali, and S. Pervez, "Folinic acid protects against suppression of growth by methotrexate in mice," *Biopharmaceutics & Drug Disposition*, vol. 22, no. 4, pp. 169–178, 2001.

Hindawi
Oxidative Medicine and Cellular Longevity
Volume 2017, Article ID 5032102, 16 pages
https://doi.org/10.1155/2017/5032102

Review Article

Effects of Antioxidant Supplements on the Survival and Differentiation of Stem Cells

Sara Shaban,[1] Mostafa Wanees Ahmed El-Husseny,[1,2] Abdelrahman Ibrahim Abushouk,[2,3,4] Amr Muhammad Abdo Salem,[2,3] Mediana Mamdouh,[1] and Mohamed M. Abdel-Daim[5,6]

[1]*Faculty of Medicine, Fayoum University, Cairo, Egypt*
[2]*NovaMed Medical Research Association, Cairo, Egypt*
[3]*Faculty of Medicine, Ain Shams University, Cairo, Egypt*
[4]*Medical Research Group of Egypt, Cairo, Egypt*
[5]*Pharmacology Department, Faculty of Veterinary Medicine, Suez Canal University, Ismailia 41522, Egypt*
[6]*Department of Ophthalmology and Micro-Technology, Yokohama City University, Yokohama, Japan*

Correspondence should be addressed to Mohamed M. Abdel-Daim; abdeldaim.m@vet.suez.edu.eg

Received 25 February 2017; Accepted 31 May 2017; Published 9 July 2017

Academic Editor: Andreas Daiber

Copyright © 2017 Sara Shaban et al. This is an open access article distributed under the Creative Commons Attribution License, which permits unrestricted use, distribution, and reproduction in any medium, provided the original work is properly cited.

Although physiological levels of reactive oxygen species (ROS) are required to maintain the self-renewal capacity of stem cells, elevated ROS levels can induce chromosomal aberrations, mitochondrial DNA damage, and defective stem cell differentiation. Over the past decade, several studies have shown that antioxidants can not only mitigate oxidative stress and improve stem cell survival but also affect the potency and differentiation of these cells. Further beneficial effects of antioxidants include increasing genomic stability, improving the adhesion of stem cells to culture media, and enabling researchers to manipulate stem cell proliferation by using different doses of antioxidants. These findings can have several clinical implications, such as improving neurogenesis in patients with stroke and neurodegenerative diseases, as well as improving the regeneration of infarcted myocardial tissue and the banking of spermatogonial stem cells. This article reviews the cellular and molecular effects of antioxidant supplementation to cultured or transplanted stem cells and draws up recommendations for further research in this area.

1. Introduction

Stem cells are undifferentiated cells, characterized by self-renewal and the ability to differentiate into several cell types (potency) [1]. They can be totipotent (differentiating into embryonic and extraembryonic cell types), pluripotent (differentiating into cells of the three germ layers), or multipotent (differentiating into cells of a closely related family) [2]. Stem cell research runs with an incredible speed and its applications are under investigation in different medical fields [3, 4]. There are two main types of stem cells: embryonic stem cells (ESCs) (present in the inner cell mass of the blastocyst) and adult stem cells (present in different mature tissues to replace dead cells) [5, 6].

Induced pluripotent stem cells (iPSCs) are adult cells, genetically reprogrammed to express genes and factors, required for maintaining the properties of ESCs. However, the reprogramming process itself results in oxidative stress by generating high levels of reactive oxygen species (ROS) [7, 8], which cause damage to DNA, RNA, and cell proteins and may induce apoptosis [9–11]. However, ROS are required in physiological levels to maintain the self-renewal capacity of stem cells and to fight invading microbes [11–14].

Antioxidants are biochemical supplements that protect cellular constituents from oxidative stress by neutralizing free radicals and terminating the oxidative reaction chain in the mitochondrial membrane [15]. They can be classified into enzymatic and nonenzymatic, endogenous and

exogenous [16], and water-soluble (reacting with oxidants in the cytosol or plasma) and lipid-soluble antioxidants (preventing lipid peroxidation of cell membranes) [17].

Over the past decade, several studies have shown that antioxidants can not only mitigate oxidative stress and improve stem cell survival but also affect the potency and differentiation of these cells. In our article, we reviewed the results of preclinical studies that investigated the effects of antioxidants on cultured or transplanted stem cells in an attempt to draw up recommendations for further research in this area.

2. Induced Pluripotent Stem Cells (iPSCs)

As highlighted earlier, the reprogramming of iPSCs is associated with generation of high ROS levels. Several reports showed that, in comparison to somatic precursor cells, iPSCs exhibit the following criteria: (1) marked protection against nuclear and mitochondrial DNA (mtDNA) damage and (2) significantly lower levels of ROS due to upregulation of intrinsic antioxidant enzymes [18, 19]. Dannenmann et al. found a 10-fold decrease in ROS level and a fourfold increase of glutathione (GSH) and glutathione reductase (GR) levels in iPSCs, compared to fibroblasts [18]. In another study by the same authors, they showed that several glutathione S-transferases (GSTs), which act as antioxidant and detoxifying enzymes, were upregulated in iPSCs, compared to their somatic precursor cells [19].

Ji and colleagues reported that mitigation of oxidative stress during cellular reprogramming by antioxidant supplementation protects the genome of reprogramming cells against DNA damage and leads to iPSCs with fewer genomic aberrations [20]. In the same vein, Luo and colleagues [21] found that iPSCs grew well and "stemness" was preserved for up to two months after the addition of a low-dose antioxidant supplement. Moreover, using comparative genomic hybridization (CGH) analysis, they showed that antioxidant supplementation lowered the levels of genetic aberrations in cultured iPSCs [21].

Hämäläinen and colleagues showed that the reprogramming and self-renewal abilities of iPSCs were diminished after subtle increases in ROS levels, originating from mtDNA mutagenesis. However, the addition of two different antioxidants [N-acetyl-L-cysteine (NAC) and mitochondria-targeted ubiquinone (MitoQ)] efficiently rescued these abilities in mutator iPSCs [22]. N-acetyl-L-cysteine raises cellular GSH pool and promotes the processing of H_2O_2 in the cytosol [23], whereas MitoQ acts upstream to prevent superoxide production within the mitochondria before H_2O_2 generation [24]. Of note, Hämäläinen et al. highlighted that the therapeutic window of MitoQ for iPSCs is narrow, while high concentrations of NAC were not associated with toxic effects on iPSCs [22].

Interestingly, other reports showed no effect of antioxidant supplementation on the expression of 53BP1 and ATM proteins (two molecules involved in DNA repair pathways) [25–27]. Recently, it has been found that high-dose antioxidants downregulates DNA repair-related kinases, which conversely results in genomic instability of iPSCs [21]. Therefore, adjusting the dose of supplementary antioxidants is critical.

3. Bone Marrow-Derived Mesenchymal (BMSCs) and Hematopoietic Stem Cells (HSCs)

Several studies showed that the ex vivo expansion of ESCs and mesenchymal stem cells (MSCs) [28–31] and the in vitro expansion of HSCs [32] may cause genomic instability. Through a serial transplantation assay, Jang and colleagues showed that elevated ROS levels reduce the self-renewal ability of HSCs [33]. Therefore, decreasing O_2 concentrations to physiological levels or adding proper dosages of antioxidants can reduce in vitro, culture-stimulated aneuploidy, providing potential methods to limit genomic alterations when expanding HSCs in vitro [32, 34, 35]. Hamid et al. conducted an in vitro study to evaluate the antioxidant effects of *Hibiscus sabdariffa* L. (roselle) on bone marrow-derived HSCs. They showed that roselle supplementation increased superoxide dismutase (SOD) expression (at 125, 500, and 1000 ng/mL) and HSCs survival (at 500 and 1000 ng/mL) and protected against H_2O_2-induced DNA damage [36].

In another study by Halabian et al., treatment of BMSCs with Lipocalin-2 (Lcn2), a natural cytoprotective factor generated upon exposure to stressful conditions, increased cellular resistance against oxidative, hypoxic, and serum deprivation stresses. Moreover, Lcn2-treated cells showed SOD gene upregulation, increased proliferation, maintained pluripotency, and improved cellular adhesion to culture media upon H_2O_2 exposure, in comparison to untreated cells [37]. Similarly, Fan and colleagues studied different methods for isolation of BMSCs, aiming at reducing the number of chromosomal abnormalities in isolated cells. They reported that culturing isolated BMSCs at a low O_2 concentration (2%) or with antioxidant (NAC) supplementation increased cellular proliferation and genomic stability, in comparison to cultured cells at normoxic concentrations (20% O_2) [38].

Another study by Choi et al. demonstrated that adding ascorbic acid 2-phosphate (AAP) at different concentrations can influence the fate of BMSCs, that is, AAP significantly increased osteogenic differentiation at 50 mM concentration, while a significant induction of adipogenic differentiation with oil droplet formation was noted at concentrations of 250 mM and higher [39].

4. Cardiomyoblasts and Vascular Progenitor Cells

According to Li and colleagues, culturing cardiac stem cells with antioxidant increased the number and severity of cytogenic abnormalities. This could be explained by the excessive decrease in ROS to subphysiological levels, which may downregulate DNA repair enzymes [40]. In another study by Rodriguez-Porcel et al., modulation of the microenvironment, using antioxidants, leads to a higher rate of cardiomyoblast survival, early after transplantation to the myocardium of small animals [41]. Therefore, oxidative stress blockade may provide a favorable microenvironment for stem cells' engraftment and survival in the heart [42].

Song and colleagues reported increased ROS production during differentiation of human ESCs into vascular progenitor cells (CD34+ cells) due to increased activity of NADPH oxidase-4 (Nox4) enzyme. They found that moderate ROS scavenging, using selenium, enhanced the vascular differentiation of human ESCs, while complete ROS scavenging, using NAC, totally inhibited the vascular differentiation of these cells. This confirms that a minimal level of ROS is required for vascular stem cell differentiation to occur [43].

5. Neural Stem Cells (NSCs)

Neural stem cells are multipotent stem cells that have been suggested as a therapeutic agent to enhance the recovery of injured tissues in neuroinflammatory diseases [44]. Park and colleagues tested the effects of GV1001, a novel antioxidant agent, derived from human telomerase reverse transcriptase, on in vitro-cultured mouse NSCs. They showed that GV1001 treatment attenuated the effects of H_2O_2 exposure, reduced lipid peroxidation and mtDNA mutation, and induced the expression of survival-related proteins [45]. Hachem et al. reported that treatment of NSCs, isolated from the spinal cords of transgenic mice, with brain-derived neurotrophic factor improved cell viability by increasing the levels of GR and SOD enzymes; however, it had no effect on cellular proliferation [46].

Nitric oxide (NO) and nitric oxide synthase (NOS)-dependent signaling pathways have been implicated in different neurodegenerative diseases [47, 48]. Moreover, NO levels were linked to neural precursor cell (NPC) survival and cell fate determination [49], that is, elevated levels of NO suppress NSC proliferation and enhance differentiation of NPCs into astrocytes [50, 51]. Melatonin is a hormone synthesized in the pineal gland [52] with indirect antioxidant abilities through induction of antioxidant enzymes [53] and inhibiting NO production in glial cultures through p38 inhibition [54]. It has been shown to protect NSCs against lipopolysaccharide- (LPS-) induced inflammation [52]. Moreover, Negi et al. demonstrated that melatonin mitigates neuroinflammation and oxidative stress via upregulating nuclear factor (erythroid-derived 2) (Nrf2) [55], a transcription factor which stimulates the PI3K-Akt survival signaling pathway [56, 57] and increases the expression of the antioxidant enzyme heme oxygenase-1 (HO-1) [55].

To test the effects of in vitro antioxidant supplementation, Petro et al. divided male rats with experimentally induced thromboembolic stroke into four groups: normal rats, untreated rats with stroke, rats receiving tissue plasminogen activator (tPA) only, and rats receiving tPA + CAT/SOD (loaded on nanoparticles) at three hours post stroke. Two days later, brain tissue samples were harvested for analysis. Brain sections from the untreated group showed evidence of NSC migration through the rostral migratory stream (through detection of NSCs markers, such as nestin, GFAP, and SOX2), confirming the occurrence of neurogenesis following stroke. However, brain tissue samples from the tPA-alone group showed reduction in NSCs migration, indicating that tPA treatment suppresses neurogenesis, either directly or through reperfusion-induced ROS generation injury. Interestingly, tPA + Nano-CAT/SOD treatment restored and significantly increased NSCs migration [58].

6. Human Adipose-Derived Stem Cells (ADSCs)

Adipose-derived stem cells are multipotent stem cells that can be isolated from the human adipose tissue and are capable of in vitro expansion. Sun and colleagues reported that both hypoxia and antioxidants promoted ADSCs proliferation by raising the number of cells in the S phase, but the maximal increase in cell number was produced in the presence of antioxidants [59]. Hypoxia is believed to influence the secretion of several growth factors [60, 61], such as insulin-like growth factor and hepatocyte growth factor [62], while antioxidants increase the expression of stemness genes (CDK2, CDK4, and CDC2) and the differentiation potential of ADSCs [59]. Another study by Higuchi et al. found that lentivirus-mediated NADPH oxidase-4 (Nox-4) overexpression did not increase ROS production in insulin, dexamethasone, indomethacin, and 3-isobutyl-1-methylxanthine (IDII)-stimulated ADSCs [63]. This finding was later explained by the increased expression of endogenous antioxidants, such as SOD and CAT during adipogenesis [63, 64].

Yang et al. showed that treatment of ADSCs with fullerol (a polyhydroxylated fullerene) potentiated the expression of the transcription factor FoxO1 and its downstream genes, such as Runx2 and SOD2. Moreover, it enhanced the osteogenic activity of ADSCs, as evidenced by increased mineralization and expression of osteogenic markers (Runx2, OCN, and alkaline phosphatase) [65]. Wang and colleagues showed that pretreatment of ADSCs with NAC (3 mM) or AAP (0.2 mM) for 20 hours suppressed advanced glycosylation end product- (AGE-) induced apoptosis via a microRNA-dependent mechanism by inhibiting AGE-induced overexpression of miRNA-223: a key modulator of intracellular apoptotic signaling [66].

7. Human Periodontal Ligament Cells (hPDLCs)

In a recent study, Chung and colleagues showed that treating hPDLCs with deferoxamine (DFO), an iron chelator, results in a dose-dependent elevation in ROS levels, 24 hours after treatment [67]. The same finding was reported in rabbit cardiomyocytes [68] and normal human hepatocytes [69]. However, DFO has the ability to act on Nrf2, increasing its nuclear translocation and the expression of its target genes, including GST and glutamate cysteine ligase (GCL) [67]. Therefore, DFO has both beneficial (Nrf2-mediated antioxidant effect) and cytotoxic (increased ROS levels) effects. GSH depletion, using buthionine sulfoximine (BSO) and diethyl maleate (DEM), was shown to inhibit DFO-stimulated hPDLC differentiation into osteoblasts [67]. Moreover, GSH depletion was also reported to repress myogenic differentiation of murine skeletal muscle (C2C12) cells [70] and phorbol-12-myristate-13-acetate- (PMA-) stimulated differentiation of human myeloid cell line (HL-60) [71].

Table 1: Summary of the results of in vitro and in vivo studies on treatment of stem cells with antioxidant supplements.

Study ID	Antioxidant (dose)	Stem cell type (source)	Findings	Possible mechanisms
Ji et al. [20]	N-Acetyl-L-cysteine (NAC) and vitamin C.	Induced pluripotent stem cells (iPSCs) generated from human neonatal foreskin fibroblasts.	In cells, infected with reprogramming factors (retroviruses encoding human OCT4, SOX2, KLF4, and c-MYC), supplementation of the culture media with NAC significantly increased iPSCs survival and reduced ROS generation and the number of DNA double-stranded breaks in the reprogrammed cells.	Antioxidants significantly reduced ROS generation and the number of copy-number variations (CNVs: an indication of genomic aberrations) in treated iPSCs, compared to the untreated control group ($p < 0.02$). Treatment with NAC had no effect on transgene expression, silencing, and viral transduction efficiency.
Luo et al. [21]	Homemade antioxidant cocktail [ascorbate, glutathione, and α-tocopherol at 20 mM, 4 mM, and 1 mM, resp.].	Two human cell lines of iPSCs (201B7 and 253G1).	(i) Measurement of cellular ROS levels showed diminished ROS levels in cells, cultured with antioxidants, compared to the untreated group. (ii) Moreover, the addition of homemade antioxidant cocktail reduced the number of genomic aberrations in treated cells.	(i) The components of homemade cocktail exerted a free-radical scavenging activity to neutralize ROS in treated cells. (ii) For two months of culturing with low doses of antioxidants, iPSCs maintained the expression of stemness-related genes (Oct3/4, Nanog, SSEA-4, and ALP).
Hamid et al. [36]	Roselle (*Hibiscus sabdariffa* L.) at 125, 500, or 1000 ng/mL.	Bone marrow-derived hematopoietic stem cells (HSCs) from murine bone marrow.	(i) Adding roselle (at 500 and 1000 ng/mL) significantly increased the survival of HSCs and protected them against H_2O_2-induced DNA damage. (ii) Roselle supplementation was genoprotective, as evidenced by the nonremarkable difference on the percentage of tail DNA, compared to the control group (untreated BMSCs).	Compared to the control group, roselle enhanced the activity of SOD in HSCs (at 125, 500, and 1000 ng/mL) with a significant increase in GSH level ($p < 0.05$). However, there was no difference in ROS levels between roselle-treated and control groups.
Ikeda et al. [77]	Poly(ethylene glycol)-b-poly [4-(2,2,6,6-tetramethylpiperidine-1-oxyl)amino-methylstyrene] (PEG-b-PMNT).	Hematopoietic stem cells (HSCs) from mice fetal liver cells.	Ikeda et al. designed a biocompatible cell culture surface that can be used during ex vivo culturing and expansion of HSCs. This new surface has several advantages, compared to the currently used one including low molecular weight and antioxidant supplementation. It decreased ROS production, inhibited apoptosis, and increased the purity of separated cells.	The antioxidant culture surface (PEG-b-PMNT) scavenged nitric oxide radicals and reduced oxidative membrane damage without changing the mitochondrial membrane potential because it is not internalized within the cell as the conventional LMW systems.

Table 1: Continued.

Study ID	Antioxidant (dose)	Stem cell type (source)	Findings	Possible mechanisms
Liu et al. [32]	N-Acetyl-L-cysteine (NAC) at 0.1 to 1 μM.	LSK cells (Lin− Sca-1+ c-Kit+, a population enriched with HSCs).	(i) Aneuploidy/chromosomal instability during in vitro expansion of HSCs is ROS-mediated and can be minimized by maintaining a hypoxic condition (3% O_2) during cell culturing. (ii) Similarly, NAC administration significantly reduced the percentage of aneuploidy in HSCs, cultured under normoxic conditions, only at low dosages (0.1 μM).	(i) At optimum concentrations, NAC significantly reduced oxidative damage due to its ROS-scavenging activity. (ii) Moreover, hypoxic conditions and NAC reduced the percentage of aneuploidy in both young and old aged stem cells.
Halabian et al. [37]	Lipocalin-2 (Lcn2), a natural cytoprotective factor, generated within the cell upon exposure to stressful conditions.	Bone marrow-derived stem cells (BMSCs) from rat bone marrow (4–6 weeks old).	(i) Lcn2-expressing BMSCs showed a more potent defense against H_2O_2, hypoxia, and serum deprivation stresses, compared to control MSCs (ii) Moreover, Lcn2 expression in MSCs increased cell proliferation and adhesion to culture media by 45% on H_2O_2 exposure, compared to control MSCs. (iii) Lcn2-expressing BMSCs showed normal multipotency into different cell lineage with mild potentiation of adipogenic lineage compared to the control group.	(i) The antioxidant effect of Lcn2 expression is due to ROS scavenging activity, associated with upregulation of antioxidant enzymes' genes, such as SOD. (ii) This antioxidant effect is associated with an antiapoptotic property as indicated by the diminished number of apoptotic cells on oxidative stress exposure, compared to the control group.
Fan et al. [38]	Alpha-phenyl-t-butyl nitrone (PBN) at 800 μM and NAC at 5 mM.	Mesenchymal stem cells (MSCs) from mice embryos.	(i) Cultured MSCs with extracellular matrix from mouse embryonic fibroblast (MEF-ECM) under hypoxic conditions (2% O_2) showed greater proliferation, lower generation of ROS, and increased chromosomal stability compared to the control group, cultured on plastic plates under normoxic conditions. (ii) To further diminish chromosomal instability and based on the increased DNA damage on H_2O_2 exposure, antioxidant supplementation to the culture media significantly reduced the number of DNA micronuclei and karyotyping abnormalities. The use of both (antioxidants and MEF-ECM) in the initial isolation of cells from the	Although authors did not investigate the underlying mechanisms for antioxidants' effects, they suggested that their findings can be attributed to the ability of both PBN and NAC to trap free radicals. Moreover, NAC serves as a precursor for glutathione, an intracellular antioxidant molecule.

Table 1: Continued.

Study ID	Antioxidant (dose)	Stem cell type (source)	Findings	Possible mechanisms
			marrow increased purity and normal cell karyotyping.	
Wang et al. [78]	2-Vinyl-8-hydroxyquinoline derivatives.	Mesenchymal stem cells (MSCs) from rat bone marrow.	In general, 2-vinyl-8-hydroxyquinoline derivatives had a positive effect on MSCs proliferation in a dose-dependent manner.	2-Vinyl-8-hydroxyquinoline derivatives are phenol compounds that perform their antioxidant activity through reaction of their hydroxyl group with free radicals.
Choi et al. [39] and Mekala et al. [79]	Ascorbic acid-2-phosphate (AAP) at 0, 5, 50 250, 500 mM.	Mesenchymal stem cells (MSCs) from adult human bone marrow [39] and human umbilical cord blood-derived stem cells (hUCB-SCs) from umbilical vein [79].	(i) Ascorbic acid significantly increased the proliferation of MSCs/hUCB-SCs, compared to the control group (with the highest proliferation rate at 250 mM). It had no effect on cellular antigenic expression and differentiation. (ii) Moreover, AAP significantly increased osteogenic differentiation at 50 mM (highest calcium deposition at this concentration). In contrast, a significant induction of adipogenic differentiation with oil droplets formation was noted at 250 mM and higher.	(i) AAP improved the amount of collagen production per cell and increased the amount of calcium (at 50 mM) and oil deposition (at ≥250 mM), enhancing MSCs/hUCB-SCs differentiation. (ii) The positive effect of AAP on cellular proliferation is dose-dependent (highest at 250 mM and decreases with higher doses due to inhibitory effect on glycosaminoglycan formation).
Ko et al. [80]	PEG-catalase (200 μg/mL) and NAC (1 mM).	Human umbilical cord blood-derived stem cells (hUCB-SCs) from umbilical vein.	(i) Exposure to genotoxic stress (H_2O_2) in culture media caused a more significant reduction in cellular proliferation and DNA synthesis in hUCB-SCs, compared to control cells (cancer cells and human primary fibroblasts). (ii) Moreover, hUCB-SCs showed low resistance to oxidative stress with cellular senescence and apoptosis at H_2O_2 levels much lower than those of control groups.	Measuring the cellular antioxidant capacity showed that hUCB-SCs had a lower antioxidant capacity than control cells. To confirm that, antioxidant supplementation increased this capacity and diminished cellular damage upon exposure to oxidative stress.
Zeng et al. [81]	Edaravone (10 μM), a clinically approved drug.	Human umbilical cord blood-derived stem cells (hUCB-SCs) from umbilical vein.	(i) Unlike the pro-oxidant (diethyl maleate), edaravone significantly reduced lipopolysaccharide (LPS)/H_2O_2-induced damage and increased stem cell viability ($p < 0.05$). (ii) In diabetic mice with severe combined immunodeficiency, only three mice died in the group, injected with (Gal/LPS and hUCB-SCs), compared to 50% loss in the group, injected with Gal/LPS only. (iii) Pretreatment with edaravone rescued all mice with potentiation of the hepatic cell regenerative power. Furthermore, it	(i) LPS/H_2O_2 challenge induced apoptosis by augmenting oxidative stress and increasing Bax/Bcl2 ratio. However, pretreatment with edaravone abolished these changes. (ii) Moreover, edaravone increased the expression of endogenous antioxidant enzymes (superoxide dismutase, catalase).

Table 1: Continued.

Study ID	Antioxidant (dose)	Stem cell type (source)	Findings	Possible mechanisms
			diminished the levels of cellular injury and proinflammatory markers in treated mice, compared to the control group.	
Rodriguez-Porcel et al. [41]	Tempol (SOD mimetic) at 0 to 10 mm/L concentration.	Rat cardiomyoblasts, transfected by a bioluminescence reporter gene for in vivo detection and transplanted into the myocardium, guided by high-resolution ultrasound.	(i) Cells, exposed to hypoxic/oxidative stress conditions during in vitro culturing, showed decreased cell viability with increased ROS production and NADPH-oxidase-1 expression, compared to the control group. These effects were significantly reduced after adding antioxidants in a dose-dependent manner. (ii) After transplantation into rat myocardium, antioxidant-treated cells showed significantly higher cell viability within the first three days of transplantation, compared to untreated cells.	Hypoxia induces oxidative stress by increasing the expression of NAD(P)H oxidase enzyme. Interestingly, adding antioxidant did not reduce NAD(P)H expression, suggesting that tempol reduces oxidative stress by neutralizing free radicals rather than decreasing their production.
Li et al. [40]	Homemade antioxidant cocktail consisting of 100 $_{M}$L-ascorbate, L-glutathione, and α-tocopherol acetate.	Cardiac stem cells (CSCs) from the endomyocardial tissue of a patient undergoing a cardiac procedure.	(i) Cells, cultured under hypoxic conditions (5% O_2) had a lower number of chromosomal abnormalities, compared to cells, cultured under normoxic conditions (20% O_2). (ii) Unexpectedly, increased cytogenic abnormalities in number and severity were recorded in cells, cultured with antioxidant supplementation. (iii) Antioxidant supplementation, if excessive, may hinder the physiological roles of ROS in stem cells' proliferation and differentiation, which raises a new concept [reductive stress].	(i) Measuring c-H2AX foci (a marker of DNA breaks) showed a biphasic relationship between ROS levels and frequency of DNA breaks, that is, increased DNA damage occurs at low antioxidant/high ROS levels, while excessive suppression of ROS levels increases DNA damage. (ii) There is an optimal level of ROS in stem cells, above which genomic instability occurs due to ROS-induced DNA damage and below which DNA repair enzymes are not activated to maintain the DNA stability.
Takahashi et al. [82]	Ascorbic acid (10^4 M/L) incubation for 12 days.	Human embryonic stem cells (ESCs).	(i) Ascorbic acid significantly increased ESCs differentiation into cardiac myocytes in a dose-dependent manner, as evidenced by increased expression of the cardiac specific gene (myosin heavy chain (MHC)). (ii) Ascorbic acid, independent of its antioxidative property, induced ESCs differentiation into cardiac myocytes. This was evidenced by the absence of this effect with other antioxidants, such as NAC, Tiron, and vitamin E.	Ascorbic acid increased the expression of cardiac muscle genes, such as GATA4, Nkx2.5, α-MHC, β-MHC, and atrial natriuretic factor (ANF), with subsequent cardiac-specific protein production.

Table 1: Continued.

Study ID	Antioxidant (dose)	Stem cell type (source)	Findings	Possible mechanisms
Song et al. [43]	Selenium (20 or 50 ng/mL) and NAC (100 μM).	Human embryonic stem cell- (ESC-) derived vascular progenitors.	(i) Following vascular differentiation of ESCs into vascular progenitor cells (CD34+ cells), a quiescent state of cellular proliferation developed with 41% of the cells in the G0 phase, upregulation of the G1 checkpoint inhibitor (p21) protein and downregulation of mitosis-related genes. (ii) Selenium increased cellular proliferation, reduced p21 expression, and decreased the number of cells in G0 phase of cell cycle. Moreover, it promoted the vascular differentiation of ESCs with no similar effect on endodermal or ectodermal potentiality. (iii) Using NAC totally inhibited the vascular differentiation of ESCs.	(i) Physiologically, ROS are produced during vascular differentiation mainly by NADPH oxidase and is responsible for this quiescent state. (ii) Selenium through increasing glutathione and thioredoxin activity moderately diminished ROS levels. (iii) However, NAC, through complete scavenging of ROS, abolished their physiological role in vascular differentiation.
Park et al. [45]	GV1001 [derived from human telomerase reverse transcriptase from 0 to 100 μM.	Neural stem cells (NSCs) from mice embryonic brain (cortical tissue).	GV1001 significantly reduced H_2O_2 effects on NSCs including diminished cellular proliferation, migration and increased apoptosis. Interestingly, GV1001 itself had no effect on normal untreated cells.	(i) GV1001 has an ROS-scavenging activity, preventing lipid peroxidation and DNA damage. (ii) At the molecular level, GV1001 induced the expression of survival-related proteins and diminished the expression of apoptosis-related proteins.
Hachem et al. [46]	Cyclosporine A (CsA), brain-derived neurotrophic factor (BDNF), and thyrotropin-releasing hormone (TRH).	Neural stem cells (NSCs) from the spinal cord of transgenic adult female rats (spinal cord injury model).	(i) Pretreatment with BDNF for 48 hours (before H_2O_2 exposure) significantly increased NSCs viability and decreased intracellular ROS accumulation, compared to the control group. However, CsA and TRH-treated cells showed no significant changes from the control group. (ii) Interestingly, BDNF-treated cells showed no changes in cellular proliferation and differentiation compared to the control group.	The neuroprotective effect of BDNF is exerted through its ROS-scavenging activity and induction of antioxidant enzymes, such as GR and SOD. Moreover, significant reductions in apoptotic features were noted in BDNF-treated cells, compared to the control group.
Song et al. [52]	Melatonin (100 nM).	Neural stem cells (NSCs) from mice embryonic cortical tissue.	(i) Melatonin significantly reduced LPS-induced toxicity and apoptosis of NSCs through reducing nitric oxide (NO) production and inducing antioxidant enzymes.	(i) Melatonin increased the expression of multiple transcriptional factors, involved in NSCs proliferation, self-renewal, and differentiation, such as orphan

Table 1: Continued.

Study ID	Antioxidant (dose)	Stem cell type (source)	Findings	Possible mechanisms
			(ii) Furthermore, it maintained the neurosphere size in NSCs, treated with LPS. (iii) Melatonin increased cell survival by activating PI3K/Akt pathway. This was confirmed by the addition of wortmannin (a PI3K inhibitor), which inhibited Nrf2 expression and subsequent antioxidant activities.	nuclear receptor TLX and fibroblast growth factor receptor-2. (ii) Melatonin upregulated the expression of nuclear factor-erythroid 2-related factor 2 (Nrf2), responsible for downstream activation of antioxidant enzymes' genes.
Sun et al. [59]	N-Acetyl-L cysteine (NAC) at 2 mM and ascorbic acid-2-phosphate (AAP) at 0.2 mM in comparison to the effect of hypoxia.	Adipose-derived stem cells (ADSCs) from human adipose tissue.	ADSCs, grown in media, supplemented by antioxidants or under hypoxic conditions (5% po2), showed a more significant increase in cell proliferation and a decrease in doubling time than the control group, supplemented by fibroblast growth factor-2. Moreover, cytometric analysis showed that cells, cultured in antioxidant-supplemented and hypoxic media, had a greater proportion of cells in S1 phase of the cell cycle with diminished G0/G1 phase cells, compared to the control group.	In antioxidant-supplemented media, PCR showed diminished levels of cyclin-dependent kinase inhibitors (CDK: important cell cycle regulators that control entering S1 phase), with enhanced expression of stemness-related genes, compared to the control group.
Lyublinskaya et al. [11]	Tempol (1-2 mM), NAC (5–20 mM), and resveratrol (20–40 μM).	Endometrial stem cells, isolated from desquamated endometrium of menstrual blood and ADSCs from adipose tissue.	(i) Reactive oxygen species are important regulators of stem cell self-renewal and proliferation upon exit of the quiescent stage. (ii) Using a synchronized cell in G0 phase, there was a transient increase in ROS levels upon stimulation of cell proliferation and during initial stages of DNA synthesis. (iii) Adding antioxidants to the medium after proliferation induction and before initiation of S1 phase blocked S1 transition. Antioxidant did not have the same effect when added after S1 initiation.	(i) Cells, treated with antioxidants, showed expression of the proliferative marker (Ki-67), which is absent in the nucleus of quiescent cells, indicating that the cell left the quiescent state and was arrested in G1 phase. (ii) Antioxidants, through dose-dependent reduction of ROS levels, can be used to control cellular proliferation during in vitro culturing.
Yang et al. [65]	Fullerol (a polyhydroxylated fullerene) at 0.1, 0.3, 1, 3, and 10 μM.	Human adipose-derived stem cells (ADSCs).	(i) Fullerol enhanced the osteogenic differentiation of ADSCs, as indicated by increased expression of osteogenic markers (Runx2, OCN, and alkaline	Fullerol exerted an antioxidant effect on ADSCs through potentiating the expression of the transcription factor FoxO1

Table 1: Continued.

Study ID	Antioxidant (dose)	Stem cell type (source)	Findings	Possible mechanisms
			phosphatase) and mineralization. (ii) Moreover, fullerol (at all concentrations) reduced ROS levels in the osteogenic culture media.	and its downstream genes (Runx2 and SOD2), which promote ROS scavenging and osteoblastic differentiation.
Yu et al. [83]	L-Ascorbic acid 2-phosphate (AAP) at 250 μM.	Adipose-derived stem cells (ADSCs) from the subcutaneous adipose tissue from a female patient, undergoing abdominoplasty.	(i) Ascorbic acid significantly increased ADSCs proliferation, preserved cellular stemness and increased the potentiality for adipogenic, hepatic, neural and osteogenic differentiation. (ii) In AAP-induced cell sheet, there was a significant increase in the genetic expression and secretion of collagen, laminin, and fibronectin proteins. (iii) The AAP-induced cell sheet improved wound healing in a murine wound model, which indicates the possibility of ADSCs differentiation in a non-mesenchymal lineage.	(i) Adding AAP to ADSCs increased the expression of stemness-related proteins. (ii) Using other antioxidants, such as NAC did not show an increase of stemness markers. In contrast, adding a collagen synthesis inhibitor abolished AAP-induced overexpression of stemness proteins, indicating that the involved mechanism in AAP action is collagen synthesis, not ROS scavenging.
Wang et al. [66]	NAC and AAP at 3 mM and 0.2 mM, respectively (for 20 hours).	Human ADSCs from 10 different human patients.	(i) Pretreated MSCs with antioxidants showed less apoptosis and lower caspase-3 levels upon exposure to advanced glycosylation end-products (AGE), compared to the control group. (ii) The effects of NAC and AAP were significantly amplified after the addition of miRNA-223 mimetics and were significantly abolished by miRNA-223 inhibitors.	Antioxidants reduced ROS generation and apoptosis, induced by AGE. This can be explained by the effect of both on miR-223 (a regulator of intracellular apoptotic singling through modulation of fibroblast-like growth factor receptor-2 protein levels.
Drowley et al. [72]	N-Acetyl-L cysteine at 10 mM in comparison to the pro-oxidant (diethyl maleate) at 50 μM.	Muscle-derived stem cells (MDSCs) from the skeletal muscle of 3-week-old female mice.	(i) In comparison to control cells, NAC-treated cells showed increased survival and differentiation into myotubes upon exposure to oxidative (H_2O_2) or inflammatory stress (tumor necrosis factor). (ii) In failed mice hearts, injection with NAC-treated cells significantly improved systolic and diastolic function on echocardiographic assessment, compared to injection with untreated and DEM-treated cells. Moreover, scar tissue formation was significantly	(i) Increased cell survival after NAC treatment is probably related to stimulation of mitogen-activated protein kinases (MAPK) and extracellular signal-regulated kinase (ERK), kinase families involved in cellular survival and proliferation. (ii) Interestingly, a similar increase in CD31+ endothelial cells in NAC-treated and untreated MDSCs was observed.

Table 1: Continued.

Study ID	Antioxidant (dose)	Stem cell type (source)	Findings	Possible mechanisms
			lower in NAC-treated cells than untreated cells.	
Aliakbari et al. [74]	Catalase (40 mL) and α-tocopherol (200 mL).	Spermatogonial stem cells (SSCs) from neonatal male mice testis.	Antioxidant supplementation of cryopreserved SSCs reduced oxidative damage to membranes and organelles and increased cell survival in a dose-dependent manner.	Catalase and α-tocopherol reduced ROS generation in treated cells, compared to control cells. Moreover, antioxidant-treated cells showed an increased expression of the anti-apoptotic BcL-2 gene with decreased expression of the pro-apoptotic BAX gene, compared to the control group.

ADSCs: adipose-derived stem cells; CAT: catalase; DEM: diethylmaleate; GSH: glutathione; HSCs: hematopoietic stem cells; iPSCs: induced pluripotent stem cells; MDSCs: muscle-derived stem cells; NAC: N-acetyl cysteine; NSCs: neural stem cells; SCC: spermatogonial stem cells; SOD: superoxide dismutase; ROS: reactive oxygen species.

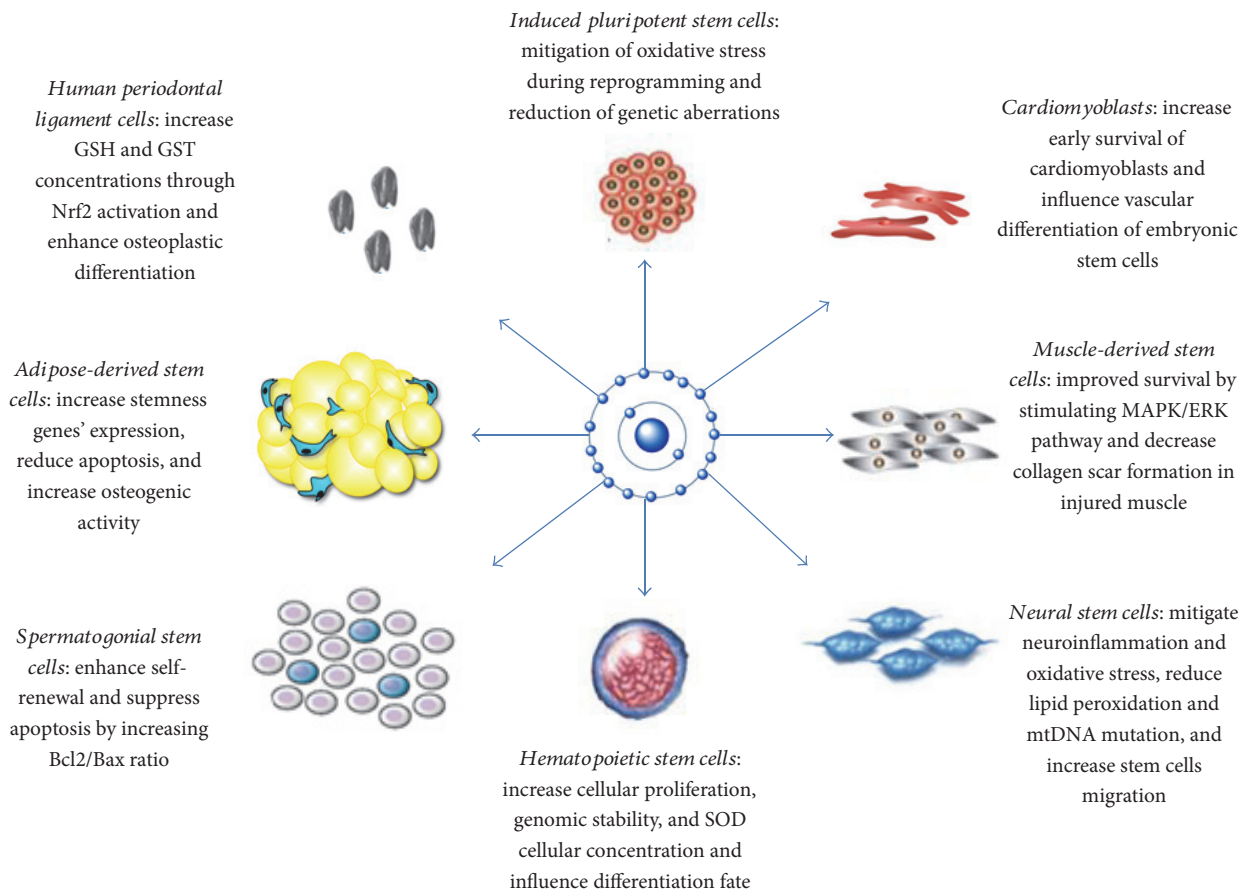

Figure 1: Summarizes the effects of antioxidants on different types of stem cells.

8. Muscle-Derived Stem Cells (MDSCs)

According to Drowley and colleagues, injection of injured skeletal muscles with NAC-treated MDSCs significantly increased muscle regeneration, compared to muscles injected with untreated or DEM-treated MDSCs. The direction of scar tissue formation was opposite the direction of the host muscle regeneration [72]. Additionally, they showed an improved survival of NAC-treated MDSCs, probably due to stimulation of extracellular signal-regulated kinase (ERK) pathway, as evidenced by decreased survival of NAC treated cells after inhibition of the ERK pathway [72, 73].

Moreover, they demonstrated that experimentally infarcted hearts, injected with NAC-treated MDSCs, showed a more significant reduction in the percentage area of collagenous scar tissue than hearts injected with either untreated, DEM-treated, or phosphate buffered saline- (PBS-) treated MDSCs. There was no difference in myocardial scar formation between hearts injected with DEM-treated MDSCs and those injected with PBS [72].

9. Spermatogonia Stem Cells (SSCs)

Cryopreservation of spermatogonial stem cells, in the presence of catalase (CAT) and α-tocopherol (α-TCP), promoted cell viability and suppressed apoptosis through inducing the expression of the antiapoptotic BcL-2 gene and inhibiting the expression of the proapoptotic BAX gene [74]. In other studies, cryopreservation with antioxidants could promote cell enrichment and increase the efficiency of colony formation in isolated SSCs [75, 76]. Spermatogonia-derived colonies showed increased SSC marker activity, enhanced expression of self-renewal genes, such as promyelocytic leukemia zinc finger (Plzf) protein and DNA-binding protein inhibitor ID4, and suppressed expression of the proto-oncogene (c-kit) in both CAT and α-TCP treated groups [74]. This technique can increase the possibility of SSCs banking for men with malignant diseases and promote the resumption of spermatogenesis in SCCs recipients. A summary of the design and main findings of included studies is illustrated in Table 1.

10. Discussion

Our review highlights that antioxidants can influence stem cell activities by [1] mitigating oxidative stress through neutralization of free radicals and increasing the expression of antioxidant enzymes and [2] influencing the differentiation fate of precursor stem cells. Further beneficial effects of antioxidant treatment include increasing genomic stability, improving the adhesion of stem cells to culture media, and enabling researchers to manipulate stem cell proliferation by using different doses of antioxidants. Figure 1 summarizes the effects of antioxidants on different types of stem cells.

We also discussed that a physiological level of ROS (oxidative optimum) is needed for proper differentiation of stem cells, especially for proper cardiogenesis and vasculogenesis [40]. These findings can have several clinical applications, such as improving neurogenesis in patients with stroke and neurodegenerative diseases, as well as improving the regeneration of infarcted myocardial tissue and the banking of SCCs.

Antioxidants are prevalent supplements worldwide. However, little is known about their cell-type-specific actions. It has been shown that a therapeutic dose may vary between different cell types: a dose that rescues a pathology in one tissue may roughly challenge the function of another [22]. Therefore, there is a need for dose-effect studies on antioxidants to confirm their safety as nutritional supplements or therapeutic agents—particularly in the case of antioxidants accumulating in the mitochondria. Our review also showed the potential of some endogenous molecules, such as melatonin, BDNF, and the adipokine (lipocalin-2) in preserving stem cell viability and differentiation potential. Whether these compounds can be used in future clinical applications of stem cells and whether other endogenous molecules with proven antioxidant activities, such as adiponectin [84], can be useful in this regard require further investigation.

11. Recommendations

(1) Multiplicity of stem cell sources within the body (different home environments) and their variable ROS scavenging capacity make them susceptible to oxidative stress at different thresholds. Therefore, we tried to review each stem cell type as a separate entity and we believe that clearing those differences on the molecular and genetic levels will optimize the clinical application of stem cells in different medical fields.

(2) Most of stem cell characteristics are established within in vitro culturing environments. More in vivo studies are required to define their interactions within the body. Furthermore, few in vivo studies have focused on the long-term survival of transplanted stem cells; therefore, this should be the interest of future studies.

(3) The effect of ROS level and redox state on the long-term oncogenicity of stem cells should be further investigated prior to in vivo clinical trials.

12. Conclusion

Using antioxidants can improve the viability and self-renewal capacity of stem cells and affect their differentiation potential. More research is needed on the dose-effect association and cell-type-specific actions of antioxidant before applying these findings in human therapeutic trials.

Abbreviations

ADSCs: Adipose-derived stem cells
BMSCs: Bone marrow-derived mesenchymal stem cells
CAT: Catalase
DEM: Diethylmaleate
DFO: Deferoxamine
GSH: Glutathione
hPDLCs: Human periodontal ligament cells
HSCs: Hematopoietic stem cells
iPSCs: Induced pluripotent stem cells
MDSCs: Muscle-derived stem cells
NAC: N-acetyl cysteine
NSCs: Neural stem cells
PBP: Phosphate buffered saline
SCCs: Spermatogonial stem cells
SOD: Superoxide dismutase
ROS: Reactive oxygen species.

Conflicts of Interest

The authors declare that they have no conflicts of interest.

Authors' Contributions

Sara Shaban, Mostafa Wanees Ahmed El-Husseny, and Abdelrahman Ibrahim Abushouk contributed equally to this work.

References

[1] J. Thomson and J. Odorico, "Human embryonic stem cell and embryonic germ cell lines," *Trends in Biotechnology*, vol. 18, no. 2, pp. 53–57, 2000.

[2] N. Knoepffler, D. Schipanski, and S. L. Sorgner, *Humanbiotechnology as Social Challenge: An Interdisciplinary Introduction to Bioethics*, Ashgate, Farnham, Surrey, United Kingdom, 2007.

[3] B. Vastag, "Stem cells step closer to the clinic," *Jama*, vol. 285, no. 13, p. 1691, 2001, American Medical Association.

[4] M. Izumikawa, R. Minoda, K. Kawamoto et al., "Auditory hair cell replacement and hearing improvement by Atoh1 gene therapy in deaf mammals," *Nature Medicine*, vol. 11, no. 3, pp. 271–276, 2005.

[5] S. D. Narasipura, J. C. Wojciechowski, N. Charles, J. L. Liesveld, and M. R. King, "P-selectin–coated microtube for enrichment of CD34+ hematopoietic stem and progenitor cells from human bone marrow," *Clinical Chemistry*, vol. 54, no. 1, pp. 77–85, 2007.

[6] M. Witkowska-Zimny and K. Walenko, "Stem cells from adipose tissue," *Cellular and Molecular Biology Letters*, vol. 16, no. 2, pp. 236–257, 2011.

[7] M. A. Esteban, T. Wang, B. Qin et al., "Vitamin C enhances the generation of mouse and human induced pluripotent stem cells," *Cell Stem Cell*, vol. 6, no. 1, pp. 71–79, 2010.

[8] M. Stadtfeld, E. Apostolou, F. Ferrari, J. Choi, and R. Walsh, "Ascorbic acid prevents loss of Dlk1-Dio3 imprinting and facilitates generation of all-iPS cell mice from terminally differentiated B cells," *Nature*, vol. 44, no. 4, pp. 398–405, 2012.

[9] W. Neeley and J. Essigmann, "Mechanisms of formation, genotoxicity, and mutation of guanine oxidation products," *Chemical Research in Toxicology*, vol. 19, no. 4, pp. 491–505, 2006.

[10] J. Silva and O. Coutinho, "Free radicals in the regulation of damage and cell death—basic mechanisms and prevention," *Drug Discoveries & Therapeutics*, vol. 4, no. 3, pp. 144–167, 2010.

[11] O. G. Lyublinskaya, Y. G. Borisov, N. A. Pugovkina et al., "Reactive oxygen species are required for human mesenchymal stem cells to initiate proliferation after the quiescence exit," *Oxidative Medicine and Cellular Longevity*, vol. 2015, Article ID 502105, 8 pages, 2015.

[12] B. J. Le, N. Orozco, A. Paucar, and J. Saxe, "Proliferative neural stem cells have high endogenous ROS levels that regulate self-renewal and neurogenesis in a PI3K/Akt-dependant manner," *Cell Stem Cell*, vol. 8, no. 1, pp. 59–71, 2011.

[13] C. Kobayashi and T. Suda, "Regulation of reactive oxygen species in stem cells and cancer stem cells," *Journal of Cellular Physiology*, vol. 227, no. 2, pp. 421–430, 2012.

[14] C. Pérez Estrada, R. Covacu, S. R. Sankavaram, M. Svensson, and L. Brundin, "Oxidative stress increases neurogenesis and oligodendrogenesis in adult neural progenitor cells," *Stem Cells and Development*, vol. 23, no. 19, pp. 2311–2327, 2014.

[15] S. Kothari, A. Thompson, A. Agarwal, and S. S. du Plessis, "Free Radicals: Their Beneficial and Detrimental Effects on Sperm Function," *Indian Journal of Experimental Biology*, vol. 48, no. 5, pp. 425–435, 2010.

[16] S. Vertuani, A. Angusti, and S. Manfredini, "The antioxidants and pro-antioxidants network: an overview," *Current Pharmaceutical Design*, vol. 10, no. 14, pp. 1677–1694, 2004.

[17] H. Sies, "Oxidative stress: oxidants and antioxidants," *Experimental Physiology*, vol. 82, no. 2, pp. 291–295, 1997.

[18] B. Dannenmann, S. Lehle, F. Essmann, and K. Schulze-Osthoff, "Genome surveillance in pluripotent stem cells: low apoptosis threshold and efficient antioxidant defense," *Molecular & Cellular Oncology*, vol. 3, no. 2, article e1052183, 2016, Taylor & Francis.

[19] B. Dannenmann, S. Lehle, D. G. Hildebrand et al., "High glutathione and glutathione peroxidase-2 levels mediate cell-type-specific DNA damage protection in human induced pluripotent stem cells," *Stem Cell Reports*, vol. 4, no. 5, pp. 886–898, 2015.

[20] J. Ji, V. Sharma, S. Qi et al., "Antioxidant supplementation reduces genomic aberrations in human induced pluripotent stem cells," *Stem Cell Reports*, vol. 2, no. 1, pp. 44–51, 2014.

[21] L. Luo, M. Kawakatsu, C.-W. Guo et al., "Effects of antioxidants on the quality and genomic stability of induced pluripotent stem cells," *Scientific Reports*, vol. 4, p. 3779, 2014, Nature Publishing Group.

[22] R. H. Hämäläinen, K. J. Ahlqvist, P. Ellonen et al., "mtDNA mutagenesis disrupts pluripotent stem cell function by altering redox signaling," *Cell Reports*, vol. 11, no. 10, pp. 1614–1624, 2015.

[23] A. M. Sadowska, B. Manuel-y-Keenoy, and W. A. De Backer, "Antioxidant and anti-inflammatory efficacy of NAC in the treatment of COPD: discordant in vitro and in vivo dose-effects: a review," *Pulmonary Pharmacology & Therapeutics*, vol. 20, no. 1, pp. 9–22, 2007.

[24] G. F. Kelso, C. M. Porteous, C. V. Coulter et al., "Selective targeting of a redox-active ubiquinone to mitochondria within cells: antioxidant and antiapoptotic properties," *The Journal of Biological Chemistry*, vol. 276, no. 7, pp. 4588–4596, 2001, American Society for Biochemistry and Molecular Biology.

[25] T. Kinoshita, G. Nagamatsu, T. Kosaka et al., "Ataxia-telangiectasia mutated (ATM) deficiency decreases reprogramming efficiency and leads to genomic instability in iPS cells," *Biochemical and Biophysical Research Communications*, vol. 407, no. 2, pp. 321–326, 2011.

[26] R. Kitagawa and M. B. Kastan, "The ATM-dependent DNA damage signaling pathway," *Cold Spring Harbor Symposia on Quantitative Biology*, vol. 70, no. 1, pp. 99–109, 2005, Cold Spring Harbor Laboratory Press.

[27] A. T. Noon and A. A. Goodarzi, "53BP1-mediated DNA double strand break repair: insert bad pun here," *DNA Repair*, vol. 10, no. 10, pp. 1071–1076, 2011.

[28] D. Foudah, S. Redaelli, E. Donzelli et al., "Monitoring the genomic stability of in vitro cultured rat bone-marrow-derived mesenchymal stem cells," *Chromosome Research*, vol. 17, no. 8, pp. 1025–1039, 2009, Springer Netherlands.

[29] Y. F. Zhou, M. Bosch-Marce, H. Okuyama et al., "Spontaneous transformation of cultured mouse bone marrow–derived stromal cells," *Cancer Research*, vol. 66, no. 22, pp. 10849–10854, 2006.

[30] D. E. C. Baker, N. J. Harrison, E. Maltby et al., "Adaptation to culture of human embryonic stem cells and oncogenesis in vivo," *Nature Biotechnology*, vol. 25, no. 2, pp. 207–215, 2007, Nature Publishing Group.

[31] A. Maitra, D. E. Arking, N. Shivapurkar et al., "Genomic alterations in cultured human embryonic stem cells," *Nature Genetics*, vol. 37, no. 10, pp. 1099–1103, 2005, Nature Publishing Group.

[32] A. M. Liu, W. W. Qu, X. Liu, and C.-K. Qu, "Chromosomal instability in in vitro cultured mouse hematopoietic cells associated with oxidative stress," *American Journal of Blood Research*, vol. 2, no. 1, pp. 71–76, 2012, e-Century Publishing Corporation.

[33] Y.-Y. Jang and S. J. Sharkis, "A low level of reactive oxygen species selects for primitive hematopoietic stem cells that may reside in the low-oxygenic niche," *Blood*, vol. 110, no. 8, pp. 3056–3063, 2007.

[34] P. Eliasson, M. Rehn, P. Hammar et al., "Hypoxia mediates low cell-cycle activity and increases the proportion of long-term–reconstituting hematopoietic stem cells during in vitro culture," *Experimental Hematology*, vol. 38, no. 4, pp. 301–310.e2, 2010.

[35] G. H. Danet, Y. Pan, J. L. Luongo, D. A. Bonnet, and M. C. Simon, "Expansion of human SCID-repopulating cells under hypoxic conditions," *The Journal of Clinical Investigation*, vol. 112, no. 1, pp. 126–135, 2003, American Society for Clinical Investigation.

[36] Z. A. Hamid, W. Hii, L. Lin et al., "The role of Hibiscus sabdariffa L. (roselle) in maintenance of ex vivo murine bone marrow-derived hematopoietic stem cells," *The Scientific World Journal*, vol. 2014, Article ID 258192, 10 pages, 2014.

[37] R. Halabian and H. A. Tehrani, "Lipocalin-2-mediated upregulation of various antioxidants and growth factors protects bone marrow-derived mesenchymal stem cells against unfavorable microenvironments," *Cell Stress and Chaperones*, vol. 18, no. 6, pp. 785–800, 2013.

[38] G. Fan, L. Wen, M. Li et al., "Isolation of mouse mesenchymal stem cells with normal ploidy from bone marrows by reducing oxidative stress in combination with extracellular matrix," *BMC Cell Biology*, vol. 12, no. 1, p. 30, 2011.

[39] K. Choi, Y. Seo, H. Yoon et al., "Effect of ascorbic acid on bone marrow-derived mesenchymal stem cell proliferation and differentiation," *Journal of Bioscience and Bioengineering*, vol. 105, no. 6, pp. 586–594, 2008.

[40] T. S. Li and E. Marbán, "Physiological levels of reactive oxygen species are required to maintain genomic stability in stem cells," *Stem Cells*, vol. 28, no. 7, pp. 1178–1185, 2010.

[41] M. Rodriguez-Porcel, O. Gheysens, R. Paulmurugan et al., "Antioxidants improve early survival of cardiomyoblasts after transplantation to the myocardium," *Molecular Imaging and Biology*, vol. 12, no. 3, pp. 325–334, 2010, Springer-Verlag.

[42] C. Napoli, S. Williams-Ignarro, F. de Nigris et al., "Beneficial effects of concurrent autologous bone marrow cell therapy and metabolic intervention in ischemia-induced angiogenesis in the mouse hindlimb," *Proceedings of the National Academy of Sciences of the United States of America*, vol. 102, no. 47, pp. 17202–17206, 2005, National Academy of Sciences.

[43] S. Song, K. Kim, J. J. Park, K. H. Min, and W. Suh, "Reactive oxygen species regulate the quiescence of CD34-positive cells derived from human embryonic stem cells," *Cardiovascular Research*, vol. 103, no. 1, pp. 1–29, 2014.

[44] M. Song, Y.-J. Kim, Y.-H. Kim, J. Roh, S. U. Kim, and B.-W. Yoon, "Effects of duplicate administration of human neural stem cell after focal cerebral ischemia in the rat," *International Journal of Neuroscience*, vol. 121, no. 8, pp. 457–461, 2011, Taylor & Francis.

[45] H. H. Park, H. J. Yu, K. Sangjae et al., "Neural stem cells injured by oxidative stress can be rejuvenated by GV1001, a novel peptide, through scavenging free radicals and enhancing survival signals," *Neurotoxicology*, vol. 55, pp. 131–141, 2016, Elsevier B.V.

[46] L. D. Hachem, A. J. Mothe, and C. H. Tator, "Effect of BDNF and other potential survival factors in models of in vitro oxidative stress on adult spinal cord–derived neural stem/progenitor cells," *BioResearch Open Access*, vol. 4, no. 1, pp. 146–159, 2015.

[47] A. A. Pieper, S. Blackshaw, E. E. Clements et al., "Poly(ADP-ribosyl)ation basally activated by DNA strand breaks reflects glutamate-nitric oxide neurotransmission," *Proceedings of the National Academy of Sciences of the United States of America*, vol. 97, no. 4, pp. 1845–1850, 2000, National Academy of Sciences.

[48] V. Calabrese, T. E. Bates, and A. M. G. Stella, "NO synthase and NO-dependent signal pathways in brain aging and neurodegenerative disorders: the role of oxidant/antioxidant balance," *Neurochemical Research*, vol. 25, no. 9/10, pp. 1315–1341, 2000, Kluwer Academic Publishers-Plenum Publishers.

[49] A. Cheng, S. L. Chan, O. Milhavet, S. Wang, and M. P. Mattson, "p38 MAP kinase mediates nitric oxide-induced apoptosis of neural progenitor cells," *The Journal of Biological Chemistry*, vol. 276, no. 46, pp. 43320–43327, 2001, American Society for Biochemistry and Molecular Biology.

[50] R. Covacu, A. I. Danilov, B. S. Rasmussen et al., "Nitric oxide exposure diverts neural stem cell fate from neurogenesis towards astrogliogenesis," *Stem Cells*, vol. 24, no. 12, pp. 2792–2800, 2006, John Wiley & Sons, Ltd.

[51] A. Torroglosa, M. Murillo-Carretero, C. Romero-Grimaldi, E. R. Matarredona, A. Campos-Caro, and C. Estrada, "Nitric oxide decreases subventricular zone stem cell proliferation by inhibition of epidermal growth factor receptor and phosphoinositide-3-kinase/Akt pathway," *Stem Cells*, vol. 25, no. 1, pp. 88–97, 2007, John Wiley & Sons, Ltd.

[52] J. Song, S. M. Kang, K. M. Lee, and J. E. Lee, "The protective effect of melatonin on neural stem cell against LPS-induced inflammation," *BioMed Research International*, vol. 2015, Article ID 854359, 13 pages, 2015, Hindawi Publishing Corporation.

[53] C. Tomás-Zapico and A. Coto-Montes, "A proposed mechanism to explain the stimulatory effect of melatonin on antioxidative enzymes," *Journal of Pineal Research*, vol. 39, no. 2, pp. 99–104, 2005, Munksgaard International Publishers.

[54] A. Vilar, L. de Lemos, I. Patraca et al., "Melatonin suppresses nitric oxide production in glial cultures by pro-inflammatory cytokines through p38 MAPK inhibition," *Free Radical Research*, vol. 48, no. 2, pp. 119–128, 2014, Taylor & Francis.

[55] G. Negi, A. Kumar, and S. S. Sharma, "Melatonin modulates neuroinflammation and oxidative stress in experimental diabetic neuropathy: effects on NF-κB and Nrf2 cascades," *Journal of Pineal Research*, vol. 50, no. 2, pp. 124–131, 2010, Blackwell Publishing Ltd.

[56] Q. Ma, "Role of nrf2 in oxidative stress and toxicity. Annual review of pharmacology and toxicology," *NIH Public Access*, vol. 53, pp. 401–426, 2013.

[57] Y.-J. Surh, J. K. Kundu, M.-H. Li, H.-K. Na, and Y.-N. Cha, "Role of Nrf2-mediated heme oxygenase-1 upregulation in adaptive survival response to nitrosative stress," *Archives of Pharmacal Research*, vol. 32, no. 8, pp. 1163–1176, 2009, Pharmaceutical Society of Korea.

[58] M. Petro, H. Jaffer, J. Yang, S. Kabu, V. B. Morris, and V. Labhasetwar, "Biomaterials tissue plasminogen activator followed by antioxidant-loaded nanoparticle delivery promotes activation/mobilization of progenitor cells in infarcted rat brain," *Biomaterials*, vol. 81, pp. 169–180, 2016, Elsevier Ltd.

[59] L.-Y. Sun, C.-Y. Pang, D.-K. Li et al., "Antioxidants cause rapid expansion of human adipose-derived mesenchymal stem cells via CDK and CDK inhibitor regulation," *Journal of Biomedical Science*, vol. 20, no. 1, p. 53, 2013, BioMed Central.

[60] K. Tamama, H. Kawasaki, S. S. Kerpedjieva, J. Guan, R. K. Ganju, and C. K. Sen, "Differential roles of hypoxia inducible factor subunits in multipotential stromal cells under hypoxic condition," *Journal of Cellular Biochemistry*, vol. 112, no. 3, pp. 804–817, 2011, Wiley Subscription Services, Inc., A Wiley Company.

[61] S.-P. Hung, J. H. Ho, and Y.-R. V. ShihT. Lo and O. K. Lee, "Hypoxia promotes proliferation and osteogenic differentiation potentials of human mesenchymal stem cells," *Journal of Orthopaedic Research*, vol. 30, no. 2, pp. 260–266, 2012, Wiley Subscription Services, Inc., A Wiley Company.

[62] I. Martin, A. Muraglia, G. Campanile, R. Cancedda, and R. Quarto, "Fibroblast growth factor-2 supports *ex vivo* expansion and maintenance of osteogenic precursors from human bone marrow," *Endocrinology*, vol. 138, no. 10, pp. 4456–4462, 1997, Endocrine Society.

[63] M. Higuchi, G. J. Dusting, H. Peshavariya et al., "Differentiation of human adipose-derived stem cells into fat involves reactive oxygen species and forkhead box O1 mediated upregulation of antioxidant enzymes," *Stem Cells and Development*, vol. 22, no. 6, pp. 878–888, 2013, Mary Ann Liebert, Inc. 140 Huguenot Street, 3rd Floor New Rochelle, NY 10801 USA.

[64] T. Kojima, T. Norose, K. Tsuchiya, and K. Sakamoto, "Mouse 3T3-L1 cells acquire resistance against oxidative stress as the adipocytes differentiate via the transcription factor FoxO," *Apoptosis*, vol. 15, no. 1, pp. 83–93, 2010, Springer US.

[65] X. Yang, C. J. Li, Y. Wan, P. Smith, G. Shang, and Q. Cui, "Antioxidative fullerol promotes osteogenesis of human adipose-derived stem cells," *International Journal of Nanomedicine*, vol. 9, pp. 4023–4031, 2014.

[66] Z. Wang, H. Li, R. Guo, Q. Wang, and D. Zhang, "Antioxidants inhibit advanced glycosylation end-product-induced apoptosis by downregulation of miR-223 in human adipose

tissue-derived stem cells," *Scientific Reports*, vol. 6, pp. 1–11, 2016, Nature Publishing Group.

[67] J.-H. Chung, Y.-S. Kim, K. Noh, Y.-M. Lee, S.-W. Chang, and E.-C. Kim, "Deferoxamine promotes osteoblastic differentiation in human periodontal ligament cells via the nuclear factor erythroid 2-related factor-mediated antioxidant signaling pathway," *Journal of Periodontal Research*, vol. 49, no. 5, pp. 563–573, 2014.

[68] S. Philipp, L. Cui, B. Ludolph et al.J. M. Downey et al., "Desferoxamine and ethyl-3,4-dihydroxybenzoate protect myocardium by activating NOS and generating mitochondrial ROS," *American Journal of Physiology-Heart and Circulatory Physiology*, vol. 290, no. 1, p. H450, 2005.

[69] C.-N. Im, J.-S. Lee, Y. Zheng, and J.-S. Seo, "Iron chelation study in a normal human hepatocyte cell line suggests that tumor necrosis factor receptor-associated protein 1 (TRAP1) regulates production of reactive oxygen species," *Journal of Cellular Biochemistry*, vol. 100, no. 2, pp. 474–486, 2007, Wiley Subscription Services, Inc., A Wiley Company.

[70] E. Ardite, J. A. Barbera, J. Roca, and J. C. Fernández-Checa, "Glutathione depletion impairs myogenic differentiation of murine skeletal muscle C2C12 cells through sustained NF-κB activation," *The American Journal of Pathology*, vol. 165, no. 3, pp. 719–728, 2004.

[71] F. Esposito, V. Agosti, G. Morrone et al., "Inhibition of the differentiation of human myeloid cell lines by redox changes induced through glutathione depletion," *Biochemical Journal*, vol. 301, no. 3, pp. 649–653, 1994.

[72] L. Drowley, M. Okada, S. Beckman et al., "Cellular antioxidant levels influence muscle stem cell therapy," *Molecular Therapy*, vol. 18, no. 10, pp. 1865–1873, 2010, Nature Publishing Group.

[73] A. Paranjpe, N. A. Cacalano, W. R. Hume, and A. Jewett, "N-acetylcysteine protects dental pulp stromal cells from HEMA-induced apoptosis by inducing differentiation of the cells," *Free Radical Biology and Medicine*, vol. 43, no. 10, pp. 1394–1408, 2007.

[74] F. Aliakbari, M. A. S. Gilani, F. Amidi et al., "Improving the efficacy of cryopreservation of spermatogonia stem cells by antioxidant supplements," *Cellular Reprogramming*, vol. 18, no. 2, pp. 87–95, 2016, Mary Ann Liebert, Inc. 140 Huguenot Street, 3rd Floor New Rochelle, NY 10801 USA.

[75] M. Koruji, M. Koruji, M. Movahedin, S. J. Mowla, and H. Gourabi, "Colony formation ability of frozen thawed spermatogonial stem cell from adult mouse," *International Journal of Reproductive BioMedicine*, vol. 5, no. 3, pp. 109–115, 2012.

[76] T. Mirzapour, M. Movahedin, T. A. Tengku Ibrahim, A. W. Haron, and M. R. Nowroozi, "Evaluation of the effects of cryopreservation on viability, proliferation and colony formation of human spermatogonial stem cells in vitro culture," *Andrologia*, vol. 45, no. 1, pp. 26–34, 2013.

[77] Y. Ikeda, T. Yoshinari, H. Miyoshi, and Y. Nagasaki, "Design of antioxidative biointerface for separation of hematopoietic stem cells with high maintenance of undifferentiated phenotype," *Journal of Biomedical Materials Research Part A*, vol. 104, no. 8, pp. 2080–2085, 2016.

[78] T. Wang, G. Zeng, X. Li, and H. Zeng, "In vitro studies on the antioxidant and protective effect of 2-substituted-8-hydroxyquinoline derivatives against H2O2-induced oxidative stress in BMSCs," *Chemical Biology & Drug Design*, vol. 75, no. 2, pp. 214–222, 2010.

[79] N. K. Mekala, R. R. Baadhe, S. R. Parcha, and D. Y. Prameela, "Enhanced proliferation and osteogenic differentiation of human umbilical cord blood stem cells by L-ascorbic acid, in vitro," *Current Stem Cell Research & Therapy*, vol. 8, no. 2, pp. 156–162, 2013.

[80] E. Ko, K. Y. Lee, and D. S. Hwang, "Human umbilical cord blood–derived mesenchymal stem cells undergo cellular senescence in response to oxidative stress," *Syem Cells and Development*, vol. 21, no. 11, pp. 1877–1886, 2012.

[81] W. Zeng, J. Xiao, G. Zheng, F. Xing, G. L. Tipoe, and X. Wang, "Antioxidant treatment enhances human mesenchymal stem cell anti-stress ability and therapeutic efficacy in an acute liver failure model," *Scientific Reports*, vol. 5, article 11100, 2015, Nature Publishing Group.

[82] T. Takahashi, B. Lord, P. C. Schulze et al., "Ascorbic acid enhances differentiation of embryonic stem cells into cardiac myocytes," *Circulation*, vol. 107, no. 14, pp. 1912–1917, 2003.

[83] J. Yu, T. Yuan-Kun, and N.-C. C. Yueh-Bih Tang, "Stemness and transdifferentiation of adipose- derived stem cells using L-ascorbic acid 2," *Biomaterials*, vol. 35, no. 11, pp. 3516–3526, 2014.

[84] M. W. El Husseny, M. Mamdouh, S. Shaban et al., "Adipokines: potential therapeutic targets for vascular dysfunction in type II diabetes mellitus and obesity," *Journal of Diabetes Research*, vol. 2017, Article ID 8095926, 11 pages, 2017.

Hindawi
Oxidative Medicine and Cellular Longevity
Volume 2017, Article ID 1351945, 13 pages
https://doi.org/10.1155/2017/1351945

Research Article

Modulatory Effect of Monochromatic Blue Light on Heat Stress Response in Commercial Broilers

Safaa E. Abdo,[1] Seham El-Kassas,[1] Abeer F. El-Nahas,[2] and Shawky Mahmoud[3]

[1]*Department of Animal Wealth Development, Faculty of Veterinary Medicine, Kafrelsheikh University, Kafr El-Shaikh, Egypt*
[2]*Department of Animal Husbandry and Animal Wealth Development, Faculty of Veterinary Medicine, Alexandria University, Alexandria, Egypt*
[3]*Department of Physiology, Faculty of Veterinary Medicine, Kafrelsheikh University, Kafr El-Shaikh, Egypt*

Correspondence should be addressed to Seham El-Kassas; seham.elkassas@vet.kfs.edu.eg and Abeer F. El-Nahas; abeer.elnahas@alexu.edu.eg

Received 4 February 2017; Revised 11 March 2017; Accepted 12 April 2017; Published 18 June 2017

Academic Editor: Kota V. Ramana

Copyright © 2017 Safaa E. Abdo et al. This is an open access article distributed under the Creative Commons Attribution License, which permits unrestricted use, distribution, and reproduction in any medium, provided the original work is properly cited.

In a novel approach, monochromatic blue light was used to investigate its modulatory effect on heat stress biomarkers in two commercial broiler strains (Ross 308 and Cobb 500). At 21 days old, birds were divided into four groups including one group housed in white light, a second group exposed to blue light, a 3rd group exposed to white light + heat stress, and a 4th group exposed to blue light + heat stress. Heat treatment at 33°C lasted for five h for four successive days. Exposure to blue light during heat stress reduced MDA concentration and enhanced SOD and CAT enzyme activities as well as modulated their gene expression. Blue light also reduced the degenerative changes that occurred in the liver tissue as a result of heat stress. It regulated, though variably, liver *HSP70*, *HSP90*, *HSF1*, and *HSF3* gene expression among Ross and Cobb chickens. Moreover, the Cobb strain showed better performance than Ross manifested by a significant reduction of rectal temperature in the case of H + B. Furthermore, a significant linear relationship was found between the lowered rectal temperature and the expression of all HSP genes. Generally, the performance of both strains by most assessed parameters under heat stress is improved when using blue light.

1. Introduction

Heat stress is one of the most serious problem facing poultry production in all subtropical countries during summer [1]. The severity of heat stress is due to the resultant oxidative stress which is characterized by accumulation of oxygen reactive species (ROS) in an excess to cellular antioxidants [2–4]. Besides heat exposure, vigorous bird handling, presence of oxidize dietary oils, and infection are associated with ROS formation [3, 5, 6]. ROS accumulation is accompanied by disturbances of cellular balance and modulation of several biological macromolecules including nucleic acid and protein [7]. The cellular antioxidant enzymes represent the first defense system which is responsible for restoring cellular hemostasis. Thus, the increase in the antioxidant enzyme activities including superoxide dismutase (SOD) and catalase (CAT) protects the cells from heat stress-ROS-associated damaged effects. This response greatly differs according to the heat stress conditions, species, and affected tissue [2].

Moreover, one of the main other consequences of heat stress is protein damage and subsequent accumulation of unfolded proteins [8, 9]. Affected cells increase the expression of chaperone proteins and heat shock protein (HSPs), leading to proteostasis and thermotolerance [10]. The HSPs include Hsp40, Hsp60, Hsp70, Hsp90, Hsp110, and the small HSPs. HSP70 and HSP90 are the most conserved HSPs. They work to protect the cell and prevent the aggregation of unfolding protein [11]. Additionally, HSPs protect the cells from heat shock deleterious impacts and enhance tissue repair [12]. HSP expression is regulated mainly at the level of transcription by four heat shock transcription factors (HSFs). HSFs include HSF-1, HSF-2, and HSF-4 (specific to

mammals) and HSF-3, which is avian specific [13]. HSFs modify HSP expression through interaction with a specific DNA sequence (heat shock element (HSE)) in their promoter [14, 15]. Hence, they regulate the HS response.

Different approaches have been done to control the destructive effects of heat stress. Among which were inclusion of feed additives in the diet and water, as well as light management [16]. However, lighting management studies in the alleviation of heat stress deleterious effects are still lacking. Previous studies looked at the effect of different monochromatic lights (white, red, green, and blue) on the broiler immune response and the breed performance [17–20]. Light management was found to increase productivity and improve animal welfare [18, 20, 21]. Thus, light color has been considered as a powerful management that can be used to modify many physiological, immunological, and behavioral pathways [22, 23]. For instance, blue light has been shown to have calming effect by reducing the negative impact of different stressors [24, 25]. Blue light modulates peripheral blood T lymphocytes proliferation, the response to Newcastle disease virus vaccine, heterophils to lymphocytes (H/L) ratio, and interleukin-1β (IL-1β) expression [22, 23]. In addition, using blue light significantly increases the numbers of intestinal intraepithelial lymphocytes, goblet cells, and IgA^+ cells [26]. Moreover, blue light significantly improves meat quality by decreasing lipid peroxidation and improving antioxidant activities by enhancing SOD, GHS, and total antioxidant capability activities and reduced MDA content both in breast and thigh muscles [27].

The aim of this work was to investigate effects of the monochromatic blue light (BL) on alleviating the negative impact of induced cyclic chronic heat stress in commercial broiler strains. We investigated the regulatory effect of using monochromatic blue light during heat stress on heat stress biomarkers activity including antioxidant enzyme activity, histopathological changes in the liver tissue, HSP gene expression, and bird's temperature.

2. Materials and Methods

2.1. Bird Management. A total of 160 one-day-old chicks from two commercial broiler strains (Ross 308 and Cobb 500) were used in this experiment. Eighty chicks of mixed sexes were used for each strain. Chicks were purchased from a reputable dealer at El-Gharbia Governorate, Egypt. The birds were housed (10 birds/m^2) in separate environmentally controlled rooms at the poultry farm, Kafrelsheikh University, Egypt. Each bird had 2.5 cm of feeder space for the first two weeks. After that, 6 cm/bird was allowed. During heat treatment, the feeder and waterer space per bird was increased. The birds were exposed, for the first three weeks, to white light (WL, 400–760 nm) using a light-emitting diode (LED) system. Light duration was adjusted according to the bird's age. Thus, birds received 24 h light length from 0 to 7 days of age and then a light-dark cycle (23 hours : 1 hour) was applied. Light intensity was adjusted according to the Council of the European Communities, 2007 [28, 29]. Thus, birds received 40 lux light intensity for the first week followed by 25 lux till the end of the experiment. Chicks had ad libitum access to feed and water, and diets were formulated to meet the nutrient recommendations for poultry by the National Research Council [30]. Additionally, birds received their regular vaccination program which consisted of Newcastle disease vaccine at days 7 and 18 of age as well as Gumboro disease vaccine at the 14th day of age. The bird's management procedures were undertaken in accordance with the requirements of the Animal Care and Ethics Committee of the Faculty of Veterinary Medicine, Kafrelsheikh University, Egypt.

Table 1: Experimental groups.

Bird strain	Group number	Temp (°C)	Treatment
Ross	W	24	Normal temperature & white light
	B	24	Normal temperature & blue light
	H + W	33 ± 2	Heat stress & white light
	H + B	33 ± 2	Heat stress & blue light
Cobb	W	24	Control & white light
	B	24	Control & blue light
	H + W	33 ± 2	Heat stress & white light
	H + B	33 ± 2	Heat stress & blue light

2.2. Experimental Design. At 21 days of age, birds were individually weighed. All birds were divided into equal eight groups (four groups for each strain ($n = 20$) (Table 1). Two groups (W and B) were housed at normal temperature of 24°C with white and blue lighting, respectively. H + W and H + B groups were exposed to an experimental cyclic chronic heat stress. In this regard, heat treatment extended for four successive days in which birds were exposed each day to 33 ± 2°C for 5 h and then the temperature was decreased to normal 24°C for the rest of the day [31]. In the case of the H + B group, white light was replaced with a monochromatic blue light (480 nm, intensity 25 lux). Air humidity was kept at 70% during the experimental period.

2.3. Sample Collection. Seven birds from each group were used for the sample collection immediately at the end of the heat treatment (at the end of fourth day heat treatment). The birds were killed by cervical dislocation. Three liver specimens were collected from each bird. One liver specimen was collected in 10% formalin for histopathological examination; the second specimen was collected in PBS and kept at −20°C for analysis of antioxidant enzymes activity while the third liver specimen was placed in 2 ml Eppendorf and immediately frozen in liquid nitrogen then kept at −80°C for RNA extraction.

2.4. Histopathological Examination. Liver tissue specimens were fixed in 10% neutral buffered formalin for 24 hours. Then, the tissue was routinely processed in paraffin. Sections (4 μm) from each specimen were obtained from each block and mounted on a glass slide. Tissue sections were subsequently stained with hematoxylin and eosin (H&E)

Table 2: Sequence of forward and reverse primers used in real-time PCR.

Gene	Primer	Ref. seq. accession number
β-Actin	F: 5′-ACCTGAGCGCAAGTACTCTGTCT-3′ R: 5′-CATCGTACTCCTGCTTGCTGAT-3′	NM_205518.1 [66]
GAPDH	F: 5′-GGGCACGCCATCACTATCTTC-3′ R: 5′-ACCTGCATCTGCCCATTTGAT-3′	NM_204305 [67]
HSP70	F: 5-CCAAGAACCAAGTGGCAATGAA-3′ R: 5-CATACTTGCGGCCGATGAGA-3′	EU747335 [49]
HSF1	F: 5-CAGGGAAGCAGTTGGTTCAC TACACG-3 R: 5-CCTTGGGTTTGGGTTGCTCAGTC-3	L06098.1 [66]
HSF3	F: 5-TCCACCTCTCCTCTCGGAAG-3 R: 5-CAACAGGACTGAGGAGCAGG-3	NM_001305041.1 [66]
HSP90	F: 5-GAGTTTGACTGACCCGAGCA-3′ R: 5-TCCCTATGCCGGTATCCACA-3′	NM_206959 [66]
SOD	F: 5-CGGGCCAGTAAAGGTTACTGGAA-3 R: 5-TGTTGTCTCCAAATTCATGCACATG-3	NM_205064.1 [49]
CAT	F: 5-ACTGGTGCTGGCAACCC-3′ R: 5-ACGTGGCCCAACTGTCAT-3′	NM_001031215 [49]

according to the method described by [32]. Liver sections were then examined using a light microscope (200x).

2.5. Assays for Measurement of Malondialdehyde (MDA) Content and Antioxidant Enzyme Activities. Liver tissue specimens were ground in sterile cold potassium phosphate buffer (pH 7). Liver homogenates were spun down at 4000 rpm for 15 min at 4°C, and supernatant was used for further assessments. For malondialdehyde (MDA), its concentration was measured using Biodiagnostic kit following the manufacture's protocol (Biodiagnostic, # MD 2529, Egypt). MDA content were measured using UV-Vis spectrophotometer at 534 nm. MDA content was determined as nmol/g of tissue. Superoxide dismutase activity (SOD) was measured following the protocol of Biodiagnostic kit (Biodiagnostic, # SD 2521, Egypt). The change in absorbance at 560 nm over 5 min was measured using UV-Vis spectrophotometer. Additionally, catalase (CAT) activity was measured based on the spectrophotometric method described by [33]. Catalase reacts with a known quantity of hydrogen peroxide, and the reaction is stopped after 1 min with catalase inhibitor. In the presence of peroxidase, the remaining hydrogen peroxide reacts with 3,5-dichloro-2-hydroxybenzene sulfonic acid and 4-aminophenazone to form a chromophore with a color intensity inversely proportional to the amount of catalase in the sample. The absorbance was measured at 240 nm over 3 min. Enzyme activities of SOD and CAT were measured as units/gram of tissue (u/g).

2.6. RNA Isolation and Reverse Transcription. Total RNA was extracted from 30 to 50 mg of liver tissue ($n = 3$ from each group) using the TRI reagent (easy-RED™, iNtRON Biotechnology), according to the manufacturer's protocol. The integrity of the RNA was verified by gel electrophoresis through visual inspection of rRNA bands (18S and 28S) in ethidium bromide-stained 2% agarose. Also, RNA concentration was measured by Nanodrop ND1000 (UV-Vis spectrophotometer Q5000/USA). Two μg of RNA sample was reverse transcribed using the SensiFAST™ cDNA synthesis kit (Bioline, United Kingdom). The cDNA product was verified by conventional PCR using HSP70 primers and analyzed by agarose gel electrophoresis.

2.7. Real-Time PCR. For gene expression of *HSP70*, *HSP90*, *HSF1*, *HSF3*, *SOD*, and *CAT*, specific primers (Table 2) were used to amplify gene products. In this regard, a real-time PCR (qPCR) was performed using the SensiFAST SYBR Lo-Rox kit (Bioline, United Kingdom) and PikoReal™ 24 Real-Time PCR System (PikoReal 24, Thermoscientific, TCR0024). The reaction mix consisted of 10 μl of SensiFAST SYBR Lo-Rox mastermix, 0.5 μM of each prime, and 2 μl of cDNA. The thermal cycling conditions were initial denaturation at 95°C for 15 min, followed by 40 cycles at 95°C for 15 s, and annealing for 1 min at 60°C for all genes. Dissociation curve analyses were performed beginning at 65°C and ending at 95°C, with incremental increases of 0.5°C every 5 s to validate the specificity of the PCR products. For all tested genes, dissociation curve analysis showed only one peak at the specific melting temperature (data not shown), showing that the PCR products were specifically amplified. All genes were tested in duplicates for three birds of each chicken strain. CT values for each sample were determined and incorporated in "fold change" calculation based on the Livac method [34], and mRNA expressions for each sample were normalized against β-actin and GAPDH.

2.8. Statistical Analysis. Statistical analysis of the data was performed using GraphPad Prism 6 software (GraphPrism Software, La Jolla, California, USA). Two-way ANOVA followed by Fisher's LSD was used to examine the statistically significant differences of the strain and light treatment effects on heat shock parameters measured including SOD, CAT MDA, and gene expression of *SOD*, *CAT*, *HSP70*, *HSP90*, *HSF1*, and *HSF3* as well as bird's body temperature. Linear regression analysis was performed to determine the association between enzyme activity of SOD and CAT and their

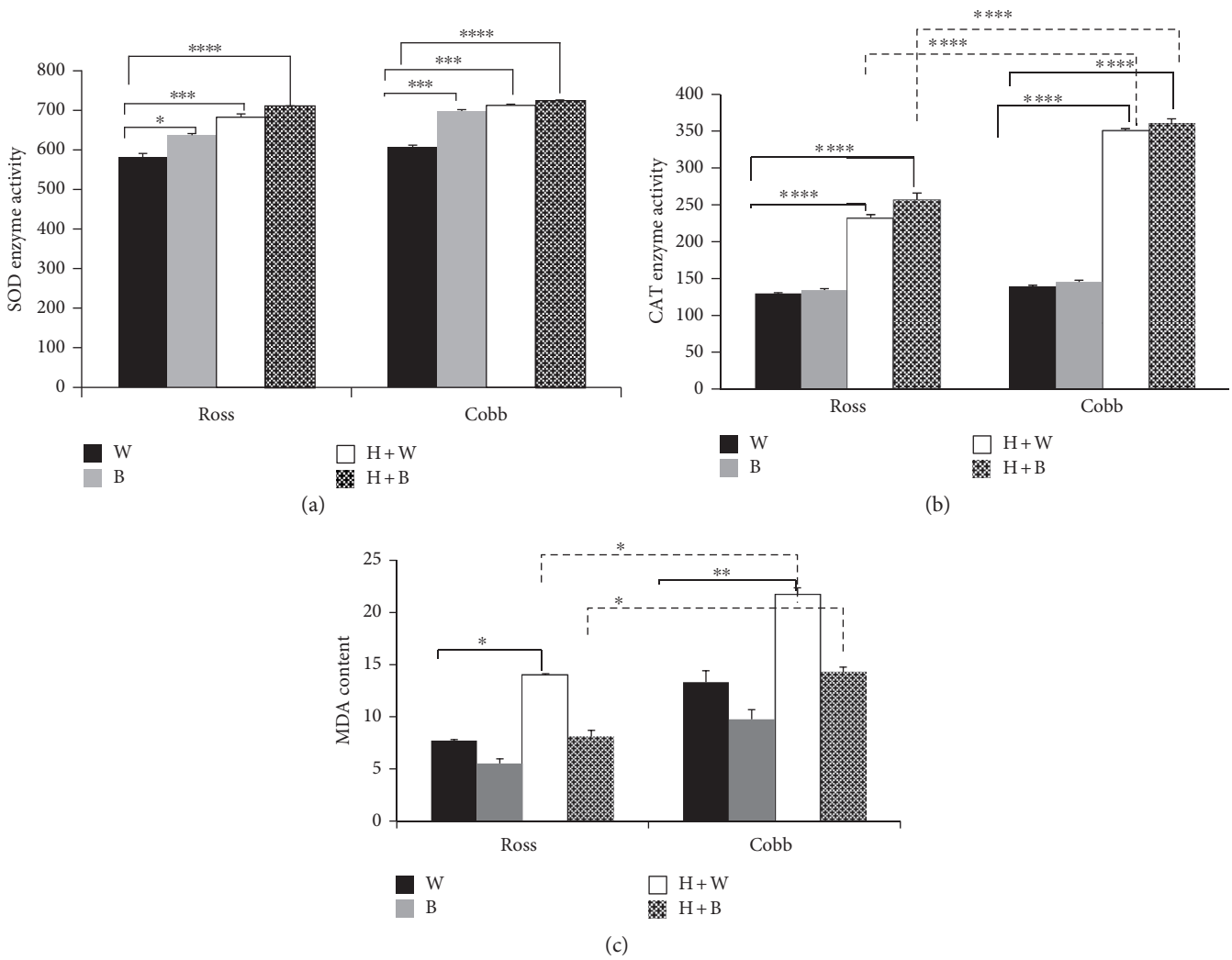

Figure 1: Blue light significantly increases antioxidant enzyme activities and lowers MDA concentration in the liver of two broiler strains (Ross 308 and Cobb 500). Chickens were reared in white light for 3 weeks and after that exposed to cyclic chronic heat stress with white and blue light (H + W and H + B), respectively. Liver samples were collected in sterile PBS for SOD and CAT as well as MDA measurement following the manufacture's protocol. (a) represents SOD enzyme activity. CAT enzyme activity and MDA cellular content were shown in (b) and (c), respectively. Mean ± SEM is shown. *, **, and *** denote statistical significance (two-way ANOVA) with a $p < 0.05$, $p < 0.01$ and $p < 0.001$, respectively.

gene expressions (*SOD* and *CAT* genes). Additionally, the relationship between the bird's body temperature and *HSP70*, *HSP90*, *HSF1*, and *HSF3* gene expression during heat stress (H + W and H + B) was assessed using linear regression analysis. The results were stated as mean ± SEM. Differences were considered to be statistically significant at p values $<0.05^{*}$, $p < 0.01^{**}$, $p < 0.001^{***}$, and $p < 0.0001^{****}$. The significant difference in the case of regression analysis was determined at $p < 0.1^{*}$, $p < 0.05^{**}$, and $p < 0.01^{**}$.

3. Results and Discussion

3.1. Blue Light Significantly Increases Antioxidant Enzyme Activities and Lowers MDA Concentration in Chicken Liver. The analysis of antioxidant enzyme activities as well as MDA content has been considered as one of the most interesting and promising approaches in this study; we reasoned that blue light management would help in treating and preventing of oxidative damage caused by heat stress. Herein, we measured MDA content and SOD as well as CAT enzyme activities in the liver tissue of Ross 308 and Cobb 500 chickens ($n = 7$) after a cyclic chronic heat stress.

Figures 1(a) and 1(b) show the effect of strain, light, and strain + light interaction on SOD and CAT enzyme activities in the liver after heat stress, respectively. Light effect on the level of SOD activity was statistically significant (two-way ANOVA, $p < 0.0001$ for light treatment). SOD activity displayed a significant increase in the case of blue light (B), heat stress (H + W), and heat stress with blue light (H + B) compared to white (W) in both Ross and Cobb chickens (two-way ANOVA, in the case of Ross, for B $p < 0.05$; for H + W $p < 0.001$; and for H + B $p < 0.0001$, in the case of Cobb $p < 0.001$ for B, H + W and $p < 0.0001$ for H + B). Besides, CAT enzyme showed a similar response to SOD

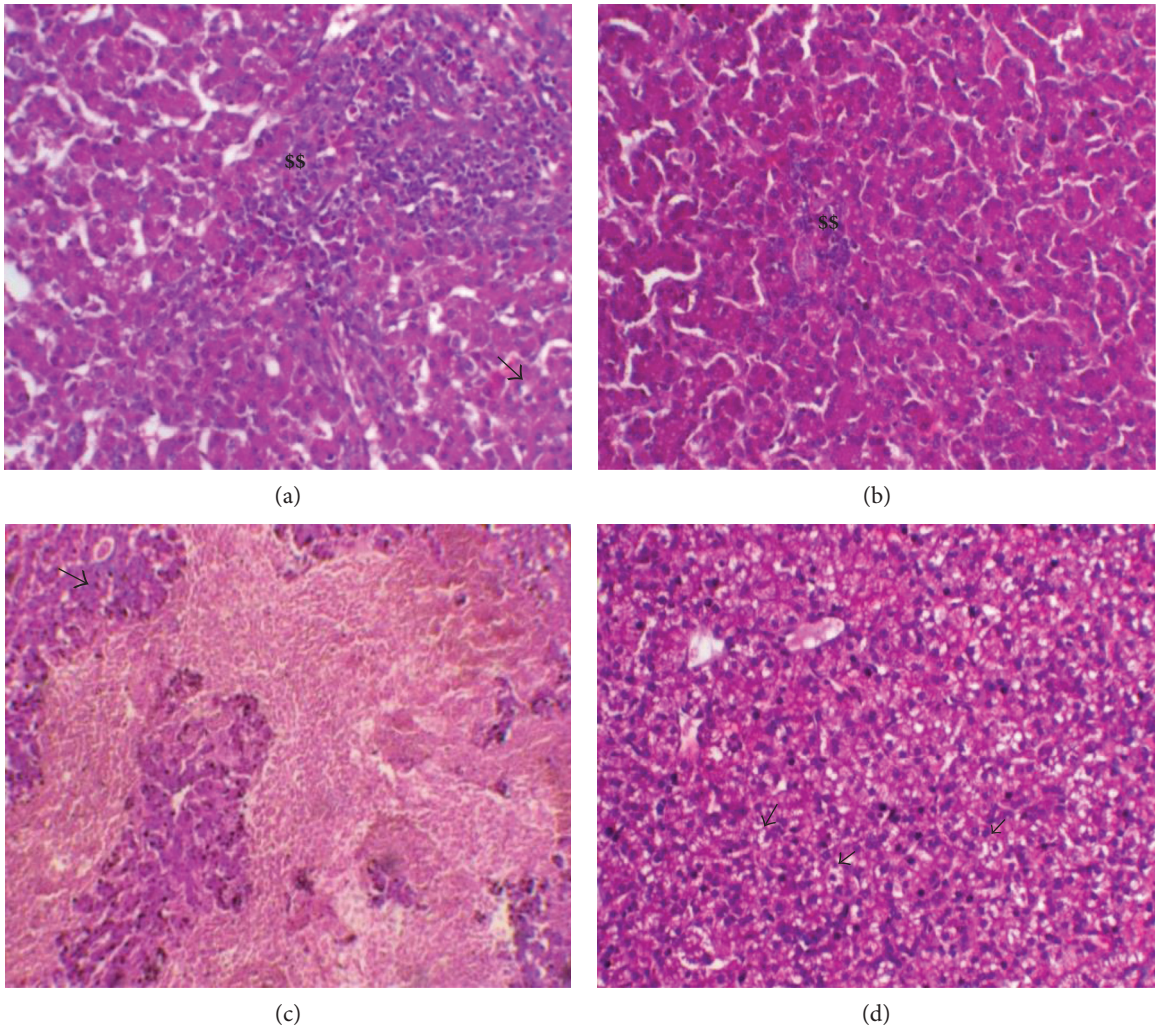

Figure 2: Hematoxylin and eosin staining of liver sections of Ross 308 and Cobb 500: (a) Ross exposed to white light during heat stress H + W and (b) Ross housed with blue light during heat stress H + B. (c, d) The same treatment in the case of Cobb, respectively. $$ refers to mononuclear cell infiltration. Arrows point the fatty changes.

enzyme activity following heat stress. Strain, light effects, and their interaction were statistically significant (two-way ANOVA, $p < 0.0001$ of the two factors and their interaction). A significant increase of CAT enzyme activity was noticed in the case of heat stress (H + W) and using blue light during heat stress (H + B) compared to white (W) in Ross and Cobb (two-way ANOVA, $p < 0.0001$ for H + W and H + B in the case of Ross and Cobb). Additionally, a significant increase of CAT enzyme activity was found in Cobb compared to Ross chicken at the level of H + W and H + B (two-way ANOVA, $p < 0.0001$ for H + W and H + B) discontinued line in Figure 1(b).

Figure 1(c) shows the MDA contents in Ross and Cobb following heat stress. Strain and light effects on MDA content were statistically significant (two-way ANOVA, $p < 0.001$ for strain and light). Since MDA is an indicator of lipid peroxidation that occurs consequently to heat stress, a significant increase in MDA concentration was detected in the case of H + W for Ross and Cobb compared to white (W) (two-way ANOVA, in the case of Ross, for H + W $p < 0.05$, in the case of Cobb $p < 0.01$ for H + W). Interestingly, using blue light only and during heat stress (B and H + B, resp.) induced a lower concentration of MDA compared to white light (W). Moreover, Ross and Cobb manifested a significantly different response in MDA content, whereas Cobb chicken had a significant higher MDA concentration compared to Ross chicken in the case of heat stress + white light (H + W) and heat stress + blue light (H + B) (two-way ANOVA, $p < 0.05$ for H + W and H + B) discontinued line Figure 1(c).

3.2. Blue Light Lowers the Tissue Damage Induced by Heat Stress in Chicken Liver. Since high temperature causes severe damage to internal organs' parenchyma such as the liver, we examined the morphological changes in the liver tissue following heat stress in the presence of blue light during treatment. Histological analysis of the liver tissue revealed that heat stress (H + W) in Ross and Cobb induced moderate to severe damage in hepatic tissue. In Cobb, this damage included moderate to severe fatty changes and perivascular mononuclear cell infiltration (in some fields it was admixed with heterophils). Besides, vascular congestion and subcapsular and interstitial hemorrhage were detected (Figure 2(c)

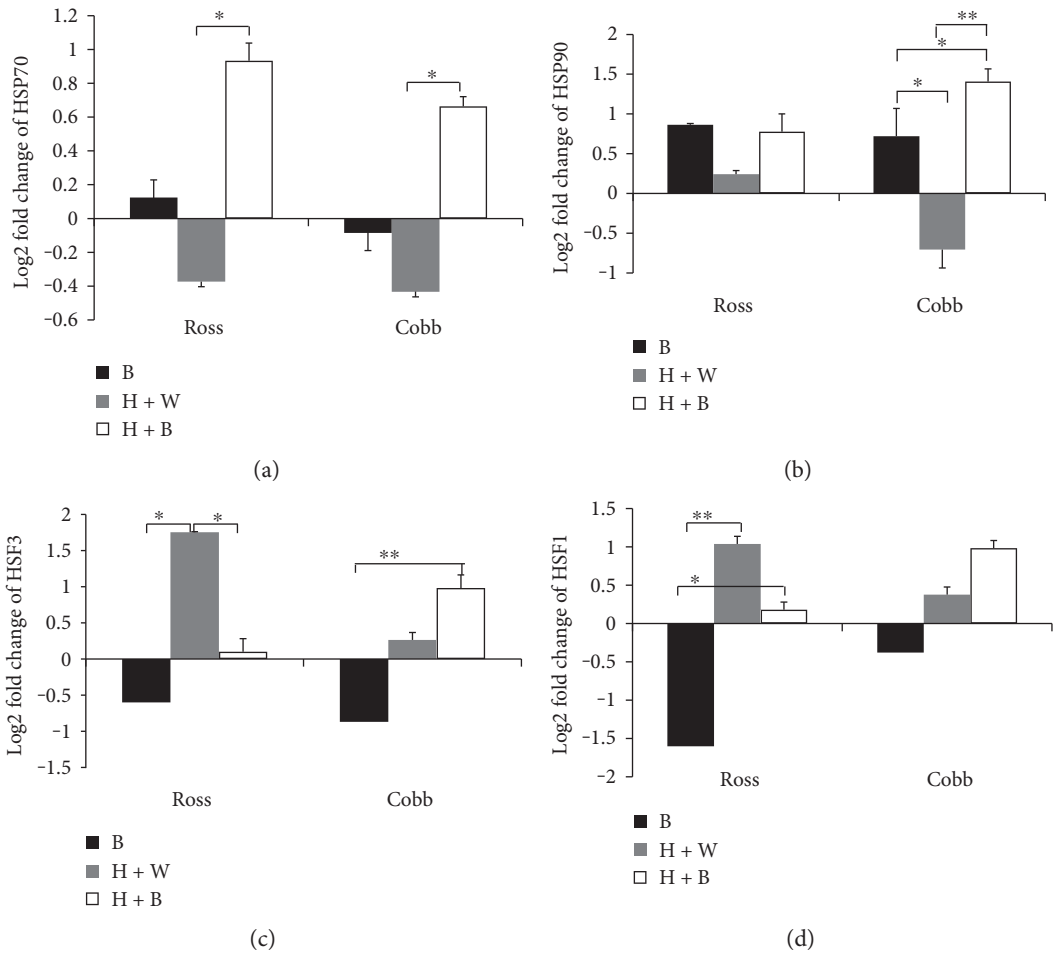

Figure 3: Blue light significantly modulates liver *HSP70*, *HSP90*, *HSF1*, and *HSF3* gene expression in the chicken liver. The relative gene expression levels of *HSP70*, *HSP90*, *HSF3*, and HSF1in the liver of Ross and Cobb exposed to blue light, heat stress in white light, and heat stress in blue light (B, H + W, and H + B, resp.) were measured. The gene expression levels were normalized against control (W) and against two housekeeping genes (β-actin and GAPDH). The expression levels were presented as log2 fold change and shown in the figure as mean ± SEM. *, **, and *** denote statistical significance (two-way ANOVA) with a $p < 0.05$, $p < 0.01$, and $p < 0.001$, respectively.

as well as in the Supporting information to Figure 2 available online at https://doi.org/10.1155/2017/1351945 H + W for Cobb). For Ross, severe mononuclear cell infiltration admixed with heterophils, hepatic degeneration, and focal necrosis were found (Figure 2(a) as well as in the Supporting information to Figure 2 H + W for Ross). Interestingly, treating heat stress effect using blue light (H + B) lowered the tissue damage caused by heat stress in the two chicken strains. Only mild to moderate vacuolation and mononuclear cell infiltration were found (Figure 2(b) in the case of Ross and Figure 2(d) in the case of Cobb).

3.3. Blue Light Significantly Modulates Liver HSP70, HSP90, HSF1, and HSF3 Gene Expression in Chicken Liver. Blue light significantly modulated bird's resistance to heat stress by increasing the level of SOD and CAT. Moreover, it reduced the damaged effect of heat stress on the liver tissue indicated by decreasing MDA concentration in Ross and Cobb (Figure 1 and Figures 2(b) and 2(d), resp.). Therefore, we further examined how blue light regulates the relative mRNA expression of *HSPs* (*HSP70* and *HSP90*) as well as *HSF3* and *HSF1*. The analysis was performed in the liver of Ross and Cobb chickens following heat stress using qPCR. Figures 3(a), 3(b), 3(c), and 3(d) represent the relative gene expression level of *HSP70*, *HSP90*, *HSF3*, and *HSF1*, respectively, from 3 birds for each treatment compared to normal white (W). Blue light, similarly modulated the expression level of *HSP70* and *HSP90* in Ross and Cobb without strain differences (two-way ANOVA, $p < 0.01$ and $p = 0.05$ for blue light effect in the case of *HSP70* and *HSP90*, resp.).

In Ross and Cobb, normally, blue light (B) did not affect much the *HSP70* gene expression where only a slight increase and decrease of *HSP70* gene expression were detected, respectively. However, heat stress caused nonsignificant downregulation of *HSP70* gene expression when used with white light (H + B) in both Ross and Cobb. Nevertheless, when blue light was used during heat stress (H + B), an interesting significant upregulation of *HSP70* gene expression was detected ($p < 0.05$) in the two chicken strains (Figure 3(a)).

For *HSP90* gene (Figure 3(b)), it showed a similar expression pattern to *HSP70* gene. There was no strain

differences and only differences due to light treatment were detected without light + strain interaction (two-way ANOVA, $p > 0.05$ for strain and interaction; $p < 0.05$ for light treatment). In Ross, B, H + B, and H + W revealed a nonsignificant upregulation of *HSP90* gene expression level. However, in Cobb, the response to *HSP90* gene was different. Normally and during heat stress, blue light (B and H + B, resp.) induced a significant upregulation of *HSP90* gene ($p < 0.05$; $p < 0.01$, resp.) when compared to heat stress only (H + W) which displayed a downregulation of *HSP90* gene expression level. Additionally, blue light during heat stress stimulated more *HSP90* gene expression compared to under normal condition (B) ($p < 0.05$). These results demonstrate that blue light variably regulates HSP (*HSP70* and *HSP90*) gene expression between the two chicken strains. It induces more *HSP70* and *HSP90* gene expression. Most of the increases in *HSP70* and *HSP90* expression occurred by using blue light during heat stress.

Further, we examined the mRNA expression level of *HSF3* and *HSF1* in the liver of Ross and Cobb chickens. Figures 3(c) and 3(d) show the effect of strain, light, and strain + light interaction on gene expression level of *HSF3* and *HSF1* in the liver of Ross and Cobb chickens, respectively. Statistical analysis revealed a nonsignificant difference due to strain and strain + light interaction. However, light treatment showed a significant effect (two-way ANOVA, $p > 0.05$ for strain and interaction; $p < 0.05$ for light treatment). The expression levels of *HSF3* and *HSF1* genes were similar in Ross. Heat stress (H + W) induced a significant upregulation of *HSF3* and *HSF1* which significantly decreased when the blue light was used during heat stress ($p < 0.05$). Moreover, blue light, alone (B), significantly downregulated the expression levels of *HSF3* and *HSF1* ($p < 0.01$) (Figures 3(c) and 3(d)).

In Cobb, the expression level of the two genes was similar to Ross. Heat stress (H + W) induced a slight increase in the expression level of both *HSF3* and *HSF1*. This effect was significantly increased when blue light was applied during heat stress (H + B). It induced a significant upregulation of *HSF3* and *HSF1* gene expression. However, in the case of using blue light alone (B), it induced a significant downregulation especially for *HSF3* ($p < 0.01$).

In conclusion, using blue light during heat stress regulated the expression levels of *HSP70*, *HSP90*, *HSF1*, and *HSF3* though variably in the different broiler strains. A similar increase in the level of expression of HSPs (*HSP70* and *HSP90*) in Ross and Cobb was found. However, in the case of *HSF1* and *HSF3*, this resulted in an upregulation in their expression levels in Cobb but a downregulation in the case of Ross.

3.4. Variations of SOD and CAT Antioxidant Enzyme Activities Could Be Predicted from Their Respective Gene Expression. Blue light significantly induced more SOD and CAT enzyme production during heat stress (H + B) (Figures 1(a) and 1(b)). To address how it modulates their gene expression levels, we measured *SOD* and *CAT* mRNA expression levels in the liver of Ross and Cobb chickens. Figures 4(a) and 4(b) show the strain, light treatment, and strain + light interaction effects on *SOD* and *CAT* gene expression levels. For *SOD*, only the light treatment caused significant difference, while in the case of *CAT*, there were significant differences due to strain, light treatment, and strain + light interaction effects (two-way ANOVA, in the case of *SOD* for strain and light + strain interaction $p > 0.05$; for light treatment $p < 0.05$; in the case of *CAT*, strain $p < 0.01$; light treatment $p = 0.05$; and strain + light interaction $p < 0.01$). *SOD* gene expression level, in Ross and Cobb, was upregulated when blue light was used (B and H + B). This upregulation was significant, in case the of Cobb, when compared to heat stress (H + W) which stimulated a significant downregulation ($p < 0.05$).

CAT gene reacted differently to heat stress and light treatment between the two chicken strains. For Cobb, it responded similarly to *SOD* gene. Thus, blue light resulted in a significant upregulation either normally (B) or when it was applied during heat stress ($p < 0.05$; $p < 0.01$, resp.) compared to heat stress (H + W) which was characterized by a significant downregulation. However, in the case of Ross, blue light significantly downregulated *CAT* gene expression when used during heat stress ($p = 0.05$). Additionally, there were significant differences in the expression level between Ross and Cobb ($p < 0.001$). In conclusion, blue light regulated *SOD* and *CAT* gene expression levels during heat stress.

To better understand how the variation in the enzymes activities could be predicted from their gene expression, linear regression analysis was performed (Figure 4(c)). For linear regression analysis, the question posed in the test was "what would best predict variations in the level of antioxidant enzymes (SOD and CAT) from their gene expression levels?" The r^2 value, a measurement of the linear relationship between these 2 parameters, and the p value set at 90% confidence level are reported.

For Ross, a strong significant association was detected between SOD enzyme and its gene expression level in the case of the control (W), blue light (B), and heat stress + blue light (H + B) ($p < 0.05$ for each). Nevertheless, a very weak nonsignificant association was detected in the case of heat stress (H + W). Additionally, CAT enzyme showed a similar strong significant relationship with its gene expression in the case of blue light (B) ($p < 0.1$). Moreover, a nonsignificant association was detected in the case of the control (W), heat stress (H + W), and heat stress + blue light (H + B).

For Cobb, SOD enzyme exhibited a similar association to its gene, as in the case of Ross. A significant association was detected in the case of the control (W), blue light (B), and heat stress + blue light (H + B) ($p = 0.1$ for W; $p < 0.0.05$ for B; and $p < 0.1$ for H + B). On the other hand, in the case of heat stress (H + W), a weak nonsignificant relationship was found. For CAT, blue light (B and H + B) induced a significant relationship between CAT enzyme and its gene expression ($p < 0.05$ for B; $p < 0.01$ for H + B). However, under normal condition (W) and in the case of heat stress (H + W) nonsignificant association was found.

3.5. Blue Light Significantly Regulates Bird's Temperature during Heat Stress Suggesting an Association with Changes in Heat Shock Biomarker Genes. Figure 5(a) represents strain, light treatment, and strain + light interaction effects on

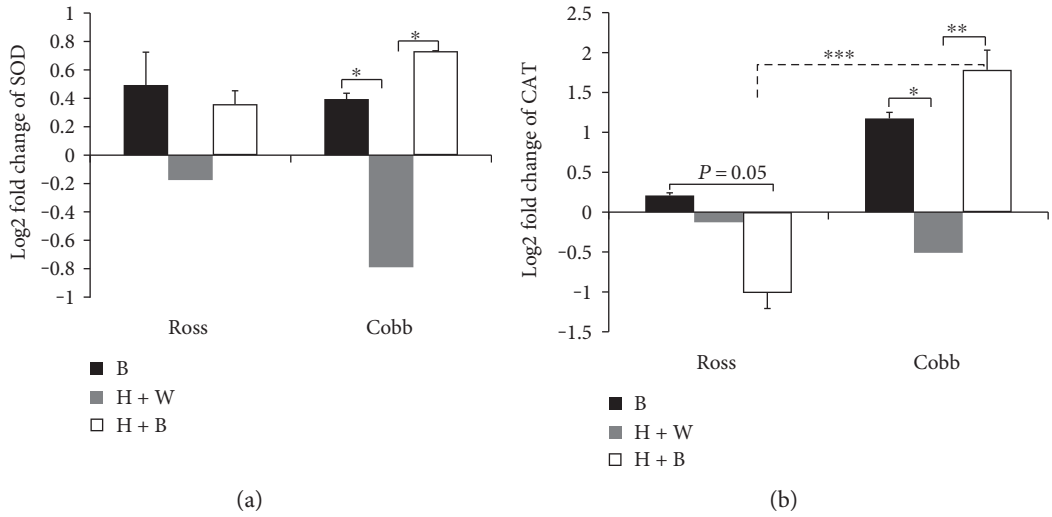

r^2	Ross		Cobb	
	SOD	Catalase	SOD	Catalase
W	0.9957**	0.9029	0.9643 $P = 0.1$	0.7500
B	0.9989**	*0.9802	0.9974**	**0.9961
H + W	0.06113	0.7048	0.2049	0.1071
H + B	**0.9153	0.6226	0.8805*	***0.9929

(c)

Figure 4: Variations of SOD and CAT antioxidant enzyme activities could be predicted from their respective gene expression. The relative gene expression levels of antioxidant enzymes SOD and CAT in Ross and Cobb in the three groups, blue light (B), heat stressed with white light (H + W), and heat stressed with blue light (H + B) compared to the control group which kept at 24°C and white light. Two housekeeping genes (β-actin and GAPDH) were used to normalize the gene expression level. The expression levels were presented as log2 fold change and shown in the figure as mean ± SEM. *, **, and *** in (a) and (b) denote statistical significance (two-way ANOVA) with a $p < 0.05$, $p < 0.01$, and $p < 0.001$, respectively. (c) represents regression analysis of the association between antioxidant enzyme activities and their gene expressions. The analysis was performed at 90% confidence level. The r^2 values are shown. *, **, and *** denote statistical significance at $p < 0.1$, $p < 0.05$, and $p < 0.01$, respectively.

bird's temperature (rectal temperature) during normal condition and heat stress. Strain and strain + light interaction did not show a statistically significant effect on the bird's temperature while light treatment did (two-way ANOVA, for strain and strain + light interaction $p > 0.05$; for light treatment $p < 0.0001$, resp.). Compared to chicken housed under control temperature (W), a significant increase in bird's temperature was recoded due to heat stress regardless of light treatment (H + W and H + B) in both Ross and Cobb ($p < 0.0001$ for each). Interestingly, a significant reduction in the bird's temperature was recorded when blue light was used during heat stress (H + B) compared to heat stress only (H + W). This reduction in body temperature was significant in the case of Cobb compared to Ross which exhibited a nonsignificant reduction in bird's temperature ($p < 0.001$ for Cobb). Moreover, birds reared in blue light during heat stress (H + B) showed less panting, were more relaxed and calm, and exhibited better feed intake in comparison to heat-stressed birds (H + W).

Since heat stress modulated heat shock biomarkers such as *HSP70*, *HSP90*, *HSF3*, and *HSF1* gene expression (Figure 3), a linear regression analysis was performed to examine how the variation in bird's temperature could be explained (Figure 5(b)). We hypothesized that the changes in bird's temperature would best predict variations in the *HSP70*, *HSP90*, *HSF3*, and *HSF1* gene expression levels. The r^2 value and the p value, set at 90% confidence level, are reported (Figure 5(b)).

For Ross, heat stress (H + W) induced a strong significant relationship between changes in bird's temperature and *HSP90* and *HSF3* gene expression ($p < 0.1$ and $p = 0.1$, resp.). Additionally, *HSP70* gene expression following heat stress showed a significant moderate correlation with the variation in bird's temperature ($p < 0.05$). However, modulation of *HSF1* gene expression due to heat stress was not significantly related to bird's temperature. Moreover, using blue light during heat stress (H + B) resulted in a significant relationship with *HSF3* gene expression

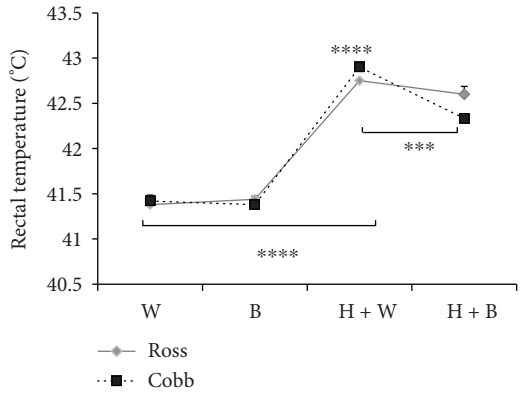

(a)

r^2	Ross				Cobb			
	HSP 70	HSP 90	HSF 1	HSF 3	HSP 70	HSP 90	HSF 1	HSF 3
HW	0.309**	0.977*	0.683	0.976 $P = 0.1$	0.976**	0.947***	0.259***	0.003**
HB	0.7976	0.8837	0.5854	0.999***	0.997**	0.234***	0.9558	0.514**

(b)

Figure 5: Blue light significantly regulates bird's temperature during heat stress which could be associated with change in heat shock biomarker genes. (a) represents mean ± SEM of the bird's temperature in the case of W, B, H + W, and H + B. *, **, and *** denote statistical significance (two-way ANOVA) with a $p < 0.05$, $p < 0.01$, and $p < 0.001$, respectively. (b) represents regression analysis of the association between the gene expression level (fold change) of heat shock protein and heat shock factor *HSP70*, *HSP90*, *HSF3*, and *HSF1*, respectively, and bird's temperature. Analysis was performed at 90% confidence level. The r^2 values are shown. *, **, and *** denote statistical significance at $p < 0.1$, $p < 0.05$, and $p < 0.01$, respectively.

($p < 0.01$). However, nonsignificant correlation was found in the case of *HSP70*, *HSP90*, and *HSF1* gene expression.

For Cobb chickens, changes in bird's temperature displayed more significant correlations with *HSP70*, *HSP90*, *HSF3*, and *HSF1* gene expression following heat stress in the case of white and blue lighting (H + W and H + B, resp.). *HSP70* gene expression demonstrated a strong significant association with the variations in bird's temperature in the case of ((H + W and H + B); $p < 0.05$ for each). Additionally, a significantly, strong and low correlation was found for *HSP90* gene expression ($p < 0.01$ in the case of H + W and H + B, resp.). Likewise, the variations of *HSF3* gene expression showed very low and moderate significant association with the changes in bird's temperature after heat stress ((H + W and H + B, resp.) ($p < 0.05$ for each)). Also, the changes in *HSF1* gene expression was significantly correlated to body temperature variation after heat stress (H + W); $p < 0.01$).

4. Discussion

Several studies addressed the destructive impact of heat stress on poultry, especially chicken, well-being, and production. Heat stress induces oxidative damage which is characterized by production of reactive oxygen species (ROS) in excess of cellular antioxidants [35, 36]. ROS are highly toxic and modify the cellular macromolecules including lipid, protein, and nucleic acid (DNA and RNA) [7]. As a result, their accumulation results in a variety of cellular dysfunctions including lipid peroxidation, protein oxidation, and cell death [35, 37]. Thus, antioxidative enzyme system (including SOD as well as CAT) represents the first line of cellular defense to heat shock. They lower the free radical concentration in the cells by preventing their formation. Additionally, they enhance the mitochondrial electron chain efficiency and diminish the electron leakage resulting in superoxide production. Likewise, they scavenge the initial radicals (such as peroxyl radicals) by stimulating the expression of various transcription factors (e.g., Nrf2 and NF-$\kappa\beta$) resulting in preventing the propagation of lipid peroxidation [38–41]. Alteration of these enzyme activities can modify the balance between the production of ROS and the antioxidant system. Consequently, a reduction in animal's productive and reproductive performances and immunity incompetence occurs [42].

In the present study, we addressed the possible regulatory mechanisms on antioxidant enzymes following exposure to blue light under heat stress in two different commercial broiler strains, Ross and Cobb. Ross 308 and Cobb 500 were used in this work because they are the most common

commercial broiler strains used for production purpose. Additionally, Cobb 500 had better overall performance than Ross 308 [43, 44]. Moreover, broiler chickens are known to be highly affected by heat stress due to that selection for higher growth rate is associated with decreased resistance to heat stress [16, 45, 46]. Figure 1 represents the effect of blue light on SOD and CAT activities and MDA content following heat stress. In this regard, during heat stress, the elevation in the level of SOD and CAT enzymes is necessary and represents one of the most crucial defense systems of cells to overcome the deleterious effect of HS [47, 48]. This limits the excessive oxidation caused by the accumulation of ROS and thereby protect the cells by maintaining the steady state level of free radicals within the cells [2, 11]. The results in Figure 1 clearly show a striking modulation in the SOD and CAT enzyme activities following exposure to blue light. Interestingly, blue light in the case of B and H + B induced more enzyme activity compared to normal and heat stress, respectively. The most notable is the significantly higher activities of these enzymes following exposure of the birds to blue light during heat stress. Considering that higher level of SOD and CAT enzymes protects against heat stress destructive effects [2], this result is a strong indication of the protective regulatory mechanisms of blue light during heat stress [27]. We suggest that using blue light during heat stress may enhance the bird's resistance to heat stress oxidative injuries to the cells.

On the molecular level, we further examined how exposure to blue light modifies gene expression levels of *SOD* and *CAT* in the two chicken strains (Figure 4). Again, using blue light during heat stress stimulated higher gene expression levels of *SOD* and *CAT* especially in Cobb chicken. However, Ross chicken showed a significant downregulation in the expression of *CAT* gene when blue light replaced the white light during heat stress. The higher gene expression levels in the case of exposure to blue light during heat stress may imply higher enzymatic activity of these antioxidant enzymes. The downregulation of *CAT* gene may explain the significantly lowered CAT enzyme activity of Ross chicken in the case of H + B group compared to Cobb chicken (Figure 1(b)). This was confirmed by using regression analysis that examined the association between antioxidant enzymes and their genes (Figure 4(c)). Significant associations between the enzyme activities and their gene expression demonstrated their tight connection. Our results are in agreement with those results by [49] which showed that the higher antioxidant enzyme activities were due to higher mRNA expression level. The higher expression in the case of H + B represents a protective mechanism of the cells from the negative impact of heat stress [50, 51]. Additionally, the lowered levels of gene expression of *SOD* and *CAT* in the case of heat stress (H + W) agree with results of [52] who reported that the higher temperature during heat stress suppressed the antioxidant activities.

Conversely, for MDA (Figure 1(c)), exposure of birds to blue light during heat stress (H + B) significantly lowered its content compared to heat stress (H + W) which showed a significant increase in MDA content. Higher MDA content is an indicator of lipid peroxidation and consequently more oxidative damage [53–56]. The lowered MDA concentration in the case of H + B suggests a possible role of blue light in lowering the negative effect of heat stress [27].

The effects of exposure to blue lighting on histology of the liver tissue were further examined in Ross and Cobb Figure 2. Heat stress (H + W) induced tissue injuries, infiltration of inflammatory cells, subcapsular and interstitial hemorrhage, hepatic degeneration, and focal necrosis. This was associated with significantly higher H/L ratio in the case of H + W in the two chicken strains (data not shown). Chicken reared under exposure to blue light during heat stress (H + B) showed a reduction in tissue damage effect by heat stress compared to those reared in white light. This was also correlated with lowered H/L ratio in the case of H + B group (data not shown). The blue light effect on the liver tissue concomitant with the lowered MDA concentration (Figure 1(c)) indicates that blue light plays a significant role during heat stress to scavenge the negative effect of heat stress as well as it enhances bird's resistance [23, 26].

Having demonstrated the protective effect of blue light during heat stress by modulating the antioxidant enzyme activity and reducing the liver tissue injuries, we examined its effect on HSPs. In this regard, it is known that one of the cellular consequences of the oxidative stress is protein damage and the subsequent aggregation of unfolded proteins [2]. Heat shock proteins (HSPs) play an essential role in protecting and repairing cells and tissues against stress [12]. They regulate protein processing in the cells and enhance refolding of the damaged protein [57]. The increased expression level of HSPs has been reported to protect against the heat shock adverse subsequent tissue injuries [2, 8, 58–60]. Hence, we examined the possible regulatory impact of blue light on HSP gene expression (Figures 3(a) and 3(b)). Heat stress (H + W) suppressed the expression of *HSP70* and *HSP90* whereas it downregulated *HSP70* and *HSP90* gene expression. The decrease in gene expression was probably due to the severe extent of stress and destructive injuries in the liver [61–63]. This was shown here by the significantly elevated body temperature in the case of (H + W). On the other hand, blue light treatment regulated the level of HSP (*HSP70* and *HSP90*) gene expression. Blue light during heat stress (H + B) induced interesting upregulation of *HSP70* and *HSP90* in the two broiler strains. This effect was tightly associated with the lowered body temperature. Accordingly, HSP upregulation would likely explain the protective effect of the blue light during heat stress.

Since expression of heat shock proteins is regulated by heat shock factor, and HSFs are involved in regulating the cellular response against it, HSF genes (*HSF1* and *HSF3*) were examined (Figures 3(c) and 3(d)). HSF genes were variably expressed during heat stress and in the case of exposure of birds to blue light. In the two chicken strains, heat stress (H + W) induced a significant upregulation of HSF gene expression level. These effects were strongly correlated to higher body temperature in the case of H + W in both strains. HSFs are stress biomarkers and their expression is induced during heat stress [11, 13]. Under normal housing temperature with blue light application (B), the expression level of HSF genes was significantly downregulated. This indicates

that blue light exposure does not induce stress on the birds. Likewise, using blue light during heat stress (H + B) led to lower expression levels of *HSF3* and *HSF1* in the Ross strain. This was significantly associated with lowered body temperature, especially for *HSF3*. On the other hand, in the Cobb strain, the expression levels of *HSF1* and *HSF3* genes showed a slight increase when white light was replaced by the blue one during heat stress (H + B). The results of HSP and HSF gene expression levels are consistent with those of [47, 64, 65] who reported that HSFs and HSPs were variably expressed after heat stress. In the latter case, *HSF3* gene expression level continued to increase while that of *HSP 70* decreased. The authors also reported that the expression levels varied depending on the species and the tissue affected.

From the foremost results we reported in this work, replacing white by blue light during heat stress significantly correlated with improved bird's resistance to heat stress and lowered the negative impacts of heat stress. This was clearly shown by reduction of bird's body temperature (Figure 5(a)) in the case of H + B compared to a significant increase in the case of heat stress without blue light exposure (H + W). Cobb chicken displayed a significant decrease in body temperature compared to Ross. This shows that there is a variation in the response to blue light effects between the two strains [55]. This variation in body temperature significantly correlated with the gene expression of heat biomarkers (HSPs and HSFs) (Figure 5(b)).

5. Conclusion

Our findings represent the first reported data on the role of monochromatic blue light in regulating the bird's resistance to heat stress. Replacing white light by the blue one during heat stress would modify the heat shock biomarker activities which might enhance the bird's resistance to negative impacts of heat stress. Finally, our results suggest that Cobb 500 have a better response to blue light than Ross 308. Therefore, using blue light during heat stress represents a cheap tool to manage and control heat stress in poultry farms. Therefore, we strongly recommend using blue light in poultry houses during summer.

Abbreviations

CAT: Catalase
HS: Heat stress
HSF: Heat shock factor
HSF1: Heat shock factor 1
HSF3: Heat shock factor 3
HSP: Heat shock protein
HSP70: Heat shock protein 70
HSP90: Heat shock protein 90
MDA: Malondialdehyde
SOD: Superoxide dismutase.

Conflicts of Interest

All authors agree about the content of the article and have no conflict of interest.

Acknowledgments

The authors are immensely grateful to Dr. T.O. Nashar, Department of Pathobiology, College of Veterinary Medicine, Nursing and Allied Health, Tuskegee University, AL, USA, for his assistance with language editing and proofreading. Also, the authors are indebted to Dr. Waleed Sobhy, Pathology Department, Kafrelsheikh University, Egypt, for help in the histopathological examination.

References

[1] C. D. Allen, A. K. Macalady, H. Chenchouni et al., "A global overview of drought and heat-induced tree mortality reveals emerging climate change risks for forests," *Forest Ecology and Management*, vol. 259, no. 4, pp. 660–684, 2010.

[2] A. Akbarian, J. Michiels, J. Degroote, M. Majdeddin, A. Golian, and S. De Smet, "Association between heat stress and oxidative stress in poultry; mitochondrial dysfunction and dietary interventions with phytochemicals," *Journal of Animal Science and Biotechnology*, vol. 7, no. 37, pp. 1–14, 2016.

[3] B. Halliwell and M. Whiteman, "Measuring reactive species and oxidative damage in vivo and in cell culture: how should you do it and what do the results mean?" *British Poultry Science*, vol. 142, no. 2, pp. 231–255, 2004.

[4] J. Feng, M. Zhang, S. Zheng, P. Xie, and A. Ma, "Effects of high temperature on multiple parameters of broilers *in vitro* and *in vivo*," *Poultry Science*, vol. 87, no. 10, pp. 2133–2139, 2008.

[5] M. Estévez, "Oxidative damage to poultry: from farm to fork," *Poultry Science*, vol. 94, no. 6, pp. 1368–1378, 2015.

[6] S. Ye, S. Lowther, and J. Stambas, "Inhibition of reactive oxygen species production ameliorates inflammation induced by influenza A viruses via upregulation of SOCS1 and SOCS3," *Journal of Virology*, vol. 89, no. 5, pp. 2672–2683, 2015.

[7] K. J. Davies, "Oxidative stress: the paradox of aerobic life," *Biochemical Society Symposium*, vol. 61, pp. 1–31, 1995.

[8] P. H. McCormick, G. Chen, S. Tlerney, C. J. Kelly, and D. J. Bouchier-Hayes, "Clinically relevant thermal preconditioning attenuates ischemia-reperfusion injury," *The Journal of Surgical Research*, vol. 109, no. 1, pp. 24–30, 2003.

[9] J. L. Staib, J. C. Quindry, J. P. French, D. S. Criswell, and S. K. Powers, "Increased temperature, not cardiac load, activates heat shock transcription factor 1 and heat shock protein 72 expression in the heart," *American Journal of Physiology. Regulatory, Integrative and Comparative Physiology*, vol. 292, no. 1, pp. R432–R439, 2007.

[10] M. Jaattela, "Heat shock proteins as cellular lifeguards," *Annals of Medicine*, vol. 31, no. 4, pp. 261–271, 1999.

[11] I. Belhadj Slimen, T. Najar, A. Ghram, and M. Abdrrabba, "Heat stress effects on livestock: molecular, cellular and metabolic aspects, a review," *Journal of Animal Physiology and Animal Nutrition*, vol. 100, no. 3, pp. 401–412, 2016.

[12] J. Yu, E. Bao, J. Yan, and L. Lei, "Expression and localization of Hsps in the heart and blood vessel of heat-stressed broilers," *Cell Stress & Chaperones*, vol. 13, no. 3, pp. 327–335, 2008.

[13] A. Nakai and R. I. Morimoto, "Characterization of a novel chicken heat shock transcription factor, heat shock factor 3, suggests a new regulatory pathway," *Molecular and Cellular Biology*, no. 13no. 4, pp. 1983–1997, 1993.

[14] R. I. Morimoto, M. P. Kline, D. N. Bimston, and J. J. Cotto, "The heat-shock response: regulation and function of heat-shock proteins and molecular chaperones," *Essays in Biochemistry*, vol. 32, pp. 17–29, 1997.

[15] M. Fujimoto and A. Nakai, "The heat shock factor family and adaptation to proteotoxic stress," *Federation of European Biochemical Societies Journal*, vol. 277, no. 20, pp. 4112–4125, 2010.

[16] L. J. Lara and M. H. Rostagno, "Impact of heat stress on poultry production," *Animals (Basel)*, vol. 3, no. 2, pp. 356–369, 2013.

[17] J. Cao, W. Liu, Z. Wang, L. J. D. Xie, and Y. Chen, "Green and blue monochromatic lights promote growth and development of broilers via stimulating testosterone secretion and myofiber growth," *Journal of Applied Poultry Research*, vol. 17, no. 2, pp. 211–218, 2008.

[18] Y. Yang, Y. Yu, J. Pan, Y. Ying, and H. Zhou, "A new method to manipulate broiler chicken growth and metabolism: response to mixed LED light system," *Scientific Reports*, vol. 6, article no. 25972, 2016.

[19] J. Pan, Y. Yang, B. Yang, and Y. Yu, "Artificial polychromatic light affects growth and physiology in chicks," *PloS One*, vol. 9, no. 12, article e113595, 2014.

[20] J. Pan, Y. Yang, B. Yang, W. Dai, and Y. Yu, "Human-friendly light-emitting diode source stimulates broiler growth," *PloS One*, vol. 10, no. 8, article e0135330, 2015.

[21] J. Pan, M. Lu, W. Lin et al., "The behavioral preferences and performance of female broilers under unevenly distributed yellow led lights with various intensities," *Transactions of the ASABE*, vol. 57, no. 4, pp. 1245–1254, 2014.

[22] R. A. Mohamed, M. M. Eltholth, and N. R. El-Saidy, "Rearing broiler chickens under monochromatic blue light improve performance and reduce fear and stress during pre-slaughter handling and transportation," *Biotechnology and Animal Husbandry*, vol. 30, no. 3, pp. 457–471, 2014.

[23] D. Xie, Z. X. Wang, Y. L. Dong et al., "Effects of monochromatic light on immune response of broilers," *Poultry Science*, vol. 87, no. 8, pp. 1535–1539, 2008.

[24] D. S. Prayitno, C. J. Phillips, and D. K. Stokes, "The effects of color and intensity of light on behavior and leg disorders in broiler chickens," *Poultry Science*, vol. 76, no. 12, pp. 1674–1681, 1997.

[25] P. Lewis and T. Morris, "Poultry and coloured light," *World's Poultry Science Journal*, vol. 56, no. 3, pp. 189–207, 2000.

[26] D. Xie, J. Li, Z. X. Wang et al., "Effects of monochromatic light on mucosal mechanical and immunological barriers in the small intestine of broilers," *Poultry Science*, vol. 90, no. 12, pp. 2697–2704, 2011.

[27] Y. Y. Ke, W. J. Liu, Z. X. Wang, and J. L. Chen, "Effects of monochromatic light on quality properties and antioxidation of meat in broilers," *Poultry Science*, vol. 90, no. 11, pp. 2632–2637, 2011.

[28] H. H. Kristensen, "The effects of light intensity, gradual changes between light and dark and definition of darkness for the behaviour and welfare of broiler chickens, laying hens, pullets and turkeys," *Scientific Report for the Norwegian Scientific Committee for Food Safety*, 2008, http://www.vkm.no/dav/7643446bd0.pdf.

[29] C. Directive, "43/EC of 28 June 2007, laying down minimum rules for the protection of chickens kept for meat production," *Official Journal of the European Union L*, vol. 182, pp. 19–28, 2007.

[30] NRC, *Nutrient Requirements of Poultry*, National Research Council. National Academy Press, Washington, USA, 1994.

[31] M. A. Azad, M. Kikusato, I. Zulkifli, and M. Toyomizu, "Electrolysed reduced water decreases reactive oxygen species-induced oxidative damage to skeletal muscle and improves performance in broiler chickens exposed to medium-term chronic heat stress," *British Poultry Science*, vol. 54, no. 4, pp. 503–509, 2013.

[32] J. D. Bancroft, H. C. Cook, and J. H. Beckstead, *Manual of Histological Techniques and Their Diagnostic Application*, Archives of Pathology and Laboratory Medicine, Churchill Livingstone, 1994.

[33] H. Aebi, "Catalase in vitro," *Methods in Enzymology*, vol. 105, pp. 121–126, 1984.

[34] K. J. Livak and T. D. Schmittgen, "Analysis of relative gene expression data using real-time quantitative PCR and the $2^{-\Delta\Delta C_T}$ method," *Methods*, vol. 25, no. 4, pp. 402–408, 2001.

[35] H. Lin, E. Decuypere, and J. Buyse, "Acute heat stress induces oxidative stress in broiler chickens," *Comparative Biochemistry and Physiology. Part a, Molecular & Integrative Physiology*, vol. 144, no. 1, pp. 11–17, 2006.

[36] M. P. Murphy, "How mitochondria produce reactive oxygen species," *The Biochemical Journal*, vol. 417, no. 1, pp. 1–13, 2009.

[37] R. Mittler, "Oxidative stress, antioxidants and stress tolerance," *Trends in Plant Science*, vol. 9, no. 7, pp. 405–410, 2002.

[38] P. F. Surai and V. I. Fisinin, "Antioxidant-prooxidant balance in the intestine: applications in chick placement and pig weaning," *Journal of Veterinary Science & Medicine*, vol. 3, no. 1, pp. 66–84, 2015.

[39] E. Shatskikh, E. Latypova, V. Fisinin, S. Denev, and P. Surai, "Molecular mechanisms and new strategies to fight stresses in egg-producing birds," *Agricultural Science and Technology*, vol. 7, no. 1, pp. 3–10, 2015.

[40] P. F. Surai, "Silymarin as a natural antioxidant: an overview of the current evidence and perspectives," *Antioxidants (Basel)*, no. 4no. 1, pp. 204–247, 2015.

[41] P. F. Surai, "Antioxidant systems in poultry biology: heat shock proteins," *Journal of Science*, vol. 5, no. 12, pp. 1188–1222, 2015.

[42] P. F. Surai, *Selenium in Nutrition and Health*, Nottingham University Press, Nottingham, UK, 2006.

[43] F. Lobago, G. Melese, B. Mideksa, and M. Tibbo, "Comparative performance of two broiler hybrids (Cobb-500 and Ross) under small-scale production system in Debre Zeit, Central Ethiopia," *AU Bulletin of Animal Health and Production in Africa*, vol. 51, no. 2, pp. 83–93, 2003, http://hdl.handle.net/10568/28367.

[44] P. Hascik, M. Kacaniova, M. Mihok, J. Pochop, E. Benczova, and T. A. Hlinku, "Performance of various broiler chicken hybrids fed with commercially produced feed mixtures," *International Journal of Poultry Science*, vol. 9, no. 11, pp. 1076–1082, 2010.

[45] W. M. Quinteiro-Filho, A. Ribeiro, V. Ferraz-de-Paula et al., "Heat stress impairs performance parameters, induces intestinal injury, and decreases macrophage activity in broiler chickens," *Poultry Science*, vol. 89, no. 9, pp. 1905–1914, 2010.

[46] S. L. Berrong and K. W. Washburn, "Effects of genetic variation on total plasma protein, body weight gains, and body

temperature responses to heat stress," *Poultry Science*, vol. 77, no. 3, pp. 379–385, 1998.

[47] T. Zeng, J. J. Li, D. Q. Wang, G. Q. Li, G. L. Wang, and L. Z. Lu, "Effects of heat stress on antioxidant defense system, inflammatory injury, and heat shock proteins of Muscovy and Pekin ducks: evidence for differential thermal sensitivities," *Cell Stress & Chaperones*, vol. 19, no. 6, pp. 895–901, 2014.

[48] P. F. Surai, "Antioxidant systems in poultry biology: superoxide dismutase," *Journal of Animal Research and Nutrition*, vol. 1, no. 1, p. 8, 2016.

[49] S. Rimoldi, E. Lasagna, F. M. Sarti et al., "Expression profile of six stress-related genes and productive performances of fast and slow growing broiler strains reared under heat stress conditions," *Meta Gene*, vol. 6, no. 6, pp. 17–25, 2015.

[50] G. S. Devi, M. H. Prasad, I. Saraswathi, D. Raghu, D. N. Rao, and P. P. Reddy, "Free radicals antioxidant enzymes and lipid peroxidation in different types of leukemias," *Clinica Chimica Acta; International Journal of Clinical Chemistry*, vol. 293, no. 1-2, pp. 53–62, 2000.

[51] M. J. Thomas, "The role of free radicals and antioxidants," *Nutrition*, vol. 16, no. 7, pp. 716–718, 2000.

[52] H. Willemsen, Q. Swennen, N. Everaert et al., "Effects of dietary supplementation of methionine and its hydroxy analog DL-2-hydroxy-4-methylthiobutanoic acid on growth performance, plasma hormone levels, and the redox status of broiler chickens exposed to high temperatures," *Poultry Science*, vol. 90, no. 10, pp. 2311–2320, 2011.

[53] K. Sahin, M. Onderci, N. Sahin, M. F. Gursu, and O. Kucuk, "Dietary vitamin C and folic acid supplementation ameliorates the detrimental effects of heat stress in Japanese quail," *The Journal of Nutrition*, vol. 133, no. 6, pp. 1882–1886, 2003.

[54] I. B. Ismail, K. A. Al-Busadah, and S. M. El-Bahr, "Oxidative stress biomarkers and biochemical profile in broilers chicken fed zinc bacitracin and ascorbic acid under hot climate," *American Journal of Biochemistry and Molecular Biology*, no. 3, pp. 202–214, 2013.

[55] O. Altan, A. Pabuçcuoğlu, A. Altan, S. Konyalioğlu, and H. Bayraktar, "Effect of heat stress on oxidative stress, lipid peroxidation and some stress parameters in broilers," *British Poultry Science*, vol. 44, no. 4, pp. 545–550, 2003.

[56] G.-Y. Tan, L. Yang, Y. Q. Fu, J. H. Feng, and M. H. Zhang, "Effects of different acute high ambient temperatures on function of hepatic mitochondrial respiration, antioxidative enzymes, and oxidative injury in broiler chicken," *Poultry Science*, vol. 89, no. 1, pp. 115–122, 2010.

[57] C. Marques, W. Guo, P. Pereira et al., "The triage of damaged proteins: degradation by the ubiquitin-proteasome pathway or repair by molecular chaperones," *Federation of American Societies for Experimental Biology Journal*, vol. 20, no. 6, pp. 741–743, 2006.

[58] J. C. Liu, M. He, L. Wan, and X. S. Cheng, "Heat shock protein 70 gene transfection protects rat myocardium cell against anoxia-reoxygeneration injury," *Chinese Medical Journal*, vol. 120, no. 7, pp. 578–583, 2007.

[59] H. Y. Zhang, N. H. Lv, Y. Xie, G. H. Guo, J. H. Zhan, and J. Chen, "Protection of heat shock preconditioning on acute gastric mucosal lesion in scalded rats and its mechanism," *Zhonghua Shao Shang Za Zhi*, vol. 23, no. 1, pp. 58–61, 2007.

[60] S. P. Luh, P. H. Kuo, T. F. Kuo et al., "Effects of thermal preconditioning on the ischemia-reperfusion-induced acute lung injury in minipigs," *Shock*, vol. 28, no. 5, pp. 615–622, 2007.

[61] J. M. Yu and E. D. Bao, "Effect of acute heat stress on heat shock protein 70 and its corresponding mRNA expression in the heart, liver, and kidney of broilers," *Asian-Australasian Journal of Animal Sciences*, vol. 21, no. 8, pp. 1116–1126, 2008.

[62] L. Lei, J. M. Yu, and E. D. Bao, "Expression of heat shock protein 90 (Hsp90) and transcription of its corresponding mRNA in broilers exposed to high temperature," *British Poultry Science*, vol. 50, no. 4, pp. 504–511, 2009.

[63] X. H. Gu, Y. Hao, and X. L. Wang, "Overexpression of heat shock protein 70 and its relationship to intestine under acute heat stress in broilers: 2. Intestinal oxidative stress," *Poultry Science*, vol. 91, no. 4, pp. 790–799, 2012.

[64] M. Zhang, Z. Yue, Z. Liu et al., "Hsp70 and HSF-1 expression is altered in the tissues of pigs transported for various periods of times," *Journal of Veterinary Science*, vol. 13, no. 3, pp. 253–259, 2012.

[65] M. Tanabe, A. Nakai, Y. Kawazoe, and K. Nagata, "Different thresholds in the responses of two heat shock transcription factors, HSF1 and HSF3," *The Journal of Biological Chemistry*, vol. 272, no. 24, pp. 15389–15395, 1997.

[66] J. J. Xie, L. Tang, L. Lu et al., "Differential expression of heat shock transcription factors and heat shock proteins after acute and chronic heat stress in laying chickens (*Gallus gallus*)," *PloS One*, vol. 9, no. 7, article e102204, 2014.

[67] J. R. Nerren, C. L. Swaggerty, K. M. MacKinnon et al., "Differential mRNA expression of the avian-specific toll-like receptor 15 between heterophils from Salmonella-susceptible and -resistant chickens," *Immunogenetics*, vol. 61, no. 1, pp. 71–77, 2009.

Hindawi
Oxidative Medicine and Cellular Longevity
Volume 2017, Article ID 5985219, 16 pages
https://doi.org/10.1155/2017/5985219

Research Article

Camellia sinensis Prevents Perinatal Nicotine-Induced Neurobehavioral Alterations, Tissue Injury, and Oxidative Stress in Male and Female Mice Newborns

Jamaan S. Ajarem,[1] Gadh Al-Basher,[1] Ahmed A. Allam,[1,2] and Ayman M. Mahmoud[3]

[1]*Department of Zoology, Faculty of Science, King Saud University, Riyadh, Saudi Arabia*
[2]*Department of Zoology, Faculty of Science, Beni-Suef University, Beni-Suef, Egypt*
[3]*Physiology Division, Department of Zoology, Faculty of Science, Beni-Suef University, Beni-Suef, Egypt*

Correspondence should be addressed to Ayman M. Mahmoud; ayman.mahmoud@science.bsu.edu.eg

Received 13 January 2017; Accepted 27 March 2017; Published 15 May 2017

Academic Editor: Kota V. Ramana

Copyright © 2017 Jamaan S. Ajarem et al. This is an open access article distributed under the Creative Commons Attribution License, which permits unrestricted use, distribution, and reproduction in any medium, provided the original work is properly cited.

Nicotine exposure during pregnancy induces oxidative stress and leads to behavioral alterations in early childhood and young adulthood. The current study aimed to investigate the possible protective effects of green tea (*Camellia sinensis*) against perinatal nicotine-induced behavioral alterations and oxidative stress in mice newborns. Pregnant mice received 50 mg/kg *C. sinensis* on gestational day 1 (PD1) to postnatal day 15 (D15) and were subcutaneously injected with 0.25 mg/kg nicotine from PD12 to D15. Nicotine-exposed newborns showed significant delay in eye opening and hair appearance and declined body weight at birth and at D21. Nicotine induced neuromotor alterations in both male and female newborns evidenced by the suppressed righting, rotating, and cliff avoidance reflexes. Nicotine-exposed newborns exhibited declined memory, learning, and equilibrium capabilities, as well as marked anxiety behavior. *C. sinensis* significantly improved the physical development, neuromotor maturation, and behavioral performance in nicotine-exposed male and female newborns. In addition, *C. sinensis* prevented nicotine-induced tissue injury and lipid peroxidation and enhanced antioxidant defenses in the cerebellum and medulla oblongata of male and female newborns. In conclusion, this study shows that *C. sinensis* confers protective effects against perinatal nicotine-induced neurobehavioral alterations, tissue injury, and oxidative stress in mice newborns.

1. Introduction

Maternal smoking during pregnancy is a versatile risk factor that represents a public health concern [1]. Adverse perinatal outcomes and health complications, including respiratory disorders and childhood cancers, are associated with exposure to smoking in utero [2–4]. Additionally, low birth weight, premature birth, neonatal death, neural tube defects, and congenital anomalies have been identified as adverse effects of maternal smoking [5, 6].

Nicotine and its metabolite cotinine can readily cross the placenta and bind to the nicotinic acetylcholine receptors [7]. These receptors are known to be expressed by the second gestational week in rodents and in the first trimester in humans [8, 9]. The study of Berlin et al. [10] showed that cotinine concentrations in newborn's cord blood are similar to that of their smoking mothers. Through binding to these receptors, nicotine disturbs the cholinergic system, brain development, neuronal migration, synaptogenesis, and neurotransmitter release [11]. These nicotine-induced adverse effects can alter fetal brain development and produce neurobehavioral impairments later in life [1].

In this context, studies have demonstrated that maternal smoking during pregnancy leads to behavioral alterations in early childhood and can extend to young adulthood [12, 13]. Experimental animals exposed to tobacco alkaloid extracts showed delayed development of several behavioral patterns [14]. Nicotine exposure in utero resulted in memory and learning [15, 16] and sensory processing defects [17] in rodents. In clinical settings, newborns exposed to nicotine

in utero exhibited poor attention, increased tremors, hypertonicity, startle responses, irritability, and deficient speech processing [18–21]. Newborns also showed an attenuated response to auditory stimuli [20, 22]. This effect, later in life, can contribute to language and learning impairments [20, 22]. In addition, exposed infants showed poor self-regulation within the first month of life [23]. Thus, continuous exposure to nicotine during fetal development in utero and early developmental period of the pups after birth has bad impacts on the developing brain tissues and neurobehavioral and cognitive functions.

Excessive production of reactive oxygen species (ROS) plays a key role in nicotine-induced neurodevelopmental alterations [24]. Nicotine has been reported to induce oxidative stress both in vivo [25, 26] and in vitro [27]. Also, nicotine-induced cell death in various brain regions and memory impairment have been attributed to excessive ROS production [28–30].

Based on the previous findings, counteracting oxidative stress could represent an effective strategy to protect against nicotine-induced alterations in newborns. Therefore, the current study aimed to demonstrate the possible protective effects of green tea (*Camellia sinensis*) extract against perinatal nicotine-induced neurodevelopmental and behavioral alterations and oxidative stress in mice newborns. *C. sinensis* and its bioactive polyphenols are well-known to possess potent antioxidant and radical scavenging efficacies [31].

2. Materials and Methods

2.1. Preparation of C. sinensis Extract. Fresh leaves of *C. sinensis* were purchased from a local herbalist and ground to a powder using an electric grinder. Fifty g of the fine powder was added to one liter of boiled water and left for 15 min. The infusion was then filtered and freshly used.

2.2. Experimental Animals and Treatments. All the experimental protocols and investigations were approved and complied with the *Guide for Care and Use of Laboratory Animals* published by the US National Institutes of Health (NIH Publication Number 85–23, revised 1996) and was approved by the Ethics Committee for Animal Experimentation at King Saud University. Twenty-eight females and 14 males of Swiss Webster mice (*Mus musculus*) of 10–12 weeks were used in this study. The mice were obtained from the animal house of the College of Pharmacy, King Saud University, Riyadh, Saudi Arabia. The animals were housed in a well-ventilated animal's room in standard mice cages at a room temperature around 25°C and 12 h light/dark cycle. Standard rodent diet and water were supplemented ad libitum. The estrous cycle of females was estimated and each 3 proestrous females were housed with a male in a standard rodent mating cage for 12 h. The appearance of the vaginal plug in the morning was considered the first day of pregnancy. After mating, each dam has been incubated single in a cage where it will incubate its newborns after delivery. The date of birth for each dam was recorded. The number of newborns for each mother was fixed to be eight. The dates of appearance and development of external features such as eye opening, fur appearing, and body weights were recorded. The newborns were exposed to some behavioral investigations.

The mice were randomly divided into 4 groups; each comprises 4-5 mothers as following:

Group 1 (Control). Pregnant mice received distilled water by oral gavage from the first day of pregnancy (PD1) until the 15th day after birth (D15) and subcutaneously injected with physiological saline from the 12th day of pregnancy (PD12) until D15 after birth.

Group 2 (C. sinensis). Pregnant mice received 50 mg/kg body weight *C. sinensis* extract [32] by oral gavage from PD1 until D15 and subcutaneously injected with saline from the PD12 until D15.

Group 3 (Nicotine). Pregnant mice received distilled water by oral gavage from PD1 until D15, and subcutaneously injected with 0.25 mg/kg body weight nicotine (SOMATCO, Riyadh, KSA) [33] dissolved in saline from PD12 until D15.

Group 4 (Nicotine + C. sinensis). Pregnant mice received 50 mg/kg body weight *C. sinensis* extract by oral gavage from PD1 until D15 and subcutaneously injected with 0.25 mg/kg body weight nicotine (SOMATCO, Riyadh, KSA) dissolved in saline from PD12 until D15.

2.3. Behavioral Study

2.3.1. Righting Reflex. This reflex was conduct according to Ajarem and Ahmad [34] where the newborns examined at postnatal days (D) 1, 5, 10, 15, and 20 for male and female newborns by placing the newborn on its back. The time consumed till righting on its four limbs was measured and recorded. The response is negative when the righting time duration exceed 120 seconds.

2.3.2. Rotating Reflex. This reflex was conducted according to Ajarem and Ahmad [35]. Each animal was placed on the inclined surface at an angle of 30 degrees and the direction of its head down and was being monitored to be moving its body in the opposite direction and the time spent was recorded. This reflex was examined at D1, D5, D10, D15, and D20; the maximum duration of this test is 120 seconds.

2.3.3. Cliff Avoidance Reflex. The newborns (males and females) were placed on the edge of a wood piece above the ground, and then, the time spent till turning the back in opposite direction by half of circle at 180 degrees angle was recorded [36].

2.3.4. Locomotion Activity Reflex. This test was conducted for male and female newborns at D22 in the locomotory box as mentioned by Ajarem and Ahmad [37]. The newborns were examined for all activities such as number of squares crossed, number of rears, number of wall rears, number of cleaning, duration of locomotion, and duration of immobility.

2.3.5. Fear and Anxiety Reflex. This reflex was conducted at D25 for male and female newborns using the elevated perpendicular plus maze according to Abu-Taweel [38]. The newborns were placed in the middle of the maze at the intersection of the arms point facing the open

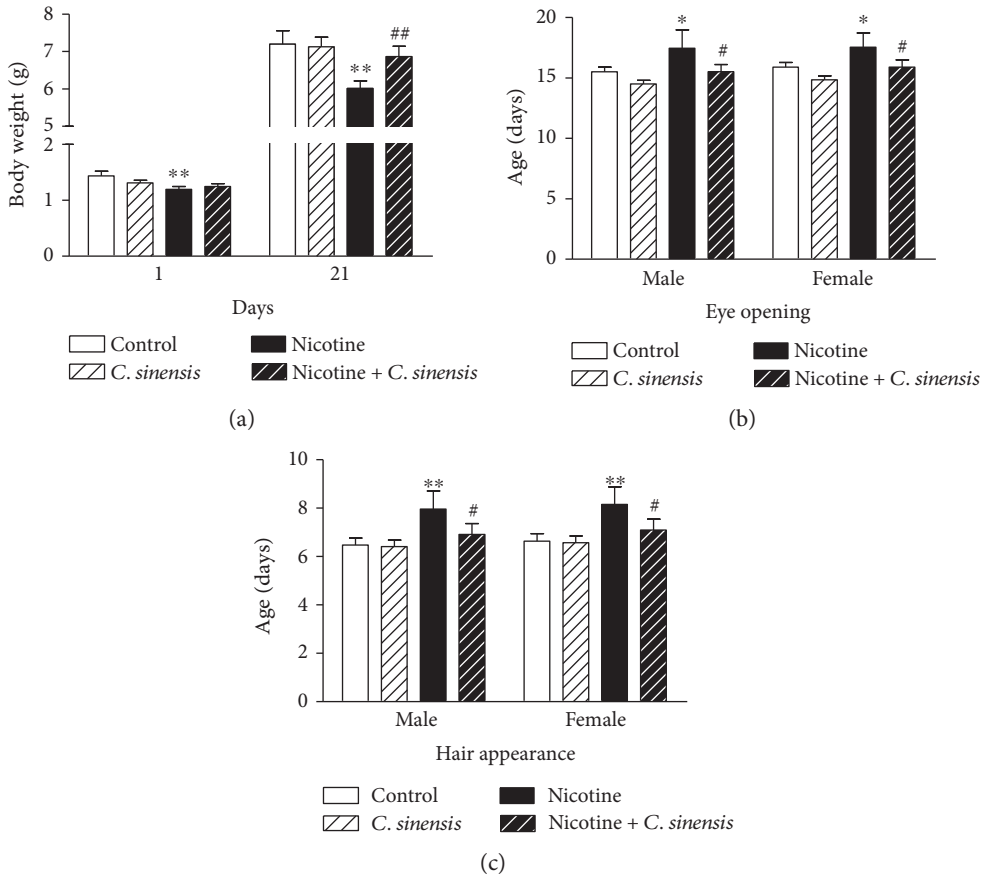

Figure 1: Effect of *C. sinensis* on (a) body weight, (b) hair appearance, and (c) eye opening in control and nicotine-induced mice newborns. Data are M ± SEM. $^{*}P < 0.05$ and $^{**}P < 0.01$ versus control. $^{\#}P < 0.05$ and $^{\#\#}P < 0.01$ versus nicotine.

arm. The examination time was 300 seconds with recording of all movements and activities, including the number of entries into the arms and center, and the time spent in the arms and center of the maze.

2.3.6. Equilibrium Reflex. This reflex was conducted at D30 using a rotarod instrument (Ugo Basile, Italy) as previously mentioned by Allam et al. [39]. The reflex measures the balance ability in the investigated mice. Each animal was placed on a horizontal rod which rotates slowly at 1 cycle/sec. The newborns will try to stay on the rod as more as they can, but finally, they fall. The instrument records the time which the animal spends on the rod. This time reflect the ability of the newborn to resist against falling.

2.3.7. Active Avoidance Reflex (Shuttle-Box Test). This reflex measures the memory and learning ability for the newborns and conducted according to the method described by Abu-Taweel et al. [40] using the shuttle-box-automated reflex conditioner (Ugo Basile, Italy). The newborns were investigated at D35, and the results were automatically recorded by the instrument. Each animal was exposed to the test for 30 trials. The lamp and the bell will be operated thirty times, and the electricity shocks depending on the animal's ability to learn. The healthy animals (who learn quickly) move from one room to another on seeing light of the lamp and hearing the bell directly to prevent stun electricity. The test begins by placing the animal in one of the two rooms and leaving it while it explores the place, then the actual test starts, which ends with the thirtieth over again, and this period can be less than the animal's ability to learn (to escape when it sees the lamp and hears the bell).

2.4. Biochemical and Histological Study. At D7, D15, and D30 after birth, 6 pups from each group were sacrificed by decapitation, and samples were collected. Samples from the cerebellum and medulla oblongata were homogenized in cold phosphate-buffered saline and used for assaying lipid peroxidation [41], reduced glutathione (GSH) [42], and superoxide dismutase (SOD) activity [43]. Other samples from the cerebellum and medulla oblongata were fixed in neutral-buffered formalin and processed for staining with hematoxylin and eosin.

2.5. Statistical Analysis. The data were analyzed by one- or two-way ANOVA followed by Tukey's test post hoc analysis using GraphPad Prism version 5 (San Diego, CA, USA). The obtained results were presented as mean ± standard error (SEM) with a P value less than 0.05 being considered significant.

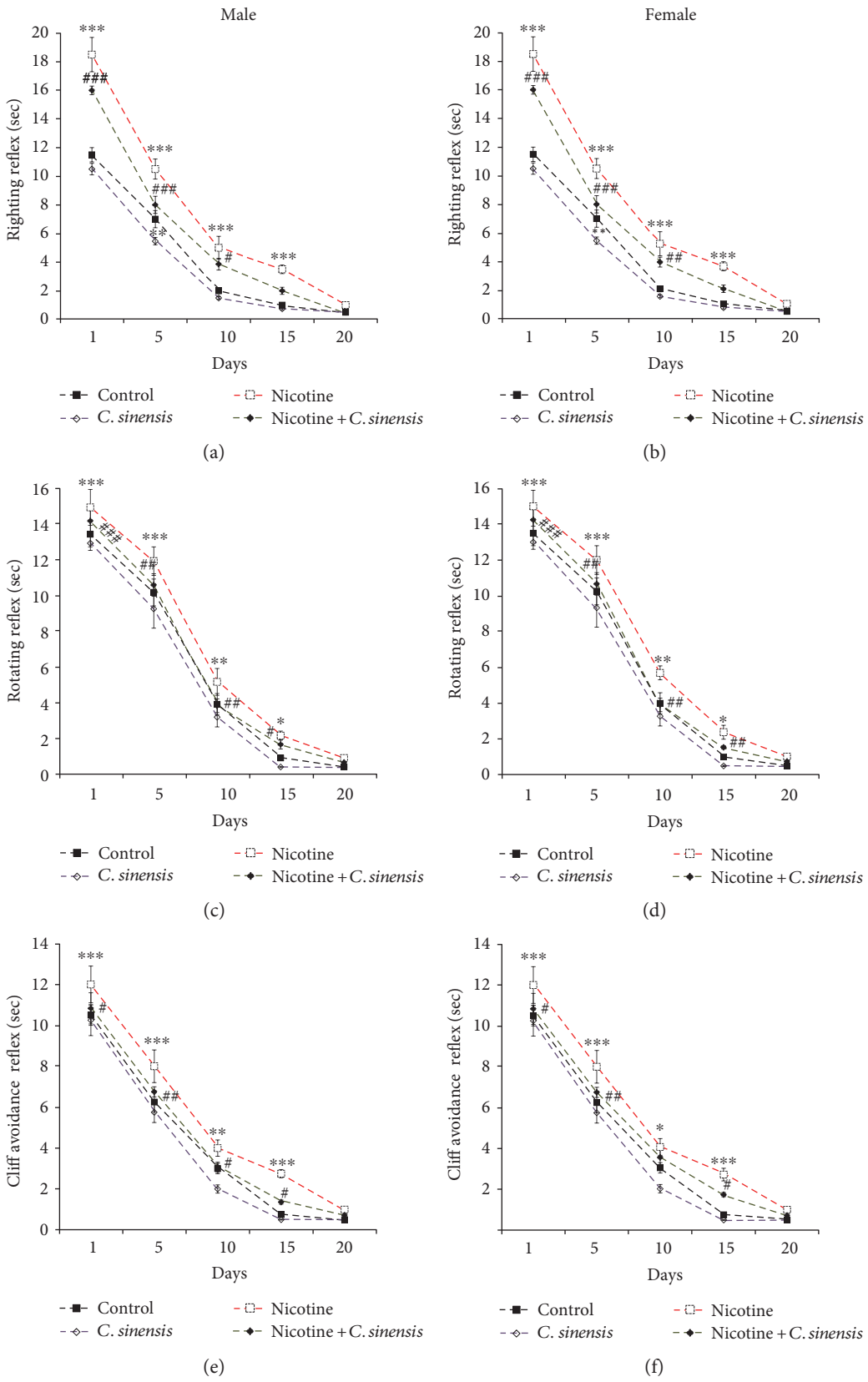

Figure 2: *C. sinensis* prevents nicotine-induced suppression of (a-b) righting, (c-d) rotating, and (e-f) cliff avoidance reflexes in mice newborns. Data are M ± SEM. $^{*}P < 0.05$, $^{**}P < 0.01$, and $^{***}P < 0.001$ versus control. $^{\#}P < 0.05$, $^{\#\#}P < 0.01$, and $^{\#\#\#}P < 0.001$ versus nicotine.

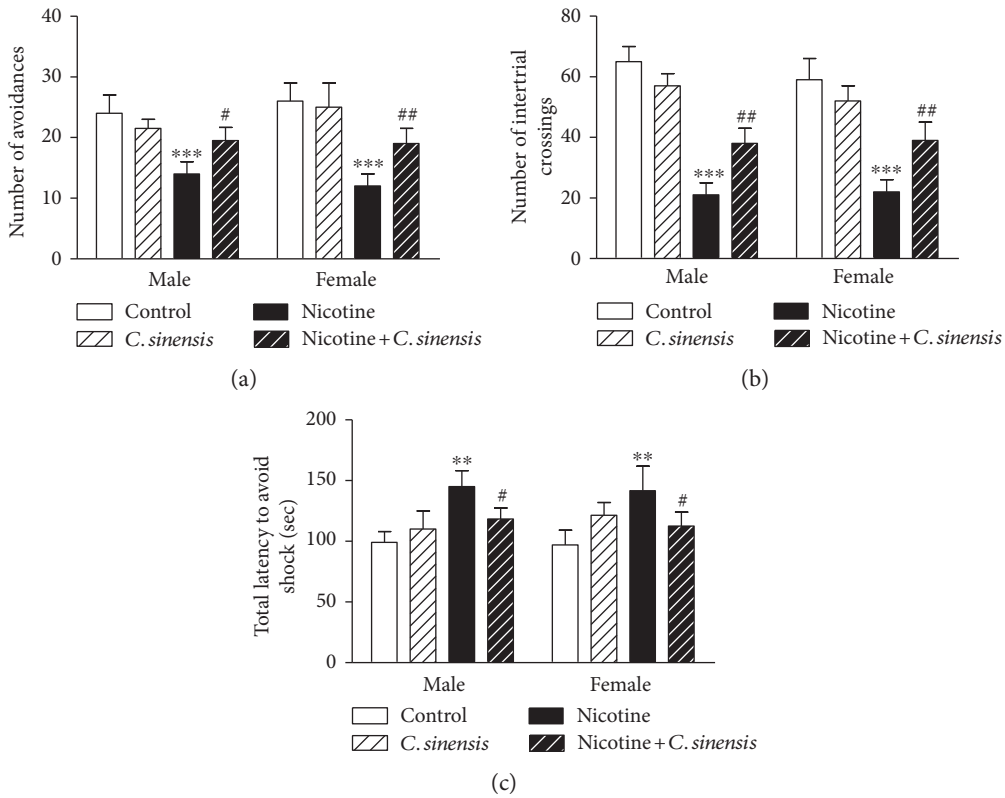

Figure 3: *C. sinensis* improves active avoidance responses in nicotine-exposed mice newborns. Data are M ± SEM. $^{**}P < 0.01$ and $^{***}P < 0.001$ versus control. $^{\#}P < 0.05$ and $^{\#\#}P < 0.01$ versus nicotine.

3. Results

3.1. Effect of C. sinensis on Body Weight, Hair Appearance, and Eye Opening in Control and Nicotine-Induced Mice Newborns. Body weight, eye opening, and hair appearance were determined as physical assessments during the weaning period. Body weight of the nicotine-induced mice newborns showed a significant ($P < 0.01$) decrease at D1 and D21 after birth when compared with that of the control group (Figure 1(a)). *C. sinensis* supplementation produced a nonsignificant ($P > 0.05$) effect on body weight of either control or nicotine-exposed mice offspring at D1. Supplementation of *C. sinensis* to nicotine-exposed pregnant mice significantly ($P < 0.01$) improved body weight of the newborns at D21 after birth. Similar effects were recorded in both male and female newborns.

C. sinensis supplementation produced nonsignificant ($P > 0.05$) effects on eye opening in both male and female mice offspring (Figure 1(b)). Both male and female nicotine-induced mice newborns showed a significant ($P < 0.05$) delay in eye opening when compared with the control groups. *C. sinensis* administration significantly ($P < 0.05$) prevented the nicotine-induced delay in eye opening in both genders.

Male and female mice born to nicotine-induced mothers showed a significant ($P < 0.01$) delay in hair appearance. Treatment of the nicotine-induced mice with *C. sinensis* significantly ($P < 0.05$) prevented the delay in hair appearance in both male and female newborns (Figure 1(c)). *C. sinensis* supplementation exerted nonsignificant ($P > 0.05$) effect on hair appearance time in either male or female newborns.

3.2. C. sinensis Prevents Nicotine-Induced Neurobehavioral Alterations in Mice Newborns

3.2.1. Neuromotor Maturation. To evaluate the effect of nicotine on the maturation of neuromotor reflexes and the protective efficacy of *C. sinensis*, the righting, rotating, and cliff avoidance reflexes were determined at D1, D5, D10, D15, and D20 after birth.

The righting reflex was significantly ($P < 0.001$) suppressed at D1, D5, D10, and D15 after birth in nicotine-exposed male (Figure 2(a)) and female (Figure 2(b)) newborn mice when compared with the corresponding controls. *C. sinensis* supplementation significantly ($P < 0.001$) improved the righting reflex at D1 and D5 in male and female newborns. At D15, the righting reflex showed significant amelioration in *C. sinensis*-treated male ($P < 0.05$) and female ($P < 0.01$) nicotine-induced newborns.

The rotating reflex showed a similar pattern where nicotine-exposed mice newborns showed reduced performance of the rotating reflex at D1 ($P < 0.001$), D5 ($P < 0.001$), D10 ($P < 0.01$), and D15 ($P < 0.05$) after birth. Treatment of the nicotine-exposed mice with *C. sinensis* significantly improved the rotating reflex throughout the weaning period in both male (Figure 2(c)) and female (Figure 2(d)) offspring.

Table 1: Effect of perinatal nicotine exposure and *C. sinensis* extract on the locomotor activity of mice newborns at adolescent age (postnatal day 22).

		Control	*C. sinensis*	Nicotine	Nicotine + *C. sinensis*
Number of squares crossed	Male	210.5 (170–230)	303* (193–320)	110*** (99–133)	157**# (153–170)
	Female	190.5 (170–211)	289* (188–310)	112*** (87–123)	145**# (134–165)
Wall rears	Male	20.5 (15–22)	27* (21–31)	11*** (10–15)	9**# (1–16)
	Female	19 (10–25)	25* (22–36)	10*** (9–14)	9**# (1–10)
Rears	Male	6 (0–14)	8* (3–13)	4 (1–4)	5 (1–6)
	Female	6 (1–11)	9* (1–14)	6 (3–11)	5 (1–11)
Wash	Male	5 (5–25)	11 (5–15)	15* (11–19)	6 (1–14)
	Female	12 (3–14)	13 (4–19)	16 (10–20)	8 (6–11)
Locomotion duration (sec)	Male	202 (173–268)	274* (261–291)	98*** (77–132)	167*# (120–187)
	Female	189 (153–256)	263* (254–282)	105*** (89–122)	154*# (110–187)
Immobility duration (sec)	Male	98 (41–127)	26* (9–39)	140.5** (101–188)	131**# (100–166)
	Female	102 (55–121)	33* (11–44)	122** (119–176)	143**# (106–153)

Date are M ± SEM. $^{*}P < 0.05$, $^{**}P < 0.01$, and $^{***}P < 0.001$ versus control, and $^{\#}P < 0.05$ versus nicotine.

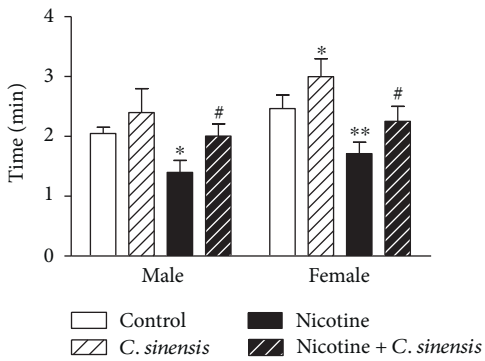

Figure 4: *C. sinensis* alleviates equilibrium reflex in nicotine-exposed mice newborns. Data are M ± SEM. $^{*}P < 0.05$ and $^{**}P < 0.01$ versus control. $^{\#}P < 0.05$ versus nicotine.

Regarding the cliff avoidance, male nicotine-exposed offspring showed significantly declined reflex at D1 ($P < 0.001$), D5 ($P < 0.001$), D10 ($P < 0.01$), and D15 ($P < 0.001$) after birth (Figure 2(e)). Similarly, the nicotine-exposed female newborn exhibited significant suppression in the cliff avoidance reflex at D1 ($P < 0.001$), D5 ($P < 0.001$), D10 ($P < 0.05$), and D15 ($P < 0.001$) after birth (Figure 2(f)). Treatment of the nicotine-exposed mice with *C. sinensis* significantly improved the cliff avoidance reflex in both male and female offspring.

Of note, supplementation of *C. sinensis* did not induce any significant changes in the neuromotor reflexes of the control group.

3.2.2. Active Avoidance Test. The effect of *C. sinensis* supplementation on memory and learning ability in control and nicotine-induced newborns was measured using the shuttle-box test.

Nicotine significantly ($P < 0.001$) decreased the number of avoidances during the trial period in both male and female offspring when compared with that in the corresponding controls (Figure 3(a)). *C. sinensis* supplementation improved the number of avoidances in nicotine-induced both male ($P < 0.05$) and female ($P < 0.01$) mice offspring, with no effect on control mice.

Nicotine-induced male and female newborns showed a significant ($P < 0.001$) decrease in the number of intertrial crossings between the chambers in the absence of shock, an effect that was significantly ($P < 0.01$) ameliorated following treatment with *C. sinensis* extract (Figure 3(b)). *C. sinensis* produced a nonsignificant ($P > 0.05$) effect on the number of intertrial crossings when supplemented to control mice.

The total time taken to avoid the shock during the entire trials was measured. As depicted in Figure 3(c), nicotine-induced both male and female mice offspring were poor learners and took significantly ($P < 0.01$) longer time in avoiding the shock when compared with the control group. Supplementation of *C. sinensis* extract markedly ($P < 0.05$) improved the learning ability of nicotine-induced male and female mice newborn, with no effect on the learning ability of control mice.

3.2.3. Locomotor Activity Test. Nicotine-induced weaned male mice showed significant decrease in the number of squares crossed ($P < 0.001$), wall rears ($P < 0.05$), and locomotion duration ($P < 0.001$) when compared with the control group (Table 1). On the other hand, the number of washes and the immobility duration were significantly increased in the nicotine-induced animals. *C. sinensis* supplementation produced a marked amelioration in all elements of the locomotor activity in both control and nicotine-induced weaned mice.

In female-weaned nicotine-induced mice, the number of squares crossed, wall rears, and locomotion duration were significantly ($P < 0.001$) decreased with a concomitant significant ($P < 0.01$) increase in the immobility duration (Table 1). However increased, the number of washes showed a nonsignificant ($P > 0.05$) change in nicotine-induced female weaned mice when compared with the corresponding control group. *C. sinensis* supplementation significantly

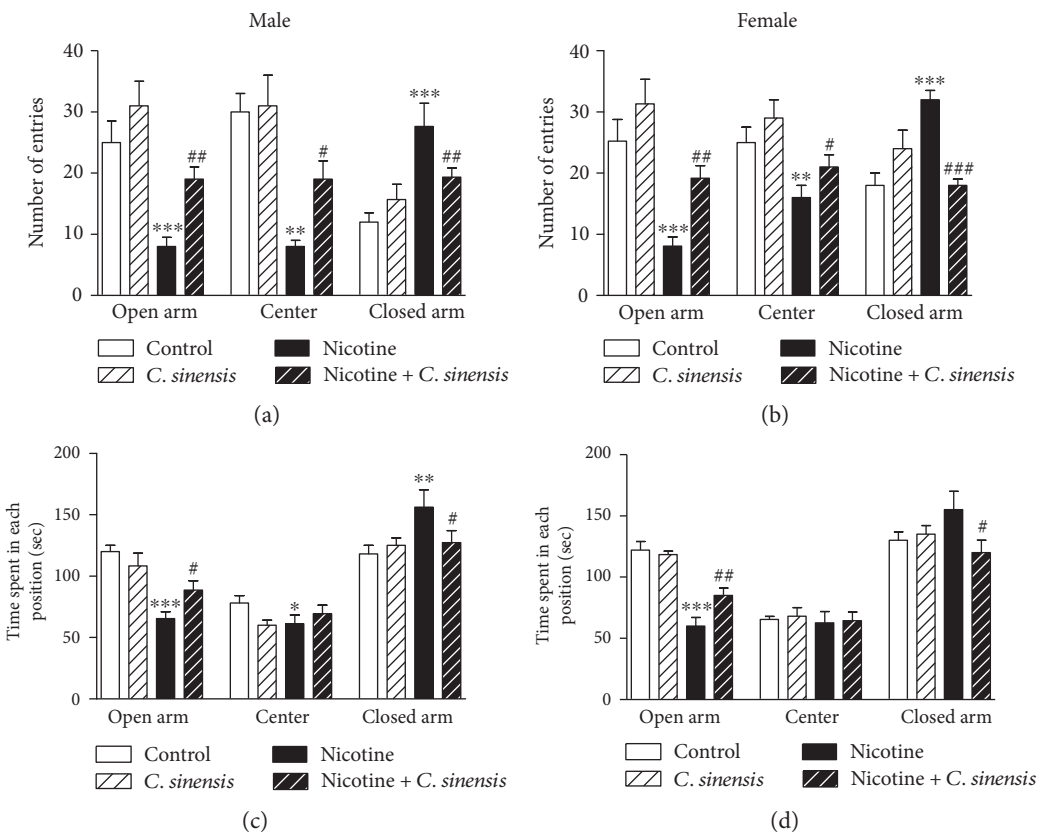

Figure 5: Protective effect of *C. sinensis* against nicotine-induced anxiety in mice newborns. Data are M ± SEM. $^{*}P < 0.05$, $^{**}P < 0.01$, and $^{***}P < 0.001$ versus control. $^{\#}P < 0.05$, $^{\#\#}P < 0.01$, and $^{\#\#\#}P < 0.001$ versus nicotine.

improved the locomotor activity in both control and nicotine-induced female mice.

3.2.4. Equilibrium Reflex. In the rotarod test, *C. sinensis* significantly ($P > 0.05$) increased the time that the mice spent on the rotating rod in female but not in male animals (Figure 4). Nicotine administered during the pregnancy period significantly affected the balance ability of the animals as evidenced by the decreased time spent on the rotating rod by both male ($P < 0.05$) and female ($P < 0.01$) mice. *C. sinensis* extract produced a significant ($P < 0.05$) improvement in the balance ability of nicotine-induced both male and female mice.

3.2.5. Anxiety Behavior in the Elevated Plus-Maze Test. The elevated plus maze is frequently used to evaluate the anxiety-like behavior in animal models [44]. In the present study, administration of nicotine during gestation significantly reduced the number of entries and the time spent to explore the open arm ($P < 0.001$) in both male (Figure 5(a)) and female (Figure 5(b)) newborn mice. *C. sinensis* significantly ($P < 0.01$) increased the number of entries to explore the open arm. Similarly, the time spent to explore the open arm was significantly increased in nicotine-induced male (Figure 5(c); $P < 0.05$) as well as female (Figure 5(d); $P < 0.01$) mice newborns. *C. sinensis* affected neither the number of entries nor the time spent to explore the open arm when supplemented to control mice.

On the contrary, nicotine administration during pregnancy significantly increased the number of entries and the time spent in the closed arm in both male and female mice newborn. *C. sinensis* supplementation significantly decreased the number of entries and time spent in the closed arm in nicotine-induced both male and female mice.

3.3. C. sinensis Prevents Nicotine-Induced Histological Alterations in the Cerebellum and Medulla Oblongata of Mice Newborns. The cerebellar histological sections of all groups showed the neural fold layer structures at D7, D15, and D30. In normal newborns, the external granular layer appeared wide at D7 (Figure 6(a)), thin at D15 (Figure 6(b)), and disappeared completely at D30 (Figure 6(c)). The molecular layer was defined at D7, wide at D15, and incubated by mature neurons at D30. The Purkinje cells were arranged in one row at D7 to form a Purkinje cell layer. The Purkinje cells became more developed and mature at D15 and D30. The internal granular layer received the migrated cells from the external granular layer, so it appeared condensed at the three investigated ages. The cerebellar sections of the *C. sinensis*-administered group showed well-developed cerebellar fold layers similar to those of the normal newborns (Figures 6(d), 6(e), and 6(f)). In the nicotine-exposed group, some aberrations in the cerebellar fold layers appeared including a delay in the external granular layer cell migration to internal granular layer that was reflected by the wide external granular layer at D7

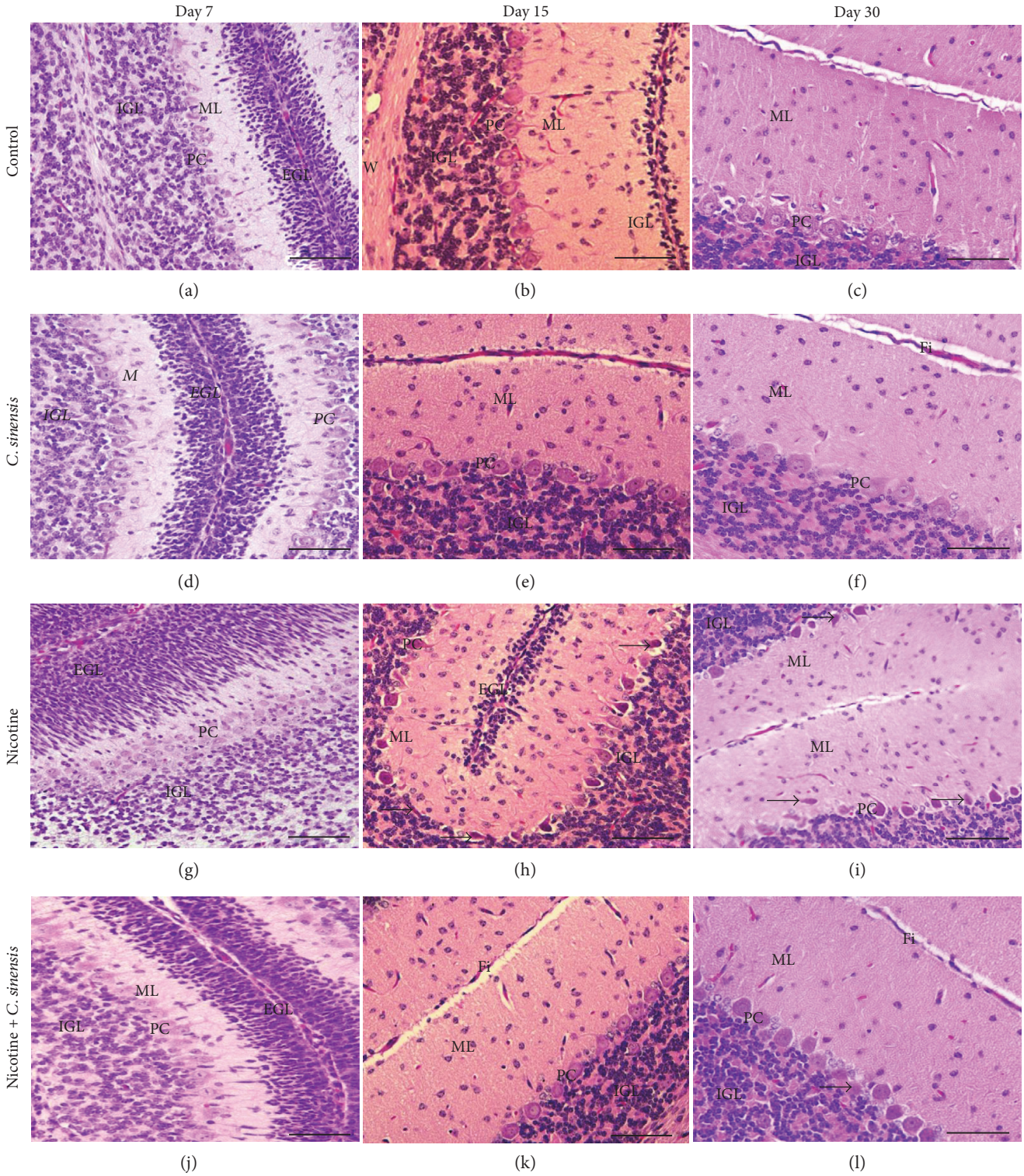

Figure 6: Sagittal sections in the cerebellum of (a–c) control newborns showing wide external granular layer (EGL) at day 7 which become thin at day 15 and disappeared at day 30. The molecular layer (ML) is defined at day 7, wide at day 15, and incubated by mature neurons at day 30. The Purkinje cells (PC) appear arranged in one row at day 7 and become more developed and mature at day 15 and day 30. The internal granular layer (IGL) received the migrated cells from the external granular layer, so it appears condensed at the three investigated ages. (d–f) The *C. sinensis*-administered group showing well-developed cerebellar fold layers similar to those of normal newborns. (g–i) The nicotine-exposed group showing a delay in the external granular layer cell migration to internal granular layer reflected by the wide external granular layer at day 7 and day 15. Purkinje cells are arranged in more than one row and appear abnormal, small, and spindle in shape. (j–l) Sections in the cerebellum of *C. sinensis*-supplemented nicotine-induced mice newborns showing improved histological structure. Scale bar = 50 μm.

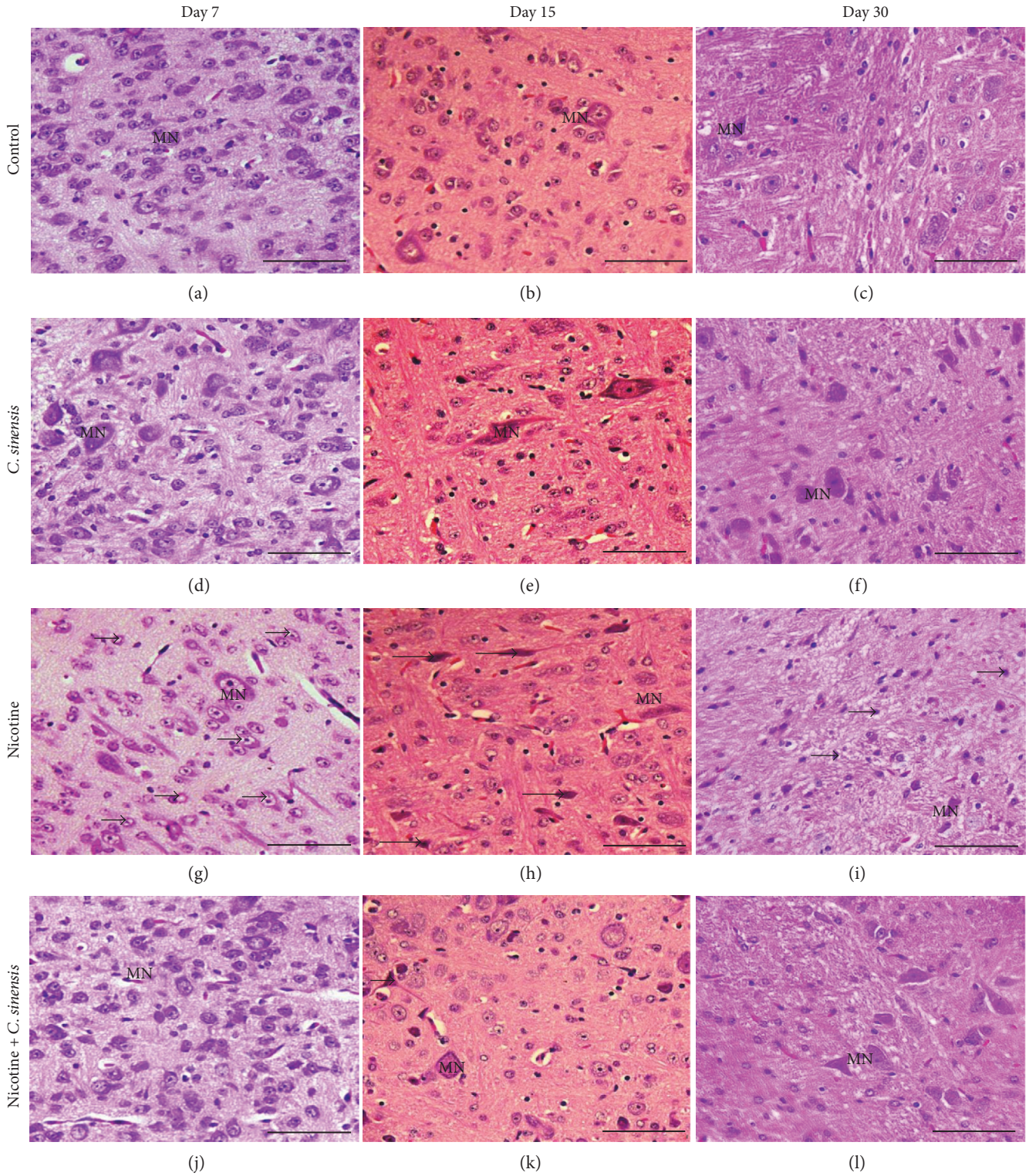

Figure 7: Sagittal sections in the medulla oblongata of (a–c) control newborns showing normal state and distribution of medullary neurons, (d–f) the *C. sinensis*-administered group showing normal histological structures of the medullary neurons, (g–i) the nicotine-exposed group revealing pyknosis and chromatolysis (arrow) of the medullary neurons (MN), and (j–l) the *C. sinensis*-supplemented nicotine-induced mice newborns showing normal histology of the medulla oblongata. Scale bar = 50 μm.

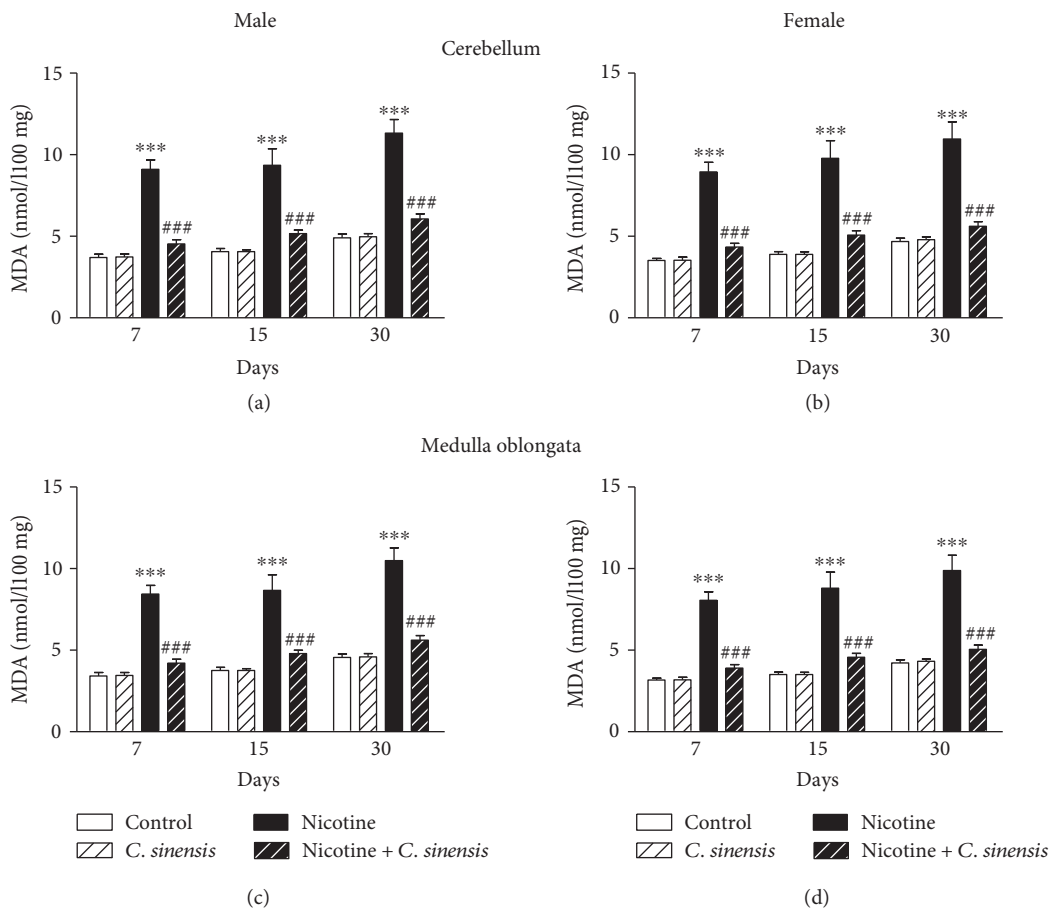

Figure 8: *C. sinensis* protects against nicotine-induced lipid peroxidation in the cerebellum and medulla oblongata of mice newborns. Data are M ± SEM. $^{***}P < 0.001$ versus control and $^{###}P < 0.001$ versus nicotine.

(Figure 6(g)) and D15 (Figure 6(h)) when compared with the control group. Purkinje cells appeared arranged in more than one row at D7. At D15 and D30 (Figure 6(i)), Purkinje cells appeared abnormal, small, and spindle in shape. Supplementation of *C. sinensis* prevented nicotine-induced malformations in the cerebellum of mice newborns at D7 (Figure 6(j)), D15 (Figure 6(k)), and D30 (Figure 6(l)).

Histological examination of the medulla oblongata sections of control newborns at D7 (Figure 7(a)), D15 (Figure 7(b)), and D30 (Figure 7(c)) showed normal state and distribution of medullary neurons. The *C. sinensis*-administered group showed normal histological structures of the medullary neurons (Figures 7(d), 7(e), and 7(f)). Perinatal nicotine exposure induced pyknosis and chromatolysis of the medullary neurons at D7 (Figure 7(g)), D15 (Figure 7(h)), and D30 (Figure 7(i)). Nicotine-induced mice newborns treated with *C. sinensis* showed normal histology of the medulla oblongata at D7 (Figure 7(j)), D15 (Figure 7(k)), and D30 (Figure 7(l)). Similar findings were observed in both male and female mice offspring.

3.4. C. sinensis Attenuates Nicotine-Induced Oxidative Stress in the Cerebellum and Medulla Oblongata of Mice Newborns. Lipid peroxidation, GSH, and SOD were determined to evaluate the protective effect of *C. sinensis* against nicotine-induced oxidative stress in the cerebellum and medulla oblongata of newborn mice.

Cerebellar lipid peroxidation showed a significant ($P < 0.001$) increase in nicotine-induced male (Figure 8(a)) and female (Figure 8(b)) mice newborns at D7, D15, and D30 after birth, an effect that was significantly ($P < 0.001$) prevented by *C. sinensis*. In the cerebellum of control male and female mice offspring, supplementation of *C. sinensis* produced nonsignificant ($P < 0.05$) effect on lipid peroxidation levels at all experimental periods.

In the medulla oblongata, nicotine induced a significant ($P < 0.001$) increase in lipid peroxidation levels in both male (Figure 8(c)) and female (Figure 8(d)) mice offspring. Oral supplementation of *C. sinensis* extract significantly ($P < 0.001$) decreased lipid peroxidation in the medulla oblongata of nicotine-induced both male and female newborn mice at D7, D15, and D30. *C. sinensis* extract produced nonsignificant ($P > 0.05$) effects on lipid peroxidation levels in the medulla oblongata of control mice offspring.

GSH content in the cerebellum of nicotine-induced male newborns showed significant decrease at D7 ($P < 0.01$), D15 ($P < 0.001$), and D30 ($P < 0.001$) after birth (Figure 9(a)). Oral supplementation of *C. sinensis* extract during pregnancy exerted nonsignificant ($P > 0.05$) effect on GSH levels at D7 while producing a significant increase at D15 ($P < 0.05$) and

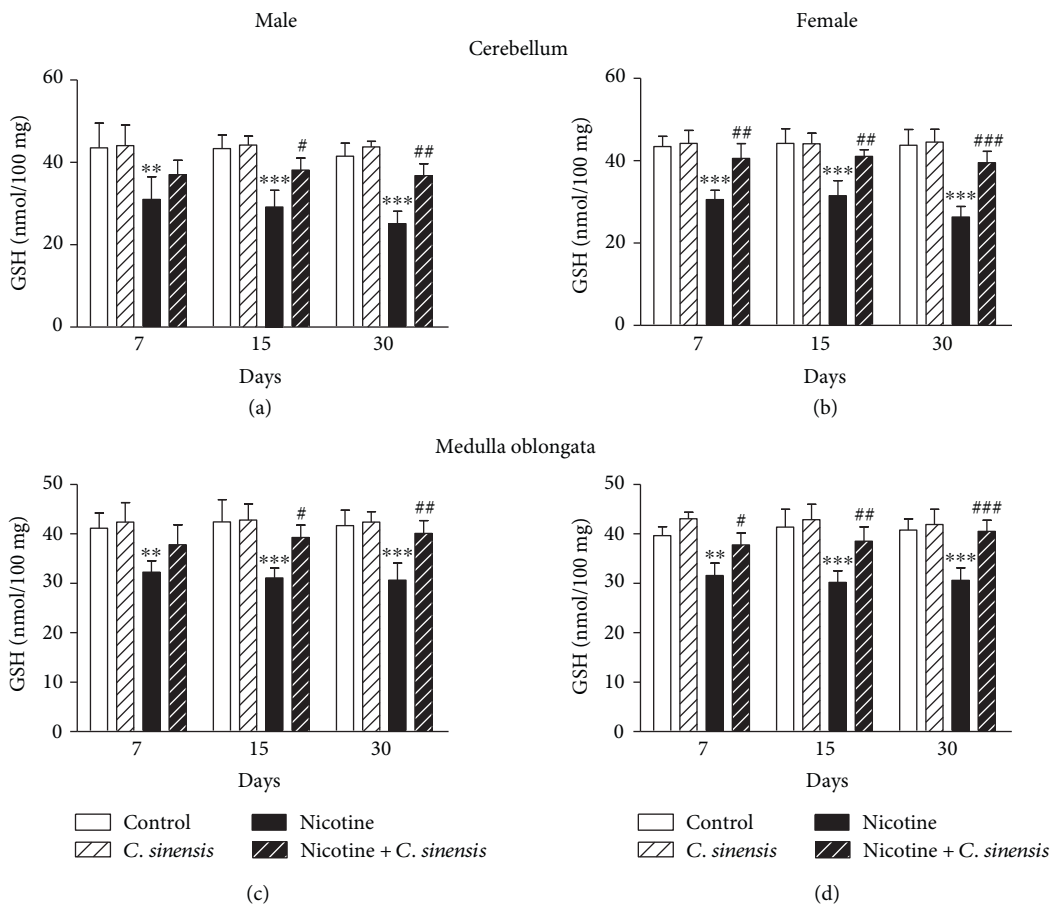

Figure 9: *C. sinensis* alleviates GSH levels in the cerebellum and medulla oblongata of nicotine-induced mice newborns. Data are M ± SEM. $^{**}P < 0.01$ and $^{***}P < 0.001$ versus control. $^{\#}P < 0.05$, $^{\#\#}P < 0.01$, and $^{\#\#\#}P < 0.001$ versus nicotine.

D30 ($P < 0.01$) in the cerebellum of nicotine-induced male offspring. Nicotine-induced female mice newborns exhibited a significant ($P < 0.001$) decrease in the cerebellar GSH levels at D7, D15, and D30 after birth (Figure 9(b)). *C. sinensis* ameliorated the cerebellar GSH levels in nicotine-induced mice newborns at D7 ($P < 0.01$), D15 ($P < 0.01$), and D30 ($P < 0.001$) after birth.

Nicotine-induced male and female mice offspring showed significant decrease in medulla oblongata GSH levels at D7 ($P < 0.01$), D15 ($P < 0.001$), and D30 ($P < 0.001$) after birth. *C. sinensis* significantly ameliorated GSH levels in the medulla oblongata of nicotine-induced male mice offspring at D15 ($P < 0.05$) and D30 ($P < 0.01$); however, its effect at D7 was nonsignificant (Figure 9(c)). In nicotine-induced female mice newborns, *C. sinensis* supplementation significantly increased GSH levels in the medulla oblongata at D7 ($P < 0.05$), D15 ($P < 0.01$), and D30 ($P < 0.001$) after birth (Figure 9(d)).

C. sinensis exerted nonsignificant effect on the levels of GSH in the cerebellum and medulla oblongata of both control male and female mice newborn at all experimental periods.

SOD activity in the cerebellum of nicotine-induced male (Figure 10(a)) and female (Figure 10(b)) mice offspring showed a significant ($P < 0.001$) decrease at D7, D15, and D30 after birth, an effect that was significantly ($P < 0.001$) prevented by *C. sinensis*. In the cerebellum of control male and female mice offspring, *C. sinensis* exerted nonsignificant ($P > 0.05$) effect on SOD activity at all experimental periods.

In the medulla oblongata, nicotine induced a significant ($P < 0.001$) decline in SOD activity in both male (Figure 10(c)) and female (Figure 10(d)) mice offspring. Oral supplementation of *C. sinensis* extract significantly ($P < 0.001$) improved SOD activity in the medulla oblongata of both male and female newborn mice at D7, D15, and D30 while exerting nonsignificant ($P > 0.05$) effect in control mice offspring.

4. Discussion

Cigarette smoking is a common problem and 10–15% women continue smoking during pregnancy even with the well-known detrimental outcomes in newborns [12, 45, 46]. Because of the dynamic nature of developmental processes, the central nervous system is vulnerable to damage by environmental toxins during fetal and early postnatal life [45, 47]. Abnormal behaviors in offspring have been associated with maternal smoking during pregnancy. These neurodevelopmental adverse effects might extend through adolescence and adulthood [12, 46]. In the present study, we demonstrated the potential protective effect of *C. sinensis* against perinatal nicotine-induced neurodevelopmental alterations in male and female offspring.

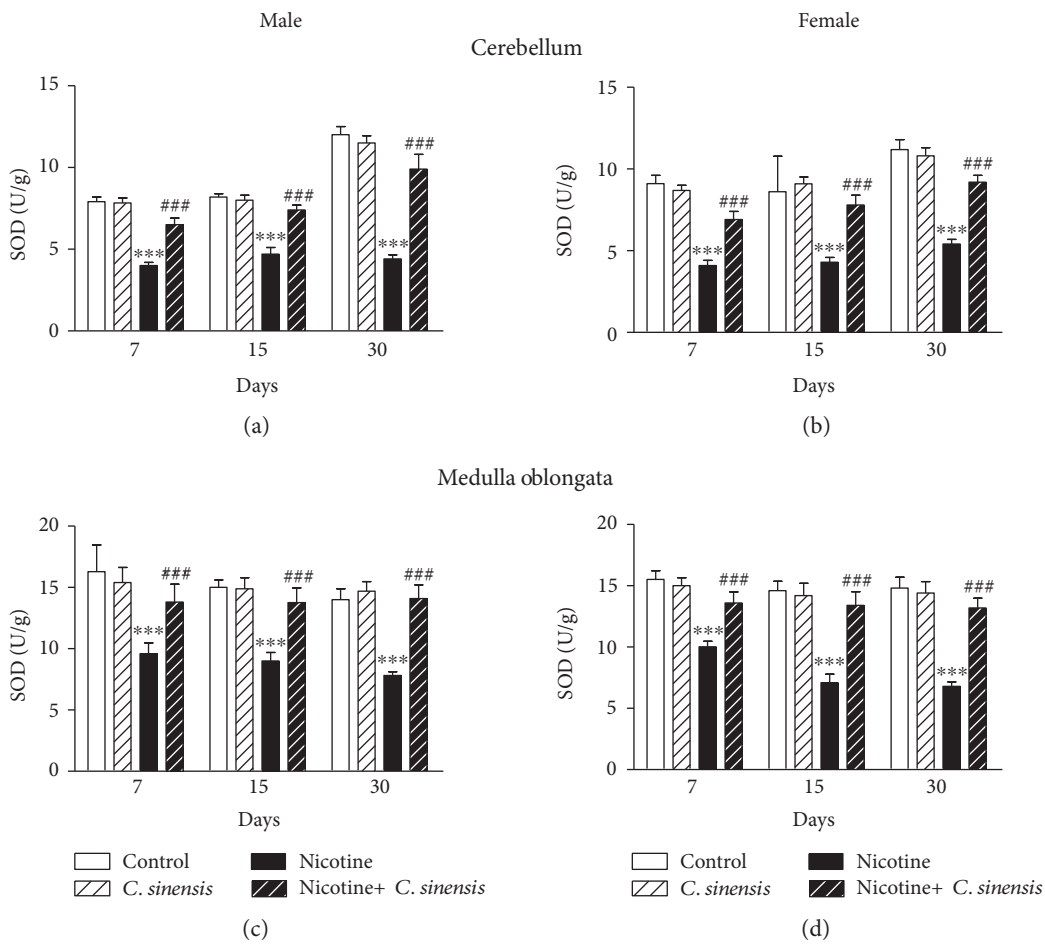

Figure 10: *C. sinensis* enhances SOD activity in the cerebellum and medulla oblongata of nicotine-induced mice newborns. Data are M ± SEM. $^{***}P < 0.001$ versus control and $^{###}P < 0.001$ versus nicotine.

Male and female offspring born to mice exposed to nicotine during pregnancy and lactation showed declined body weight and a delay in eyes opening and body hair appearance, indicating the adverse effects of nicotine on the physical growth in mice offspring. Maternal exposure to nicotine during pregnancy has been associated with reduced fat index in monkeys [48] and fetal body weight in rats [49, 50]. The declined body weight could be also explained, at least in part, by the increased lipolysis [51], energy expenditure, and metabolic rate [52]. These experimental data were supported by the clinical findings where infants, exposed to nicotine during the third trimester, showed smaller body weight at birth [18, 53]. Recently, Chan et al. [54] reported decreased body weight of male mice born to mice exposed to cigarette smoke. Oral supplementation of *C. sinensis* significantly prevented nicotine-induced in utero growth retardation. This physical improvement could be explained in terms of improved energy homeostasis by *C. sinensis*.

Nicotine and its metabolite cotinine pass through the placenta and bind to the nicotinic acetylcholine receptors [7], which are expressed by the second gestational week in rodents and in the first trimester in humans [8, 9]. Studies have demonstrated that the developmental exposure to nicotine disturbs the cholinergic system and therefore disrupts brain development, neuronal migration, synaptogenesis, and neurotransmitter release [11]. These adverse effects might produce neurobehavioral impairments in the offspring.

Here, perinatal exposure to nicotine markedly affected the motor development, active avoidance response, and locomotory behavior. The righting, rotating, and cliff avoidance reflexes were significantly suppressed in male and female pups born to mothers exposed to nicotine. These findings suggest a direct impact of nicotine exposure in utero and during lactation period on the neuromotor development.

Nicotine-induced male and female mice newborns showed declined memory and learning ability as measured by the shuttle-box test. Additionally, the mice took longer time exploring the closed arm while spending short time to explore the open arm, therefore, showing increased anxiety-like behavior. Furthermore, nicotine-exposed male and female mice showed suppressed locomotory activity and equilibrium reflex.

In line with our findings, the study of Khalki et al. [14] demonstrated delayed development of similar behavioral patterns in rats exposed to tobacco alkaloid extracts. Studies have also reported poor performance of memory and learning test, including two-way active avoidance [16] and the radial arm maze [15, 55] in rodents exposed to nicotine in

utero. Perinatal exposure to nicotine can also lead to spatial memory deficits [56]. Mice in the radial arm maze took longer time to reach the criterion when injected with nicotine [57]. Moreover, mice exposed to nicotine exhibited sensory processing defects evidenced by hypersensitive passive avoidance [17]. These experimental data were in agreement with multiple clinical findings where exposure to nicotine in utero induced several alterations, including poor attention, increased tremors, hypertonicity, startle responses, irritability, and deficient speech processing in newborns [18–21]. In addition, infants exposed to nicotine in utero showed an attenuated response to auditory stimuli which, later in life, can possibly lead to language and learning impairments [20, 22].

Interestingly, supplementation of *C. sinensis* to mice markedly prevented nicotine-induced neurobehavioral alterations. *C. sinensis* significantly improved motor development, active avoidance responses, locomotory behavior, equilibrium reflex, and memory and learning ability.

We thought that the protective effects of *C. sinensis* extract originate from its ability to counteract nicotine-induced tissue damage and oxidative stress. Nonhuman primates exposed to tobacco smoke during gestation and lactation exhibited neuronal cell loss and decreased cell size [58]. Juvenile and adult rats exposed to nicotine in utero showed changes in dendritic length and dendritic branching [59]. Pauly and Slotkin [60] stated that these changes can alter the development and contribute to functional deficits later in life. The study of Ernst et al. [61] attributed impaired cognitive function in prenatal nicotine-exposed rats to a disruption of neuronal migration in the brain. In the present study, nicotine induced a delay in cell migration from the external granular layer to the internal layer and altered shape and pyknosis in Purkinje cells in the cerebellum and chromatolysis of neurons in the medulla oblongata, an effect that was markedly prevented in the *C. sinensis*-supplemented groups. These findings highlight the efficacy of *C. sinensis* in preventing cell damage induced by nicotine.

Attenuation of oxidative stress and alleviation of the antioxidant defenses is another mechanism we hypothesized to contribute to the protective effect of *C. sinensis* on nicotine-induced neurodevelopmental and behavioral changes in mice newborn. Our hypothesis is supported by findings of multiple studies demonstrating alleviated neurobehavioral performance in experimental animals supplemented with antioxidants [30, 62]. Previous studies have attributed memory impairment following prenatal nicotine exposure to excessive production of ROS and its subsequent cell death in various brain regions [28–30]. Because the cerebellum is involved in motor control, cognitive functions, and regulating fear and pleasure and the medulla oblongata is responsible for the regulation of reflexes, we assayed lipid peroxidation and antioxidant defenses in these brain regions. Exposure to nicotine increased lipid peroxidation in the cerebellum and medulla oblongata of both male and female newborns as evidenced by the elevated levels of MDA. On the other hand, GSH and SOD were significantly declined in the cerebellum and medulla oblongata of male and female newborns. These alterations were observed at D7, D15, and D30 after birth. Brain neurons are sensitive to oxidative stress [63], and maternal nicotine and cigarette smoke exposure has been confirmed to induce oxidative stress in the brain of offspring. Chan et al. [54] demonstrated increased oxidative stress and declined antioxidant defenses in the brain of mice offspring whose mothers were exposed to cigarette smoke during pregnancy. Recently, we reported increased lipid peroxidation and declined antioxidants in the cerebrum of offspring born to mice exposed to nicotine during gestation and early period of lactation [26].

C. sinensis supplementation during pregnancy and early postnatal period significantly prevented nicotine-induced lipid peroxidation and improved the antioxidant defenses in the cerebellum and medulla oblongata of both male and female newborns. Therefore, we assumed that the antioxidant potential of *C. sinensis* protected the newborns against nicotine-induced oxidative stress, cell death, and neurodevelopmental alterations. The antioxidant efficacy of *C. sinensis* and its active constituents such as polyphenols has been well-established in several studies [64, 65]. Polyphenols of *C. sinensis* prevented 6-hydroxydopamine-induced damage of dopaminergic neurons in a rat model of Parkinson's disease [66]. Epigallocatechin-3-gallate (EGCG), a major bioactive catechin of *C. sinensis*, protected the rat cortex against acrylamide-induced apoptosis and astrogliosis [64] and oxidative stress in PC12 cells [65]. The neuroprotective effect induced by catechins is thought to occur through potentiation of antioxidant defenses [67], activation of protein kinase C, and upregulation of cell survival genes [68].

In summary, the current findings show that *C. sinensis* confers protective effect against nicotine-induced neurobehavioral alterations and oxidative stress. Perinatal nicotine exposure induced potential neurotoxic effects evidenced by chromatolysis of neurons, increased ROS production and neurobehavioral alterations in male and female newborns. *C. sinensis* significantly protected male and female newborns against nicotine-induced neurotoxicity. Therefore, *C. sinensis* represents a potential candidate conferring protection against nicotine-induced neurotoxicity in offspring, pending further studies to determine the exact mechanisms of action.

Conflicts of Interest

The authors declare that they have no conflict of interests.

Acknowledgments

The authors extend their appreciation to the Dean of Scientific Research, King Saud University, for funding the work through the research group Project no. RGP-1438-017.

References

[1] N. Chahal, A. C. McLain, A. Ghassabian et al., "Maternal smoking and newborn cytokine and immunoglobulin levels," *Nicotine and Tobacco Research*, 2016.

[2] S. Higgins, "Smoking in pregnancy," *Current Opinion in Obstetrics and Gynecology*, vol. 14, no. 2, pp. 145–151, 2002.

[3] S. P. Ng and J. T. Zelikoff, "Smoking during pregnancy: subsequent effects on offspring immune competence and disease vulnerability in later life," *Reproductive Toxicology*, vol. 23, no. 3, pp. 428–437, 2007.

[4] M. N. Hylkema and M. J. Blacquiere, "Intrauterine effects of maternal smoking on sensitization, asthma, and chronic obstructive pulmonary disease," *Proceedings of the American Thoracic Society*, vol. 6, no. 8, pp. 660–662, 2009.

[5] L. Suarez, M. Felkner, J. D. Brender, M. Canfield, and K. Hendricks, "Maternal exposures to cigarette smoke, alcohol, and street drugs and neural tube defect occurrence in offspring," *Maternal and Child Health Journal*, vol. 12, no. 3, pp. 394–401, 2008.

[6] A. Dalgic, E. Armagan, F. Helvacioglu et al., "High dose cotinine may induce neural tube defects in a chick embryo model," *Turkish Neurosurgery*, vol. 19, no. 3, pp. 224–229, 2009.

[7] D. S. Lambers and K. E. Clark, "The maternal and fetal physiologic effects of nicotine," *Seminars in Perinatology*, vol. 20, no. 2, pp. 115–126, 1996.

[8] J. B. Dwyer, R. S. Broide, and F. M. Leslie, "Nicotine and brain development," *Birth Defects Research Part C: Embryo Today*, vol. 84, no. 1, pp. 30–44, 2008.

[9] J. B. Dwyer, S. C. McQuown, and F. M. Leslie, "The dynamic effects of nicotine on the developing brain," *Pharmacology and Therapeutics*, vol. 122, no. 2, pp. 125–139, 2009.

[10] I. Berlin, C. Heilbronner, S. Georgieu, C. Meier, and O. Spreux-Varoquaux, "Newborns' cord blood plasma cotinine concentrations are similar to that of their delivering smoking mothers," *Drug and Alcohol Dependence*, vol. 107, no. 2-3, pp. 250–252, 2010.

[11] T. A. Slotkin, "Cholinergic systems in brain development and disruption by neurotoxicants: nicotine, environmental tobacco smoke, organophosphates," *Toxicology and Applied Pharmacology*, vol. 198, no. 2, pp. 132–151, 2004.

[12] M. D. Cornelius, L. Goldschmidt, and N. L. Day, "Prenatal cigarette smoking: long-term effects on young adult behavior problems and smoking behavior," *Neurotoxicology and Teratology*, vol. 34, no. 6, pp. 554–559, 2012.

[13] M. D. Cornelius, L. Goldschmidt, N. M. De Genna, and C. Larkby, "Long-term effects of prenatal cigarette smoke exposure on behavior dysregulation among 14-year-old offspring of teenage mothers," *Maternal and Child Health Journal*, vol. 16, no. 3, pp. 694–705, 2012.

[14] H. Khalki, L. Khalki, R. Aboufatima et al., "Prenatal exposure to tobacco extract containing nicotinic alkaloids produces morphological and behavioral changes in newborn rats," *Pharmacology Biochemistry and Behavior*, vol. 101, no. 3, pp. 342–347, 2012.

[15] E. D. Levin, S. J. Briggs, N. C. Christopher, and J. E. Rose, "Prenatal nicotine exposure and cognitive performance in rats," *Neurotoxicology and Teratology*, vol. 15, no. 4, pp. 251–260, 1993.

[16] J. Vaglenova, K. Parameshwaran, V. Suppiramaniam, C. R. Breese, N. Pandiella, and S. Birru, "Long-lasting teratogenic effects of nicotine on cognition: gender specificity and role of AMPA receptor function," *Neurobiology of Learning and Memory*, vol. 90, no. 3, pp. 527–536, 2008.

[17] C. J. Heath, S. L. King, C. Gotti, M. J. Marks, and M. R. Picciotto, "Cortico-thalamic connectivity is vulnerable to nicotine exposure during early postnatal development through alpha4/beta2/alpha5 nicotinic acetylcholine receptors," *Neuropsychopharmacology*, vol. 35, no. 12, pp. 2324–2338, 2010.

[18] K. A. Espy, H. Fang, C. Johnson, C. Stopp, and S. A. Wiebe, "Prenatal tobacco exposure: developmental outcomes in the neonatal period," *Developmental Psychology*, vol. 47, no. 1, pp. 153–156, 2011.

[19] A. P. Key, M. Ferguson, D. L. Molfese, K. Peach, C. Lehman, and V. J. Molfese, "Smoking during pregnancy affects speech-processing ability in newborn infants," *Environmental Health Perspectives*, vol. 115, no. 4, pp. 623–629, 2007.

[20] G. Mansi, F. Raimondi, S. Pichini et al., "Neonatal urinary cotinine correlates with behavioral alterations in newborns prenatally exposed to tobacco smoke," *Pediatric Research*, vol. 61, no. 2, pp. 257–261, 2007.

[21] L. R. Stroud, R. L. Paster, M. S. Goodwin et al., "Maternal smoking during pregnancy and neonatal behavior: a large-scale community study," *Pediatrics*, vol. 123, no. 5, pp. e842–e848, 2009.

[22] J. A. Kable, C. D. Coles, M. E. Lynch, and J. Carroll, "The impact of maternal smoking on fast auditory brainstem responses," *Neurotoxicology and Teratology*, vol. 31, no. 4, pp. 216–224, 2009.

[23] L. R. Stroud, R. L. Paster, G. D. Papandonatos et al., "Maternal smoking during pregnancy and newborn neurobehavior: effects at 10 to 27 days," *Journal of Pediatrics*, vol. 154, no. 1, pp. 10–16, 2009.

[24] C. Lin, J. M. Yon, J. T. Hong et al., "4-O-methylhonokiol inhibits serious embryo anomalies caused by nicotine via modulations of oxidative stress, apoptosis, and inflammation," *Birth Defects Research Part B: Developmental and Reproductive Toxicology*, vol. 101, no. 2, pp. 125–134, 2014.

[25] A. R. Sudheer, K. Chandran, S. Marimuthu, and V. P. Menon, "Ferulic acid modulates altered lipid profiles and prooxidant/antioxidant status in circulation during nicotine-induced toxicity: a dose-dependent study," *Toxicology Mechanisms and Methods*, vol. 15, no. 6, pp. 375–381, 2005.

[26] G. Al-Basher, J. S. Ajarem, A. A. Allam, and A. M. Mahmoud, "Green tea protects against perinatal nicotine-induced histological, biochemical and hematological alterations in mice offspring," *International Journal of Pharmacology*, vol. 13, no. 2, pp. 109–121, 2017.

[27] A. R. Sudheer, S. Muthukumaran, N. Devipriya, and V. P. Menon, "Ellagic acid, a natural polyphenol protects rat peripheral blood lymphocytes against nicotine-induced cellular and DNA damage in vitro: with the comparison of N-acetylcysteine," *Toxicology*, vol. 230, no. 1, pp. 11–21, 2007.

[28] Z. Z. Guan, W. F. Yu, and A. Nordberg, "Dual effects of nicotine on oxidative stress and neuroprotection in PC12 cells," *Neurochemistry International*, vol. 43, no. 3, pp. 243–249, 2003.

[29] T. A. Slotkin, F. J. Seidler, D. Qiao et al., "Effects of prenatal nicotine exposure on primate brain development and attempted amelioration with supplemental choline or vitamin C: neurotransmitter receptors, cell signaling and cell development biomarkers in fetal brain regions of rhesus monkeys," *Neuropsychopharmacology*, vol. 30, no. 1, pp. 129–144, 2005.

[30] S. R. Sirasanagandla, R. K. Rooben, Rajkumar, S. N. Narayanan, and R. Jetti, "Ascorbic acid ameliorates nicotine exposure induced impaired spatial memory performances in rats," *West Indian Medical Journal*, vol. 63, no. 4, pp. 318–324, 2014.

[31] M. S. Butt, R. S. Ahmad, M. T. Sultan, M. M. Qayyum, and A. Naz, "Green tea and anticancer perspectives: updates from last decade," *Critical Reviews in Food Science and Nutrition*, vol. 55, no. 6, pp. 792–805, 2015.

[32] H. Ghafurniyan, M. Azarnia, M. Nabiuni, and L. Karimzadeh, "The effect of green tea extract on reproductive improvement in estradiol valerate-induced polycystic ovarian syndrome in rat," *Iranian Journal of Pharmaceutical Research*, vol. 14, no. 4, pp. 1215–1233, 2015.

[33] T. Umezu, "Unusual effects of nicotine as a psychostimulant on ambulatory activity in mice," *ISRN Pharmacology*, vol. 2012, Article ID 170981, p. 12, 2012.

[34] J. S. Ajarem and M. Ahmad, "Teratopharmacological and behavioral effects of coffee in mice," *Acta Physiologica et Pharmacologica Bulgarica*, vol. 22, no. 2, pp. 51–61, 1996.

[35] J. S. Ajarem and M. Ahmad, "Behavioral and biochemical consequences of perinatal exposure of mice to instant coffee: a correlative evaluation," *Pharmacology Biochemistry and Behavior*, vol. 40, no. 4, pp. 847–852, 1991.

[36] J. S. Ajarem, "Effects of prenatal nicotine exposure on some morphological, behavioral and enzymatic characteristics in mice offspring," *Journal of Union of Arab Biologists*, vol. 14, no. 4, pp. 197–210, 2000.

[37] J. S. Ajarem and M. Ahmad, "Prenatal nicotine exposure modifies behavior of mice through early development," *Pharmacology Biochemistry and Behavior*, vol. 59, no. 2, pp. 313–318, 1998.

[38] G. M. Abu-Taweel, "Effects of perinatal exposure of lithium on neuro-behaviour of developing mice offspring," *Indian Journal of Experimental Biology*, vol. 50, no. 10, pp. 696–701, 2012.

[39] A. A. Allam, S. N. Maodaa, R. Abo-Eleneen, and J. Ajarem, "Protective effect of parsley juice (Petroselinum crispum, Apiaceae) against cadmium deleterious changes in the developed albino mice newborns (Mus musculus) brain," *Oxididative Medicine and Cellular Longevity*, vol. 2016, Article ID 2646840, p. 15, 2016.

[40] G. M. Abu-Taweel, A. ZM, J. S. Ajarem, and M. Ahmad, "Cognitive and biochemical effects of monosodium glutamate and aspartame, administered individually and in combination in male albino mice," *Neurotoxicology and Teratology*, vol. 42, pp. 60–67, 2014.

[41] H. G. Preuss, S. T. Jarrell, R. Scheckenbach, S. Lieberman, and R. A. Anderson, "Comparative effects of chromium, vanadium and Gymnema sylvestre on sugar-induced blood pressure elevations in SHR," *Journal of the American College of Nutrition*, vol. 17, no. 2, pp. 116–123, 1998.

[42] E. Beutler, O. Duron, and B. M. Kelly, "Improved method for the determination of blood glutathione," *The Journal of Laboratory and Clinical Medicine*, vol. 61, pp. 882–888, 1963.

[43] S. Marklund and G. Marklund, "Involvement of the superoxide anion radical in the autoxidation of pyrogallol and a convenient assay for superoxide dismutase," *European Journal of Biochemistry*, vol. 47, no. 3, pp. 469–474, 1974.

[44] P. M. Wall and C. Messier, "Methodological and conceptual issues in the use of the elevated plus-maze as a psychological measurement instrument of animal anxiety-like behavior," *Neuroscience and Biobehavioral Reviews*, vol. 25, no. 3, pp. 275–286, 2001.

[45] R. M. Amos-Kroohs, M. T. Williams, A. A. Braun et al., "Neurobehavioral phenotype of C57BL/6J mice prenatally and neonatally exposed to cigarette smoke," *Neurotoxicology and Teratology*, vol. 35, pp. 34–45, 2013.

[46] H. Elmasry, R. D. Goodwin, M. B. Terry, and P. Tehranifar, "Early life exposure to cigarette smoke and depressive symptoms among women in midlife," *Nicotine and Tobacco Research*, vol. 16, no. 10, pp. 1298–1306, 2014.

[47] G. Balsevich, A. Poon, D. Goldowitz, and J. A. Wilking, "The effects of pre- and post-natal nicotine exposure and genetic background on the striatum and behavioral phenotypes in the mouse," *Behavioural Brain Research*, vol. 266, pp. 7–18, 2014.

[48] K. L. Grove, H. S. Sekhon, R. S. Brogan, J. A. Keller, M. S. Smith, and E. R. Spindel, "Chronic maternal nicotine exposure alters neuronal systems in the arcuate nucleus that regulate feeding behavior in the newborn rhesus macaque," *Journal of Clinical Endocrinology and Metabolism*, vol. 86, no. 11, pp. 5420–5426, 2001.

[49] C. C. Paccola, F. M. Neves, I. Cipriano, T. Stumpp, and S. M. Miraglia, "Effects of prenatal and lactation nicotine exposure on rat testicular interstitial tissue," *Andrology*, vol. 2, no. 2, pp. 175–185, 2014.

[50] C. Mao, X. Yuan, H. Zhang et al., "The effect of prenatal nicotine on mRNA of central cholinergic markers and hematological parameters in rat fetuses," *International Journal of Developmental Neuroscience*, vol. 25, no. 5, pp. 467–475, 2008.

[51] M. K. Hellerstein, N. L. Benowitz, R. A. Neese et al., "Effects of cigarette smoking and its cessation on lipid metabolism and energy expenditure in heavy smokers," *Journal of Clinical Investigation*, vol. 93, no. 1, pp. 265–272, 1994.

[52] J. F. Nunn, "Chapter 19 - smoking," in *Nunn's Applied Respiratory Physiology*, pp. 378–383, Butterworth-Heinemann, Oxford, Boston, 1993.

[53] S. K. Himes, L. R. Stroud, K. B. Scheidweiler, R. S. Niaura, and M. A. Huestis, "Prenatal tobacco exposure, biomarkers for tobacco in meconium, and neonatal growth outcomes," *Journal of Pediatrics*, vol. 162, no. 5, pp. 970–975, 2013.

[54] Y. L. Chan, S. Saad, C. Pollock et al., "Impact of maternal cigarette smoke exposure on brain inflammation and oxidative stress in male mice offspring," *Scientific Reports*, vol. 6, article 25881, 2016.

[55] C. A. Sorenson, L. A. Raskin, and Y. Suh, "The effects of prenatal nicotine on radial-arm maze performance in rats," *Pharmacology Biochemistry and Behavior*, vol. 40, no. 4, pp. 991–993, 1991.

[56] A. K. Eppolito and R. F. Smith, "Long-term behavioral and developmental consequences of pre- and perinatal nicotine," *Pharmacology Biochemistry and Behavior*, vol. 85, no. 4, pp. 835–841, 2006.

[57] J. Yanai, C. G. Pick, Y. Rogel-Fuchs, and E. A. Zahalka, "Alterations in hippocampal cholinergic receptors and hippocampal behaviors after early exposure to nicotine," *Brain Research Bulletin*, vol. 29, no. 3-4, pp. 363–368, 1992.

[58] T. A. Slotkin, K. E. Pinkerton, and F. J. Seidler, "Perinatal environmental tobacco smoke exposure in rhesus monkeys: critical periods and regional selectivity for effects on brain cell development and lipid peroxidation," *Environmental Health Perspectives*, vol. 114, no. 1, pp. 34–39, 2006.

[59] A. Muhammad, R. Mychasiuk, A. Nakahashi, S. R. Hossain, R. Gibb, and B. Kolb, "Prenatal nicotine exposure alters neuroanatomical organization of the developing brain," *Synapse*, vol. 66, no. 11, pp. 950–954, 2012.

[60] J. R. Pauly and T. A. Slotkin, "Maternal tobacco smoking, nicotine replacement and neurobehavioural development," *Acta Paediatrica*, vol. 97, no. 10, pp. 1331–1337, 2008.

[61] M. Ernst, E. T. Moolchan, and M. L. Robinson, "Behavioral and neural consequences of prenatal exposure to nicotine," *Journal of the American Academy of Child and Adolescent Psychiatry*, vol. 40, no. 6, pp. 630–641, 2001.

[62] S. N. Narayanan, R. S. Kumar, J. Paval, and S. Nayak, "Effect of ascorbic acid on the monosodium glutamate-induced neurobehavioral changes in periadolescent rats," *Bratislava Medical Journal*, vol. 111, no. 5, pp. 247–252, 2010.

[63] P. J. Urrutia, N. P. Mena, and M. T. Nunez, "The interplay between iron accumulation, mitochondrial dysfunction, and inflammation during the execution step of neurodegenerative disorders," *Frontiers in Pharmacology*, vol. 5, article 38, 2014.

[64] Y. He, D. Tan, B. Bai, Z. Wu, and S. Ji, "Epigallocatechin-3-gallate attenuates acrylamide-induced apoptosis and astrogliosis in rat cerebral cortex," *Toxicology Mechanisms and Methods*, vol. 27, no. 4, pp. 298–306, 2017.

[65] Y. He, D. Tan, Y. Mi et al., "Effect of epigallocatechin-3-gallate on acrylamide-induced oxidative stress and apoptosis in PC12 cells," *Human and Experimental Toxicology*, 2016.

[66] S. Guo, J. Yan, T. Yang, X. Yang, E. Bezard, and B. Zhao, "Protective effects of green tea polyphenols in the 6-OHDA rat model of Parkinson's disease through inhibition of ROS-NO pathway," *Biological Psychiatry*, vol. 62, no. 12, pp. 1353–1362, 2007.

[67] A. L. Al-Malki and S. S. Moselhy, "Protective effect of vitamin E and epicatechin against nicotine-induced oxidative stress in rats," *Toxicology and Industrial Health*, vol. 29, no. 2, pp. 202–208, 2013.

[68] S. A. Mandel, Y. Avramovich-Tirosh, L. Reznichenko et al., "Multifunctional activities of green tea catechins in neuroprotection. Modulation of cell survival genes, iron-dependent oxidative stress and PKC signaling pathway," *Neurosignals*, vol. 14, no. 1-2, pp. 46–60, 2005.

Hindawi
Oxidative Medicine and Cellular Longevity
Volume 2017, Article ID 7528090, 9 pages
https://doi.org/10.1155/2017/7528090

Research Article

MitoTEMPO Prevents Oxalate Induced Injury in NRK-52E Cells via Inhibiting Mitochondrial Dysfunction and Modulating Oxidative Stress

Jiaqiao Zhang,[1] Qing Wang,[1] Chuou Xu,[2] Yuchao Lu,[1] Henglong Hu,[1] Baolong Qin,[1] Yufeng Wang,[1] Deng He,[3] Cong Li,[1] Xiao Yu,[1] Shaogang Wang,[1] and Jihong Liu[1]

[1]*Department and Institute of Urology, Tongji Hospital, Tongji Medical College, Huazhong University of Science and Technology, Wuhan, Hubei, China*
[2]*Department of Radiology, Tongji Hospital, Tongji Medical College, Huazhong University of Science and Technology, Wuhan, Hubei, China*
[3]*Department of Gynecology and Obstetrics, Tongji Hospital, Tongji Medical College, Huazhong University of Science and Technology, Wuhan, Hubei, China*

Correspondence should be addressed to Shaogang Wang; sgwangtjm@163.com

Received 23 October 2016; Revised 2 December 2016; Accepted 15 December 2016; Published 2 January 2017

Academic Editor: Mohamed M. Abdel-Daim

Copyright © 2017 Jiaqiao Zhang et al. This is an open access article distributed under the Creative Commons Attribution License, which permits unrestricted use, distribution, and reproduction in any medium, provided the original work is properly cited.

As one of the major risks for urolithiasis, hyperoxaluria can be caused by genetic defect or dietary intake. And high oxalate induced renal epithelial cells injury is related to oxidative stress and mitochondrial dysfunction. Here, we investigated whether MitoTEMPO, a mitochondria-targeted antioxidant, could protect against oxalate mediated injury in NRK-52E cells via inhibiting mitochondrial dysfunction and modulating oxidative stress. MitoSOX Red was used to determine mitochondrial ROS (mtROS) production. Mitochondrial membrane potential ($\Delta\psi$m) and quantification of ATP synthesis were measured to evaluate mitochondrial function. The protein expression of Nox4, Nox2, and p22 was also detected to explore the effect of oxalate and MitoTEMPO on NADPH oxidase. Our results revealed that pretreatment with MitoTEMPO significantly inhibited oxalate induced lactate dehydrogenase (LDH) and malondialdehyde (MDA) release and decreased oxalate induced mtROS generation. Further, MitoTEMPO pretreatment restored disruption of $\Delta\psi$m and decreased ATP synthesis mediated by oxalate. In addition, MitoTEMPO altered the protein expression of Nox4 and p22 and decreased the protein expression of IL-6 and osteopontin (OPN) induced by oxalate. We concluded that MitoTEMPO may be a new candidate to protect against oxalate induced kidney injury as well as urolithiasis.

1. Introduction

Hyperoxaluria is considered as one of the primary risk factors for urolithiasis [1]. High oxalate can cause renal tubular cells injury, and this effect is related to reactive oxygen species (ROS) production and imbalance of oxidation-reduction [2]. Mitochondria and NADPH oxidase are the major sources of ROS generation in renal tubular cells, and mitochondrial dysfunction was regarded as a key event in oxalate mediated renal cell injury [3–7].

Various antioxidant treatments including NADPH oxidase inhibitors had been applied to prevent renal cell injury and/or renal crystal formation [8–13]. However, limited research focused on preventing oxalate mediated renal cell toxicity via targeting mitochondria. Further, mitochondria-targeted antioxidant may scavenge mitochondrial ROS (mtROS) without affecting physiological ROS production outside the mitochondria [14].

Targeted therapies for mtROS species have not been reported in oxalate mediated injury in renal tubular cells. MitoTEMPO, a mitochondria-targeted antioxidant can specifically accumulate in the mitochondrial matrix 1000-fold due to its positive charge [15]. We hypothesized that MitoTEMPO prevents oxalate induced injury in renal tubular

cell via inhibiting mitochondrial dysfunction and modulating oxidative stress. We hoped to find new and more specific drugs to treat oxalate induced kidney injury as well as urolithiasis.

2. Materials and Methods

2.1. Reagents. MitoTEMPO was purchased from Sigma-Aldrich (St. Louis, MO, USA) and was dissolved in deionized water according to the molecular weight. Cell counting kit 8 (CCK-8) was purchased from Signalway Antibody LLC (Maryland, USA). LDH cytotoxicity assay kit, 2,7-dichlorodihydrofluorescein diacetate (DCF-DA), JC-1 dye and MDA assay kit, and ATP assay kit were purchased from Beyotime Institute of Biotechnology (Jiangsu, China). MitoSOX Red was purchased from Molecular Probes-Invitrogen (Carlsbad, CA, USA). OPN and Nox4 antibodies were purchased from Abcam (Cambridge, MA, USA); IL6 antibody was purchased from Biorbyt (Cambridge, United Kingdom); p22 antibody was purchased from Santa Cruz Biotechnology (Santa Cruz, CA, USA); Nox2 and β-actin antibodies were purchased from Proteintech (Wuhan, China).

2.2. Cell Culture. The NRK-52E (normal rat proximal tubular epithelial cell line) was obtained from the Type Culture Collection of the Chinese Academy of Sciences (Shanghai, China). Cells were maintained in Dulbecco's Modified Eagle's Medium (DMEM) (Hyclone; USA) supplemented with 10% fetal bovine serum (Gibco; Grand Island, NY, USA) at 37°C under a humidified 5% CO_2 atmosphere. Under these conditions, the cells achieved 90% to confluence. They were washed with serum and sodium pyruvate-free DMEM media.

2.3. Detection of Cell Viability (CCK-8). The NRK-52E cells were seeded at the concentration of 2×10^3/well in 96-well plates and incubated overnight. Following pretreatment with or without MitoTEMPO (10 μM) for 1 hour, the cells were treated with or without oxalate (700 μmol/l) for 24 or 48 hours at 37°C. After treatment, 100 μl DMEM media with 10% CCK-8 were added to replace previous media in each well and incubated for another 3 hours. The absorbance at 450 nm was detected. The viability of the cells was recorded as the percentage relative to untreated controls.

2.4. Lactate Dehydrogenase (LDH) Assay. The release of LDH into media was measured to detect the injury effect on NRK-52E cells. Cells were seeded in 96-well plates and cultured overnight. Before treatment, they were replaced with serum and sodium pyruvate-free DMEM media. After treatment for various periods, supernatants were collected and detected according to related instruction manual. The LDH release activity was presented as the fold increase over the control group.

2.5. Detection of Total Intracellular ROS by Flow Cytometry. Intracellular ROS production was detected using the ROS assay kit as the fluorescence of 2,7-dichlorofluorescein diacetate (DCF-DA) significantly increases after oxidation. Cells were seeded in a 6-well plate and stimulated by oxalate with or without 1 hour of preincubation with MitoTEMPO. After 3 h, cells were treated with DCF-DA (10 μM) for 30 min. Then, the cells were collected and resuspended in 200 μl of PBS buffer. Then intracellular ROS levels were performed by flow cytometry (BD Biosciences) with extinction and emission at 485 and 538 nm. All determinations were performed in triplicate.

2.6. Determination of mtROS Levels by Flow Cytometry. MitoSOX Red mitochondrial superoxide indicator was used to determine mtROS production. The cells were treated as the same when detecting intracellular ROS. After treatment, cells were loaded with 5 μM MitoSOX Red reagent for 10 min at 37°C. Then the cells were collected, washed, and resuspended in 200 μl Hanks' balanced salt solution. Flow cytometric analyses were performed with extinction and emission at 510 and 580 nm to determine mtROS. All determinations were performed in triplicate.

2.7. Assay of Lipid Peroxidation (MDA). Lipid peroxidation was measured as malondialdehyde (MDA) content. MDA was determined according to the instructions. The levels of MDA were expressed as percentage relative to the controls.

2.8. Detection of Mitochondrial Membrane Potential (MMP) by Fluorescence Microscopy. MMP assay kit (JC-1) was used to detect MMP. Cells were cultured in six-well plates. After stimulation by oxalate with or without 1 hour of preincubation with MitoTEMPO for 3 hours, cells were incubated with dyeing working solution for 20 minutes at 37°C, protected from light. JC-1 selectively entering mitochondria exists as a monomer with green fluorescence (Em 530 nm) at relatively low membrane potential and aggregates with red fluorescence (Em 590 nm) at high membrane potential. Then cells were observed by the fluorescence microscope (Olympus IX73, Japan).

2.9. Determination of Cellular ATP. Cellular ATP levels were determined using a commercial ATP assay kit based on the luciferin-luciferase reaction. After treatments, NRK-52E cells were lysed and centrifuged at 12,000g for 5 min. Then, 20 μL supernatants were mixed with 100 μL detection working solution in a black 96-well plate. Then, the chemiluminescence was measured. The level of ATP was expressed as percentage relative to the controls.

2.10. Western Blotting Analysis. After treatment, the cells were washed and lysed with RIPA buffer that contained protease inhibitor. Same amounts of proteins in each sample were analyzed on 10% SDS-PAGE. After being transferred to PVDF membranes, the membranes were blocked with 3% BSA for 2 h and then the membranes were incubated with primary antibody (1 : 500 for rabbit polyclonal anti-Nox2; 1 : 1,000 for rabbit monoclonal anti-NADPH oxidase 4; 1 : 250 for mouse monoclonal anti-P22; 1 : 1000 for rabbit monoclonal anti-OPN; 1 : 200 for rabbit polyclonal anti-IL6; 1 : 500 for mouse monoclonal β-actin) at 4°C overnight; the signals of the membranes were visualized using enhanced

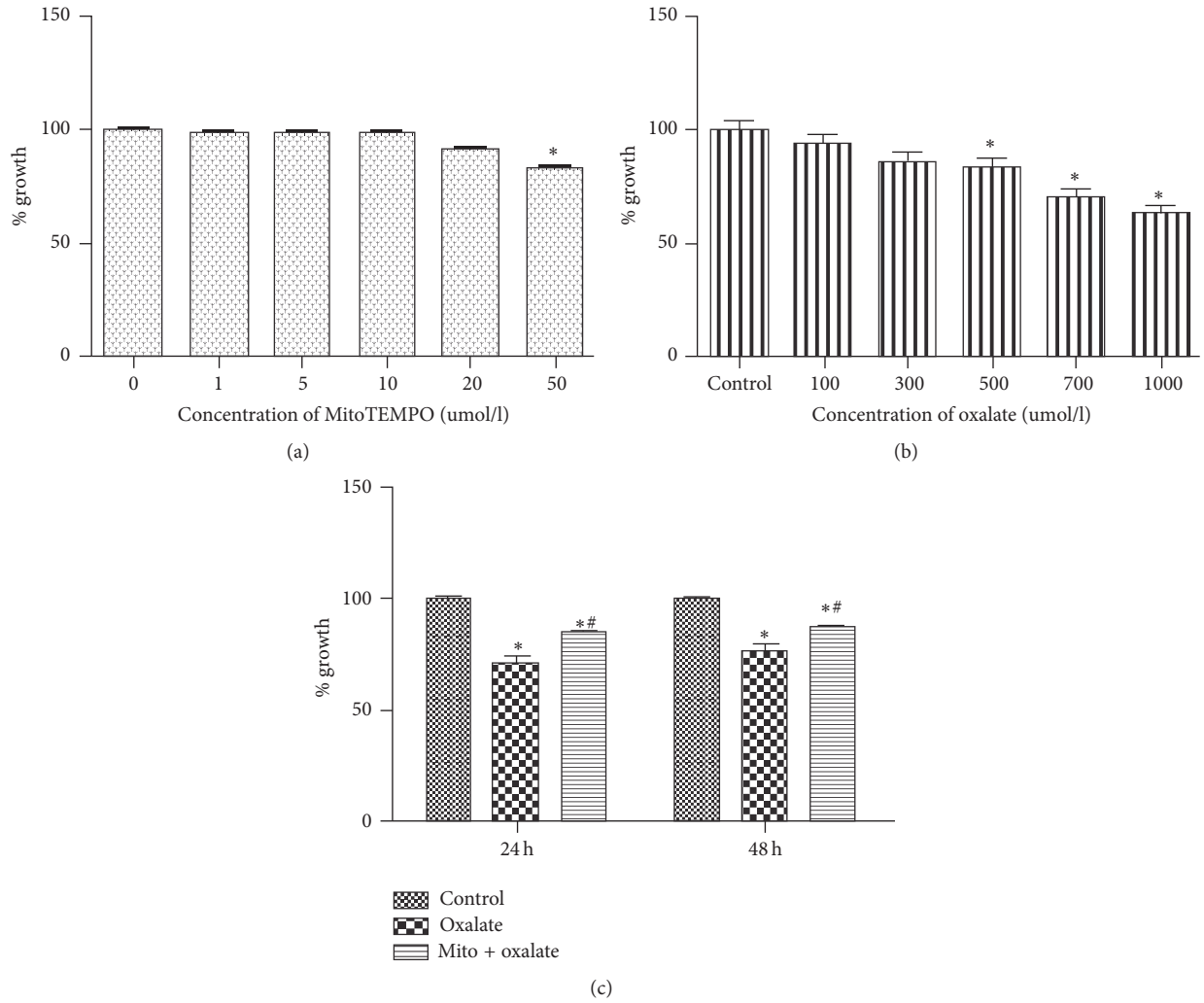

Figure 1: Effects of oxalate and MitoTEMPO on NRK-52E cell viability (a, b, c). The viability of NRK-52E cells was assessed by performing a CCK-8 assay. (a) Cells were treated with MitoTEMPO in different concentrations (0–50 μM). (b) Cells were treated with potassium oxalate in different concentrations (0–1000 μM). (c) MitoTEMPO (10 μM, pretreatment for 1 hour) increased NRK-52E cell viability in the presence of oxalate (700 μM) at 24 and 48 hours. $^{*}P < 0.05$ versus control; $^{\#}P < 0.05$ versus oxalate treated group (*Mito: MitoTEMPO).

chemiluminescence (ECL) after being incubated with secondary antibody (anti-rabbit or anti-mouse IgG) for 1 h at room temperature. Anti-β-actin was used to normalize the protein expression.

2.11. Statistical Analysis. Results were expressed as the mean ± SEM. One-way ANOVA was used to determine statistically significant differences in these experiments by GraphPad Prism 5 software.

3. Results

3.1. Effects of Oxalate and MitoTEMPO on NRK-52E Cell Viability. No significant toxicity of MitoTEMPO (1 to 20 μM) was found for NRK-52E cells for 24 hours (Figure 1(a)). The oxalate treatment (for 24 hours) decreased the viability of cells in a dose-dependent manner (Figure 1(b)). According to that, oxalate with concentration of 700 μM was selected for the following experiments. After pretreatment with MitoTEMPO (10 μM) for 1 hour, cells were exposed to oxalate (700 μM) for 24 hours to check cell viability. And we found that treatment with MitoTEMPO could significantly increase the cells viability (Figure 1(c)).

3.2. MitoTEMPO Attenuates Oxalate Mediated Cell Injury. To further test the protection of MitoTEMPO against oxalate induced cell injury, the LDH release activity was detected. Exposure of the cells to oxalate (700 μM) resulted in the release of LDH, significantly more than in the controls. In contrast, MitoTEMPO effectively reduced LDH leakage caused by oxalate at different periods (3 to 24 hours) (Figure 2(a)).

3.3. MitoTEMPO Reduces Lipid Peroxidation Injury in NRK-52E Cells Exposed to Oxalate. MDA levels were examined as

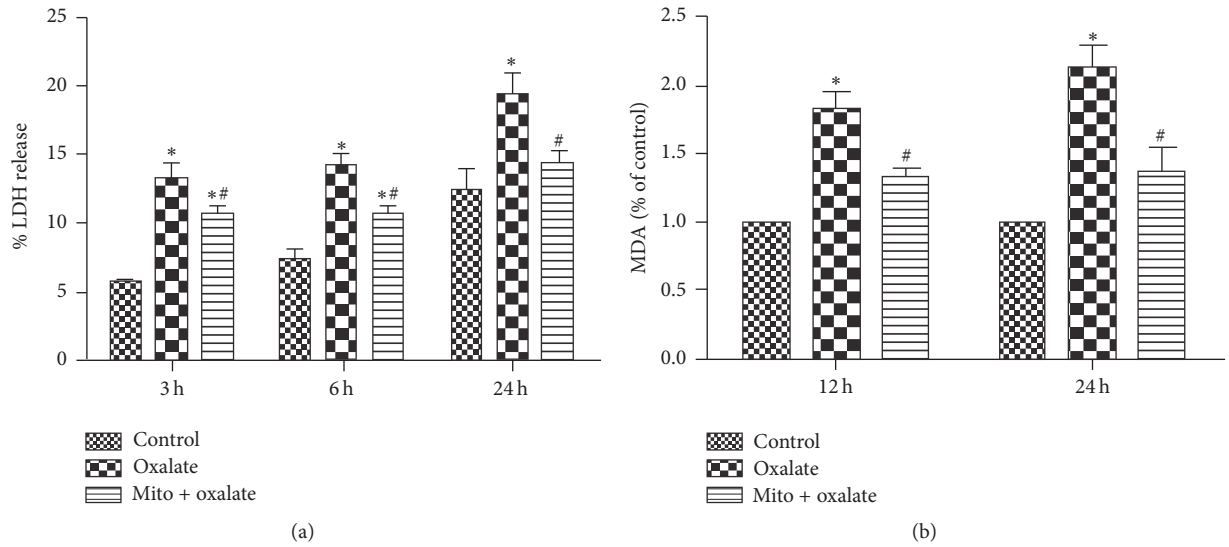

Figure 2: Mito attenuates oxalate induced cell injury and lipid peroxidation (a, b). (a) Mito decreased oxalate induced LDH release at 3, 6, and 24 hours. (b) Lipid peroxidation was assessed by detecting MDA level in the supernatants of NRK cell lysates. Pretreatment with Mito (1 hour) obviously attenuated MDA generation compared with oxalate induced group. $^{*}P < 0.05$ versus control; $^{\#}P < 0.05$ versus oxalate treated group (*Mito: MitoTEMPO).

the marker of lipid peroxidation injury and oxidative stress. Treatment with oxalate significantly increased cellular MDA content, and pretreatment with MitoTEMPO significantly decreased the cellular MDA levels compared with oxalate induced cells (Figure 2(b)).

3.4. MitoTEMPO Attenuates Oxalate Induced Mitochondrial ROS (mtROS) but not Intracellular ROS Generation. The DCF-DA fluorescence was measured to determine total intracellular ROS level and the intensity of MitoSOX Red fluorescence to determine the mtROS level. Pretreatment with MitoTEMPO significantly decreased the mtROS generation compared with oxalate induced cells; however it had no obvious impact on intracellular ROS generation (Figure 3).

3.5. MitoTEMPO Ameliorates Oxalate Induced Disruption of Mitochondrial Membrane Potential. Relative to the control group, oxalate exposure produced an obvious reduction in the initial $\Delta\psi_m$, as estimated by the decreased JC-1 fluorescence at 596 nm (red) and concomitant increased fluorescence at 534 nm (green). With MitoTEMPO pretreatment for 1 h, an obvious restoration of MMP was observed (Figure 4). The results indicate that oxalate induced mitochondrial dysfunction, and MitoTEMPO could inhibit this effect.

3.6. MitoTEMPO Increases ATP Levels in the NRK-52E Cells Exposed to Oxalate. Decreased MMP is related to reduction of ATP synthesis. Our results showed that oxalate could induce ATP deficiency in the NRK-52E cells, and MitoTEMPO treatment restored this effect (Figure 5).

3.7. MitoTEMPO Selectively Modulated the Protein Expression of NADPH Oxidase Subunits. It was reported that oxalate exposure could regulate mRNA expression of NADPH oxidase subunits in a human renal epithelial-derived cell line [5]. In this research, we detected the effect of oxalate and MitoTEMPO on the protein expression of NADPH oxidase subunits. Oxalate treatment decreased the protein expression of Nox4, elevated the protein expression of p22 significantly, and did not change the protein expression of Nox2. MitoTEMPO pretreatment reversed the change of protein expression of Nox4 and p22 without affecting the protein expression of Nox2 (Figure 6).

3.8. MitoTEMPO Reduced the Expression of OPN and IL-6 in NRK-52E Cells Exposed to Oxalate. Oxalate significantly increased the protein expression of OPN and IL-6. Furthermore, the increased expression of OPN and IL-6 was significantly attenuated when cells were pretreated with MitoTEMPO (Figure 7).

4. Discussion

Numerous studies have indicated that ROS and oxidative stress were involved in the stone formation as well as oxalate induced renal epithelial cells injury. As two important sources of ROS production, both mitochondria and NADPH oxidases were involved in oxalate induced renal epithelial cells injury [3, 6, 13, 16, 17].

However, ROS generation is not always detrimental, as it is involved in both physiological and pathological processes. Many intervention trials with antioxidants supposed to prevent oxidative stress and improve disease outcomes have been mostly invalid or harmful. An important reason for these failures may be attributed to inappropriate inhibition of physiological ROS [18]. Therefore, theoretically we should intervene

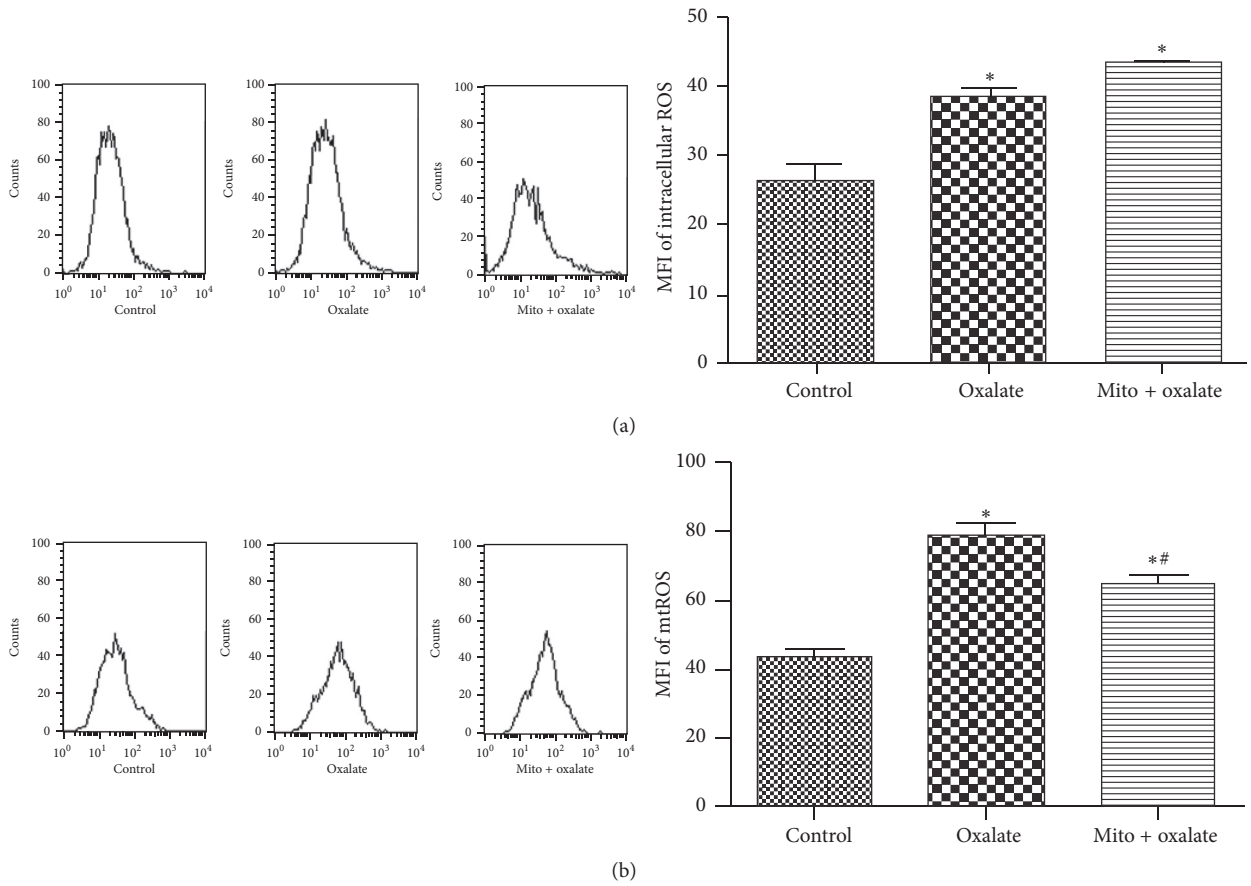

Figure 3: Effect of MitoTEMPO on oxalate induced intracellular ROS and mtROS generation (a, b). NRK-52E cells were stimulated with oxalate (700 μM) for 3 hours with or without preincubation with MitoTEMPO for 1 hour. (a) The intracellular ROS levels were indicated by the fluorescence intensity of DCF analyzed by flow cytometry. (b) The mtROS levels were indicated by the fluorescence intensity of MitoSOX Red analyzed by flow cytometry. Mean ± SEM of three independent experiments. $^{*}P < 0.05$ versus control; $^{\#}P < 0.05$ versus oxalate treated group (*Mito: MitoTEMPO).

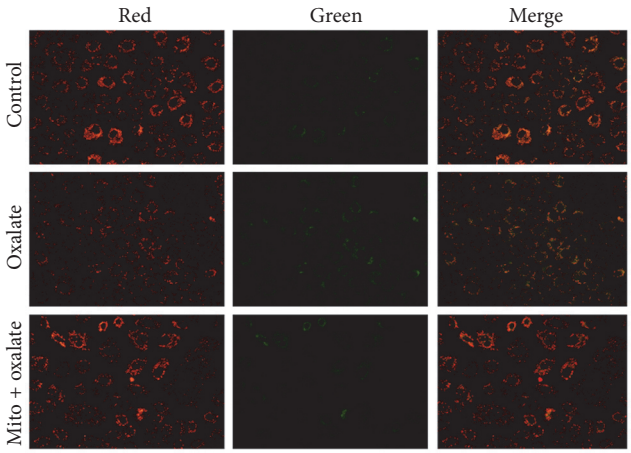

Figure 4: Mito ameliorates oxalate induced disruption of mitochondrial membrane potential. NRK-52E cells were stimulated with oxalate (700 μM) for 1 hour with or without preincubation with MitoTEMPO for 1 hour. Mitochondrial membrane potential was observed using a mitochondrial potential-sensitive dye, JC-1. Cells in control group showed bright red fluorescence. Oxalate treatment attenuated red fluorescence compared with control, and pretreatment with MitoTEMPO reversed these changes (*Mito: MitoTEMPO).

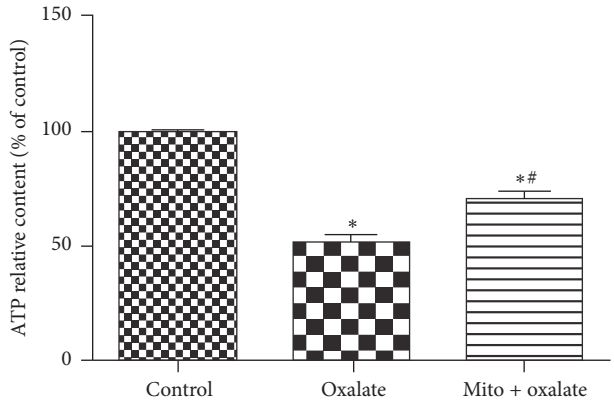

Figure 5: Mito increases ATP levels in the oxalate induced cultured NRK52E cells. NRK-52E cells were stimulated with oxalate (700 μM) for 3 hours with or without preincubation with MitoTEMPO for 1 hour. Oxalate treatment decreased ATP levels significantly. ATP levels in MitoTEMPO pretreatment group significantly increased compared with oxalate treatment group and still was lower compared with control group. $^{*}P < 0.05$ versus control; $^{\#}P < 0.05$ versus oxalate treated group (*Mito: MitoTEMPO).

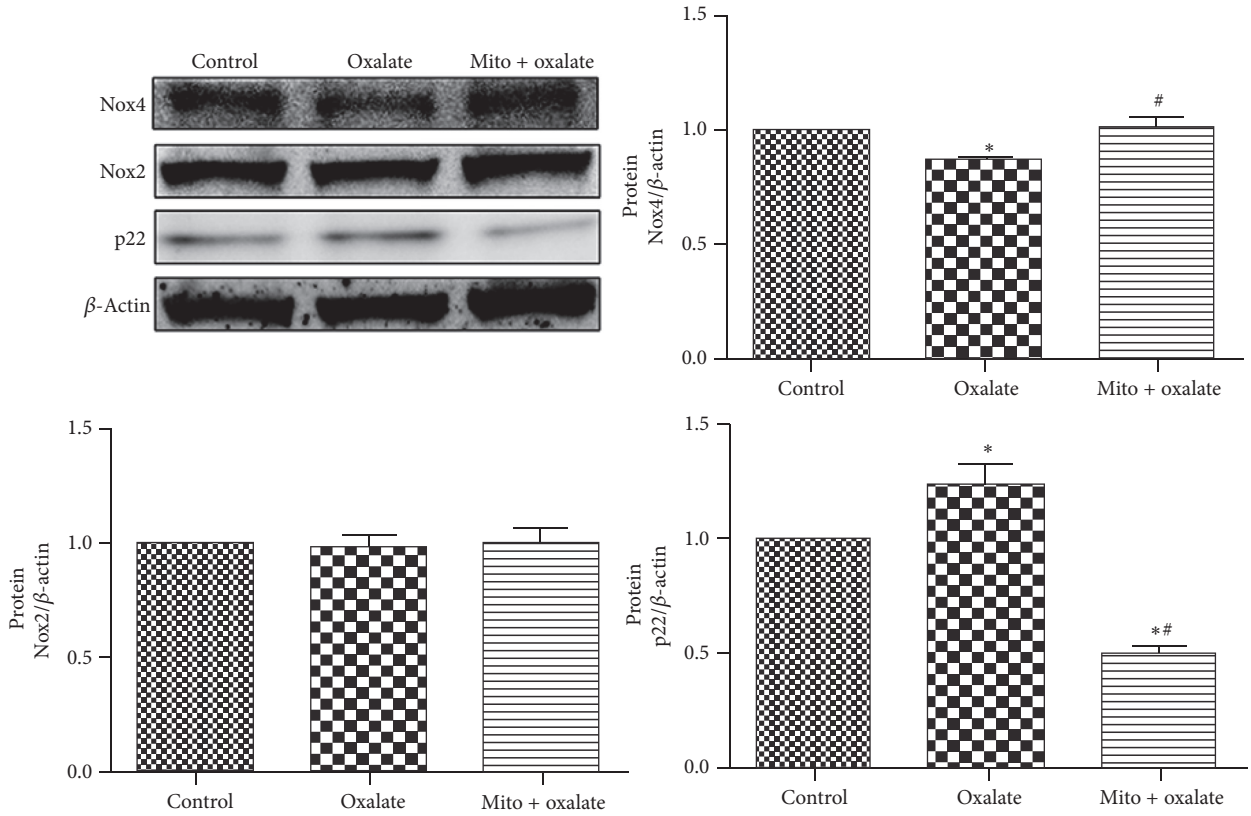

Figure 6: MitoTEMPO selectively modulated the protein expression of NADPH oxidase subunits in NRK-52E cells exposed to oxalate. NRK-52E cells were stimulated with oxalate (700 μM) for 24 hours with or without preincubation with MitoTEMPO for 1 hour. Oxalate treatment decreased the protein expression of Nox4 and elevated the protein expression of p22 significantly compared with the control group. MitoTEMPO pretreatment elevated the protein expression of Nox4 and decreased the protein expression of p22. The protein expression of Nox2 was not changed after oxalate stimulation with or without MitoTEMPO pretreatment. $^{*}P < 0.05$ versus control; $^{\#}P < 0.05$ versus oxalate treated group (*Mito: MitoTEMPO).

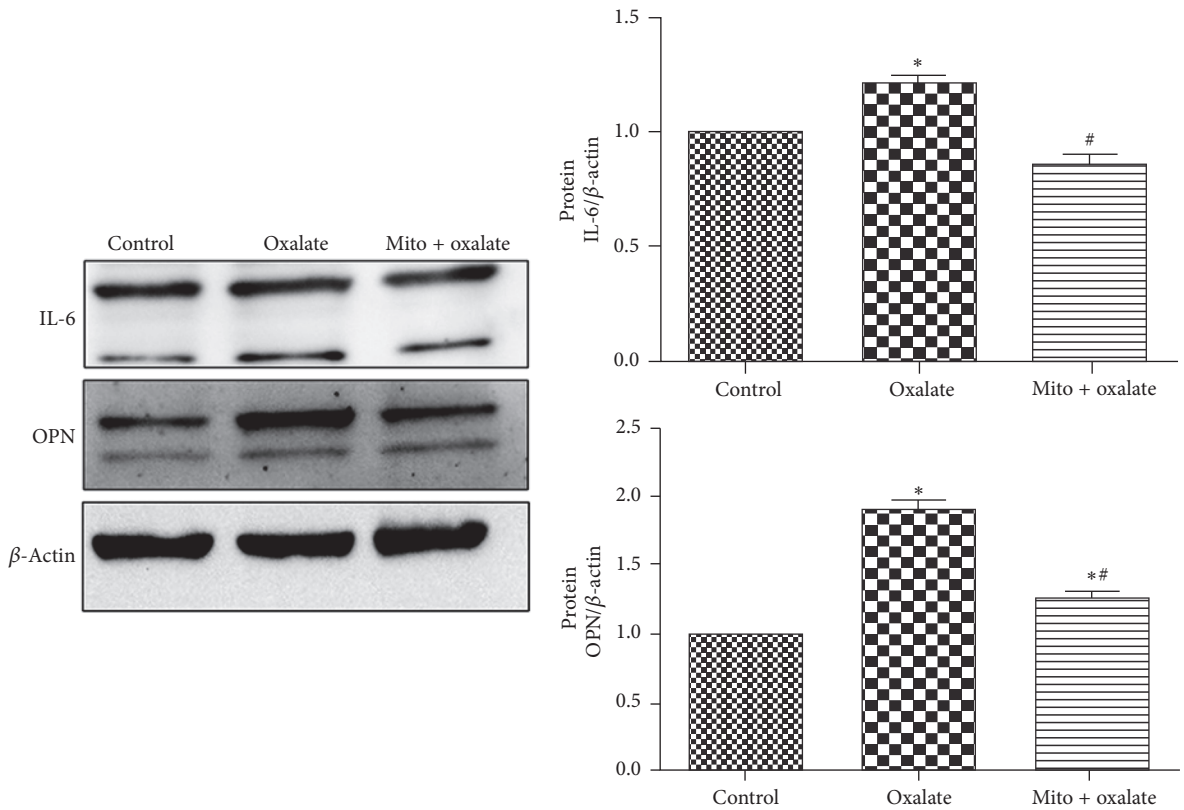

Figure 7: MitoTEMPO reduced the expression of stone modulators of IL-6 and OPN in NRK-52E cells exposed to oxalate. NRK-52E cells were stimulated with oxalate (700 μM) for 24 hours with or without preincubation with MitoTEMPO for 1 hour (*Mito: MitoTEMPO).

by targeting pathological ROS while making physiologically relevant ROS unaffected. Interestingly, it was reported that mtROS could directly contribute to inflammatory cytokine production and we suggested that mtROS may be a type of pathological ROS [19, 20]. Based on these evidences, we propose a hypothesis that MitoTEMPO, a mitochondria-targeted antioxidant, would exert a protective effect against oxalate induced renal epithelial cells injury via specifically acting on mitochondria and modulating ROS generation.

In our study, MitoTEMPO significantly increased the cells viability following exposure to oxalate. Also pretreatment with MitoTEMPO obviously decreased NRK-52E cells injury assessed by LDH release. The marker of oxidative stress, MDA level, was also decreased in MitoTEMPO-treated group. We also demonstrated that MitoTEMPO increased the cells viability via inhibiting mitochondrial ROS generation and restoration of mitochondrial membrane potential as well as promoting ATP synthesis.

Interestingly, our research found that MitoTEMPO attenuated mtROS generation caused by oxalate stimulation but not intracellular ROS generation. This phenomenon may be because MitoTEMPO can selectively accumulate in the mitochondria. Of course, there may be interaction between mitochondria and NADPH oxidase. Research indicated that oxidative stress provokes a positive-feedback loop between the two, although exact mechanism is undefined [15, 21]. As previous studies have indicated oxalate could activate the NADPH oxidase and upregulate the expression of some NADPH oxidase subunits [5, 17], we wondered if NADPH oxidase subunits could be regulated by MitoTEMPO treatment. And we observed that the protein expressions of Nox4 and p22 were also changed after oxalate and oxalate and MitoTEMPO combination treatment. This result also indicated mtROS may regulate NADPH oxidase activity via regulating the protein expression of NADPH oxidase subunits although we did not detect the activity of the NADPH oxidase.

The family of NADPH oxidases consists of seven isoforms (Nox1–5, Duox1, and Duox2). Of the seven isoforms, Nox4 and Nox2 are the two major components in the kidney, and activation of both Nox4 and Nox2 depends on p22 [22]. In contrast to NADPH oxidase Nox2, Nox4 produces hydrogen peroxide rather than superoxide [23]. Based on these evidences, we speculate that MitoTEMPO may play a protective role in oxalate mediated cell injury through modulating not only "dose" but also "type" of ROS generation.

As one of the proinflammatory cytokines, IL-6 may be involved in pathogenesis of urolithiasis. It was reported that patients of urolithiasis were associated with elevated level of IL-6 [24]. Study also indicated that oxalate could increase the expression of IL-6 in a time- and concentration-dependent manner [25]. As publications have discovered that mtROS acted as signaling molecules to lead inflammatory cytokine production [26–28], we determine the effect of oxalate and

MitoTEMPO on the expression of IL-6. And our results demonstrated that oxalate also upregulated the expression of IL-6 in NRK-52E cells, and MitoTEMPO treatment could weaken this effect.

Osteopontin (OPN), secreted by renal tubular epithelial cells, is considered as an important macromolecular modulator in the development of urolithiasis. The OPN expression is upregulated in both hyperoxaluric rats and genetic hypercalciuric rats [29, 30]. Studies also revealed that high concentration of calcium, oxalate, or calcium oxalate monohydrate (COM) crystals could stimulate OPN expression in renal tubular cells [4, 31, 32]. In our study, MitoTEMPO modulated ROS (including mitochondrial and intracellular) generation and OPN expression induced by oxalate. It is consistent with previous reports that OPN expression is regulated by ROS [4, 33].

There are some limitations in our study. Firstly, we just determined a part of NADPH oxidase subunits and did not include NADPH oxidase activity. Secondly, we did not detect specific type of intracellular ROS, for example, hydrogen peroxide or superoxide anion. At last, how MitoTEMPO affects downstream redox signaling such as p38, JNK, and ERK1/2 pathways is yet to be known.

In our study, MitoTEMPO may play a role to inhibit "harmful" ROS to confer protection against oxalate induced cell injury. Furthermore, MitoTEMPO decreased protein expression of IL-6 and OPN which are sensitive to redox regulation. To our knowledge, it is the first time to apply mitochondria-targeted antioxidant to inhibit oxalate induced cytotoxicity. Our present study implicates that MitoTEMPO may be an ideal candidate to control oxalate induced kidney injury as well as urolithiasis.

Competing Interests

The authors declare that no conflict of interests exists.

Authors' Contributions

Jihong Liu, Shaogang Wang, Xiao Yu, Cong Li, and Jiaqiao Zhang conceived and designed the study. Yuchao Lu, Deng He, Baolong Qin, Yufeng Wang, Qing Wang, Chuou Xu, and Jiaqiao Zhang performed the experiments. Henglong Hu and Jiaqiao Zhang analyzed the data. Jiaqiao Zhang wrote the manuscript. All authors read and approved the manuscript.

Acknowledgments

This work was supported by National Natural Science Foundation of China (81270787, 81570631).

References

[1] D. W. Kaufman, J. P. Kelly, G. C. Curhan et al., "Oxalobacter formigenes may reduce the risk of calcium oxalate kidney stones," *Journal of the American Society of Nephrology*, vol. 19, no. 6, pp. 1197–1203, 2008.

[2] H. Tsuji, W. Wang, J. Sunil et al., "Involvement of renin–angiotensin–aldosterone system in calcium oxalate crystal induced activation of NADPH oxidase and renal cell injury," *World Journal of Urology*, vol. 34, no. 1, pp. 89–95, 2016.

[3] F. D. Khand, M. P. Gordge, W. G. Robertson, A. A. Noronha-Dutra, and J. S. Hothersall, "Mitochondrial superoxide production during oxalate-mediated oxidative stress in renal epithelial cells," *Free Radical Biology & Medicine*, vol. 32, no. 12, pp. 1339–1350, 2002.

[4] T. Umekawa, H. Tsuji, H. Uemura, and S. R. Khan, "Superoxide from NADPH oxidase as second messenger for the expression of osteopontin and monocyte chemoattractant protein-1 in renal epithelial cells exposed to calcium oxalate crystals," *BJU International*, vol. 104, no. 1, pp. 115–120, 2009.

[5] S. R. Khan, A. Khan, and K. J. Byer, "Temporal changes in the expression of mRNA of NADPH oxidase subunits in renal epithelial cells exposed to oxalate or calcium oxalate crystals," *Nephrology Dialysis Transplantation*, vol. 26, no. 6, pp. 1778–1785, 2011.

[6] S. Joshi, A. B. Peck, and S. R. Khan, "NADPH oxidase as a therapeutic target for oxalate induced injury in kidneys," *Oxidative Medicine and Cellular Longevity*, vol. 2013, Article ID 462361, 18 pages, 2013.

[7] L.-C. Cao, T. W. Honeyman, R. Cooney, L. Kennington, C. R. Scheid, and J. A. Jonassen, "Mitochondrial dysfunction is a primary event in renal cell oxalate toxicity," *Kidney International*, vol. 66, no. 5, pp. 1890–1900, 2004.

[8] H.-S. Huang, J. Chen, C.-F. Chen, and M.-C. Ma, "Vitamin E attenuates crystal formation in rat kidneys: roles of renal tubular cell death and crystallization inhibitors," *Kidney International*, vol. 70, no. 4, pp. 699–710, 2006.

[9] X. Li, J. Lu, P. Shang, J. Bao, and Z. Yue, "The selective NADPH oxidase inhibitor apocynin has potential prophylactic effects on melamine-related nephrolithiasis in vitro and in vivo," *Molecular and Cellular Biochemistry*, vol. 399, no. 1, pp. 167–178, 2015.

[10] M. Alex, M. V. S. Paul, M. Abhilash, V. V. Mathews, T. V. Anilkumar, and R. H. Nair, "Astaxanthin modulates osteopontin and transforming growth factor β1 expression levels in a rat model of nephrolithiasis: a comparison with citrate administration," *BJU International*, vol. 114, no. 3, pp. 458–466, 2014.

[11] S. Thamilselvan and M. Menon, "Vitamin E therapy prevents hyperoxaluria-induced calcium oxalate crystal deposition in the kidney by improving renal tissue antioxidant status," *BJU International*, vol. 96, no. 1, pp. 117–126, 2005.

[12] J. Zuo, A. Khan, P. A. Glenton, and S. R. Khan, "Effect of NADPH oxidase inhibition on the expression of kidney injury molecule and calcium oxalate crystal deposition in hydroxy-L-proline-induced hyperoxaluria in the male Sprague-Dawley rats," *Nephrology Dialysis Transplantation*, vol. 26, no. 6, pp. 1785–1796, 2011.

[13] S. Joshi, B. T. Saylor, W. Wang, A. B. Peck, and S. R. Khan, "Apocynin-treatment reverses hyperoxaluria induced changes in NADPH oxidase system expression in rat kidneys: a transcriptional study," *PLoS ONE*, vol. 7, no. 10, Article ID e47738, 2012.

[14] L. C. A. Tábara, J. Poveda, C. Martin-Cleary, R. Selgas, A. Ortiz, and M. D. Sanchez-Niño, "Mitochondria-targeted therapies for acute kidney injury," *Expert reviews in molecular medicine*, vol. 16, article e13, 2014.

[15] S. Dikalov, "Cross talk between mitochondria and NADPH oxidases," *Free Radical Biology & Medicine*, vol. 51, no. 7, pp. 1289–1301, 2011.

[16] S. M. Farooq, N. B. Boppana, D. Asokan et al., "C-phycocyanin confers protection against oxalate-mediated oxidative stress and mitochondrial dysfunctions in MDCK cells," *PLoS ONE*, vol. 9, no. 4, Article ID e93056, 2014.

[17] A. Khan, K. Byer, and S. R. Khan, "Exposure of madin-darby canine kidney (MDCK) cells to oxalate and calcium oxalate crystals activates nicotinamide adenine dinucleotide phosphate (NADPH)-oxidase," *Urology*, vol. 83, no. 2, pp. 510.e1–510.e7, 2014.

[18] A. I. Casas, V. T.-V. Dao, A. Daiber et al., "Reactive oxygen-related diseases: therapeutic targets and emerging clinical indications," *Antioxidants & Redox Signaling*, vol. 23, no. 14, pp. 1171–1185, 2015.

[19] X. Li, P. Fang, J. Mai, E. T. Choi, H. Wang, and X.-F. Yang, "Targeting mitochondrial reactive oxygen species as novel therapy for inflammatory diseases and cancers," *Journal of Hematology & Oncology*, vol. 6, article 19, 2013.

[20] E. Naik and V. M. Dixit, "Mitochondrial reactive oxygen species drive proinflammatory cytokine production," *The Journal of Experimental Medicine*, vol. 208, no. 3, pp. 417–420, 2011.

[21] D. B. Zorov, M. Juhaszova, and S. J. Sollott, "Mitochondrial reactive oxygen species (ROS) and ROS-induced ROS release," *Physiological Reviews*, vol. 94, no. 3, pp. 909–950, 2014.

[22] M. Sedeek, R. Nasrallah, R. M. Touyz, and R. L. Hébert, "NADPH oxidases, reactive oxygen species, and the kidney: friend and foe," *Journal of the American Society of Nephrology*, vol. 24, no. 10, pp. 1512–1518, 2013.

[23] I. Takac, K. Schröder, L. Zhang et al., "The E-loop is involved in hydrogen peroxide formation by the NADPH oxidase Nox4," *The Journal of Biological Chemistry*, vol. 286, no. 15, pp. 13304–13313, 2011.

[24] E. Rhee, L. Santiago, E. Park, P. Lad, and G. C. Bellman, "Urinary IL-6 is elevated in patients with urolithiasis," *The Journal of Urology*, vol. 160, no. 6, part 1, pp. 2284–2288, 1998.

[25] M. Y. Huang, L. S. Chaturvedi, S. Koul, and H. K. Koul, "Oxalate stimulates IL-6 production in HK-2 cells, a line of human renal proximal tubular epithelial cells," *Kidney International*, vol. 68, no. 2, pp. 497–503, 2005.

[26] A. C. Bulua, A. Simon, R. Maddipati et al., "Mitochondrial reactive oxygen species promote production of proinflammatory cytokines and are elevated in TNFR1-associated periodic syndrome (TRAPS)," *The Journal of Experimental Medicine*, vol. 208, no. 3, pp. 519–533, 2011.

[27] K. Nakahira, J. A. Haspel, V. A. K. Rathinam et al., "Autophagy proteins regulate innate immune responses by inhibiting the release of mitochondrial DNA mediated by the NALP3 inflammasome," *Nature Immunology*, vol. 12, no. 3, pp. 222–230, 2011.

[28] R. Zhou, A. S. Yazdi, P. Menu, and J. Tschopp, "A role for mitochondria in NLRP3 inflammasome activation," *Nature*, vol. 469, no. 7329, pp. 221–225, 2011.

[29] S. R. Khan, S. Joshi, W. Wang, and A. B. Peck, "Regulation of macromolecular modulators of urinary stone formation by reactive oxygen species: transcriptional study in an animal model of hyperoxaluria," *American Journal of Physiology—Renal Physiology*, vol. 306, no. 11, pp. F1285–F1295, 2014.

[30] Z. Jia, S. Wang, J. Tang et al., "Does crystal deposition in genetic hypercalciuric rat kidney tissue share similarities with bone formation?" *Urology*, vol. 83, no. 2, pp. 509.e7–509.e14, 2014.

[31] K. Tozawa, T. Yasui, A. Okada et al., "NF-κB activation in renal tubular epithelial cells by oxalate stimulation," *International Journal of Urology*, vol. 15, no. 10, pp. 924–928, 2008.

[32] Q. Xi, J. Ouyang, J. Pu, J. Hou, and S. Wang, "High concentration of calcium stimulates calcium oxalate crystal attachment to rat tubular epithelial NRK cells through osteopontin," *Urology*, vol. 86, no. 4, pp. 844.e1–844.e5, 2015.

[33] T. Hu, R. Luan, H. Zhang et al., "Hydrogen peroxide enhances osteopontin expression and matrix metalloproteinase activity in aortic vascular smooth muscle cells," *Clinical and Experimental Pharmacology & Physiology*, vol. 36, no. 7, pp. 626–630, 2009.

Hindawi Publishing Corporation
Oxidative Medicine and Cellular Longevity
Volume 2016, Article ID 8715185, 11 pages
http://dx.doi.org/10.1155/2016/8715185

Research Article

Nephroprotective Effects of N-Acetylcysteine Amide against Contrast-Induced Nephropathy through Upregulating Thioredoxin-1, Inhibiting ASK1/p38MAPK Pathway, and Suppressing Oxidative Stress and Apoptosis in Rats

Xuezhong Gong,[1] Yiru Duan,[1] Junli Zheng,[1] Yiquan Wang,[1] Guohua Wang,[1] Svante Norgren,[2] and Tom K. Hei[3]

[1] *Department of Nephrology, Shanghai Municipal Hospital of Traditional Chinese Medicine, Shanghai University of Traditional Chinese Medicine, 274 Zhijiang Middle Road, Shanghai 200071, China*
[2] *Department of Women's and Children's Health, Karolinska Institutet, Karolinska University Hospital, 171 77 Stockholm, Sweden*
[3] *Center for Radiological Research, Department of Radiation Oncology, College of Physician and Surgeons, Columbia University, 630 West 168th Street, New York, NY 10032, USA*

Correspondence should be addressed to Xuezhong Gong; shnanshan@hotmail.com

Received 1 October 2016; Accepted 30 November 2016

Academic Editor: Mohamed M. Abdel-Daim

Copyright © 2016 Xuezhong Gong et al. This is an open access article distributed under the Creative Commons Attribution License, which permits unrestricted use, distribution, and reproduction in any medium, provided the original work is properly cited.

Contrast-induced nephropathy (CIN) is a leading cause of hospital-acquired acute kidney injury (AKI) due to apoptosis induced in renal tubular cells. Our previous study demonstrated the novel N-acetylcysteine amide (NACA); the amide form of N-acetyl cysteine (NAC) prevented renal tubular cells from contrast-induced apoptosis through inhibiting p38 MAPK pathway in vitro. In the present study, we aimed to compare the efficacies of NACA and NAC in preventing CIN in a well-established rat model and investigate whether thioredoxin-1 (Trx1) and apoptosis signal-regulating kinase 1 (ASK1) act as the potential activator for p38 MAPK. NACA significantly attenuated elevations of serum creatinine, blood urea nitrogen, and biomarkers of AKI. At equimolar concentration, NACA was more effective than NAC in reducing histological changes of renal tubular injuries. NACA attenuated activation of p38 MAPK signal, reduced oxidative stress, and diminished apoptosis. Furthermore, we demonstrated that contrast exposure resulted in Trx1 downregulation and increased ASK1/p38 MAPK phosphorylation, which could be reversed by NACA and NAC. To our knowledge, this is the first report that Trx1 and ASK1 are involved in CIN. Our study highlights a renal protective role of NACA against CIN through modulating Trx1 and ASK1/p38 MAPK pathway to result in the inhibition of apoptosis among renal cells.

1. Introduction

CIN (contrast-induced nephropathy) has become a leading cause of hospital-acquired acute kidney injury as a result of the increasing use of iodine contrast media and the simultaneous increase in number of at-risk patients, for example, due to diabetes or hypertension [1–4]. The most common clinical course is a transient nonoliguric and asymptomatic decline in renal function with serum creatinine levels peaking at days 3–5, but CIN can also cause long-term adverse events and need for chronic dialysis [1–4]. Thus, it is essential not only to investigate the pathogenesis of CIN but also to develop preventive interventions [5].

There is accumulating evidence that CIN is caused by a combination of a reduction in medullary blood flow resulting in hypoxia and direct tubular damage, including apoptosis [6–8]. Oxidative stress has been identified as an important driver mechanism in the pathogenesis, and this has triggered trials of antioxidants to prevent CIN [6, 9]. Although there is no consensus or standard practice regarding the most effective intervention to prevent CIN besides adequate hydration, the international work group Kidney Disease:

Improving Global Outcomes (KDIGO) suggested using oral administration of the antioxidant N-acetylcysteine (NAC) along with intravenous fluids in patients at increased risk to develop CIN [10, 11]. There is, however, an inconsistency in guidelines regarding the benefit of NAC [3, 4], which highlights the need for more investigation to seek new antioxidants and address the effectiveness of antioxidants in the prevention of the disease.

NACA, also termed AD4, as the amide form of NAC, is a thiol antioxidant with enhanced properties of lipophilicity, membrane permeability, and antioxidant capacity when compared with NAC [12]. Recently emerging evidence confirmed NACA as a protective agent against oxidative stress in vitro and in vivo [13–16]. Our previous study also indicated NACA could protect renal tubular epithelial cell against contrast-induced apoptosis in vitro [6]. We thus hypothesized NACA could be a better renoprotective agent against CIN than NAC in vivo through its prominent antioxidant activity.

We have previously demonstrated that the low-osmolar, nonionic contrast agent iohexol, the most widely used radiocontrast media, induces renal tubular cell apoptosis through activation of the p38 MAPK/iNOS signal pathway in vitro and vivo [6, 7]. This signal pathway has been confirmed by others in a human renal tubular cell line (HK2) and cultured renal tubular cells isolated from CIN patients [17, 18]. We have subsequently identified the Forkhead box O1 transcriptional factor (FoxO1) as a downstream element of the p38 MAPK cascade [7]. However, little is known of the upstream modulators of the p38 MAPK pathway in CIN as well as in kidney disease [19].

One putative candidate for the upstream signal activator of p38 MAPK is Apoptosis Signal-regulating Kinase 1 (ASK1) [20]. As a serine/threonine kinase belonging to the mitogen activated protein kinase kinase kinase (MAP3K) family, ASK1 has been reported to play a critical role in reactive oxygen species (ROS)-induced apoptosis in various cell types and oxidative stress-related diseases such as D-galactosamine/lipopolysaccharide induced hepatotoxicity and cardiovascular disease [21–24]. Meanwhile, as an important redox regulator, thioredoxin-1 (Trx1) could bind to the N terminal non catalytic region of ASK1 and act as an upstream inhibitor of ASK1 [25, 26].

In the present study, we aimed to compare the efficacies of NACA and NAC in preventing CIN and further investigated whether Trx1/ASK1 signal, as the potential upstream modulators of p38 MAPK, were involved in CIN pathogenesis.

2. Materials and Methods

2.1. Reagents. All chemicals were purchased from Sigma (St. Louis, MO, USA) unless otherwise stated. N-Acetylcysteine amide (NACA) was provided by Dr. Glenn Goldstein (New York, NY, USA). The contrast media iohexol (Omnipaque) was purchased from Amersham Health (Princeton, NJ, USA).

2.2. Animals. The study was approved by Medicine Animal Ethics Committee of Shanghai University of Traditional Chinese Medicine. A total of 40 adult 8–10-week-old male Sprague-Dawley rats weighing 200–250 g were purchased from Shanghai Lab Animal Research Center (certificate number: 2016-0021). Rats were housed in an air-conditioned room at 23°C with a cycle of 12 h/12 h light/dark. Food and water were provided ad libitum except for the day of dehydration.

2.3. Experimental Protocol and Drugs. We used a well-established rat model of CIN [7, 27–29]. Rats were randomly divided into 5 groups of 8 rats each: controls (CON), rats injected with CM (CIN), rats treated with 150 mg/kg/d NAC and injected with CM (CIN+NAC), rats treated with 50 mg/kg/d NACA and injected with CM (CIN+NACA1), and rats treated with 150 mg/kg/d NACA and injected with CM (CIN+NACA2). NAC and NACA were injected intraperitoneally (i.p.) once daily for 4 consecutive days (days 1–4). CON and CIN rats were given the same volume of saline. On day 3, all rats were left without water for 24 h. On day 4, 20 min after injections of saline, NAC or NACA, CIN, CIN+NAC, CIN+NACA1, and CIN+NACA2 rats were injected with a nitric oxide synthase inhibitor (NG-nitro-L-arginine methyl ester, L-NAME, 10 mg/kg, i.p.), followed after 15 and 30 min, respectively, by injection of an inhibitor of prostaglandin synthesis (indomethacin, 10 mg/kg, i.p.) and iohexol (1.5–2 g iodine/kg, i.p.). CON rats received injections of equivalent volume of saline. On day 5, all rats were allowed regular chow and tap water in metabolic cages for 24 h.

Baseline blood samples were collected from the tail vein under ether anaesthesia for analysis of serum creatine (Scr), blood urea nitrogen (BUN), and plasma Cystatin-C (CysC). Urine samples (24-h) were collected on day 1 (baseline) and on day 5 for determination of urinary N-acetyl-β-glucosaminidase (UNAG) and urinary γ-glutamyl transpeptidase (UGGT). At the end of day 5, blood samples were collected from the abdominal aorta under pentobarbital (50 mg/kg) anesthesia for determination of Scr, BUN, and CysC. Subsequently the rats were killed and kidneys removed for biochemical and morphological studies.

2.4. Histopathological Examinations

2.4.1. Light Microscopy. Left kidney samples were fixed in 10% formalin and prepared for examination by light microscopy by hematoxylin and eosin (HE) staining, TUNEL staining, or immunohistochemistry (IHC).

For TUNEL staining, sections were stained using In Situ Cell Death Detection Kit (Roche Applied Science, Mannheim, Germany). TUNEL-positive tubular cell numbers were counted in 20 nonoverlapping random cortical fields under a 400x magnification.

For IHC, sections (4 mm) were immersed in citrate buffer and autoclaved at 120°C for 10 min and then immersed in 3% aqueous hydrogen peroxide (H_2O_2). The sections were incubated with a rabbit polyclonal antibody (phospho-p38 MAPK, #9211, Cell Signaling Technology, Danvers, MA, USA, 1 : 200) for 1 h at room temperature. Immunodetection was performed using biotinylated anti-rabbit IgG and peroxidase-labeled avidin chain working fluid (Beijing Zhong Shan

Golden Bridge Biotechnology Co., China), with diaminobenzidine as the substrate. Finally, the slides were lightly counterstained with hematoxylin for 30 sec. The positive signals were measured using Motic Med 6.0 CMIAS Image Analysis System (Motic China Group Co., Ltd., China). The area density representing the positive staining intensity was calculated as the ratio between the stained area and the total analyzed field. Two blinded examiners independently analyzed all slides.

2.4.2. Transmission Electron Microscopy (TEM). The right renal cortex samples were cut into pieces (2 × 2 mm) on ice and fixed in 2.5% (v/v) glutaraldehyde-polyoxymethylene solution for 6–8 h at 4°C and subsequently embedded in Epon 812. Ultrathin sections (60–70 nm) were stained with uranyl acetate and alkaline lead citrate and visualized under a JEM 100CX transmission electron microscope.

2.4.3. Analysis of Renal Oxidative Stress Indicators. Superoxide dismutase (SOD), malondialdehyde (MDA), and glutathione (GSH) levels in renal tissues were determined using SOD kit, MDA kit, and GSH kit, respectively (Sigma, St. Louis, MO, USA). Briefly, tissue blocks of the appropriate size were placed in ice-cold normal saline and homogenated in a ratio of 1 : 9, w (g) : v (ml). After 15 min of centrifugation at 3000 rpm, the supernatant was removed and used for determination of SOD, MDA, and GSH using the respective kits and an UV-visible spectrophotometer.

2.4.4. Quantitative Real-Time PCR (QPCR). Renal cortexes were dissected and total RNA was extracted using Trizol according to the manufacturer's instructions (Invitrogen, Carlsbad, USA). cDNA was synthesized using random primer and a High Capacity cDNA Reverse Transcription Kit (Applied Biosystems, USA). The following primers were used: Trx1 F-GTGGTGTGGACCTTGCAAAA, R-GGAAGGTCGGCATGCATTTG; beta-actin F-CTGTGTGGATTGGTGGCTCT, R-GCAGCTCAGTAACAGTCCGC. QPCR was performed on a 7500 Real-Time PCR System (Applied Biosystems, USA).

2.4.5. Western Blot Analysis. Western blotting was performed as described [6, 7, 30, 31]. Renal cortex samples were lysed in a lysis buffer, separated by electrophoresis in 6–12% polyacrylamide gel, and transferred to polyvinylidene fluoride (PVDF) membranes. Protein expression was quantified by Image J 1.45 software (Wayne Rasband, NIH, Bethesda, MD, USA) after scanning the film. Primary antibodies used included anti-ASK1 (abcam); anti-phospho-ASK1 (abcam, Ser966); anti-Trx1 (abcam); anti-p38 MAPK (Cell Signaling Technology); anti-phospho-p38 MAPK (Cell Signaling Technology, Thr180/Tyr182); anti-cleaved caspase 3 (Cell Signaling Technology); and anti-beta-actin (Cell Signaling Technology). All experiments were performed at least 3 times (i.e., 3 separate protein preparations) under the same conditions.

2.4.6. Statistical Analysis. Results are expressed as means ± SD. One-way analysis of variance (ANOVA) with Tukey's post hoc multiple-comparison test was used to determine the significance of differences in multiple comparisons. Differences were considered significant if $p < 0.05$ and highly significant if $p < 0.01$.

3. Results

3.1. Effects of Induction of CIN (Table 1). At baseline, there was no difference in blood levels of markers of renal functional among the 5 groups. CIN was effectively induced in CIN group as evident from drastic deterioration in renal function (Table 1) and morphological changes, including severe vacuolization of the renal cortex, intratubular cast formation, and medullary congestion (Figure 1(b)).

3.2. Effect of NAC and NACA on Renal Function Parameters. Pretreatment with NAC or NACA preserved renal function as evident from analysis of renal function parameters (Table 1). At the same dose (150 mg/kg/d), NACA was uniformly more effective than NAC as demonstrated by lower Scr, BUN, UNAG, and UGGT (Table 1, $p < 0.05$ versus CIN+NAC). In fact, 50 mg/kg/d NACA had similar effects to 150 mg/kg/d of NAC.

3.3. Effects of NAC and NACA on Histopathology and Ultrastructures (Figure 1). Histopathological examinations of renal samples from CIN rats revealed normal glomerulus structure but severe renal tubular interstitial injury (Figure 1(b)). Pretreatment with NAC or NACA markedly attenuated the development of these lesions (Figures 1(c), 1(d), and 1(e)).

Renal tubular epithelial cell apoptosis in CIN rats was evident by TEM. Cells undergoing apoptosis were characterized by injuries to ultrastructures (Figure 1(g)), for example, condensation of the nuclear chromatin, wrinkling of nuclear membranes, swelling of mitochondria, fracture of cristae, and shedding of microvilli of cell cavity. In comparison, both the apoptotic cell number and injuries to ultrastructures were obviously reduced in CIN+NAC, CIN+NACA1, and CIN+NACA2 rats compared to CIN rats (Figures 1(h), 1(i), and 1(j)). Consistent with the findings under light microscopy, no obvious glomerular lesions were observed by TEM in CIN rats (Figures 1(k) and 1(l)).

3.4. Effects of NAC and NACA on Renal Tubular Apoptosis as Assessed by TUNEL Staining and Analysis of Cleaved Caspase 3 (Figure 2). In addition to TEM, apoptosis was assessed with two independent methods: TUNEL staining in kidney sections and analysis of cleaved caspase 3 by western blotting. Compared to CON rats, CIN rats exhibited markedly increased numbers of TUNEL-positive tubular cells (Figures 2(a), 2(b), and 2(f), $p < 0.01$ versus CON) and also increased cleavage of caspase 3 (Figures 2(g) and 2(h), $p < 0.01$ versus CON). Pretreatment with NAC or NACA significantly decreased both apoptotic cell numbers (Figures 2(c)–2(f), $p < 0.01$ versus CIN) and caspase 3 cleavage (Figures 2(g) and 2(h), $p < 0.01$ versus CIN). At the same dose (150 mg/kg/d), NACA exhibited better protection than NAC

Table 1: Effects of NACA on renal function parameters. The baseline levels of Scr, BUN, CysC, UNAG, and UGGT did not differ among the groups. In CIN rats, BUN, Scr, CysC, UNAG, and UGGT were markedly increased on day 5 as compared to CON rats ($p < 0.01$). Pretreatment with NAC or NACA attenuated the effect of CM, and the increases in Scr, BUN, CysC, UGGT, and UNAG were significantly lower than in CIN group ($p < 0.05$ or 0.01). At the same dose (150 mg/kg/d), NACA was significantly more effective than NAC (CIN+NACA2 versus CIN+NAC).

	CON ($n = 8$)	CIN ($n = 8$)	CIN+NAC ($n = 8$)	CIN+NACA1 ($n = 8$)	CIN+NACA2 ($n = 8$)
Scr (μmol/l)					
Baseline	23.30 ± 3.12	22.38 ± 3.07	23.35 ± 4.52	23.45 ± 2.72	24.75 ± 3.28
Day 8	22.49 ± 2.65	82.23 ± 13.08**	52.89 ± 11.33$^{**\#}$	50.71 ± 7.03$^{**\#}$	37.12 ± 5.69$^{*\#\#\&}$
Serum BUN (mmol/l)					
Baseline	5.83 ± 0.82	5.91 ± 0.84	5.52 ± 1.03	5.70 ± 0.29	5.62 ± 0.78
Day 8	5.77 ± 0.44	44.54 ± 6.54**	16.45 ± 2.42$^{**\#\#}$	15.79 ± 2.87$^{**\#\#}$	10.65 ± 2.08$^{*\#\#\&}$
Serum Cystatin-C (U/l)					
Baseline	1.04 ± 0.05	1.15 ± 0.20	1.19 ± 0.31	1.13 ± 0.16	1.11 ± 0.19
Day 8	1.28 ± 0.25	6.71 ± 1.30**	3.55 ± 0.89$^{**\#}$	3.25 ± 0.91$^{**\#}$	2.92 ± 0.61$^{**\#\#}$
UNAG (U/l)					
Baseline	33.71 ± 5.20	35.25 ± 5.38	35.60 ± 3.20	35.95 ± 6.12	33.12 ± 5.50
Day 8	35.55 ± 6.18	69.27 ± 10.28**	51.25 ± 7.37$^{**\#}$	48.69 ± 8.27$^{**\#}$	41.50 ± 9.50$^{*\#\#\&}$
UGGT (IU/l)					
Baseline	667.74 ± 89.10	648.26 ± 112.08	650.38 ± 117.90	640.73 ± 59.07	639.41 ± 137.55
Day 8	673.28 ± 26.69	6690.15 ± 257.48**	3236.77 ± 536.80$^{**\#\#}$	3064.73 ± 350.29$^{**\#\#}$	2537.17 ± 400.50$^{**\#\#\&}$

Data are means ± SD. $^{*}p < 0.05$ versus CON, $^{**}p < 0.01$ versus CON, $^{\#}p < 0.05$ versus CIN, $^{\#\#}p < 0.01$ versus CIN, and $^{\&}p < 0.05$ versus CIN+NAC.

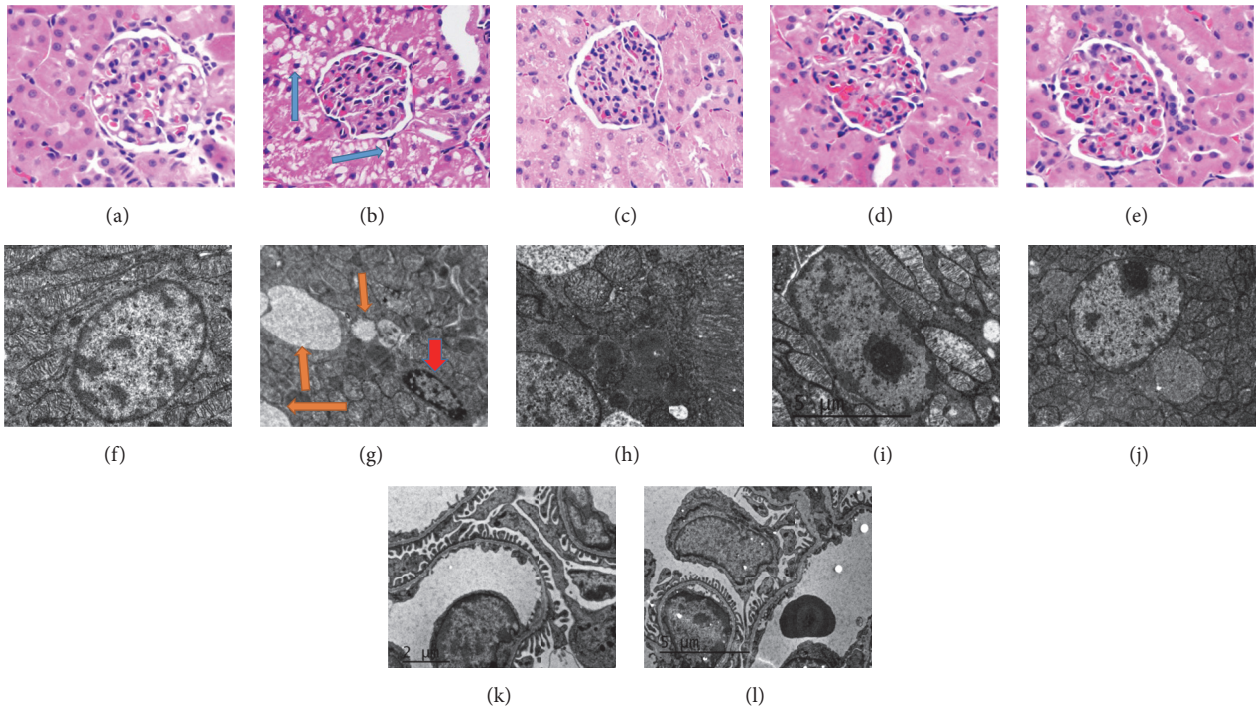

Figure 1: NACA attenuated CM-induced morphological changes. HE staining of kidney sections (magnification ×200) from CON rats (a), CIN rats (b), NAC+CIN rats (c), NACA1+CIN rats (d), and NACA2+CIN rats (e). Representative changes of ultrastructure by TEM (magnifications ×4200) from CON rats (f), CIN rats (g), NAC+CIN rats (h), NACA1+CIN rats (i), NACA2+CIN group (j), normal glomerular basement membrane and podocyte in CON rats (k), and CIN rats (l). Note the condensation of the nuclear chromatin (red arrow) and cytoplasm vacuoles (orange arrow) in CIN rats. Blue arrows refer to severe vacuolization of the renal cortex. Figures are representative of 5 to 8 rats from each group.

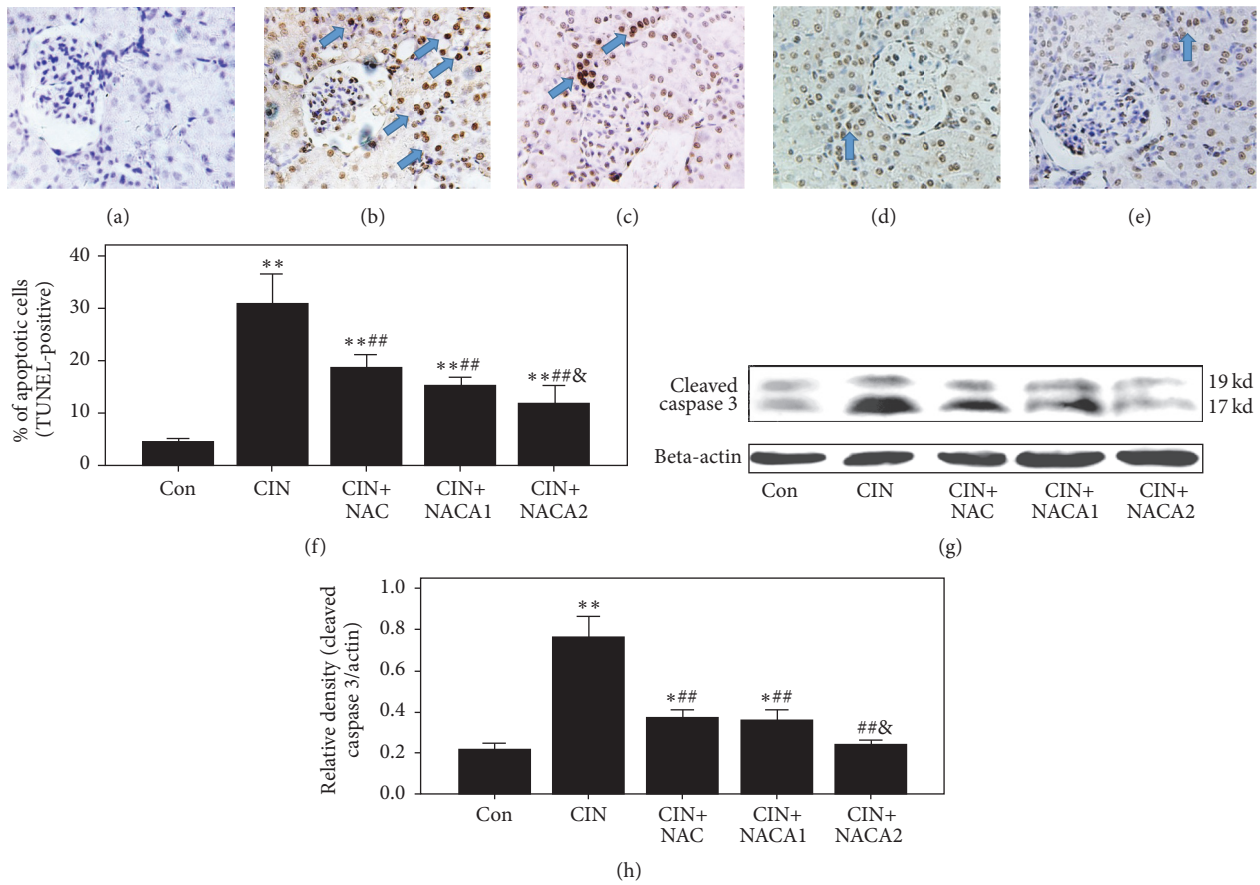

Figure 2: NACA inhibited CM-induced renal tubular cell apoptosis as detected by TUNEL staining and western blot analyses of cleaved caspase 3. CM increased the number of TUNEL-positive renal tubular cells (blue arrows), and pretreatment with NAC or NACA blocked this effect. TUNEL-stained kidney sections (magnifications ×200) from CON rats (a), CIN rats (b), NAC+CIN rats (c), NACA1+CIN rats (d), and NACA2+CIN rats (e). TUNEL-positive cells are marked by blue arrows. (f) Quantitative analysis of TUNEL-positive cell number. (g) Western blot analyses of cleaved capsase-3. (h) Relative densitometry analysis of the ratio of cleaved caspase 3 to beta-actin. Figures are representative of 5 to 8 rats from each group. The values are means ± SD ($n = 5$). $^{*}p < 0.05$ versus CON, $^{**}p < 0.01$ versus CON, $^{\#\#}p < 0.01$ versus CIN, and $^{\&}p < 0.05$ versus CIN+NAC.

(Figure 2(f), $p < 0.05$ versus CIN+NAC, and Figures 2(g) and 2(h), $p < 0.05$ versus CIN+NAC).

3.5. Effects of NAC and NACA on Indicators of Oxidative Stress in Renal Tissue. Induction of CIN attenuated renal SOD (Figure 3(a)) and GSH (Figure 3(c)) and increased MDA (Figure 3(b)) levels ($p < 0.01$ versus CON). Pretreatment with NAC or NACA significantly prevented this (Figure 3, $p < 0.05$ and $p < 0.01$ versus CIN, resp.). At equimolar concentrations, NACA was more effective than NAC at preserving SOD, MDA, and GSH levels ($p < 0.05$ versus CIN+NAC, Figures 3(a)–3(c)).

3.6. Effects of NAC and NACA on P38 MAPK Phosphorylation. Activation of p38 MAPK was confirmed by a significant increase in phospho-p38 MAPK levels as detected by western blotting and IHC (Figures 4(b) and 4(g), $p < 0.01$ versus CON). Pretreatment with NAC or NACA significantly prevented the CIN-induced p38 MAPK activation in kidney (Figures 4(c), 4(d), 4(e), and 4(g), $p < 0.01$ versus CIN). Again, NACA was more effective than NAC at the same dose (Figures 4(f) and 4(h), $p < 0.05$ versus CIN+NAC).

3.7. Effects of NAC and NACA on ASK1 Phosphorylation. We next examined whether ASK1, a potential upstream signal of p38 MAPK, was involved in CIN pathogenesis. As shown in Figures 5(a) and 5(b), phospho-ASK1 level was upregulated in CIN rats ($p < 0.01$ versus CON). Pretreatment with NAC ($p < 0.01$ versus CIN) or, more effectively, NACA (Figures 5(a) and 5(b), $p < 0.05$ versus CIN+NAC) inhibited this activation.

3.8. Effects of NAC and NACA on Trx1 mRNA and Protein Expressions. In order to deduce the role of Trx1 in CIN, Trx1 mRNA and protein expressions were evaluated by QPCR and western blotting, respectively. As shown in Figure 5, Trx1 protein expression (c, d) and mRNA level (e) were decreased in renal cortex following CIN induction ($p < 0.01$ CON

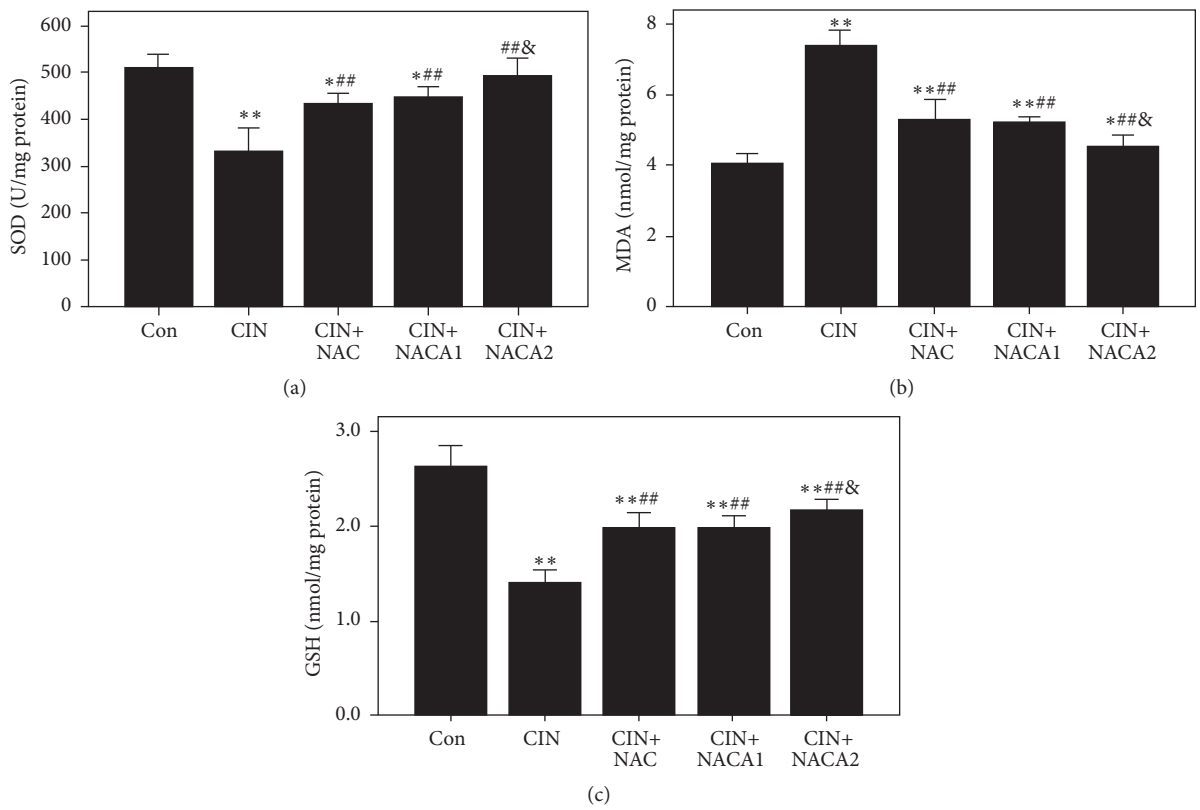

Figure 3: NACA inhibited CM-induced indicators of oxidative stress in kidney. Exposure to CM significantly attenuated renal SOD (a) and GSH levels and increased MDA (b) levels. Pretreatment with NAC or NACA blocked the CIN-induced changes. Figures are representative of 5 to 8 rats in each group. The values are means ± SD ($n = 5$). $^{*}p < 0.05$ versus CON, $^{**}p < 0.01$ versus CON, $^{\#\#}p < 0.01$ versus CIN, and $^{\&}p < 0.05$ versus CIN+NAC.

versus CIN). However, the downregulated expressions of Trx1 were markedly blocked by NAC and NACA ($p < 0.01$ versus CIN).

4. Discussion

Although the mechanisms underlying CIN have not been fully clarified, several studies have shown that ROS-induced oxidative stress and direct cytotoxicity of contrast media are important in the pathogenesis of the disease [2, 6, 32, 33]. Here, we confirm the importance of oxidative stress and demonstrate that the novel antioxidant NACA, an amide derivate of NAC with better tissue penetration, offers more effective prevention against CIN. Furthermore, we show that Txr1/ASK1 signal act as the upstream modulator of the p38 MAPK and present a potential drug target for prevention. To our knowledge, this is the first report demonstrating that Trx1/ASK1 signal are involved in CIN.

The oxidative stress induced in rats with CIN was evident by drastically decreased levels of SOD and GSH, as well as an increased level of MDA, which is consistent with our previous data [6, 7] and other reports [34, 35]. The findings that NACA consistently exhibited better renoprotection than NAC may be related to its better membrane penetration. However, whether other mechanisms of action are involved is not clear and needs further studies. Overall, the present findings confirmed again that oxidative stress is an important factor in the pathogenesis of CIN.

Since there is significant inconsistency in the guidelines regarding the benefit of NAC to reduce the risk for CIN [1, 35], large-scale, randomized clinical trials that are adequately powered have been proposed to determine the effectiveness of NAC for prevention of CIN. Our present findings suggest that consideration should be given to the use of NACA as a result of its superior renoprotective function relative to NAC.

CIN, also called contrast-induced acute kidney injury (CI-AKI), is typically defined by an increase in serum creatinine after intravascular administration of contrast media, but serum creatinine is a late and insensitive indicator of AKI [7, 36–38]. Thus, several additional biomarkers have been investigated in order to improve both prediction and diagnosis of AKI. Our previous study first reported that urinary γ-glutamyl transpeptidase (UGGT) has good sensitivity in early detection of contrast-induced acute renal injury and thus in early diagnosing AKI [7]. UGGT as a potential early diagnostic biomarker of AKI has been confirmed in AKI patients after liver transplantation [39]. Furthermore, another GSH-dependent enzyme present in large amount in liver, urinary glutathione S-transferases (UGST), has recently been

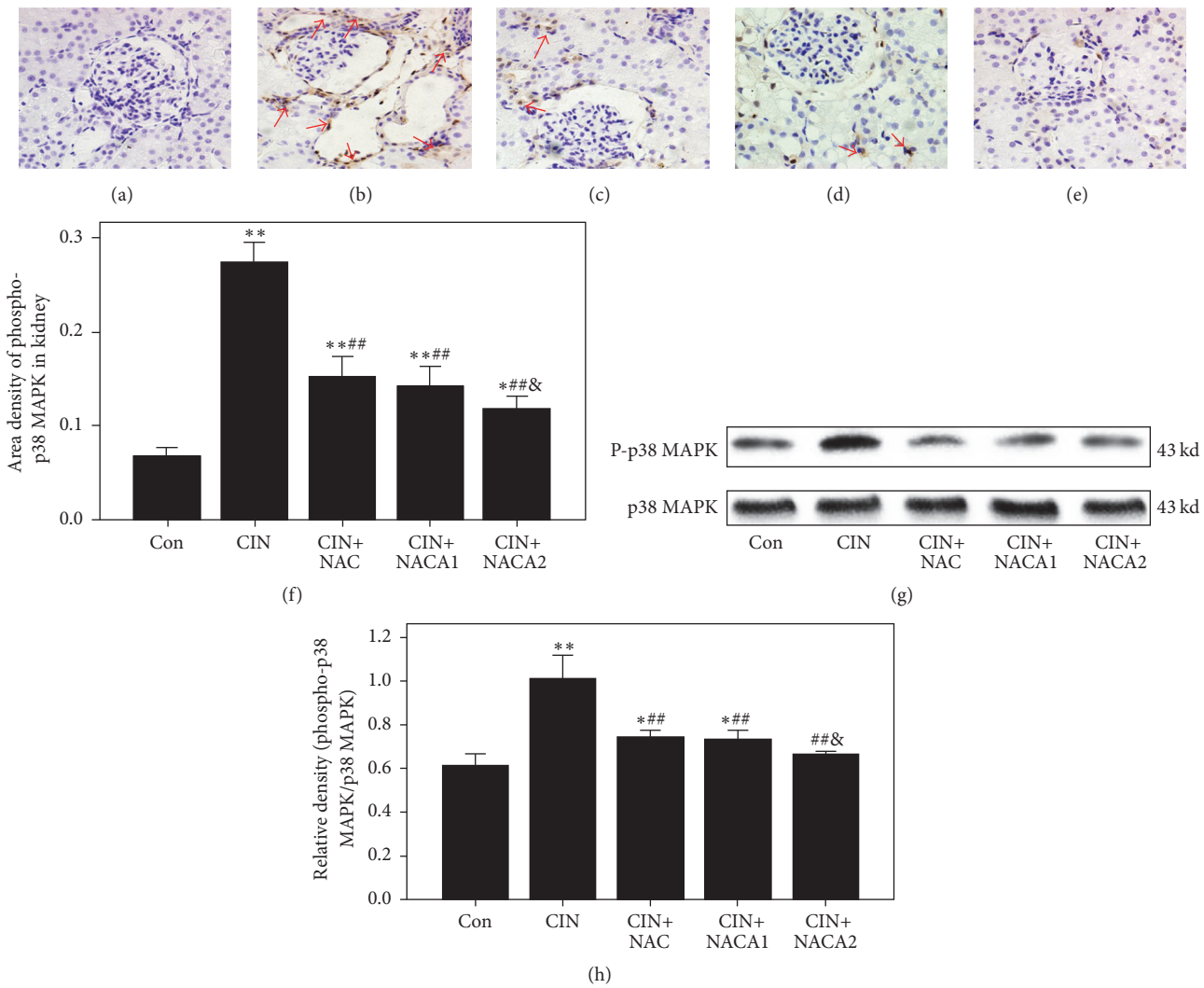

Figure 4: Effects of NACA on p38 MAPK phosphorylation in kidney. IHC staining of phospho-p38 MAPK in CON (a), CIN (b), NAC+CIN (c), NACA1+CIN (d), and NACA2+CIN (e) rats, respectively (figures are representative of 5 to 8 rats in each group). Note positive stained area (yellow) of IHC staining (arrow). (f) Semiquantitative analysis of phosphor-p38 MAPK expression in kidneys with IHC. (g) Phospho-p38 MAPK and total-p38 MAPK expressions by western blotting ($n = 3$ each). (h) Relative densitometry analysis of the ratio of phospho-p38 MAPK to total-p38 MAPK. Data are shown as means ± SD ($n = 3$ each). $^{*}p < 0.05$ versus CON, $^{**}p < 0.01$ versus CON, $^{\#\#}p < 0.01$ versus CIN, and $^{\&}p < 0.05$ versus CIN+NAC.

identified as a biomarker of AKI [40]. Subsequent studies should address usefulness of these and other biomarkers in terms of sensitivity and early detection of kidney injury.

Previous work from our laboratory and others has confirmed that contrast-induced apoptotic cell death via p38 MAPK pathway is an important pathogenic mechanism in CIN [6, 7, 17, 18]. There is evidence that p38 MAPK activation is associated with renal injury, which highlights p38 MAPK pathway as an attractive therapeutic target. However, the potential pathway by which p38 MAPK is activated in CIN is still not well defined so far.

Since MAPKs could be regulated upstream by the MAPK kinase kinase kinase (MAP3K) and p38 MAPK could act as the target of ASK1, we investigated the effect of contrast media on activation of ASK1, a member of MAP3K family [20, 41]. The present data demonstrated increased ASK1 phosphorylation in CIN, which could be blocked by NACA and NAC. Our present data indicated clearly that contrast media could activate the stress/death signaling mitogen-activated protein kinase (MAPK) phosphorylation cascade and thus confirmed that ASK1/p38 MAPK could be a potential drug target for preventing CIN. The study of Ma et al. has also identified ASK1 as a potential therapeutic target in renal fibrosis [20].

Reduced Trx1 could be a direct inhibitor or negative regulator of ASK1, while ROS stimulation could dissociate Trx1 from Trx1/ASK1 complex and lead to ASK1 activation and in turn result in the phosphorylation of its downstream substrate p38 MAPK [22, 26]. As mentioned above, we previously reported that contrast media exposure directly increased cellular oxidation and induced p38 AMPK/iNOS

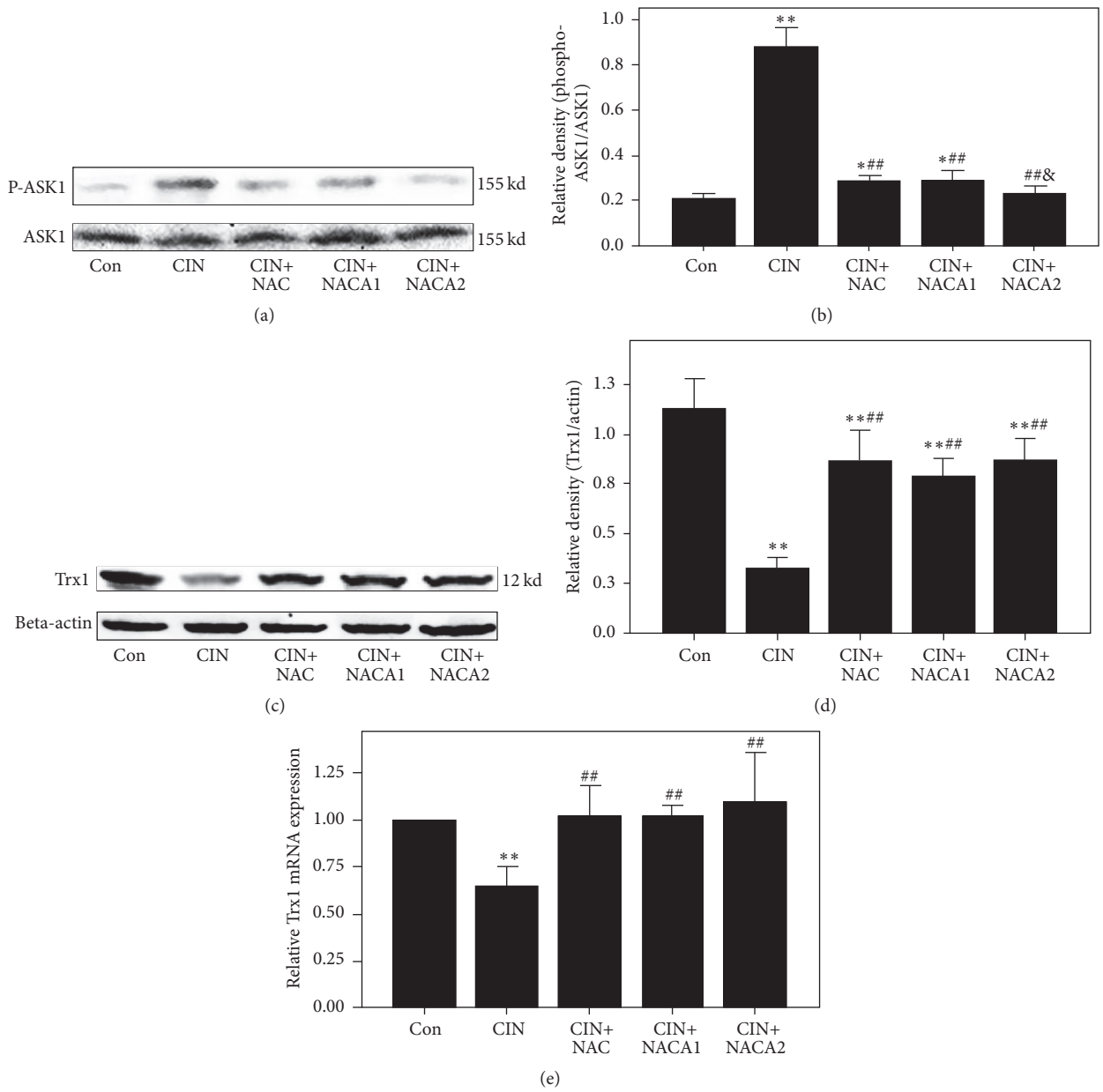

Figure 5: NACA blocked CM-induced p38 MAPK activation by inhibiting ASK1 phosphorylation and upregulating Trx1 mRNA and protein expression. (a) Phospho-ASK1 and ASK1 expressions by western blotting ($n = 3$ each). (b) Relative densitometry analysis of the ratio of phospho-ASK1 to ASK1. (c) Trx1 expression by western blotting ($n = 3$ each). (d) Relative densitometry analysis of the ratio of Trx1 to beta-actin. (e) QPCR analysis for Trx1 mRNA in renal cortex. Data are shown as means ± SD ($n = 3$ each). $^{*}p < 0.05$ versus CON, $^{**}p < 0.01$ versus CON, $^{\#\#}p < 0.01$ versus CIN, and $^{\&}p < 0.05$ versus CIN+NAC.

pathway mediated apoptosis in renal tubular cells in vitro and vivo [6, 7]. Additionally, our present data further clearly indicated that contrast media exposure downregulated Trx1 and increased ASK1 phosphorylation in CIN rat model. Thus we could speculate that the more complete signal mechanism for CIN should include the following key steps (Figure 6); first, contrast medium exposure increased ROS production of kidney, resulting in suppression of Trx1, which lead to Trx1/ASK1 complex dissociation to facilitate the activation of ASK1. This results in the downstream activation of its substrate p38 MAPK and an imbalance of pro- and antiapoptotic members of the Bcl-2 family and finally induced apoptotic cell death. Interestingly, such a pathologic process could be efficiently inhibited by NACA through its antioxidant activity and by upregulating Trx1.

5. Conclusion

Summarily, based on our present and previous studies, we demonstrated that NACA is more effective than NAC in preventing CIN both in vivo and in vitro and identified the

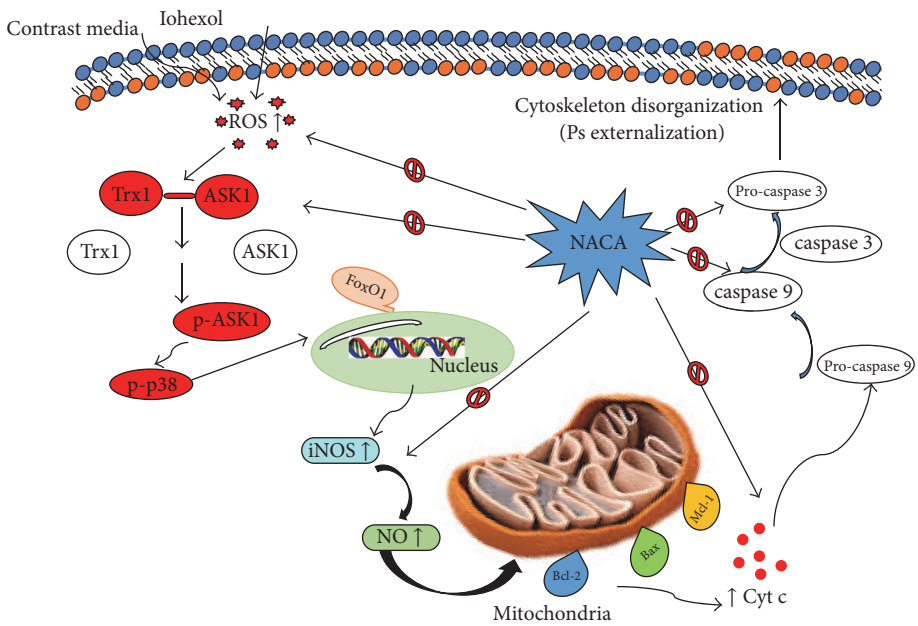

Figure 6: Schematic diagram illustrates the signal mechanism for CIN and the renoprotection of NACA. Contrast media exposure increases ROS production in kidney, resulting in suppression of Trx1 and thus dissociating the Trx1/ASK1 complex to facilitate the activation of ASK1 (phosphorylation). Subsequently, activated ASK1 results in the downstream activation of its substrate p38 MAPK, an imbalance of pro- and antiapoptotic members of the Bcl-2 family, and finally induces apoptosis. NACA efficiently inhibits such a pathologic process through its antioxidant activity and by upregulating Trx1. p, phosphorylation. Ps, phosphatidylserine.

underlying mechanisms including suppression of oxidative stress, upregulating Trx1 and in turn inhibiting ASK1/p38 MAPK pathway, and preventing renal tubular cell apoptosis.

Competing Interests

The authors declare that there is no conflict of interests regarding the publication of this paper.

Acknowledgments

The authors would like to thank Dr. Glenn Goldstein for providing N-acetylcysteine amide. This work was supported by National Natural Science Foundation of China (Grants 81573936 and 81373614) and sponsored by Shanghai Pujiang Program.

References

[1] J. J. Keaney, C. M. Hannon, and P. T. Murray, "Contrast-induced acute kidney injury: how much contrast is safe?" *Nephrology Dialysis Transplantation*, vol. 28, no. 6, pp. 1376–1383, 2013.

[2] H. Li, C. Wang, C. Liu, R. Li, M. Zou, and G. Cheng, "Efficacy of short-term statin treatment for the prevention of contrast-induced acute kidney injury in patients undergoing coronary angiography/percutaneous coronary intervention: a meta-analysis of 21 randomized controlled trials," *American Journal of Cardiovascular Drugs*, vol. 16, no. 3, pp. 201–219, 2016.

[3] R. J. Owen, S. Hiremath, A. Myers, M. Fraser-Hill, and B. J. Barrett, "Canadian association of radiologists consensus guidelines for the prevention of contrast-induced nephropathy: update 2012," *Canadian Association of Radiologists Journal*, vol. 65, no. 2, pp. 96–105, 2014.

[4] R. Rear, R. M. Bell, and D. J. Hausenloy, "Contrast-induced nephropathy following angiography and cardiac interventions," *Heart*, vol. 102, no. 8, pp. 638–648, 2016.

[5] R. M. Bell, R. Rear, J. Cunningham, A. Dawnay, and D. M. Yellon, "Effect of remote ischaemic conditioning on contrast-induced nephropathy in patients undergoing elective coronary angiography (ERICCIN): rationale and study design of a randomised single-centre, double-blind placebo-controlled trial," *Clinical Research in Cardiology*, vol. 103, no. 3, pp. 203–209, 2014.

[6] X. Gong, G. Celsi, K. Carlsson, S. Norgren, and M. Chen, "N-acetylcysteine amide protects renal proximal tubular epithelial cells against iohexol-induced apoptosis by blocking p38 MAPK and iNOS signaling," *American Journal of Nephrology*, vol. 31, no. 2, pp. 178–188, 2010.

[7] X. Gong, Q. Wang, X. Tang et al., "Tetramethylpyrazine prevents contrast-induced nephropathy by inhibiting p38 MAPK and FoxO1 signaling pathways," *American Journal of Nephrology*, vol. 37, no. 3, pp. 199–207, 2013.

[8] T. B. Sterenborg, T. P. Menting, Y. de Waal et al., "Remote ischemic preconditioning to reduce contrast-induced nephropathy: study protocol for a randomized controlled trial," *Trials*, vol. 15, article 119, 2014.

[9] J. A. Neyra, S. Shah, R. Mooney, G. Jacobsen, J. Yee, and J. E. Novak, "Contrast-induced acute kidney injury following coronary angiography: a cohort study of hospitalized patients with or without chronic kidney disease," *Nephrology Dialysis Transplantation*, vol. 28, no. 6, pp. 1463–1471, 2013.

[10] J. Kooiman, Y. W. J. Sijpkens, J.-P. P. M. De Vries et al., "A randomized comparison of 1-h sodium bicarbonate hydration versus standard peri-procedural saline hydration in patients with chronic kidney disease undergoing intravenous contrast-enhanced computerized tomography," *Nephrology Dialysis Transplantation*, vol. 29, no. 5, pp. 1029–1036, 2014.

[11] N. Lameire, J. A. Kellum, P. Aspelin et al., "Contrast-induced acute kidney injury and renal support for acute kidney injury: a KDIGO summary (part 2)," *Critical Care*, vol. 17, no. 1, article 205, 2013.

[12] K. A. Carver and D. Yang, "N-acetylcysteine amide protects against oxidative stress–induced microparticle release from human retinal pigment epithelial cells," *Investigative Ophthalmology and Visual Science*, vol. 57, no. 2, pp. 360–371, 2016.

[13] M. Paul, M. Hemshekhar, R. M. Thushara et al., "Methotrexate promotes platelet apoptosis via JNK-mediated mitochondrial damage: alleviation by *N*-acetylcysteine and *N*-acetylcysteine amide," *PLoS ONE*, vol. 10, no. 6, Article ID e0127558, 2015.

[14] T. Benterud, M. B. Ystgaard, S. Manueldas et al., "N-acetylcysteine amide exerts possible neuroprotective effects in newborn pigs after perinatal asphyxia," *Neonatology*, vol. 111, no. 1, pp. 12–21, 2016.

[15] K. Sunitha, M. Hemshekhar, R. M. Thushara et al., "N-Acetylcysteine amide: a derivative to fulfill the promises of N-Acetylcysteine," *Free Radical Research*, vol. 47, no. 5, pp. 357–367, 2013.

[16] X. Gong, G. Celsi, K. Carlsson, and S. Norgren, "Protective effects of N-acetylcysteine amide (NACA) on gentamicin-induced apoptosis in LLC-PK1 cells," *Renal Failure*, vol. 34, no. 4, pp. 487–494, 2012.

[17] M. Andreucci, G. Lucisano, T. Faga et al., "Differential activation of signaling pathways involved in cell death, survival and inflammation by radiocontrast media in human renal proximal tubular cells," *Toxicological Sciences*, vol. 119, no. 2, pp. 408–416, 2011.

[18] C. Quintavalle, M. Brenca, F. De Micco et al., "In vivo and in vitro assessment of pathways involved in contrast media-induced renal cells apoptosis," *Cell Death and Disease*, vol. 2, no. 5, article no. e155, 2011.

[19] F. Y. Ma, G. H. Tesch, and D. J. Nikolic-Paterson, "ASK1/p38 signaling in renal tubular epithelial cells promotes renal fibrosis in the mouse obstructed kidney," *American Journal of Physiology - Renal Physiology*, vol. 307, no. 11, pp. F1263–F1273, 2014.

[20] F. Y. Ma, G. H. Tesch, and D. J. Nikolic-Paterson, "ASK1/p38 signaling in renal tubular epithelial cells promotes renal fibrosis in the mouse obstructed kidney," *American Journal of Physiology—Renal Physiology*, vol. 307, no. 11, pp. F1263–F1273, 2014.

[21] W. Hao, T. Takano, J. Guillemette, J. Papillon, G. Ren, and A. V. Cybulsky, "Induction of apoptosis by the Ste20-like kinase SLK, a germinal center kinase that activates apoptosis signal-regulating kinase and p38," *Journal of Biological Chemistry*, vol. 281, no. 6, pp. 3075–3084, 2006.

[22] R. M. Hashem, K. M. Hassanin, L. A. Rashed, M. O. Mahmoud, and M. G. Hassan, "Effect of silibinin and vitamin E on the ASK1-p38 MAPK pathway in D-galactosamine/lipopolysaccharide induced hepatotoxicity," *Experimental Biology and Medicine*, vol. 241, no. 11, pp. 1250–1257, 2016.

[23] Q.-Q. Wu, M. Xu, Y. Yuan et al., "Cathepsin B deficiency attenuates cardiac remodeling in response to pressure overload via TNF-α/ASK1/JNK pathway," *American Journal of Physiology—Heart and Circulatory Physiology*, vol. 308, no. 9, pp. H1143–H1154, 2015.

[24] Y. Huang, L. Wu, J. Wu, Y. Li, and L. Hou, "Cellular FLICE-like inhibitory protein protects against cardiac hypertrophy by blocking ASK1/p38 signaling in mice," *Molecular and Cellular Biochemistry*, vol. 397, no. 1-2, pp. 87–95, 2014.

[25] K. Shen, F. Lu, J. Xie et al., "Cambogin exerts anti-proliferative and pro-apoptotic effects on breast adenocarcinoma through the induction of NADPH oxidase 1 and the alteration of mitochondrial morphology and dynamics," *Oncotarget*, vol. 7, no. 31, pp. 50596–50611, 2016.

[26] R. Jin, Y. Gao, S. Zhang et al., "Trx1/TrxR1 system regulates post-selected DP thymocytes survival by modulating ASK1-JNK/p38 MAPK activities," *Immunology and Cell Biology*, vol. 93, no. 8, pp. 744–752, 2015.

[27] Y. Agmon, H. Peleg, Z. Greenfeld, S. Rosen, and M. Brezis, "Nitric oxide and prostanoids protect the renal outer medulla from radiocontrast toxicity in the rat," *Journal of Clinical Investigation*, vol. 94, no. 3, pp. 1069–1075, 1994.

[28] Y. Yokomaku, T. Sugimoto, S. Kume et al., "Asialoerythropoietin prevents contrast-induced nephropathy," *Journal of the American Society of Nephrology*, vol. 19, no. 2, pp. 321–328, 2008.

[29] H. T. Lee, M. Jan, C. B. Soo et al., "A1 adenosine receptor knock-out mice are protected against acute radiocontrast nephropathy in vivo," *American Journal of Physiology—Renal Physiology*, vol. 290, no. 6, pp. F1367–F1375, 2006.

[30] X. Gong, V. N. Ivanov, and T. K. Hei, "2,3,5,6-Tetramethylpyrazine (TMP) down-regulated arsenic-induced heme oxygenase-1 and ARS2 expression by inhibiting Nrf2, NF-κB, AP-1 and MAPK pathways in human proximal tubular cells," *Archives of Toxicology*, vol. 90, no. 9, pp. 2187–2200, 2015.

[31] X. Gong, V. N. Ivanov, M. M. Davidson, and T. K. Hei, "Tetramethylpyrazine (TMP) protects against sodium arsenite-induced nephrotoxicity by suppressing ROS production, mitochondrial dysfunction, pro-inflammatory signaling pathways and programed cell death," *Archives of Toxicology*, vol. 89, no. 7, pp. 1057–1070, 2014.

[32] L. Tongqiang, L. Shaopeng, Y. Xiaofang et al., "Salvianolic acid B prevents iodinated contrast media-induced acute renal injury in rats via the PI3K/Akt/Nrf2 pathway," *Oxidative Medicine and Cellular Longevity*, vol. 2016, Article ID 7079487, 11 pages, 2016.

[33] M. Buyuklu, F. M. Kandemir, M. Ozkaraca, T. Set, E. M. Bakirci, and E. Topal, "Protective effect of curcumin against contrast induced nephropathy in rat kidney: what is happening to oxidative stress, inflammation, autophagy and apoptosis?" *European Review for Medical and Pharmacological Sciences*, vol. 18, no. 4, pp. 461–470, 2014.

[34] A. Tasanarong, S. Kongkham, and A. Itharat, "Antioxidant effect of *Phyllanthus emblica* extract prevents contrast-induced acute kidney injury," *BMC Complementary and Alternative Medicine*, vol. 14, article 138, 2014.

[35] N. Wang, R.-B. Wei, Q.-P. Li et al., "Renal protective effect of probucol in rats with contrast-induced nephropathy and its underlying mechanism," *Medical Science Monitor*, vol. 21, pp. 2886–2892, 2015.

[36] M. Lichosik, A. Jung, K. Jobs, A. Mierzejewska, R. Zdanowski, and B. Kalicki, "Interleukin 18 and neutrophil-gelatinase associated lipocalin in assessment of the risk of contrast-induced nephropathy in children," *Central European Journal of Immunology*, vol. 40, no. 4, pp. 447–453, 2016.

[37] G. F. Lehner, L. G. Forni, and M. Joannidis, "Oliguria and biomarkers of acute kidney injury: star struck lovers or strangers in the night?" *Nephron*, vol. 134, no. 3, pp. 183–190, 2016.

[38] S. S. Waikar and J. V. Bonventre, "Creatinine kinetics and the definition of acute kidney injury," *Journal of the American Society of Nephrology*, vol. 20, no. 3, pp. 672–679, 2009.

[39] P. Marcelino, I. Tavares, D. Carvalho et al., "Is urinary γ-glutamyl transpeptidase superior to urinary neutrophil gelatinase-associated lipocalin for early prediction of acute kidney injury after liver transplantation?" *Transplantation Proceedings*, vol. 46, no. 6, pp. 1812–1818, 2014.

[40] K. H. Shu, C. Wang, C. Wu et al., "Urinary π-glutathione S-transferase predicts advanced acute kidney injury following cardiovascular surgery," *Scientific Reports*, vol. 6, article 26335, 2016.

[41] A. Ray, N. Sehgal, S. Karunakaran, G. Rangarajan, and V. Ravindranath, "MPTP activates ASK1-p38 MAPK signaling pathway through TNF-dependent Trx1 oxidation in parkinsonism mouse model," *Free Radical Biology and Medicine*, vol. 87, Article ID 12501, pp. 312–325, 2015.

Hindawi Publishing Corporation
Oxidative Medicine and Cellular Longevity
Volume 2016, Article ID 5454963, 9 pages
http://dx.doi.org/10.1155/2016/5454963

Research Article

Dietary Supplementation of *Phoenix dactylifera* Seeds Enhances Performance, Immune Response, and Antioxidant Status in Broilers

Ali H. El-Far,[1] Hamada A. Ahmed,[2] and Hazem M. Shaheen[3]

[1]*Department of Biochemistry, Damanhour University, Damanhour, Egypt*
[2]*Department of Nutrition and Veterinary Clinical Nutrition, Damanhour University, Damanhour, Egypt*
[3]*Department of Pharmacology, Damanhour University, Damanhour, Egypt*

Correspondence should be addressed to Hazem M. Shaheen; dr_hazemshaheen3010@yahoo.com

Received 9 August 2016; Revised 20 October 2016; Accepted 24 October 2016

Academic Editor: Kota V. Ramana

Copyright © 2016 Ali H. El-Far et al. This is an open access article distributed under the Creative Commons Attribution License, which permits unrestricted use, distribution, and reproduction in any medium, provided the original work is properly cited.

The date palm (*Phoenix dactylifera*) seeds were utilized in some traditional medical remedies and have been investigated for their possible health benefits. This proposed study wanted to assess the effect of date palm seeds (DPS) dietary supplementation in comparison to mannan-oligosaccharides (Bio-Mos®) and β-glucan over antioxidant and immunity events that have effect on growth and carcass performances of broilers. An aggregate of 180, one-day-old, chicks were raised in the wire-floored cages and allotted into control, Bio-Mos (0.1% Bio-Mos), β-glucan (0.1% β-glucan), DPS2 (2% date crushed seeds), DPS4 (4% date crushed seeds), and DPS6 (6% date crushed seeds) groups. Broilers in DPS2 and DPS4 groups showed significant variations ($P < 0.05$) in relative growth rate (RGR), feed conversion ratio (FCR), and efficiency of energy utilization in comparison to control group. Moreover, all DPS fed groups showed significant increases ($P < 0.05$) in serum reduced glutathione (GSH) values. Meanwhile, both serum interferon-gamma (IFN-γ) and interleukin-2 (IL-2) levels were significantly increased ($P < 0.05$) in DPS2. Consequently, obtained data revealed a substantial enhancement of performance, immunity, and antioxidant status by DPS supplementation in broiler that might be related to the antioxidant and immune-stimulant constituents of *P. dactylifera* seeds.

1. Introduction

Wide usage of antimicrobial agents has added to an imbalance among pathogenic and ordinary intestinal microflora as well as the development of multiple antibacterial resistance cases. In the poultry industry, natural feed additives have got the potential of reduction of poultry enteric diseases [1, 2]. Both mannan-oligosaccharides and β-glucan are extracted from *Saccharomyces cerevisiae* [3] and both were used as a feed additive in many poultry farms to enhance poultry execution and lower the liability to the pathogens propagation of the gastrointestinal tract and respiratory system [4, 5]. β-Glucan is a glucose polymer as basic component in the yeast and fungi that enhances defenses against bacterial challenge and increases the growth performance [6].

Phoenix dactylifera is a major source of nutrients for mankind [7]. The date palm seeds (DPS) are also called pips, stones, kernels, or pits that represent about 6–12% of whole date [8]. DPS are rich in minerals and vitamins. The chemical composition of DPS varies according to the nature of cultivating land. As far as dry weight, the chemical components of DPS have contained about 5–10% of moisture, 5–7% of protein, 7–10% of oil, 10–20% of crude fiber, 55–65% of carbohydrates, and 1-2% of ash [9]. The antioxidant effect of DPS regards its phenolic compounds of anticarcinogenic and anti-inflammatory activities [10].

Using medicinal herbs to decrease the participation of chemicals through the worldwide tendency to return to the natural supplements has been supported by the World Health Organization [11]. Many studies were done to investigate the usage of the medicinal plant as feed additives such as basil supplementation and/or chamomile that improves the immunity and performance of broiler [12] and *P. dactylifera* in New Zealand rabbits [13]. *P. dactylifera* is a prevalent diet among

the Middle Eastern populations; its fruits are framed of a fleshy pericarp and seed, constituting between 10% and 15% of date fruit weight [14]. *P. dactylifera* has been developed in the Middle East over no less than 6000 years ago [15].

This trial was designed to compare the possible effects of mannan-oligosaccharides, β-glucan, and different levels of *P. dactylifera* seeds (DPS) on performance, and carcass characteristics, beside the oxidative and immunity events in broilers.

2. Materials and Methods

2.1. Chemical Analysis of Phoenix dactylifera Seeds. *P. dactylifera* seeds were collected at tamr stage from Al-Beheira Governorate, Egypt, and kept at 4°C. DPS were crushed to produce a fine powder subsequently analyzed [16] for the dry matter at 105°C for 3 hours in a hot air oven. Crude protein was determined by Kjeldahl method using Gerhardt Vapodest 10 and Gerhardt Turbotherm and lipid by ether extraction (Gerhardt Soxtherm). Fibers were determined by extraction with 0.5 M H_2SO_4 and 0.5 M NaOH (Gerhardt Fibertherm), drying, and ashing, after which ash substance was resolved after burning in a furnace at 550°C for 12 hours. Moreover, lysine and methionine were determined by calculation [17].

2.2. Phoenix dactylifera Seeds Extract. The crushed *P. dactylifera* seeds were extracted with methanol [18]. Quickly, 15 g of *P. dactylifera* seeds powder was extracted with 100 mL of methanol for 24 hours with occasional shaking. The extract was filtered and evaporated to dryness in a vacuum.

2.3. Gas Chromatography-Mass Spectrometry (GC-MS) Analysis. The chemical components of *P. dactylifera* seeds were carried on using Trace GC Ultra-ISQ mass spectrometer with a direct capillary column TG-5MS with 30 m × 0.25 mm × 0.25 μm film thickness. The oven temperature was adjusted at 60°C and then raised by 5°C/minute to 280°C. The temperatures of both injector and detector were adjusted at 250°C. Helium was used as a carrier gas at a constant flow rate of 1 mL/minute for 21.03 minutes. The solvent retention time was 2 minutes and the diluted samples of 1 μL were injected by using autosampler AS3000 in the splitless mode. The segments were recognized by examination of their delay times and mass spectra with those of NIST 11 mass spectral database [19].

2.4. Birds and Dietary Treatments. This work was completed at the Faculty of Veterinary Medicine, Damanhour University, to evaluate the possible effects of Bio-Mos (mannan-oligosaccharides, produced by Alltech Co., USA), β-glucan ((1,3) β-D-glucan) which is produced by Beta-Mune™, Germany, and different levels of DPS supplementations on growth profile, carcass attributes, oxidative status, and immune events in broilers. One hundred eighty of one-day-old Ross 308 chicks with a mean body weight of 39.50 g were acquired from the local broiler chicken hatchery and then randomly allocated into six experimental groups (three replicates each of ten birds).

The study convention was affirmed by the Committee on the Ethics of Animal Experiments of Alexandria University, Egypt. The birds were raised in wire-floored cages and fed on a starter diet from the beginning of the experiment till the 3rd week of age, followed by a finishing diet to the end of experiment. The chicks were allocated into control (received the basal eating program), Bio-Mos (received the basal diet containing 0.1% Bio-Mos), β-glucan (got the basal eating routine containing 0.1% β-glucan), DPS2 (received diet containing 2% date crushed seeds), DPS4 (received diet containing 4% date crushed seeds), and DPS6 (received diet containing 6% date crushed seeds) groups from 1st to 42nd days of age.

The incubation temperature of 32°C was gradually decreased until reaching 26°C by the third week of age. The chicks were exposed to a 23-hour light regimen. Both components and synthetic materials of the basal diets are showed in Tables 1 and 2. The basal diets were mixed using National Research Council instruction [20] where protein percentages are 22.6 and 18.14 g/100 g for starter and finisher diets, respectively. Birds were vaccinated as follows: Clone Ma5 by eye drop on the 7th day of age, Gumboro Intermediate Plus (Bursine Plus vaccine) eye drop on the 14th day, LaSota vaccine eye drop on the 18th day of age, and finally LaSota vaccine plus IBD vaccine eye drop on the 28th day.

2.5. Evaluation of Growth Performance. Body mass development and intake of feed in the treatment groups were weekly recorded. The weight gain in grams was calculated as the difference between two consecutive body weights. In addition, feed conversion ratio, relative growth rate (RGR), and efficiency of energy utilization were also calculated.

2.6. Hemagglutination Inhibition (HI) Test. Three categories of blood specimens were taken from the birds of each experimental group on the 14th, 21st, and 42nd days of age. Blood specimens were taken for collection of sera to examine the antibodies titer against Newcastle disease vaccine, using the HI test as an indicator of the bird's immune health in the different experimental classes. Microtechnique to HI test was carried out following [21], while geometric mean titer (GMT) was measured after [22].

2.7. Carcass Properties. After 6 weeks of the experiment, five chickens per class were randomly chosen, fasted for 12 hours, and then weighed after which they were sacrificed and weighed to determine the dressing percentage, whereas liver, spleen, thymus, and bursa were weighed and the relative weights of chickens to their body mass were calculated. Gizzards, heart, and visible fat, from each chick, were also weighed.

2.8. Biochemical Analysis. Blood samplings were gathered from the wing vein on the 21st and 42nd days of the trial. Centrifugation of blood at 3000 rpm for 5 minutes to harvest clear sera was done. The gathered sera were exposed to biochemical

Table 1: Ingredients percentages and calculated composition analysis of the experimental starter diets (as fed basis).

Ingredients	Basal diet	DPS2	DPS4	DPS6
Corn	55	53.09	51.17	49.27
SBM (CP 44%)	32.04	32	32	32
Corn gluten (CP 62%)	5.5	5.6	5.66	5.7
Corn oil	3.5	3.39	3.27	3.17
Limestone	1.35	1.33	1.31	1.28
Dicalcium phosphate	1.74	1.74	1.74	1.74
L-lysine*	0.28	0.28	0.28	0.27
Dl-methionine**	0.14	0.12	0.12	0.12
P. dactylifera seeds	0	2	4	6
Vitamin and mineral premix***	0.3	0.3	0.3	0.3
NaCl	0.15	0.15	0.15	0.15
Total	100	100	100	100
Estimated and analyzed composition				
ME	3069.59	3070.39	3069.38	3070.05
CP %	22.6	22.6	22.59	22.58
Lysine %	1.34	1.34	1.34	1.34
Methionine %	0.5	0.5	0.5	0.5
Calcium %	1	1	1	1
Av. (P) %	0.45	0.45	0.45	0.45

SBM: soybean meal. ME: metabolizable energy (Kcal/kg diet). CP: crude protein. Av. (P): available phosphorous. *L-lysine, 99% feed grade. **Dl-methionine, 99% feed grade, China. ***Vitamin and mineral premix (Hero mix) produced by Hero pharm Co., Egypt.

Table 2: Ingredients percentages and calculated composition analysis of the experimental finisher diets (as fed basis).

Ingredients %	Basal diet	DPS2	DPS4	DPS6
Corn	67.58	65.54	63.64	61.55
SBOM (CP 44%)	23	23.09	23.20	23.35
Corn gluten (CP 62%)	3.0	3.0	3.0	3.0
Corn oil	3.4	3.36	3.27	3.17
Limestone	1.15	1.12	1.10	1.05
Dicalcium phosphate	1.27	1.30	1.30	1.30
L-lysine*	0.14	0.13	0.13	0.12
Dl-methionine**	0.01	0.01	0.01	0.01
P. dactylifera seeds	0.0	2.0	4.0	6.0
Vitamin and mineral premix***	0.3	0.3	0.3	0.3
NaCl	0.15	0.15	0.15	0.15
Total	100	100	100	100
Calculated and analyzed composition				
ME	3187.63	3189.41	3188.58	3188.10
CP %	18.14	18.13	18.12	18.14
Lysine %	0.96	0.96	0.96	0.96
Methionine %	0.32	0.32	0.32	0.32
Calcium %	0.80	0.80	0.80	0.80
Av. (P)	0.35	0.35	0.35	0.35

SBM: soybean meal. ME: metabolizable energy (Kcal/ kg diet). CP: crude protein. Av. (P): available phosphorous. *L-lysine, 99% feed grade. **Dl-methionine, 99% feed grade, China. ***Vitamin and mineral premix (Hero mix) produced by Hero pharm Co., Egypt.

Table 3: GC-MS analysis of *P. dactylifera* seeds.

Peak	Retention time (minutes)	Name	Area%	Molecular weight	Molecular formula
1	2.47	1-Ethynyl-3,trans(1,1-dimethylethyl)-4,cis-methoxycyclohexan-1-ol	1.83	210	$C_{13}H_{22}O_2$
2	3.09	Ethanol, 2-ethoxy-	2.77	90	$C_4H_{10}O_2$
3	3.82	Pentane, 3-ethyl-2,4-dimethyl-	2.14	128	$C_9H_2O_2$
4	4.45	α-Aminobutyric acid	8.98	103	$C_4H_9NO_2$
5	4.82	sec-Butyl acetate	4.48	116	$C_6H_{12}O_2$
6	4.94	4,6-Dimethyl-3-(4-methoxyphenyl) coumarin	14.73	280	$C_{18}H_{16}O_3$
7	7.04	cis-5,8,11,14-Eicosatetraenoic acid	25.64	304	$C_{20}H_{32}O_2$
8	7.68	4-Methylcinnamic acid	11.44	162	$C_{10}H_{10}O_2$
9	8.82	7-Allyloxy-4-methylcoumarin	2.20	216	$C_{13}H_{12}O_3$
10	9.00	Minoxidil	8.20	209	$C_9H_{15}N_5O$
11	9.15	1-(N-Methylamino)-1-phenylpropane	2.05	149	$C_{10}H_{15}N$
12	9.52	2-Ethyl-2-(p-tolyl) malonamide	2.50	220	$C_{12}H_{16}N_2O_2$
13	9.81	6-Hydroxy-7-methoxycoumarin	8.71	192	$C_{10}H_8O_4$
14	10.63	Mesitylene	1.91	120	C_9H_{12}
15	13.32	2H-Pyran, tetrahydro-2-(12-pentadecynyloxy)-	2.42	308	$C_{20}H_{36}O_2$

investigations of reduced glutathione (GSH) levels [23]. Meanwhile, the interferon-gamma (IFN-γ) and interleukin-2 (IL-2) levels were determined by ELISA kits that were purchased from Cusabio Company, while nitric oxide (NO) ELISA kit was purchased from WKEA Company ELISA kits. The UNICO 2100UV-Spectrophotometers, ELx800 Absorbance Microplate Reader, and other lab hardware help were utilized as a part of biochemical examinations.

2.9. Statistical Analysis. All values were stated as means ± SD. The statistical measures were handled by the SPSS programming (SPSS 22). One-way ANOVA was used followed by Duncan's multiple range tests, when the impact was significant, in order to separate the significant contrasts between dietary applications. All declarations of significance were depending on $P < 0.05$.

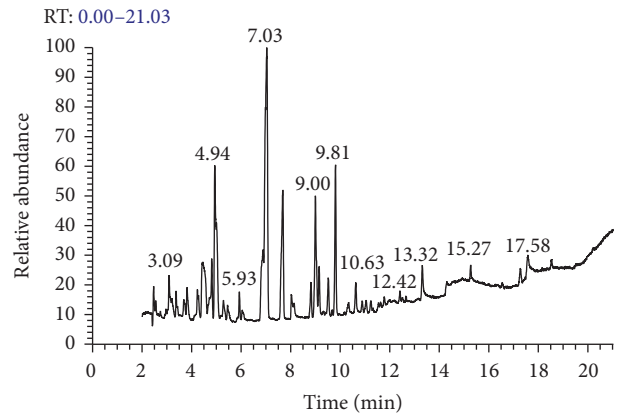

Figure 1: GC-MS chromatogram of *P. dactylifera* seeds methanolic extract.

3. Results and Discussion

The data presented in Figure 1 and illustrated in Table 3 explore 15 major different components present in *P. dactylifera* seeds that were analyzed by GC-MS. The obtained data identified the presence of some antioxidant and immune-stimulant compounds such as 4,6-dimethyl-3-(4-methoxyphenyl) coumarin (14.73%), 4-methylcinnamic acid (11.44%), 6-hydroxy-7-methoxycoumarin (8.71%), and 7-allyloxy-4-methylcoumarin (2.20%). Cinnamic acid and its derivatives were identified in *P. dactylifera* seeds of different date varieties [24–27]. More than 1300 coumarins have been documented from plant seeds, roots, and leaves possess an antioxidant, anticancer, anti-inflammatory, and antimicrobial properties [28–32].

The mean body weights of broiler nourished on basal diets and Bio-Mos and β-glucan supplemented diets compared with broiler chicks fed on diets that contained DPS at 2, 4, and 6% were illustrated in Table 4 that revealed higher significant increases in body weights and weight gain of broilers fed diets containing Bio-Mos, β-glucan, and DPS at levels of 2% and 4% when compared with the control one. Also, it was noticed that there were significant differences in relative growth rate (RGR) in all treated groups except those of DPS6 group when compared with the control one (Table 4); the highest RGR was observed in Bio-Mos, β-glucan, DPS2, and DPS4 groups (192.91 ± 0.13, 192.90 ± 0.07, 193.19 ± 0.07, and 193.06 ± 0.09, resp.). In regard to the feed intake, it was increased in all treated broiler groups in comparison to those of the control one (Table 4). Concerning total feed conversion ratio, chicks of DPS2 and DPS4 groups recorded the best feed

Table 4: Growth performance parameters of control and treated groups.

Group	IWT	FWT	WG	FI	FCR	RGR	PER	EEU	Mort. rate %
Control	39.83 ± 0.55^{a}	2073.7 ± 52.6^{b}	2033.87 ± 52.09^{b}	3501.07 ± 0.24^{f}	1.75 ± 0.04^{ab}	192.51 ± 0.10^{c}	0.10 ± 0.001^{a}	5.46 ± 0.14^{ab}	8
Bio-Mos	39.91 ± 0.33^{a}	2204.14 ± 54.56^{a}	2164.23 ± 54.25^{a}	3550 ± 0.27^{a}	1.67 ± 0.05^{bc}	192.91 ± 0.13^{b}	0.03 ± 0.001^{b}	5.20 ± 0.14^{bc}	4
β-Glucan	40.08 ± 0.24^{a}	2195.83 ± 34.26^{a}	2155.75 ± 34.03^{a}	3539.94 ± 0.28^{b}	1.65 ± 0.03^{bc}	192.9 ± 0.07^{b}	0.03 ± 0.001^{b}	5.16 ± 0.08^{bc}	4
DPS2	39.96 ± 0.37^{a}	2290.63 ± 44.46^{a}	2250.67 ± 44.10^{a}	3519.13 ± 0.23^{e}	1.58 ± 0.03^{c}	193.19 ± 0.07^{a}	0.03 ± 0.001^{b}	4.94 ± 0.10^{c}	4
DPS4	40.08 ± 0.25^{a}	2255.21 ± 40.60^{a}	2215.13 ± 40.37^{a}	3525.05 ± 0.20^{c}	1.60 ± 0.03^{c}	193.06 ± 0.09^{ab}	0.03 ± 0.001^{b}	5.02 ± 0.10^{c}	12
DPS6	40.13 ± 0.25^{a}	2023.96 ± 32.5^{b}	1983.83 ± 32.27^{b}	3520 ± 0.26^{d}	1.78 ± 0.03^{a}	192.31 ± 0.08^{c}	0.03 ± 0.001^{b}	5.59 ± 0.09^{a}	4

Means within the same column carrying different letters are significantly different at $P < 0.05$.
Values are expressed as means ± SE.
IWT: initial body weight. FWT: final body weight. WG: weight gain. FI: feed intake. FCR: feed conversion ratio. RGR: relative growth rate. PER: protein efficiency ratio. EEU: efficiency of energy utilization.

Table 5: Hemagglutination inhibition (HI) titer of Newcastle disease virus in control and treated groups at 14th, 21st, and 42nd day of age.

Group	14th day	21st day	42nd day
Control	4.30 ± 0.06^{a}	5.17 ± 0.19^{c}	5.27 ± 0.15^{b}
Bio-Mos	4.47 ± 0.03^{a}	5.30 ± 0.15^{bc}	5.47 ± 0.03^{ab}
β-Glucan	4.43 ± 0.03^{a}	5.20 ± 0.06^{c}	5.43 ± 0.03^{b}
DPS2	4.37 ± 0.09^{a}	5.50 ± 0.06^{abc}	5.73 ± 0.15^{a}
DPS4	4.43 ± 0.03^{a}	5.63 ± 0.03^{ab}	5.67 ± 0.09^{a}
DPS6	4.23 ± 0.07^{a}	5.70 ± 0.10^{a}	5.63 ± 0.07^{a}

Means within the same column carrying different letters are significantly different at $P < 0.05$.
Values are expressed as means ± SE.

conversion ratio in comparison with those of control one (1.58 ± 0.03 and 1.60 ± 0.03 versus 1.75 ± 0.04, resp.) and achieved the best energy utilization efficiency (4.94 ± 0.10 and 5.02 ± 0.10 versus 5.46 ± 0.14, resp.).

The increase in body weight and higher body weight gain due to the presence of Bio-Mos and β-glucan agree with those of [5, 33] which concluded the effect of mannan-oligosaccharides and β-glucans supplementation shows significant increase in body weight gain and enhancement in the feed efficiency in relation to the control diet. This advance may be with regard to the improvement of intestinal mucosal integrity and the increase in the absorption and utilization of the dietary nutrients [34].

DPS containing diets at levels of 2% and 4% showed higher significant increases in body weights and weight gain in broilers. The research study on DPS conveys the increment in the body weight due to DPS to mannan-oligosaccharides that were already detected in DPS [35] in addition to selenium, phenolic, and carotenoid compounds of DPS [36].

The effects of diets containing Bio-Mos and β-glucan comparing with different levels of DPS at 2, 4, and 6% on antibody level against Newcastle disease virus (NDV) of broiler chickens during 14th, 21st, and 42nd day of age in relation to control group were presented in Table 5. On the 14th day of age, there were insignificant differences among different treated groups. Meanwhile, on the 21st day, the birds fed diets containing DP at levels 6 and 4% showed a significant antibody titer against NDV, respectively, when compared with control one; also on the 42nd day the DPS2, DPS4, and DPS6 showed a significant antibody titer against NDV.

The data presented in Table 6 stated the carcass characteristics of control and treated birds. The dressing percentages in different experimental groups showed significant improvement in dressing percentage when compared with control one except those of DPS6 group. Conversely, the liver, heart, and gizzard weights showed no significant difference among different experimental groups. Table 6 also shows an enhancement in immune organ weight; spleen weight showed a numerical increase in treated groups. Also, thymus weights showed significant increases in DPS2 and DPS4 groups. The increment in antioxidant status of animals improves their growth performance, production, and reproduction [37]. Because mannan-oligosaccharides are not digested, they stimulate the lymphatic system of the gastrointestinal tract and general immunity [38].

The data belonging to the biochemical study were illustrated in Tables 7 and 8. The serum levels of GSH were significantly increased ($P < 0.05$) in DPS treated group, especially at 21st day. Indeed, its levels in Bio-Mos and β-glucan treated groups were significantly increased ($P < 0.05$) at 42nd day of the experiment. In regard to serum NO, its levels were unchanged at 21st day and slightly decreased in all treated groups in comparison to control one (Table 7). The antioxidant activity of Bio-Mos, β-glucan, and DPS treated group is evidenced by the significant increase in the serum levels of GSH. The obtained data reported a talented antioxidant effective feed additive in broiler diets through DPS besides yeast cell wall prebiotics [39]. The methanolic extract of DPS is considered as an antioxidant source of β-carotene and phenolic compounds [40]. This antioxidant effect became proportional to the phenolic contents [41]. The significant decrease in MDA level in testicular tissue of DPS treated male rats in comparison with control one may be attributed to the antioxidant effect of p-coumaric acid, ferulic acid, flavonoids, sinapic acids, and procyanidins [42].

The data of cellular immunity were obtained in Table 8 in which both IFN-γ and IL-2 were significantly increased ($P < 0.05$) in all DPS treated groups. In DPS2 group the highest levels of IFN-γ and IL-2 were at 42nd day while being at 21st day in Bio-Mos group. In regard to the comparison between the different concentrations of date seeds supplementations, the DPS2 group improved the antioxidant and cellular immunity in treating chicks. Dietary antioxidants exert their positive effects on the elimination of reactive oxygen species and subsequently prevent the activation of the inflammation process [43]. With regard to the serum production of cytokines, which were used for further understanding of immune status, we observed an upregulation of IL-2 and IFN-γ in broiler chickens in the Bio-Mos, β-glucan, and DPS groups comparable to the control one, in which IFN-γ is a soluble cytokine that is the only member of type II class of interferon known as immune interferon [44]. In addition, IL-2 is a type of cytokine that regulates the activities of leukocytes, often lymphocytes that are accountable for immunity [45]. In addition, IFN-γ production was augmented due to β-glucan in poultry [46, 47].

4. Conclusion

From the obtained data, we can conclude that the supplementation of broilers with ration containing DPS at levels 2% and 4% is of great beneficial improvements in broiler health producing healthy birds with higher body weight, despite enhancements of body weight, gain, organ weight, antibody titer, IFN-γ, IL-2, and antioxidant status in comparison to mannan-oligosaccharides and β-glucan.

Table 6: Dressing percentage and relative weights for liver, heart, gizzard and spleen, and thymus and bursa of control and treated groups.

Item	Dressing %	Liver	Heart	Gizzard	Spleen	Thymus	Bursa
Control	68% ± 0.01[c]	40 ± 2.08[a]	9.83 ± 0.09[a]	31 ± 1.53[a]	1.7 ± 0.06[a]	2.83 ± 0.03[c]	2.10 ± 0.06[a]
Bio-Mos	71% ± 0.01[ab]	40.67 ± 1.76[a]	10.5 ± 0.29[a]	34.33 ± 0.67[a]	1.93 ± 0.07[a]	3.20 ± 0.06[a]	2.23 ± 0.07[a]
β-Glucan	72% ± 0.01[a]	42 ± 1.15[a]	10.67 ± 0.17[a]	34.33 ± 0.67[a]	1.9 ± 0.06[a]	3.23 ± 0.03[a]	2.23 ± 0.07[a]
DPS2	71% ± 0.01[ab]	41.67 ± 2.03[a]	10.33 ± 0.44[a]	32.67 ± 2.33[a]	1.83 ± 0.09[a]	3.13 ± 0.07[ab]	2.13 ± 0.09[a]
DPS4	71% ± 0.01[ab]	41.67 ± 2.03[a]	10.17 ± 0.6[a]	31 ± 0.58[a]	1.9 ± 0.06[a]	2.97 ± 0.09[ab]	2.20 ± 0.06[a]
DPS6	69% ± 0.01[bc]	40.33 ± 1.86[a]	10.43 ± 0.23[a]	32 ± 1.0[a]	1.77 ± 0.03[a]	3.03 ± 0.09[abc]	2.10 ± 0.06[a]

Means within the same column carrying different letters are significantly different at $P < 0.05$.
Values are expressed as means ± SE.

Table 7: The mean values of serum GSH and NO in control and treated groups.

	GSH (μg/mL)		NO (μmol/L)	
	21st day	42nd day	21st day	42nd day
Control	49.55 ± 3.29[b]	23.56 ± 4.71[b]	8.97 ± 0.04[a]	8.24 ± 0.27[bc]
Bio-Mos	22.31 ± 3.21[c]	45.97 ± 13.56[a]	8.09 ± 0.21[a]	7.68 ± 0.12[c]
β-Glucan	16.75 ± 1.86[d]	47.55 ± 13.59[a]	8.11 ± 0.62[a]	8.19 ± 0.21[b]
DPS2	67.44 ± 5.82[a]	34.65 ± 9.42[ab]	8.09 ± 0.32[a]	8.07 ± 0.04[ab]
DPS4	55.91 ± 2.67[ab]	31.71 ± 0.4[ab]	8.18 ± 0.55[a]	8.15 ± 0.14[a]
DPS6	55.46 ± 4.69[ab]	34.2 ± 1.74[ab]	8.17 ± 0.31[a]	8.00 ± 0.09[bc]

Means within the same column carrying different letters are significantly different at $P < 0.05$.
Values are expressed as means ± SE.

Table 8: The mean values of serum IFN-γ and IL-2 in control and treated groups.

	IFN-γ (pg/mL)		IL-2 (pg/mL)	
	21st day	42nd day	21st day	42nd day
Control	149.99 ± 34.33[c]	217.02 ± 68.32[c]	1.30 ± 0.55[a]	1.27 ± 0.08[b]
Bio-Mos	532.76 ± 33.16[a]	373.23 ± 14.54[b]	1.39 ± 0.20[a]	1.86 ± 0.06[ab]
β-Glucan	314.54 ± 8.67[b]	314.54 ± 8.67[bc]	1.54 ± 0.25[a]	1.77 ± 0.12[b]
DPS2	253.43 ± 56.19[ab]	490.45 ± 36.16[a]	1.79 ± 0.52[a]	2.62 ± 0.47[a]
DPS4	238.19 ± 42.08[ab]	431.70 ± 10.50[ab]	1.61 ± 0.28[a]	1.48 ± 2.20[b]
DPS6	437.39 ± 47.68[ab]	448.23 ± 4.98[ab]	1.78 ± 0.33[a]	1.26 ± 0.17[bc]

Means within the same column carrying different letters are significantly different at $P < 0.05$.
Values are expressed as means ± SE.

Competing Interests

The authors have no conflict of interests.

Acknowledgments

The authors thank Dr. Mamoun Abd El Kareem (Atomic and Molecular Physics Unit, Experimental Nuclear Physics Department, Nuclear Research Center, Egyptian Atomic Energy Authority) for his assistance and advices.

References

[1] T. Ayasan, "Effects of dietary inclusion of protexin (probiotic) on hatchability of Japanese quails," *Indian Journal of Animal Sciences*, vol. 83, no. 1, pp. 78–81, 2013.

[2] A. Gupta and S. Das, "The benefits of probiotics in poultry production: an overview," *International Journal of Livestock Research*, vol. 2, no. 1, p. 18, 2012.

[3] P. W. Waldroup, E. O. Oviedo-Rondon, and C. A. Fritts, "Comparison of Bio-Mos® and antibiotic feeding programs in broiler diets containing copper sulfate," *International Journal of Poultry Science*, vol. 2, no. 1, pp. 28–31, 2003.

[4] D. Mikulski, K. Kozłowski, J. Jankowski, J. Blok, and Z. Sobolewski, "Efficacy of yeast extract *Saccharomyces cerevisiae* in Turkey feeding," *Medycyna Weterynaryjna*, vol. 64, no. 11, pp. 1331–1334, 2008.

[5] A. A. Alsenosy, H. S. A. El-Hamid, U. B. El-Gazzar, and A. El-Far, "Biochemical effect of some feed additives and immunological response in broiler chickens," *Alexandria Journal of Veterinary Sciences*, vol. 35, pp. 131–142, 2012.

[6] V. Vetvicka and C. Oliveira, "β(1-3)(1-6)-D-glucans modulate immune status in pigs: potential importance for efficiency of

commercial farming," *Annals of Translational Medicine*, vol. 2, no. 2, article 16, 2014.

[7] S. Besbes, C. Blecker, C. Deroanne, N.-E. Drira, and H. Attia, "Date seeds: chemical composition and characteristic profiles of the lipid fraction," *Food Chemistry*, vol. 84, no. 4, pp. 577–584, 2004.

[8] W. H. Barreveld, *Date Palm Products*, Food and Agriculture Organization of the United Nations, 1993.

[9] W. Al-Shahib and R. J. Marshall, "Fatty acid content of the seeds from 14 varieties of date palm *Phoenix dactylifera* L.," *International Journal of Food Science and Technology*, vol. 38, no. 6, pp. 709–712, 2003.

[10] J. Peterson and J. Dwyer, "Flavonoids: dietary occurrence and biochemical activity," *Nutrition Research*, vol. 18, no. 12, pp. 1995–2018, 1998.

[11] A. H. Mohamed, B. E. El-Saidy, and I. A. El-Seidy, "Influence of some medicinal plants supplementation: 1—on digestibility, nutritive value, rumen fermentation and some blood biochemical parameters in sheep," *Egyptian Journal of Nutrition and Feeds*, vol. 6, pp. 139–150, 2003.

[12] H. A. Ahmed, K. M. Sadek, and A. E. Taha, "Impact of two herbal seeds supplementation on growth performance and some biochemical blood and tissue parameters of broiler chickens," *World Academy of Science, Engineering and Technology*, vol. 2, no. 3, 2015.

[13] U. B. El-Gazzar, A. H. El-Far, and H. A. Abdel Maksoud, "The ameliorative effect of *Phoenix dactylifera* extract on CCl_4 hepatotoxicity in New Zealand rabbits," *Journal of Applied Sciences Research*, vol. 5, no. 9, pp. 1082–1087, 2009.

[14] A. S. Hussein, G. A. Alhadrami, and Y. H. Khalil, "The use of dates and date pits in broiler starter and finisher diets," *Bioresource Technology*, vol. 66, no. 3, pp. 219–223, 1998.

[15] M. S. Copley, P. J. Rose, A. Clapham, D. N. Edwards, M. C. Horton, and R. P. Evershed, "Detection of palm fruit lipids in archaeological pottery from Qasr Ibrim, Egyptian Nubia," *Proceedings of the Royal Society B: Biological Sciences*, vol. 268, no. 1467, pp. 593–597, 2001.

[16] AOAC, *Official Methods of Analysis* , AOAC Int, Arlington, Va, USA, 2005.

[17] B. S. Kamel, M. F. Diab, M. A. Ilian, and A. J. Salman, "Nutritional Value of whole dates and date pits in broiler rations," *Poultry Science*, vol. 60, no. 5, pp. 1005–1011, 1981.

[18] B. N. Shyamala, S. Gupta, A. Jyothi Lakshmi, and J. Prakash, "Leafy vegetable extracts—antioxidant activity and effect on storage stability of heated oils," *Innovative Food Science and Emerging Technologies*, vol. 6, no. 2, pp. 239–245, 2005.

[19] D. Barakat, A. El-Far, K. Sadek, U. Mahrous, H. Ellakany, and M. Abdel-Latif, "Anise (*Pimpinella anisum*) enhances the growth performance, immunity and antioxidant activities in broilers," *International Journal of Pharmaceutical Sciences Review and Research*, vol. 37, no. 24, pp. 134–140, 2016.

[20] NRC, Ed., *Nutrient Requirements of Poultry*, National Academies Press, Washington, DC, USA, 1994.

[21] G. Takátsy, "The use of spiral loops in serological and virological micro-methods. 1955," *Acta Microbiologica et Immunologica Hungarica*, vol. 50, no. 4, pp. 369–382, 2003.

[22] M. Brugh Jr., "A simple method for recording and analyzing serological data," *Avian Diseases*, vol. 22, no. 2, pp. 362–365, 1978.

[23] E. Beutler, O. Durno, and B. M. Kelly, "Improved method for the determination of blood glutathione," *Journal of Laboratory and Clinical Medicine*, vol. 61, pp. 882–888, 1963.

[24] P. K. Vayalil, "Date fruits (*Phoenix dactylifera* Linn): an emerging medicinal food," *Critical Reviews in Food Science and Nutrition*, vol. 52, no. 3, pp. 249–271, 2012.

[25] I. Hamad, H. AbdElgawad, S. Al Jaouni et al., "Metabolic analysis of various date palm fruit (*Phoenix dactylifera* L.) cultivars from Saudi Arabia to assess their nutritional quality," *Molecules*, vol. 20, no. 8, pp. 13620–13641, 2015.

[26] W. Kchaou, F. Abbès, R. B. Mansour, C. Blecker, H. Attia, and S. Besbes, "Phenolic profile, antibacterial and cytotoxic properties of second grade date extract from Tunisian cultivars (*Phoenix dactylifera* L.)," *Food Chemistry*, vol. 194, pp. 1048–1055, 2016.

[27] Z. Benmeddour, E. Mehinagic, D. Le Meurlay, and H. Louaileche, "Phenolic composition and antioxidant capacities of ten Algerian date (*Phoenix dactylifera* L.) cultivars: a comparative study," *Journal of Functional Foods*, vol. 5, no. 1, pp. 346–354, 2013.

[28] G. Cravotto, S. Tagliapietra, R. Cappello, G. Palmisano, M. Curini, and M. Boccalini, "Long-chain 3-acyl-4-hydroxycoumarins: Structure and antibacterial activity," *Archiv der Pharmazie*, vol. 339, no. 3, pp. 129–132, 2006.

[29] M.-H. Lin, Y.-S. Chou, Y.-J. Tsai, and D.-S. Chou, "Antioxidant properties of 5,7-dihydroxycoumarin derivatives in in vitro cell-free and cell-containing systems," *Journal of Experimental and Clinical Medicine*, vol. 3, no. 3, pp. 126–131, 2011.

[30] D. Završnik, S. Muratović, D. Makuc et al., "Benzylidene-bis-(4-hydroxycoumarin) and benzopyrano-coumarin derivatives: synthesis, $^{1}H/^{13}C$-NMR conformational and X-ray crystal structure studies and in vitro antiviral activity evaluations," *Molecules*, vol. 16, no. 7, pp. 6023–6040, 2011.

[31] T. Nasr, S. Bondock, and M. Youns, "Anticancer activity of new coumarin substituted hydrazide-hydrazone derivatives," *European Journal of Medicinal Chemistry*, vol. 76, pp. 539–548, 2014.

[32] A. A. Al-Amiery, Y. K. Al-Majedy, A. A. H. Kadhum, and A. B. Mohamad, "Novel macromolecules derived from coumarin: synthesis and antioxidant activity," *Scientific Reports*, vol. 5, Article ID 11825, 2015.

[33] R. C. Shendare, M. A. Gongle, A. B. Rajput, B. V. Wanjari, and S. M. Mandlekar, "Effect of supplementation of Manno-Oligosaccharide and b-glucans on maize based meal on commercial broilers," *Veterinary World*, vol. 1, no. 1, pp. 13–15, 2008.

[34] G. T. Bradley and T. F. Savage, "Enhance utilization of dietary calcium, phosphorus, nitrogen and metabolizable energy in poults feed diet containing a yeast culture," *Poultry Science*, vol. 73, p. 124, 1994.

[35] F. Daneshyar, N. Afzali, and H. Farhangfar, "Effects of different levels of date pits in broilers' feed contaminated with aflatoxin B1 on broilers' performance and carcass characteristic," *African Journal of Biotechnology*, vol. 13, no. 1, pp. 185–193, 2014.

[36] M. A. Al-Farsi and C. Y. Lee, "Nutritional and functional properties of dates: a review," *Critical Reviews in Food Science and Nutrition*, vol. 48, no. 10, pp. 877–887, 2008.

[37] Y. Wu, Q. Wu, Y. Zhou, H. Ahmad, and T. Wang, "Effects of clinoptilolite on growth performance and antioxidant status in broilers," *Biological Trace Element Research*, vol. 155, no. 2, pp. 228–235, 2013.

[38] A. Czech, E. R. Grela, A. Mokrzycka, and Z. Pejsak, "Efficacy of mannanoligosaccharides additive to sows diets on colostrum, blood immunoglobulin content and production parameters of piglets," *Polish Journal of Veterinary Sciences*, vol. 13, no. 3, pp. 525–531, 2010.

[39] L. Križková, Z. Ďuračková, J. Šandula, V. Sasinková, and J. Krajčovič, "Antioxidative and antimutagenic activity of yeast cell

wall mannans in vitro," *Mutation Research*, vol. 497, no. 1-2, pp. 213–222, 2001.

[40] S. M. M. Shanab, E. A. Hanafy, and E. A. Shalaby, "Biodiesel production and antioxidant activity of different Egyptian date palm seed cultivars," *Asian Journal of Biochemistry*, vol. 9, no. 3, pp. 119–130, 2014.

[41] M. R. S. Ardekani, M. Khanavi, M. Hajimahmoodi, M. Jahangiri, and A. Hadjiakhoondi, "Comparison of antioxidant activity and total phenol contents of some date seed varieties from Iran," *Iranian Journal of Pharmaceutical Research*, vol. 9, no. 2, pp. 141–146, 2010.

[42] S. H. Orabi and S. M. Shawky, "Effect of date palm (*Phoenix dactylifera*) seeds extracts on hematological, biochemical parameters and some fertility indices in male rats," *International Journal of Sciences: Basic and Applied Research*, vol. 17, no. 1, pp. 137–147, 2014.

[43] E. M. Conner and M. B. Grisham, "Inflammation, free radicals, and antioxidants," *Nutrition*, vol. 12, no. 4, pp. 274–277, 1996.

[44] E. Katsoulidis, S. Kaur, and L. C. Platanias, "Deregulation of interferon signaling in malignant cells," *Pharmaceuticals*, vol. 3, no. 2, pp. 406–418, 2010.

[45] W. Liao, J.-X. Lin, and W. J. Leonard, "IL-2 family cytokines: new insights into the complex roles of IL-2 as a broad regulator of T helper cell differentiation," *Current Opinion in Immunology*, vol. 23, no. 5, pp. 598–604, 2011.

[46] B. Zhang, Y. Guo, and Z. Wang, "The modulating effect of β-1, 3/1, 6-glucan supplementation in the diet on performance and immunological responses of broiler chickens," *Asian-Australasian Journal of Animal Sciences*, vol. 21, no. 2, pp. 237–244, 2008.

[47] T. Harada, N. N. Miura, Y. Adachi, M. Nakajima, T. Yadomae, and N. Ohno, "IFN-γ induction by SCG, 1,3-β-D-glucan from *Sparassis crispa*, in DBA/2 mice in vitro," *Journal of Interferon and Cytokine Research*, vol. 22, no. 12, pp. 1227–1239, 2002.